

Organic geochemical analysis of gravity core samples collected off West Greenland, 2006

J. A. Bojesen-Koefoed, F. Dalhoff, H. P. Nytoft & M. Schoell



GEOLOGICAL SURVEY OF DENMARK AND GREENLAND
MINISTRY OF THE ENVIRONMENT



Organic geochemical analysis of gravity core samples collected off West Greenland, 2006

J. A. Bojesen-Koefoed, F. Dalhoff, H. P. Nytoft & M. Schoell

1. Introduction

During the summer of 2006, a seabed sampling program was carried out in the West Greenland offshore, using the research vessel m/s Dana. Sampling was carried out by dredging, grabbing and gravity coring, covering an area from approximately 64°N to 72°N (Fig. 1).

The objectives of the sampling program were:

- Collect lithologies that crop out on the seabed – particularly with the objective to investigate the possible presence of petroleum source rocks
- Attempt to confirm and substantiate suspected petroleum seepage on the seabed as suggested by the presence of oil slicks recorded by remote sensing
- Investigate the nature of suspected mud diapirs noted on seismic from the southern part of the area covered.

The seabed sampling programme is a cooperative project of the Bureau of Minerals and Petroleum under the Greenland Government (BMP), Nunaoil, and the Geological Survey of Denmark and Greenland (GEUS).

This report summarises the results of organic geochemical analysis of gravity core samples collected during the cruise. Details of sampling and sample positions can be found in the cruise report (Dalhoff & Kuijpers 2007).

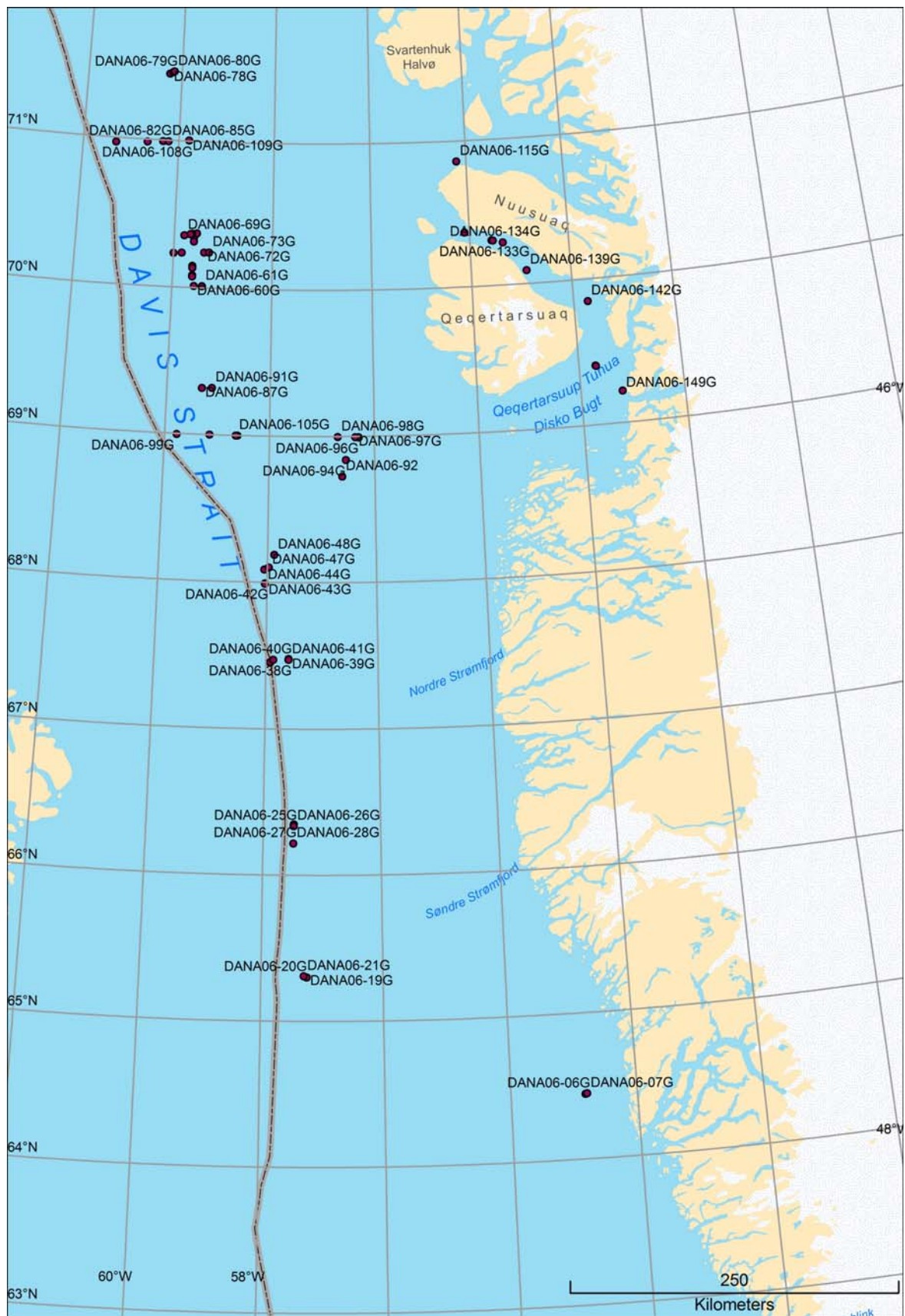


Fig. 1

2. Samples and methods

A total of 196 canned samples, collected from 60 different gravity cores were analysed (Table 1). The gravity cores were up to 6 metres long.

Each gravity core was numbered, the number being succeeded by the letter "G" to indicate "Gravity Core" – e.g. "48G" .

Subsamples were collected from the gravity cores on deck, and stored in sealed tin cans. The tins were stored upside down to prevent loss of gas through potential leaks at the rim of the lid.

Frequently, several subsamples were taken - typically with a distance of 1m - from a single gravity core. Such subsamples are identified by an index succeeding the letter "G" in the gravity core number, e.g. 48G-1, 48G-2, 48G-3, so on and so forth, with 1 being the deeper of the subsamples and higher numbers being taken successively closer to the seabed.

Headspace gases were sampled and analysed by APT, Kjeller Norway. The analyses included C₁₋₅ hydrocarbons and CO₂, plus stable carbon isotope composition of methane.

After recovery of headspace gas, sample aliquots were collected from the cans, wrapped in 5 micron polyethylene filters and washed by demineralised water in a soxhlet extraction unit until free of chloride (AgNO₃ assay). Subsequently the samples were dried at 50 °C and analysed.

Total Carbon (TC) and Total Sulphur (TS) were determined using a LECO CS-200 apparatus. Total organic carbon (TOC) was determined after treatment of sample aliquots by several batches of sulphurous acid to remove carbonates without losing soluble organic matter such as fulvic acids. Acid-treated samples were then analysed by a LECO CS-200 apparatus and TOC calculated on the basis of weight-loss.

Rock-Eval type screening pyrolysis was carried out using SRA instrumentation (Humble Instruments and Services, HISI). The instrument setup was similar to the standard Rock-

Eval cycle 1 mode, and testing show the data to be fully comparable and correlatable to normal Rock-Eval data.

Porewater sulphate content was determined in a number of selected samples that show systematic variation in headspace gas composition with depth. The following procedure was used: Plugs from the sediment core were transferred into 50 ml Eppendorf vials and frozen until use. A minor part 2-5 g of frozen sediment was transferred to a new 50 ml centrifuge vial and the vial was immediately filled with deoxygenated water to the top and closed. The sediment was afterwards suspended in the water for 10 min and then centrifuged at 1100 g in 5 min. 5 ml water was sampled by pipette and put into reagents for sulphide and sulphate determination.

Sulphide was determined using colorimetric reaction with N,N'-dimethyl-1,4-phenylenediamin and Fe(III) and measured at 665 nm. Sulphate and chloride was analysed on DIONEX-ion chromatograph with an A4S column.

Selected samples were subjected to solvent extraction, using a soxtec™ instrument. DCM/Meoh (93/7 vol./vol.) was used as solvent.

Due to low extract recovery, total hydrocarbon fractions were prepared by elution of total extracts by n-hexane through silica-microcolumns.

Gas chromatography of total hydrocarbon fractions was carried out using a Shimadzu 2010 GC, furnished with a 25 m HP-1 WCOT column and FID.

GC-MS-MS and GC-MS(SIM) analyses were performed using an Agilent 6890N gas chromatograph connected to a Waters (Micromass) Quattro Micro GC tandem quadropole mass spectrometer. A Phenomenex ZB-5 capillary column (30 m x 0.25 mm i.d., film thickness 0.10 µm) was used. The temperature program was 30°C/min from 70 to 100°C and 4°C/min from 100 to 308°C followed by 8 min at 308°C.

3. Results

3.1 TC/TOC/TS analysis and Rock-Eval screening pyrolysis

TC/TOC/TS and Rock-Eval type screening pyrolysis data are listed in table 3.1.

In general the total organic carbon (TOC) content of all samples is low. None of the samples show TOC exceeding 2% and more than half of the samples, 103 out of a total of 196 samples, show TOC below 0.5% (Fig. 3.1.1).

Pyrolysis yields are also very low with only 6 out of a total of 196 samples showing S2 pyrolysis yields exceeding 1 mg/g (Fig. 3.1.2).

Standard plots of Tmax vs. Hydrogen Index and TOC vs. S2 pyrolysis yield are shown in Fig. 3.1.3 and 3.1.4, respectively.

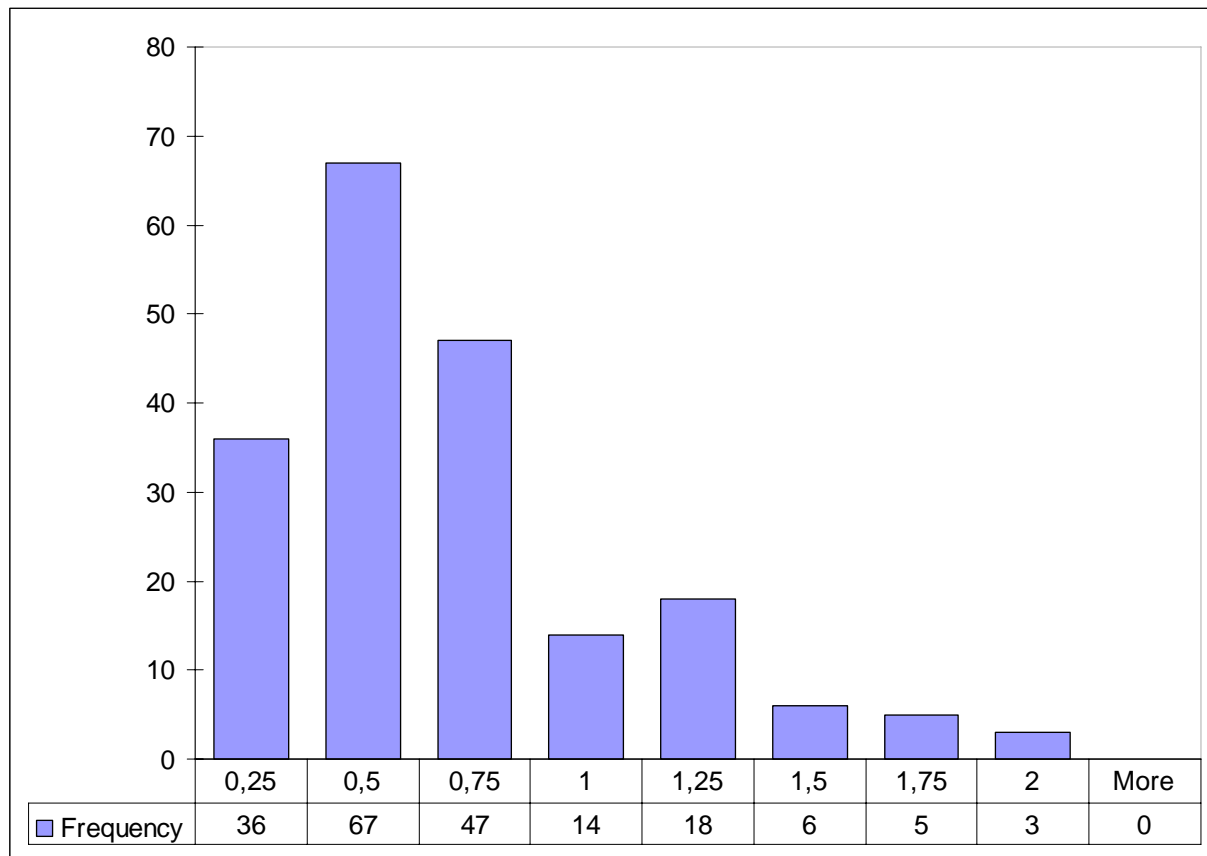


Fig. 3.1.1. Distribution of TOC in seabed samples from off West Greenland. Interval labels indicate maximum value of interval, i.e. "0.25" means 0.0–0.25, "0.5" means 0.25–0.5, ...

Fig. 3.1.5 shows TOC profiles of cores from which more than 3 subsamples were taken. With few exceptions the profiles show either a decreasing trend or no clear trend with depth. Dana06-07G was collected on a suspected mud diapir close to coast in the southern part of the study area (fig 1). This core shows a marked shift in TOC-level as well as in other parameters such as pyrolysis yield and TS/TOC ratio approximately at the middle of the core. As mentioned above most cores show very low overall TOC levels, but a few cores, Dana06-115G and Dana06-131G through Dana06-142G show TOC levels close to 1 or even higher, with little variation through the cores.

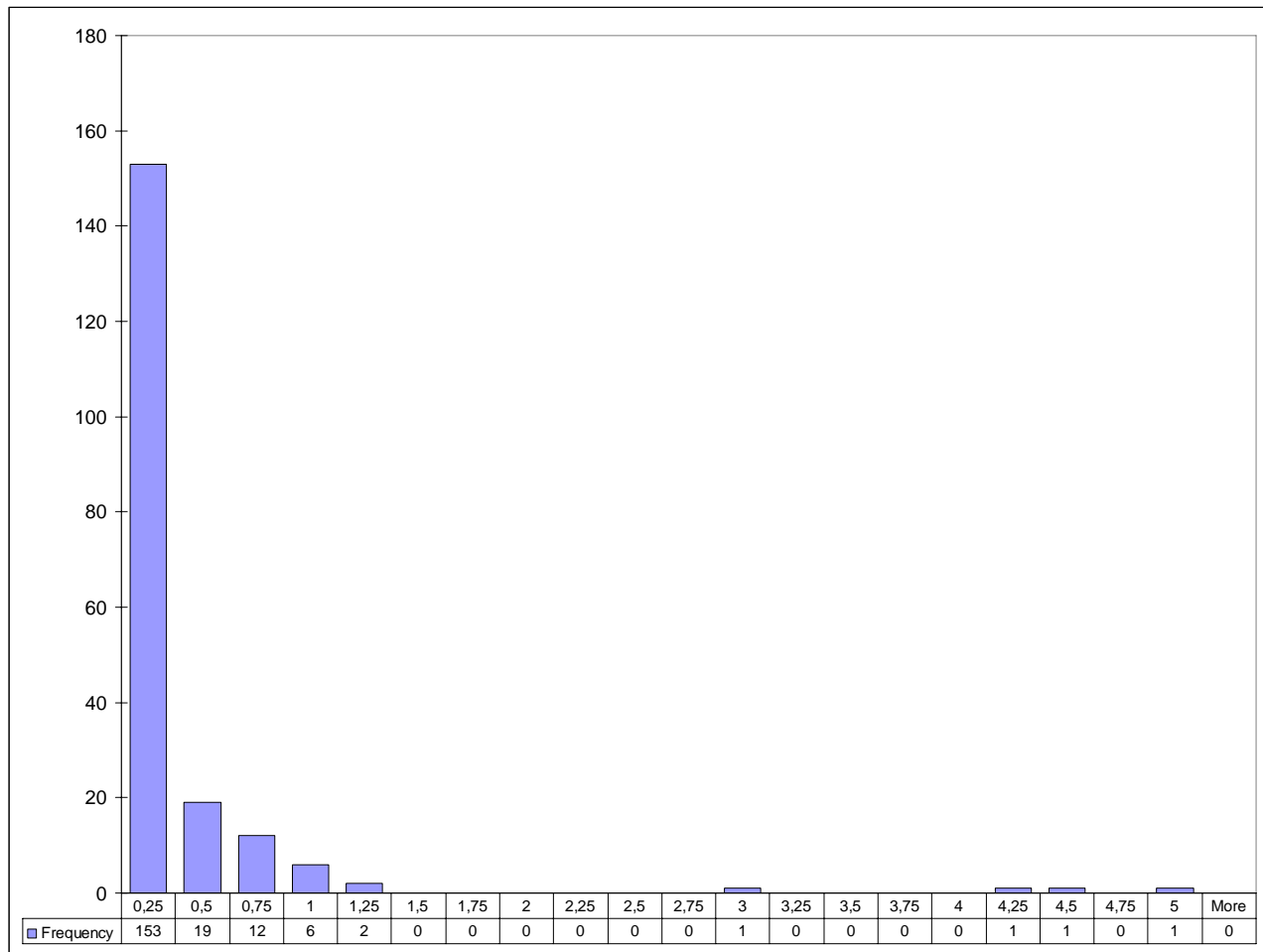


Fig. 3.1.2. Distribution of S2 pyrolysis yields in seabed samples from off West Greenland
Interval labels indicate maximum value of interval, i.e. “0.25” means 0.0–0.25, “0.5” means 0.25–0.5,,,

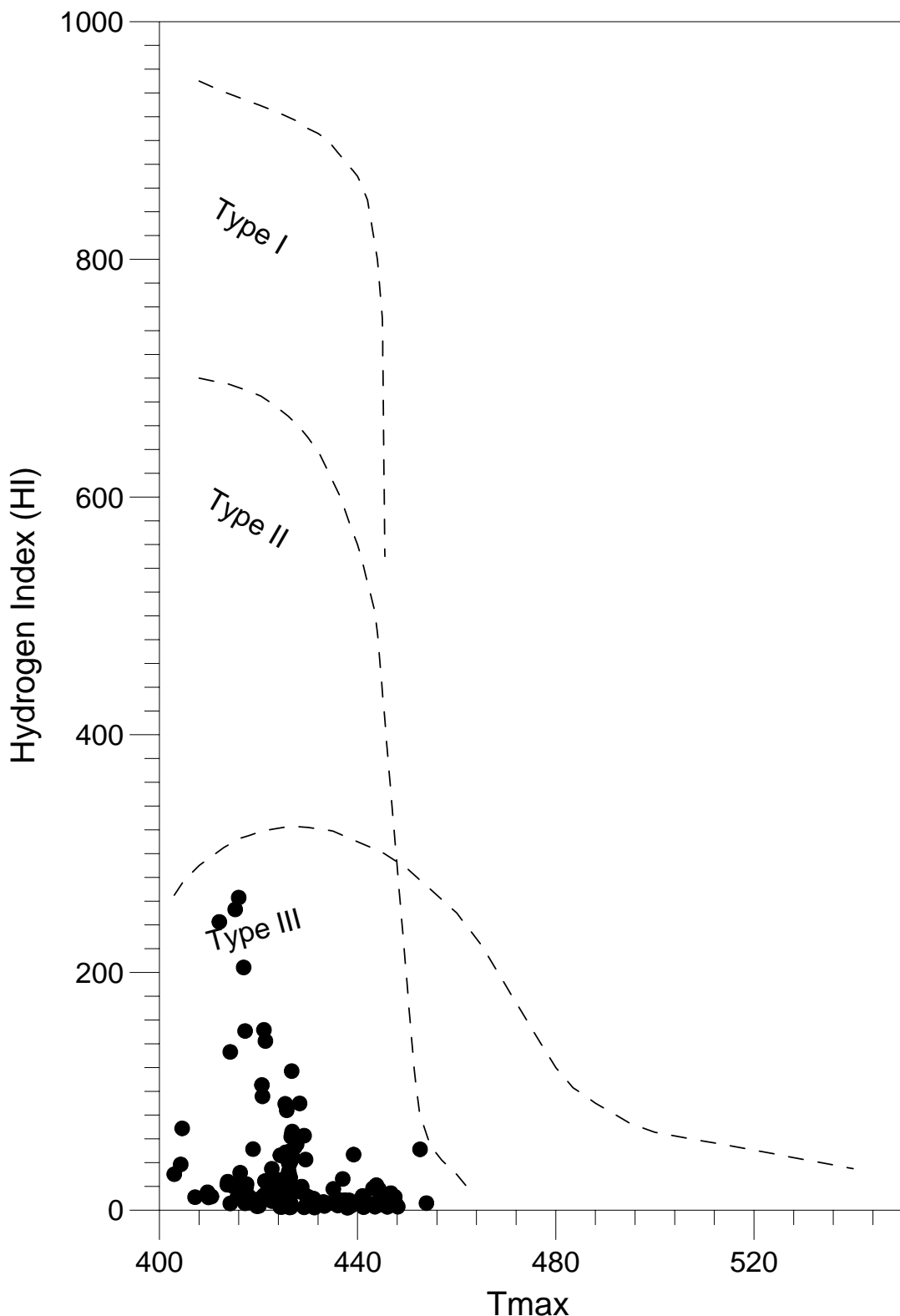


Fig. 3.1.3. Tmax vs. Hydrogen Index for seabed samples. Data clipping at axis limits has been carried out.

S2 (kg hydrocarbons/ton rock)

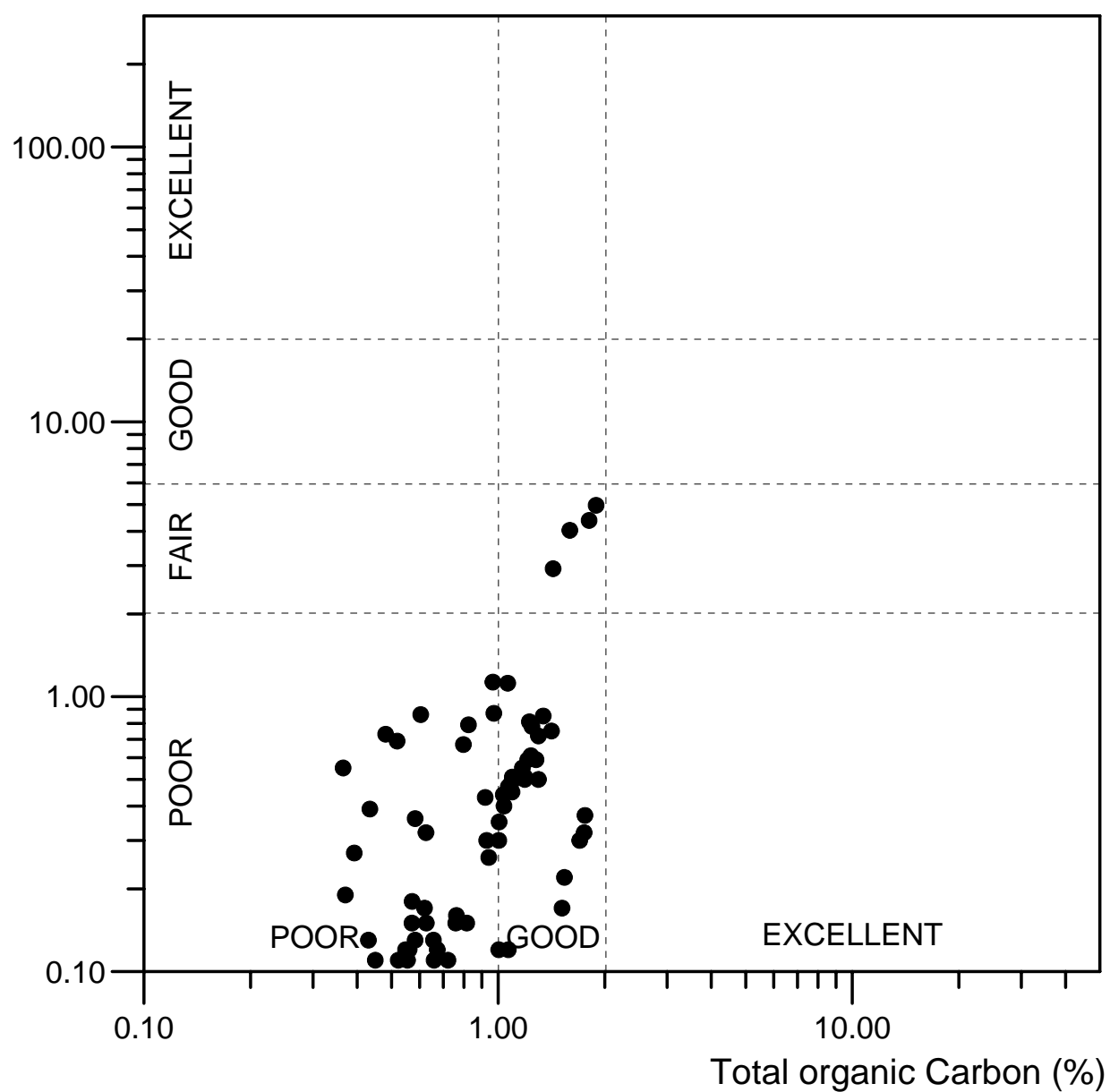


Fig. 3.1.4. TOC vs. S2 for seabed samples. Data clipping at axis limits has been carried out. Note that except for a few samples S2 pyrolysis yields are very low.

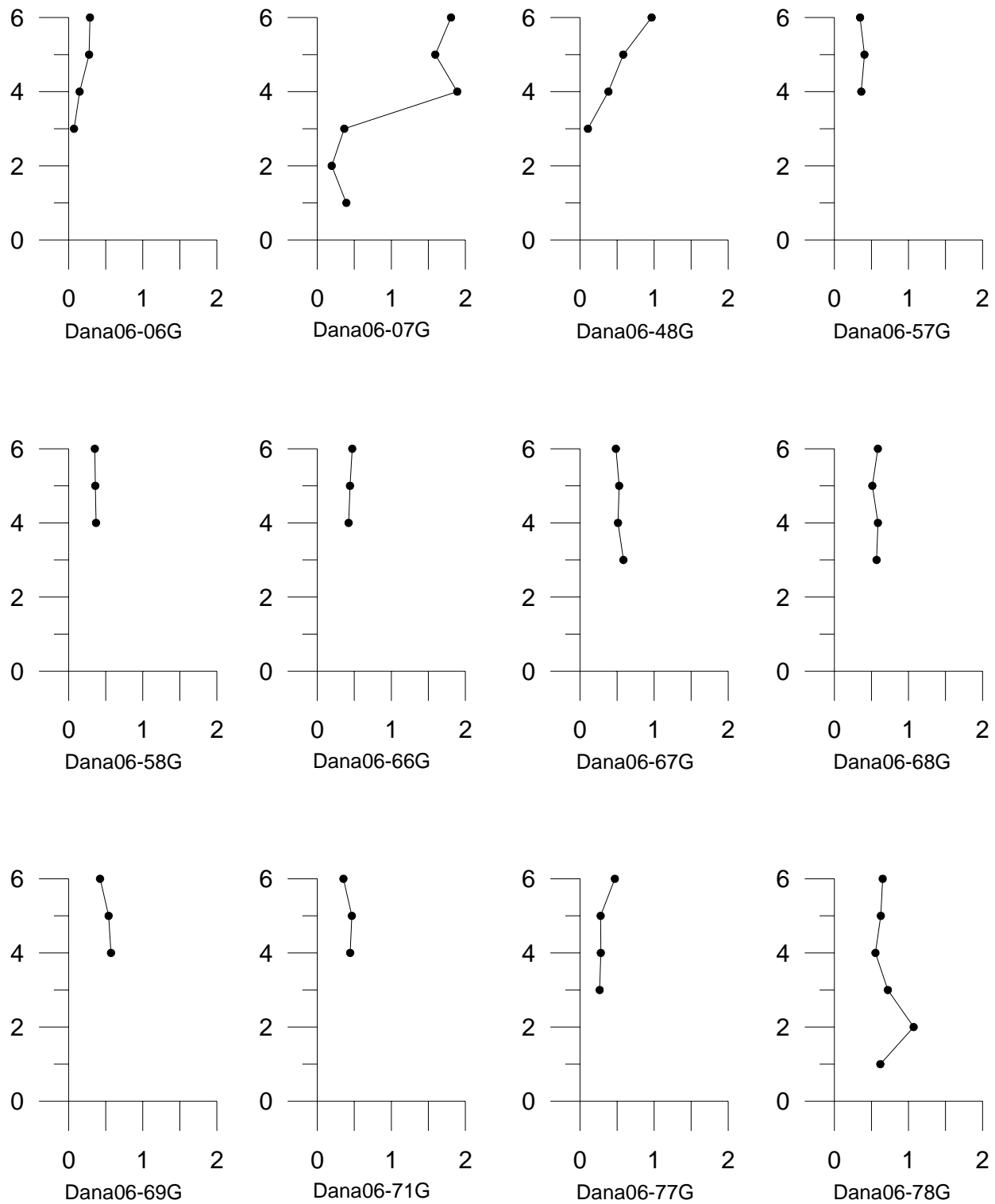


Fig. 3.1.5. Total organic carbon (TOC) profiles through gravity cores from off West Greenland. Only cores from which three or more subsamples were taken are included. Only relative sample depths are shown: "6" is closest to the seabed, lower numbers progressively deeper.

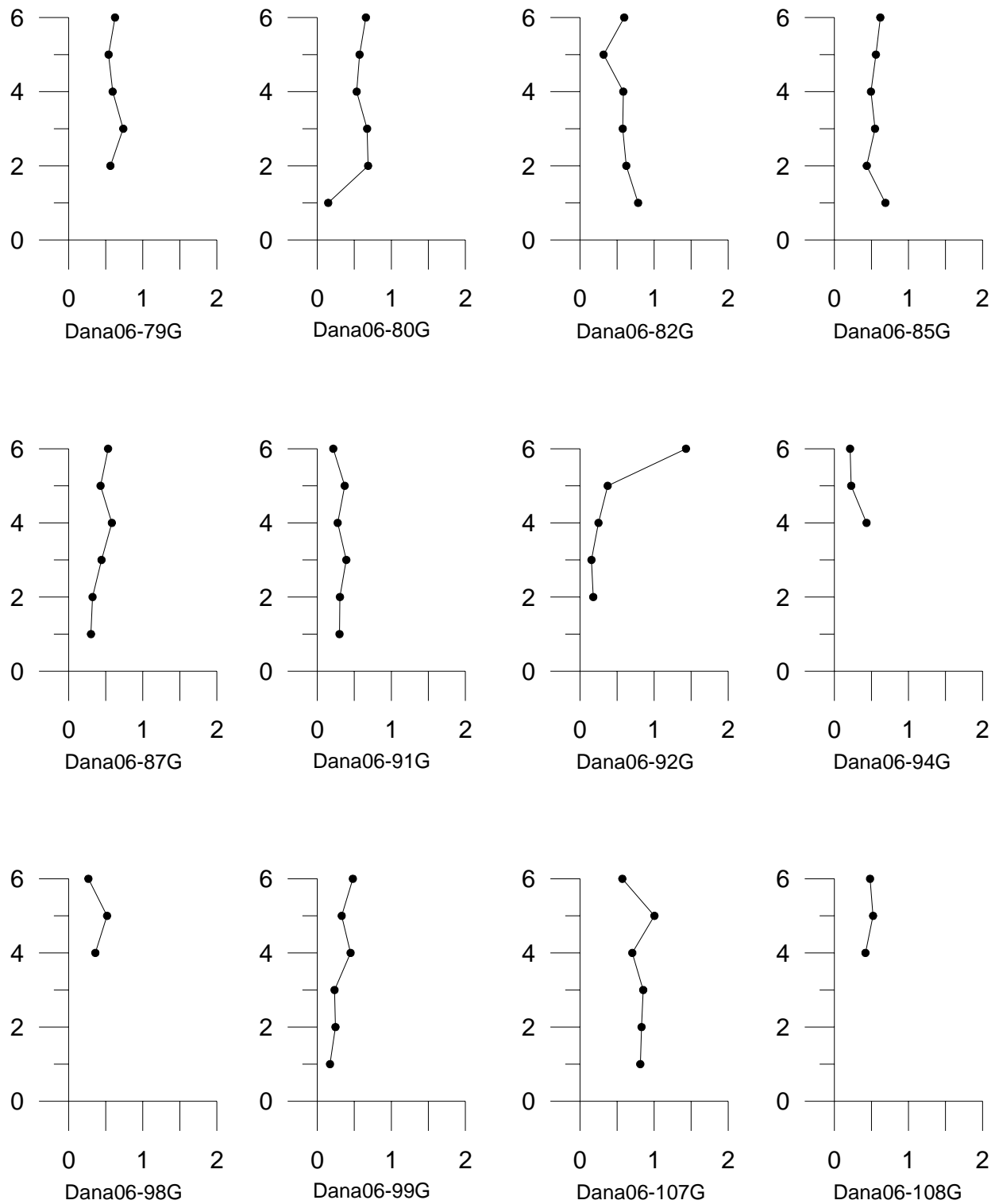


Fig. 3.1.5 continued. Total organic carbon (TOC) profiles through gravity cores from off West Greenland. Only cores from which three or more subsamples were taken are included. Only relative sample depths are shown: "6" is closest to the seabed, lower numbers progressively deeper.

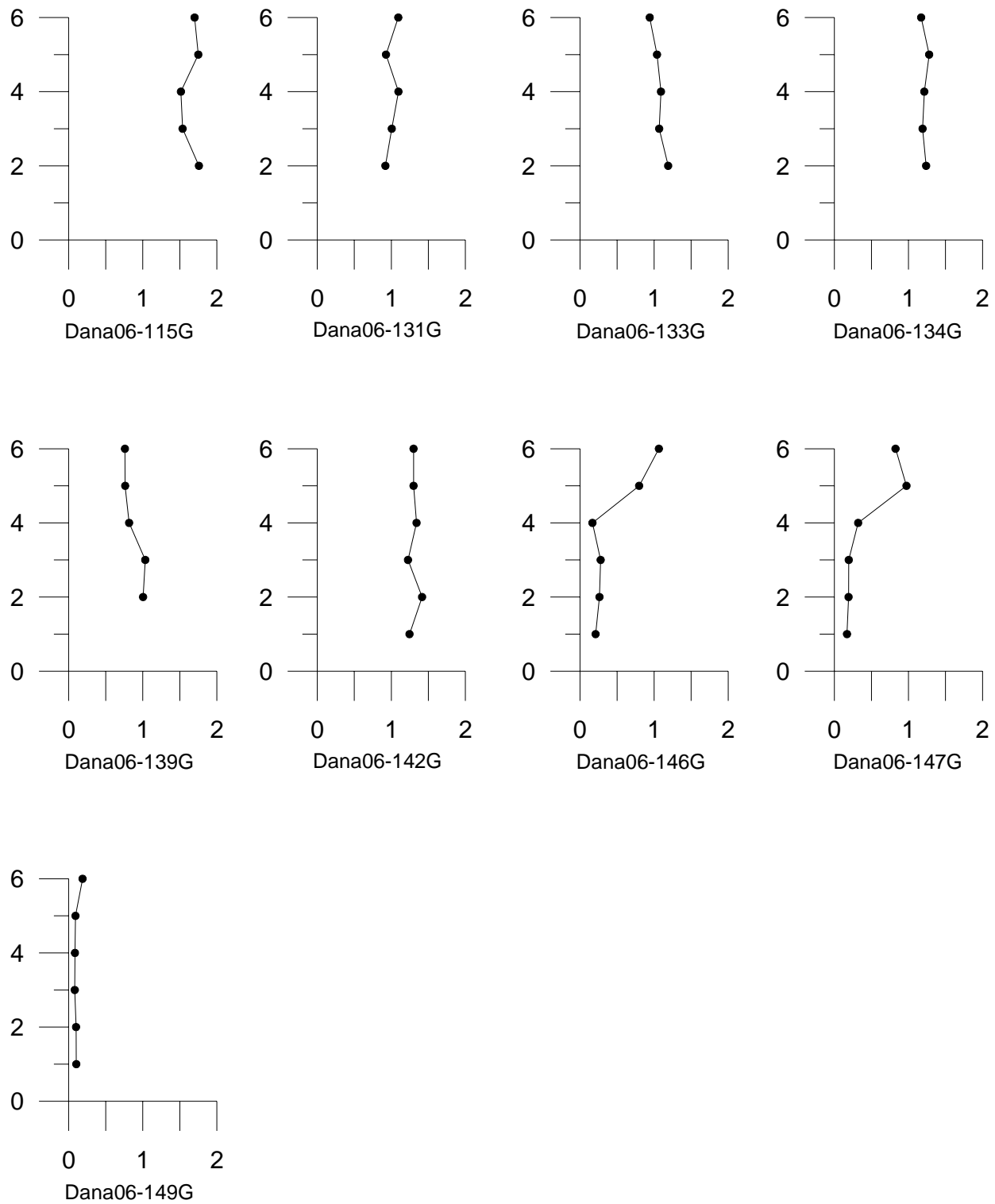


Fig. 3.1.5 *continued*. Total organic carbon (TOC) profiles through gravity cores from off West Greenland. Only cores from which three or more subsamples were taken are included. Only relative sample depths are shown: “6” is closest to the seabed, lower numbers progressively deeper.

Two separate populations seem to be present in the TOC vs. TS plot shown in Fig. 3.1.6. The major population show characteristics very similar to most normal marine shales, whereas a subordinate population, principally defined by the Dana06-115G core shows significantly lower TS/TOC ratio.

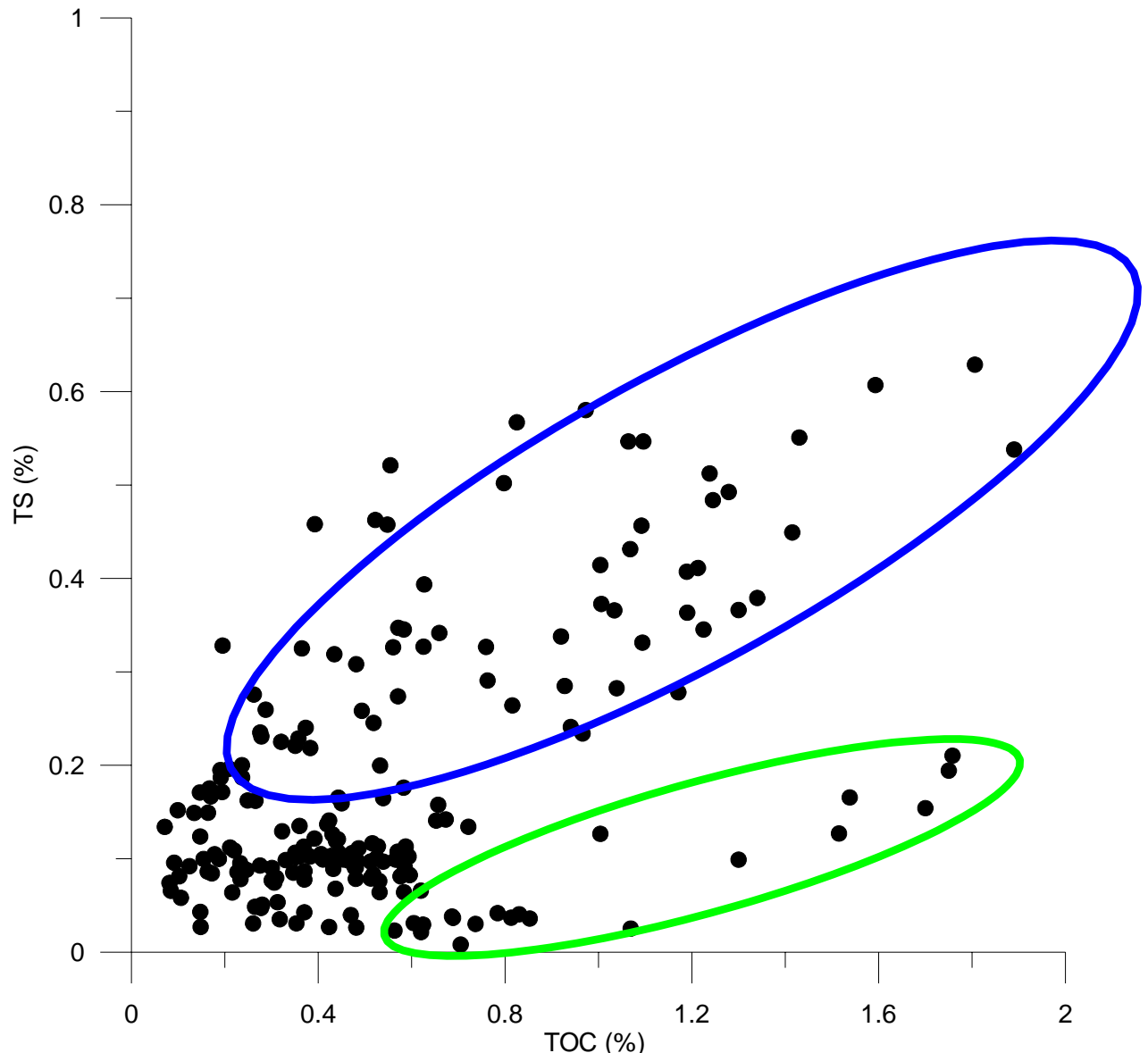


Fig. 3.1.6. TOC vs TS. Note that at levels of TOC>0.6%, two separate populations seem to exist.

Sample	GEUS#	TOC %	TC %	TS %	Tmax (°C)	S1 (mg/g)	S2 (mg/g)	HI
DANA06-06G 1	13990	0,07	0,10	0,13	354	0,00	0,00	
DANA06-06G 2	13991	0,15	0,17	0,12	356	0,00	0,00	
DANA06-06G 3	13992	0,28	0,31	0,24	407	0,00	0,03	11
DANA06-06G 4	13993	0,29	0,32	0,26	394	0,00	0,09	31
DANA06-07G 1	13994	0,39	0,43	0,46	405	0,00	0,27	69
DANA06-07G 2	13995	0,20	0,25	0,33	327	0,00	0,00	
DANA06-07G 3	13996	0,36	0,95	0,33	417	1,00	0,55	151
DANA06-07G 4	13997	1,89	0,32	0,54	416	0,33	4,97	263
DANA06-07G 5	13998	1,59	1,80	0,61	415	0,29	4,03	253
DANA06-07G 6	13999	1,81	1,96	0,63	412	0,32	4,38	243
DANA06-20G 1	14000	0,16	1,47	0,09	423	0,00	0,00	
DANA06-20G 2	14001	0,15	1,06	0,04	429	0,00	0,00	
DANA06-21G 1	14002	0,22	1,54	0,11	422	0,00	0,00	
DANA06-21G 2	14003	0,23	1,46	0,10	422	0,00	0,00	
DANA06-42G 1	14004	0,48	0,66	0,03	421	0,06	0,73	152
DANA06-43G 1	14005	0,60	0,74	0,03	421	0,06	0,86	142
DANA06-44G 1	14006	0,15	0,56	0,17	414	0,00	0,00	
DANA06-44G 2	14007	0,36	0,46	0,23	414	0,00	0,02	6
DANA06-47G 1	14008	0,19	0,45	0,19	407	0,00	0,00	
DANA06-47G 2	14009	0,35	0,46	0,22	417	0,00	0,02	6
DANA06-48G 1	14010	0,11	0,32	0,06	432	0,00	0,00	
DANA06-48G 2	14011	0,38	0,47	0,22	416	0,00	0,04	10
DANA06-48G 3	14012	0,58	0,69	0,35	427	0,01	0,36	62
DANA06-48G 4	14013	0,97	1,09	0,23	427	0,05	1,13	117
DANA06-52G 1	14014	0,49	0,81	0,11	438	0,00	0,01	2
DANA06-52G 2	14015	0,52	0,73	0,12	434	0,00	0,03	6
DANA06-53G 1	14016	0,48	0,66	0,09	438	0,00	0,02	4
DANA06-54G 1	14017	0,48	0,69	0,09	437	0,01	0,04	8
DANA06-54G 2	14018	0,52	0,75	0,10	423	0,01	0,04	8
DANA06-55G 1	14019	0,43	0,63	0,09	448	0,00	0,02	5
DANA06-56G 1	14020	0,38	0,57	0,10	432	0,00	0,00	
DANA06-56G 2	14021	0,48	0,64	0,09	446	0,00	0,04	8
DANA06-57G 1	14022	0,36	0,53	0,11	446	0,00	0,01	3
DANA06-57G 2	14023	0,41	0,56	0,10	441	0,00	0,01	2
DANA06-57G 3	14024	0,35	0,48	0,09	430	0,00	0,00	
DANA06-58G 1	14025	0,37	0,53	0,11	424	0,00	0,01	3
DANA06-58G 2	14026	0,36	0,51	0,10	429	0,00	0,00	
DANA06-58G 3	14027	0,35	0,53	0,10	424	0,00	0,00	
DANA06-59G 1	14028	0,35	0,51	0,11	444	0,00	0,01	3
DANA06-60G 1	14029	0,26	0,39	0,03	444	0,00	0,00	
DANA06-61G 1	14030	0,31	0,47	0,08	434	0,00	0,00	
DANA06-61G 2	14031	0,45	0,60	0,10	432	0,00	0,00	
DANA06-66G 1	14032	0,42	0,72	0,14	429	0,00	0,01	2
DANA06-66G 2	14033	0,44	0,66	0,12	431	0,00	0,03	7
DANA06-66G 3	14034	0,47	0,70	0,11	433	0,00	0,03	6
DANA06-67G 1	14035	0,59	0,81	0,09	441	0,00	0,05	9
DANA06-67G 2	14036	0,51	0,75	0,10	436	0,00	0,02	4
DANA06-67G 3	14037	0,53	0,75	0,11	438	0,00	0,04	8
DANA06-67G 4	14038	0,48	0,69	0,10	438	0,00	0,04	8
DANA06-68G 1	14039	0,57	0,78	0,11	438	0,00	0,04	7
DANA06-68G 2	14040	0,59	0,78	0,11	436	0,00	0,04	7
DANA06-68G 3	14041	0,51	0,72	0,08	435	0,00	0,03	6
DANA06-68G 4	14042	0,59	0,78	0,11	436	0,00	0,03	5
DANA06-69G 1	14043	0,57	0,82	0,11	436	0,00	0,05	9
DANA06-69G 2	14044	0,54	0,78	0,10	446	0,00	0,05	9
DANA06-69G 3	14045	0,42	0,69	0,03	425	0,00	0,08	19
DANA06-70G 1	14046	0,53	0,73	0,08	439	0,00	0,02	4
DANA06-70G 2	14047	0,52	0,71	0,08	441	0,00	0,02	4
DANA06-71G 1	14048	0,44	0,69	0,11	438	0,00	0,01	2
DANA06-71G 2	14049	0,47	0,64	0,10	431	0,00	0,01	2
DANA06-71G 3	14050	0,35	0,55	0,03	423	0,00	0,09	25
DANA06-72G 1	14051	0,43	0,59	0,10	430	0,00	0,03	7
DANA06-72G 2	14052	0,41	0,60	0,10	431	0,00	0,04	10
DANA06-73G 1	14053	0,44	0,64	0,12	426	0,00	0,01	2
DANA06-73G 2	14054	0,41	0,59	0,10	427	0,00	0,01	2
DANA06-75G 1	14055	0,37	0,41	0,04	427	0,00	0,00	
DANA06-76G 1	14056	0,31	0,34	0,05	449	0,00	0,00	
DANA06-77G 1	14057	0,26	0,29	0,05	432	0,00	0,00	
DANA06-77G 2	14058	0,28	0,30	0,05	404	0,00	0,00	
DANA06-77G 3	14059	0,28	0,29	0,05	351	0,00	0,00	
DANA06-77G 4	14060	0,47	0,50	0,04	423	0,00	0,00	
DANA06-78G 1	14061	0,62	0,80	0,02	448	0,00	0,00	
DANA06-78G 2	14062	1,07	1,15	0,03	447	0,00	0,12	11
DANA06-78G 3	14063	0,72	0,88	0,13	426	0,00	0,11	15
DANA06-78G 4	14064	0,55	0,59	0,52	426	0,00	0,11	20
DANA06-78G 5	14065	0,63	0,71	0,39	414	0,00	0,15	24
DANA06-78G 6	14066	0,65	0,89	0,14	429	0,00	0,10	15

Table 3.1

Sample	GEUS#	TOC %	TC %	TS %	Tmax (°C)	S1 (mg/g)	S2 (mg/g)	HI
DANA06-79G 1	14067	0,56	0,65	0,02	447	0,00	0,00	
DANA06-79G 2	14068	0,74	0,81	0,03	442	0,00	0,04	5
DANA06-79G 3	14069	0,59	1,19	0,10	426	0,00	0,04	7
DANA06-79G 4	14070	0,54	0,62	0,16	426	0,00	0,05	9
DANA06-79G 5	14071	0,63	0,72	0,33	453	0,01	0,32	51
DANA06-80G 1	14072	0,15	0,37	0,03	436	0,00	0,00	
DANA06-80G 2	14073	0,69	0,80	0,04	444	0,00	0,03	4
DANA06-80G 3	14074	0,67	0,94	0,14	435	0,00	0,12	18
DANA06-80G 4	14075	0,53	0,62	0,20	425	0,00	0,05	9
DANA06-80G 5	14076	0,57	0,65	0,35	416	0,01	0,18	32
DANA06-80G 6	14077	0,66	0,99	0,16	429	0,00	0,13	20
DANA06-82G 1	14078	0,78	0,94	0,04	444	0,00	0,05	6
DANA06-82G 2	14079	0,62	0,67	0,03	440	0,00	0,00	
DANA06-82G 3	14080	0,58	0,67	0,08	431	0,00	0,05	9
DANA06-82G 4	14081	0,58	0,64	0,06	433	0,00	0,04	7
DANA06-82G 5	14082	0,32	0,38	0,04	348	0,00	0,00	
DANA06-82G 6	14083	0,60	0,85	0,08	429	0,00	0,09	15
DANA06-85G 1	14084	0,69	0,82	0,04	448	0,00	0,02	3
DANA06-85G 2	14085	0,44	0,50	0,07	426	0,00	0,03	7
DANA06-85G 3	14086	0,55	0,60	0,46	418	0,00	0,12	22
DANA06-85G 4	14087	0,49	0,55	0,26	415	0,00	0,10	20
DANA06-85G 5	14088	0,56	0,63	0,33	416	0,00	0,12	21
DANA06-85G 6	14089	0,62	0,86	0,07	426	0,00	0,17	27
DANA06-87G 1	14090	0,30	0,37	0,09	357	0,00	0,00	
DANA06-87G 2	14091	0,32	0,46	0,13	361	0,00	0,00	
DANA06-87G 3	14092	0,44	0,65	0,17	420	0,00	0,04	9
DANA06-87G 4	14093	0,58	0,75	0,18	422	0,00	0,13	22
DANA06-87G 5	14094	0,43	0,47	0,13	403	0,00	0,13	30
DANA06-87G 6	14095	0,53	1,01	0,06	430	0,00	0,06	11
DANA06-91G 1	14096	0,30	0,30	0,08	419	0,00	0,00	
DANA06-91G 2	14097	0,31	0,42	0,07	420	0,00	0,01	3
DANA06-91G 3	14098	0,39	0,80	0,12	423	0,00	0,06	15
DANA06-91G 4	14099	0,28	0,39	0,09	420	0,00	0,01	4
DANA06-91G 5	14100	0,37	1,38	0,09	425	0,00	0,01	3
DANA06-91G 6	14101	0,22	1,61	0,06	425	0,00	0,00	
DANA06-92 1	14102	0,18	0,24	0,10	347	0,00	0,00	
DANA06-92 2	14103	0,15	0,21	0,10	348	0,00	0,00	
DANA06-92 3	14104	0,25	0,28	0,16	363	0,00	0,00	
DANA06-92 4	14105	0,37	0,41	0,24	410	0,00	0,04	11
DANA06-92 5	14106	1,43	1,55	0,55	417	0,19	2,92	204
DANA06-94G 1	14107	0,43	0,69	0,32	428	0,01	0,39	90
DANA06-94G 2	14108	0,23	0,26	0,09	353	0,00	0,00	
DANA06-94G 3	14109	0,21	0,24	0,11	346	0,00	0,00	
DANA06-95G 1	14110	0,13	0,18	0,15	353	0,00	0,00	
DANA06-96G 1	14111	0,12	0,17	0,09	350	0,00	0,00	
DANA06-96G 2	14112	0,24	0,35	0,20	422	0,00	0,04	17
DANA06-97G 1	14113	0,24	0,31	0,19	424	0,00	0,06	25
DANA06-98G 1	14114	0,36	0,39	0,14	360	0,00	0,02	6
DANA06-98G 2	14115	0,52	0,63	0,25	414	0,04	0,69	133
DANA06-98G 3	14116	0,27	0,30	0,16	410	0,00	0,04	15
DANA06-99G 1	14117	0,17	0,25	0,08	430	0,00	0,00	
DANA06-99G 2	14118	0,25	0,32	0,09	418	0,00	0,00	
DANA06-99G 3	14119	0,23	0,32	0,08	423	0,00	0,00	
DANA06-99G 4	14120	0,45	1,23	0,16	421	0,00	0,11	24
DANA06-99G 5	14121	0,33	0,42	0,10	420	0,00	0,03	9
DANA06-99G 6	14122	0,48	1,59	0,08	426	0,00	0,06	12
DANA06-104G 1	14123	0,37	0,55	0,08	419	0,01	0,19	51
DANA06-105G 1	14124	0,16	0,34	0,15	405	0,00	0,00	
DANA06-107G 1	14125	0,81	0,95	0,04	438	0,00	0,04	5
DANA06-107G 2	14126	0,83	1,02	0,04	446	0,00	0,05	6
DANA06-107G 3	14127	0,85	1,03	0,04	442	0,00	0,05	6
DANA06-107G 4	14128	0,70	0,71	0,01	444	0,00	0,00	
DANA06-107G 5	14129	1,00	1,11	0,13	441	0,00	0,12	12
DANA06-107G 6	14130	0,57	0,63	0,27	437	0,00	0,15	26
DANA06-108G 1	14131	0,42	0,47	0,14	418	0,00	0,05	12
DANA06-108G 2	14132	0,52	0,64	0,46	416	0,00	0,11	21
DANA06-108G 3	14133	0,48	0,55	0,31	415	0,00	0,10	21
DANA06-109G 1	14134	0,52	0,72	0,08	433	0,00	0,03	6
DANA06-109G 2	14135	0,57	0,74	0,10	433	0,00	0,02	4
DANA06-115G 1	14136	1,76	2,19	0,21	444	0,01	0,37	21
DANA06-115G 2	14137	1,54	1,93	0,17	447	0,01	0,22	14
DANA06-115G 3	14138	1,52	1,80	0,13	448	0,01	0,17	11
DANA06-115G 4	14139	1,75	2,04	0,19	443	0,02	0,32	18
DANA06-115G 5	14140	1,70	1,95	0,15	444	0,02	0,30	18
DANA06-126G 1	14141	0,66	0,97	0,34	428	0,00	0,11	17
DANA06-131G 1	14142	0,92	1,03	0,34	439	0,01	0,43	47
DANA06-131G 2	14143	1,01	1,09	0,37	423	0,02	0,35	35
DANA06-131G 3	14144	1,10	1,16	0,55	425	0,03	0,51	47
DANA06-131G 4	14145	0,93	0,96	0,28	426	0,01	0,30	32
DANA06-131G 5	14146	1,09	1,17	0,33	427	0,03	0,45	41

Table 3.1 continued

Sample	GEUS#	TOC %	TC %	TS %	Tmax (°C)	S1 (mg/g)	S2 (mg/g)	HI
DANA06-133G 1	14147	1,19	1,23	0,41	426	0,02	0,50	42
DANA06-133G 2	14148	1,07	1,13	0,43	427	0,02	0,47	44
DANA06-133G 3	14149	1,09	1,17	0,46	426	0,02	0,49	45
DANA06-133G 4	14150	1,04	1,17	0,28	426	0,01	0,40	38
DANA06-133G 5	14151	0,94	0,98	0,24	426	0,01	0,26	28
DANA06-134G 1	14152	1,24	1,30	0,51	426	0,02	0,61	49
DANA06-134G 2	14153	1,19	1,22	0,36	426	0,02	0,51	43
DANA06-134G 3	14154	1,21	1,31	0,41	426	0,03	0,59	49
DANA06-134G 4	14155	1,28	1,35	0,49	424	0,03	0,59	46
DANA06-134G 5	14156	1,17	1,26	0,28	427	0,03	0,55	47
DANA06-139G 1	14157	1,00	1,07	0,41	426	0,01	0,30	30
DANA06-139G 2	14158	1,03	1,15	0,37	430	0,01	0,44	43
DANA06-139G 3	14159	0,82	0,81	0,26	428	0,00	0,15	18
DANA06-139G 4	14160	0,76	0,78	0,29	422	0,00	0,16	21
DANA06-139G 5	14161	0,76	0,76	0,33	418	0,00	0,15	20
DANA06-142G 1	14162	1,25	1,30	0,48	429	0,03	0,78	63
DANA06-142G 2	14163	1,42	1,50	0,45	427	0,05	0,75	53
DANA06-142G 3	14164	1,23	1,37	0,35	427	0,04	0,81	66
DANA06-142G 4	14165	1,34	1,47	0,38	427	0,03	0,85	63
DANA06-142G 5	14166	1,30	1,45	0,37	428	0,04	0,72	55
DANA06-142G 6	14167	1,30	1,36	0,10	404	0,03	0,50	38
DANA06-146G 1	14168	0,21	0,23	0,20	420	0,00	0,00	
DANA06-146G 2	14169	0,26	0,29	0,28	411	0,00	0,03	11
DANA06-146G 3	14170	0,28	0,29	0,23	417	0,00	0,03	11
DANA06-146G 4	14171	0,17	0,21	0,18	339	0,00	0,00	
DANA06-146G 5	14172	0,80	0,91	0,50	426	0,02	0,67	84
DANA06-146G 6	14173	1,06	1,17	0,55	421	0,05	1,12	105
DANA06-147G 1	14174	0,17	0,22	0,17	454	0,00	0,01	6
DANA06-147G 2	14175	0,19	0,21	0,19	348	0,00	0,00	
DANA06-147G 3	14176	0,19	0,20	0,17	367	0,00	0,00	
DANA06-147G 4	14177	0,32	0,34	0,23	421	0,00	0,04	12
DANA06-147G 5	14178	0,97	1,08	0,58	425	0,03	0,87	89
DANA06-147G 6	14179	0,83	0,94	0,57	421	0,04	0,79	96
DANA06-149G 1	14180	0,10	0,19	0,08	344	0,00	0,00	
DANA06-149G 2	14181	0,10	0,11	0,15	351	0,00	0,00	
DANA06-149G 3	14182	0,08	0,13	0,07	454	0,00	0,00	
DANA06-149G 4	14183	0,08	0,08	0,07	349	0,00	0,00	
DANA06-149G 5	14184	0,09	0,13	0,10	338	0,00	0,00	
DANA06-149G 6	14185	0,19	0,24	0,10	414	0,00	0,04	21

Table 3.1 continued

3.2 Solvent extracts analysis (GC and GC-MS)

Total extract recoveries are low, 2.0 to 12.4 milligram, and extracts consist predominantly of heteroatomic compounds. Total hydrocarbon recoveries are between 0.1 and 3.6 milligram, typically <1 milligram.

Individual Gas Chromatograms and key Ion Fragmentograms from GC-MS and GC-MSMS are shown in Appendix 1.

Gas chromatograms generally show rather irregular distributions of normal alkanes, typically comprising a broad background, approximately ranging from nC₁₅ to nC₄₀, superimposed by variable proportions strongly odd-number dominated C₂₃-C₃₃ n-alkanes. Hence, depending on the proportion of heavy material, the distributions may be either

bimodal or heavy-end skewed unimodal. A few samples show very high proportions of heavy n-alkanes: Dana06-07G-4, Dana06-07G-5, Dana06-07G-6, and Dana06-146G-6.

Note that the necessary use of total hydrocarbon fractions rather than pure saturated fractions for gas chromatography has a negative impact on the data quality.

Due to low extract recoveries and the use of total hydrocarbon fractions, only tandem GC-MS-MS data have been used, since interference from aromatic compounds prevented the use of GC-MS_{SIM} technique.

All data show the same overall character. The hopane distributions clearly show a strong predominance of thermally labile compounds such as $\beta\beta$ -hopanes, and sometimes even hopenes. Homohopane isomerisation ratios are far from equilibrium, and although a few samples, notably Dana06-91G-6 and to a lesser extent also Dana06-21G-1 and Dana06-73G-3, show somewhat higher isomerisation ratios, none of the samples analysed even approaches a level of thermal maturity near the onset of petroleum generation. 28,30-bisnorhopane is common in most samples, whereas extended 28-norhopanes seem to be absent. Sterane data are also dominated by thermally unidentified labile moieties, often to an extent that renders the data useless for standard purposes.

3.3 Headspace gas analysis

The results of headspace gas analyses are listed in table 3.3.

With few exceptions the headspace gas composition is dominated by CO₂ that typically constitute more than 95% of the total headspace gases.

A number of gravity cores show strong trends in gas composition with depth below the sediment-water interface. The trends are defined by strongly decreasing CO₂ concentrations and increasing CH₄ concentrations with depth. These include the Dana06-07G, Dana06-131G, Dana06-133G, Dana06-134G and Dana06-142G gravity cores that also show remarkably dry gas composition, i.e. CH₄ is essentially the only hydrocarbon gas present – all higher carbon number gases are lacking.

In general the concentration of hydrocarbon gases is very variable, covering three orders of magnitude from a few hundred ppm to more than 100000 ppm. Moreover, the gases are mostly very dry, only one single sample yield hydrocarbon gases heavier than propane, and none of the samples contain pentanes.

Methane $\delta^{13}\text{C}$ values are strongly variable, approximately covering the range -30‰ to -85‰. This range comprises the $\delta^{13}\text{C}$ values typical of both bacterial and thermogenic methane. A standard Bernard-type plot of methane $\delta^{13}\text{C}$ vs. $\text{C}_1/(\text{C}_2+\text{C}_3)$ with the standard interpretation of bacterial and thermogenic gases indicated is shown in Fig. 3.3.1. (Bernard et al., 1978). Bernard type plots for individual gravity cores with four or more subsamples are shown in Figs 3.3.2 through 3.3.7.

A closer scrutiny of the data shows that several gravity cores show significant variation in isotopic composition and, to a lesser extent, gas wetness from base to top. Hence, in several cores the isotopic composition of the methane becomes less depleted from the base of the core to the top (Fig. 3.3.8). This pattern is paralleled by the gas wetness that seems to increase from the base of the cores towards the top (Fig. 3.3.9). In addition, several cores show strongly decreasing concentrations of methane from base to top (Fig. 3.3.10).

Core	GEUS #	C1%	C2%	C3%	iC4%	nC4%	CO2%	Sum C1-C5	Wetness	ppm	C1 δ¹³C	C1/(C2+C3)
06G-1	13990	0,92	0,1	0	0	0,07	98,9	1,1	15,7	1612	-33,5	9,2
06G-2	13991	1,1	0,04	0			98,9	1,1	3,5	1798	-35,1	27,5
06G-3	13992	0,98	0,03	0			99	1	3,2	2208	-37,5	32,7
06G-4	13993	2,2	0,04	0,02			97,7	2,3	2,5	1453	-50,5	36,7
07G-1	13994	61,7	0,01	0			38,3	61,7	0,02	15227	-79,6	6170,0
07G-2	13995	7,7	0,03	0			92,3	7,7	0,34	4380	-64,8	256,7
07G-3	13996	5,1	0,03	0,01			94,9	5,1	0,74	3684	-64,4	127,5
07G-4	13997	0,6	0,03	0,02			99,4	0,65	8,3	4189	-42,1	12,0
07G-5	13998	2,5	0,02	0,01			97,4	2,6	1,2	4188	-60,6	83,3
07G-6	13999	2,8	0,02	0,01			97,2	2,8	1,2	4230	-63,5	93,3
20G-1	14000	3,7	0,04	0,01			96,3	3,7	1,4	2172	-48,0	74,0
20G-2	14001	1,2	0,08	0,05			98,6	1,4	9,7	1370	-38,1	9,2
21G-1	14002	1,4	0,07	0,03			98,5	1,5	7,2	1081	-42,1	14,0
21G-2	14003	1	0,04	0,01			98,9	1,1	4,9	1671	-43,9	20,0
42G-1	14004	6,7	0,04	0,02			93,2	6,8	0,85	2079	-48,6	111,7
43G-1	14005	1,6	0,06	0,02			98,3	1,7	4,6	1450	-45,2	20,0
44G-1	14006	1	0,06	0,03			98,9	1,1	8,2	995	-38,1	11,1
44G-2	14007	0,89	0,07	0,03			99	0,98	9,7	1167	-43,3	8,9
47G-1	14008	0,71	0,04	0,01			99,2	0,76	7	1361	-43,5	14,2
47G-2	14009	1,1	0,05	0,01			98,8	1,2	5,9	1715	-43,6	18,3
48G-1	14010	0,76	0,06	0			99,2	0,82	7,5	1551	-40,8	12,7
48G-2	14011	0,44	0,03	0,01			99,5	0,48	6,8	2374	-38,1	11,0
48G-3	14012	1,2	0,08	0,03			98,7	1,3	8,2	1096	-43,0	10,9
48G-4	14013	3,2	0,06	0,03			96,8	3,2	2,6	1376	-41,5	35,6
52G-1	14014	0,88	0,04	0,01			99,1	0,93	4,9	1546	-38,5	17,6
52G-2	14015	1,2	0,1	0,02			98,7	1,3	9,4	900	-43,8	10,0
53G-1	14016	0,75	0,04	0			99,2	0,78	5	1020	-42,1	18,8
54G-1	14017	0,97	0,06	0,02			99	1	7,2	1209	-42,0	12,1
54G-2	14018	1	0,07	0,02			98,9	1,1	8,2	1111	-43,2	11,1
55G-1	14019	1	0,03	0,01			98,9	1,1	3,6	1547	-44,4	25,0
56G-1	14020	1,3	0,06	0,02			98,6	1,4	5,8	927	-42,5	16,3
56G-2	14021	1,1	0,04	0,01			98,9	1,1	4,1	1549	-43,5	22,0
57G-1	14022	1,4	0,06	0,01			98,5	1,5	5,3	1232	-42,7	20,0
57G-2	14023	1,8	0,05	0,01			98,2	1,8	3,2	1263	-44,7	30,0
57G-3	14024	1,5	0,08	0,02			98,4	1,6	6,7	793	-39,1	15,0
58G-1	14025	0,88	0,06	0,05			99	1	11,2	1481	-37,6	8,0
58G-2	14026	0,79	0,02	0,01			99,2	0,82	3,7	2316	-26,3	
58G-3	14027	0,8	0,03	0			99,2	0,83	3,9	1742	-43,6	26,7
59G-1	14028	0,65	0,03	0			99,3	0,68	4,2	1493	-43,6	21,7
60G-1	14029	0,94	0,07	0			99	1	6,7	1205	-40,8	13,4
61G-1	14030	0,81	0,05	0,01			99,1	0,86	6,3	1483	-41,6	13,5
61G-2	14031	0,83	0,04	0			99,1	0,88	5	1093	-40,0	20,8
66G-1	14032	0,69	0,01	0			99,3	0,71	1,8	3642	-51,1	69,0
66G-2	14033	0,64	0,03	0,01			99,3	0,68	6,4	1941	-36,2	16,0
66G-3	14034	1,2	0,11	0,06			98,6	1,4	12,5	1806	-42,5	7,1
67G-1	14035	0,54	0,03	0,01			99,4	0,59	7,4	2563	-43,8	13,5
67G-2	14036	0,55	0,02	0,01			99,4	0,58	4,6	2575	-34,5	18,3
67G-3	14037	0,69	0,04	0,02			99,2	0,75	7,5	1835	-36,1	11,5
67G-4	14038	0,87	0,05	0,01			99,1	0,94	6,6	1362	-38,6	14,5
68G-1	14039	1,1	0,04	0,01			98,8	1,2	4,3	1601	-38,7	22,0
68G-2	14040	0,88	0,03	0,02			99,1	0,92	4,7	1549	-36,9	17,6
68G-3	14041	1,1	0,04	0,02			98,8	1,2	4,5	1626	-41,2	18,3
68G-4	14042	0,78	0,04	0,01			99,2	0,83	6,6	1413	-39,7	15,6
69G-1	14043	0,6	0,02	0,01			99,4	0,63	4,9	2106	-41,4	20,0
69G-2	14044	0,85	0,05	0,02			99,1	0,92	7,7	1476	-43,0	12,1
69G-3	14045	4,2	0,09	0,03			95,7	4,3	2,7	1445	-49,5	35,0
70G-1	14046	0,85	0,04	0,01			99,1	0,9	6,1	1325	-43,5	17,0
70G-2	14047	2,2	0,05	0,01			97,7	2,3	2,6	1125	-47,0	36,7
71G-1	14048	0,67	0,02	0			99,3	0,7	3,3	2095	-44,3	33,5
71G-2	14049	0,8	0,03	0,01			99,2	0,84	5	2109	-43,0	20,0
71G-3	14050	4,8	0,05	0,02			95,2	4,8	1,4	1465	-54,0	68,6
72G-1	14051	0,56	0,02	0			99,4	0,58	3,2	2487	-45,1	28,0
72G-2	14052	1	0,05	0,02			98,9	1,1	6,2	1105	-44,7	14,3
73G-1	14053	0,78	0,03	0,01			99,2	0,81	4,7	1377	-43,6	19,5
73G-2	14054	2,7	0,04	0,01			97,2	2,8	1,7	1225	-38,1	54,0
75G-1	14055	6	0,07	0,01			93,9	6,1	1,4	1077		75,0
76G-1	14056	5,9	0,04	0,02			94	6	0,97	1112		98,3
77G-1	14057	2,5	0,05	0,02			97,4	2,6	2,4	834	-47,8	35,7
77G-2	14058	1,7	0,1	0,04			98,1	1,9	7,8	827		12,1
77G-3	14059	25,4	0,06	0,02			74,5	25,5	0,31	1696	-46,5	317,5
77G-4	14060	3,9	0,04	0,01			96,1	3,9	1,2	997	-52,3	78,0
78G-1	14061	1,2	0,02	0,01			98,8	1,2	2	2698	-41,8	40,0
78G-2	14062	1,9	0,03	0			98,1	1,9	1,5	1613	-50,2	63,3
78G-3	14063	1,1	0,01	0			98,9	1,1	1,1	3364	-46,7	110,0
78G-4	14064	1,3	0,03	0,01			98,6	1,4	3,5	1652	-34,9	32,5
78G-5	14065	2	0,03	0,01			97,9	2,1	1,6	1854	-44,6	50,0
78G-6	14066	5,1	0,02	0,01			94,9	5,1	0,49	2387	-53,3	170,0

Table 3.3

Core	GEUS #	C1%	C2%	C3%	iC4%	nC4%	CO2%	Sum C1-C5	Wetness	ppm	C1 δ¹³C	C1/(C2+C3)
79G-1	14067	2,7	0,09	0,04			97,2	2,8	4,5	685	-40,3	20,8
79G-2	14068	1,6	0,03	0,01			98,3	1,7	2,5	1552	-47,4	40,0
79G-3	14069	4,1	0,02	0,01			95,9	4,1	0,74	2058	-52,1	136,7
79G-4	14070	1,6	0,04	0,01			98,3	1,7	2,6	1587	-47,3	32,0
79G-5	14071	1,2	0,02	0,01			98,8	1,2	2,4	2358	-45,9	40,0
80G-1	14072	0,57	0,04	0,02			99,4	0,64	10,1	2237	-39,5	9,5
80G-2	14073	0,89	0,03	0			99,1	0,92	3,6	1813	-45,8	29,7
80G-3	14074	1	0,02	0			99	1	2,3	1770	-41,8	50,0
80G-4	14075	1,2	0,03	0,01			98,8	1,2	3,5	1390	-39,3	30,0
80G-5	14076	1,1	0,03	0,01			98,8	1,2	2,8	1605	-44,7	27,5
80G-6	14077	1,1	0,05	0,01			98,9	1,1	5,3	1637	-38,4	18,3
82G-1	14078	0,52	0,02	0			99,4	0,55	5	3169	-45,4	26,0
82G-2	14079	0,43	0,02	0,01			99,5	0,46	6,9	2739	-32,2	14,3
82G-3	14080	0,97	0,04	0,01			99	1	5,1	1682	-33,8	19,4
82G-4	14081	0,99	0,03	0,01			99	1	4,4	1200	-45,3	24,8
82G-5	14082	0,69	0,03	0,01			99,3	0,73	5,4	2006	-38,5	17,3
82G-6	14083	0,85	0,04	0,02			99,1	0,9	6,1	1767	-43,7	14,2
85G-1	14084	1,6	0,02	0,01			98,4	1,6	2	1821	-42,1	53,3
85G-2	14085	0,62	0,03	0,01			99,3	0,66	6	1712	-43,9	15,5
85G-3	14086	0,79	0,02	0,01			99,2	0,82	3,4	1910	-45,0	26,3
85G-4	14087	0,58	0,02	0,01			99,4	0,62	5,1	1928	-43,4	19,3
85G-5	14088	1	0,02	0			99	1	2,2	1846		50,0
85G-6	14089	6,7	0,04	0,01			93,2	6,8	0,84	1690	-46,0	134,0
87G-1	14090	0,4	0,01	0			99,6	0,41	2	6715	-42,6	40,0
87G-2	14091	0,31	0,01	0			99,7	0,32	2,7	6096		31,0
87G-3	14092	0,37	0,02	0			99,6	0,39	4,4	4496	-40,4	18,5
87G-4	14093	0,42	0,01	0,01			99,6	0,44	4,3	4781	-39,2	21,0
87G-5	14094	0,33	0,01	0,01			99,7	0,35	4,3	4569		16,5
87G-6	14095	0,61	0,02	0,01			99,4	0,64	3,7	2898	-39,5	20,3
91G-1	14096	0,37	0,02	0			99,6	0,39	5,1	3748	-44,0	18,5
91G-2	14097	0,3	0,01	0			99,7	0,31	3,1	5400	-42,5	30,0
91G-3	14098	0,43	0,02	0,01			99,5	0,45	5,7	3781	-44,0	14,3
91G-4	14099	0,72	0,02	0,01			99,3	0,75	4,4	3214	-35,5	24,0
91G-5	14100	0,63	0,02	0,01			99,4	0,65	3,4	3372	-44,9	21,0
91G-6	14101	1	0,02	0,01			99	1	2,5	3255	-49,8	33,3
92G-1	14102	1,1	0,02	0,01			98,9	1,1	2,2	2372	-36,1	36,7
92G-2	14103	0,76	0,03	0,01			99,2	0,8	4,7	2000	-37,1	19,0
92G-3	14104	1	0,04	0,01			98,9	1,1	4,5	1589	-43,9	20,0
92G-4	14105	1,4	0,02	0			98,6	1,4	1,6	2049	-47,1	70,0
92G-5	14106	5,9	0,08	0,06			93,9	6,1	2,3	1761	-54,2	42,1
94G-1	14107	1,7	0,02	0,01			98,3	1,7	2,1	3248	-50,3	56,7
94G-2	14108	1,3	0,03	0,01			98,7	1,3	2,9	1494	-46,2	32,5
94G-3	14109	0,87	0,04	0,02			99,1	0,93	6,6	1564	-43,7	14,5
95G-1	14110	1,9	0,05	0,02			98	2	3,9	956	-44,8	27,1
96G-1	14111	1,4	0,08	0,03			98,5	1,5	7,6	765	-41,9	12,7
96G-2	14112	1,8	0,07	0,04			98	2	5,5	785	-38,5	16,4
97G-1	14113	1,8	0,03	0,02			98,1	1,9	2,6	1610	-37,7	36,0
98G-1	14114	0,73	0,01	0,01			99,2	0,75	2,3	2987	-40,4	36,5
98G-2	14115	3,3	0,02	0,01			96,6	3,4	1	2879	-59,9	110,0
98G-3	14116	1,7	0,03	0,01			98,3	1,7	2,1	1853	-49,2	42,5
99G-1	14117	0,49	0,01	0,01			99,5	0,51	4	3500	-37,8	24,5
99G-2	14118	0,46	0,01	0,01			99,5	0,48	3,7	4151	-36,3	23,0
99G-3	14119	0,49	0,01	0,01			99,5	0,51	3,9	3788	-38,7	24,5
99G-4	14120	0,53	0,02	0,01			99,4	0,55	4	2999	-44,9	17,7
99G-5	14121	0,61	0,02	0,01			99,4	0,65	5	2733	-45,7	20,3
99G-6	14122	0,68	0,03	0,01			99,3	0,72	5,4	2267	-45,0	17,0
104G-1	14123	3,8	0,11	0,05			96	4	4	1033	-47,1	23,8
105G-1	14124	0,73	0,03	0,01			99,2	0,77	5,3	1507		18,3
107G-1	14125	2	0,03	0,01			98	2	2,4	1591	-48,1	50,0
107G-2	14126	1,5	0,04	0			98,4	1,6	2,5	1858	-38,3	37,5
107G-3	14127	1,7	0,02	0,01			98,3	1,7	1,6	2208	-48,1	56,7
107G-4	14128	0,82	0,03	0,01			99,1	0,85	4	2462	-43,9	20,5
107G-5	14129	1	0,04	0			98,9	1,1	3,5	1492	-38,3	25,0
107G-6	14130	0,93	0,05	0			99	0,98	4,9	1127		18,6
108G-1	14131	1,2	0,02	0			98,8	1,2	1,7	1793	-41,3	60,0
108G-2	14132	1,4	0,02	0,01			98,6	1,4	1,7	1996	-39,9	46,7
108G-3	14133	2,1	0,02	0			97,9	2,1	0,81	2089	-48,1	105,0
109G-1	14134	0,83	0,03	0,01			99,1	0,86	4,2	1879	-41,1	20,8
109G-2	14135	0,98	0,04	0,01			99	1	4,8	1192	-44,7	19,6
115G-1	14136	3,7	0,08	0			96,2	3,8	2,2	1163	-42,5	46,3
115G-2	14137	2,1	0,06	0,01			97,8	2,2	3,3	1087	-40,9	30,0
115G-3	14138	2,7	0,06	0			97,2	2,8	2,3	882	-42,5	45,0
115G-4	14139	4,7	0,05	0,92			94,3	5,7	17,1	1408	-46,3	4,8
115G-5	14140	1,2	0,03	0,17			98,6	1,4	14	1558	-40,3	6,0
126G-1	14141	1,2	0,05	0,03			98,7	1,3	5,7	1104		15,0
131G-1	14142	92,4	0	0			7,6	92,4	0	179658	-82,1	
131G-2	14143	92,6	0	0			7,4	92,6	0	178737	-86,4	
131G-3	14144	89,3	0	0			10,7	89,3	0	136390	-88,8	
131G-4	14145	78,4	0	0			21,6	78,4	0	55402	-81,6	
131G-5	14146	10,5	0	0			89,5	10,5	0,02	11731		
133G-1	14147	95,6	0	0			4,4	95,6	0	379762	-87,0	
133G-2	14148	92,3	0	0			7,7	92,3	0	189129	-76,3	
133G-3	14149	86,4	0	0			13,5	86,5	0	87250	-84,7	
133G-4	14150	66,7	0	0			33,3	66,7	0	31897	-81,6	
133G-5	14151	48,8	0	0			51,2	48,8	0	16974	-48,6	

Table 3.3 continued

Core	GEUS #	C1%	C2%	C3%	iC4%	nC4%	CO2%	Sum C1-C5	Wetness	ppm	C1 $\delta^{13}\text{C}$	C1/(C2+C3)
134G-1	14152	93,5	0	0			6,5	93,5	0	190586	-84,6	
134G-2	14153	92,6	0	0			7,4	92,6	0	151326	-82,0	
134G-3	14154	87,7	0	0			12,3	87,7	0	94788	-81,0	
134G-4	14155	60,3	0	0			39,7	60,3	0	23625	-84,2	
134G-5	14156	8,8	0	0			91,2	8,8	0,07	9868	-64,9	
139G-1	14157	4,2	0,02	0,01			95,7	4,3	0,65	2261	-31,1	140,0
139G-2	14158	2	0,02	0,01			98	2	1,4	2489	-57,1	66,7
139G-3	14159	1,5	0,01	0,01			98,5	1,5	1,4	2460	-51,3	75,0
139G-4	14160	1,2	0,02	0,01			98,8	1,2	2,4	2057	-49,8	40,0
139G-5	14161	6,6	0,03	0,02			93,3	6,7	0,68	1616	-52,7	132,0
142G-1	14162	92,1	0	0			7,9	92,1	0	161969	-80,9	
142G-2	14163	77	0	0			23	77	0	47208	-75,6	
142G-3	14164	74,4	0	0			25,6	74,4	0	37257	-81,6	
142G-4	14165	12,4	0	0			87,6	12,4	0,04	12270	-66,6	
142G-5	14166	4,2	0	0			95,8	4,2	0,12	9792	-69,9	
142G-6	14167	44,2	0,01	0,01			55,8	44,2	0,04	4140	-64,1	2210,0
146G-1	14168	6,1	0,01	0,01			93,9	6,1	0,25	2808	-67,6	305,0
146G-2	14169	2,6	0,01	0,01			97,4	2,6	0,8	3392	-53,4	130,0
146G-3	14170	1,5	0,02	0,01			98,5	1,5	1,6	2476	-50,9	50,0
146G-4	14171	1,1	0,02	0			98,8	1,2	1,4	1861	-40,5	55,0
146G-5	14172	1,6	0,05	0,02			98,4	1,6	4,2	1880	-49,5	22,9
146G-6	14173	1,3	0,05	0,03			98,6	1,4	5,9	1159	-37,7	16,3
147G-1	14174	2,3	0,02	0,01			97,7	2,3	1,1	2197	-45,1	76,7
147G-2	14175	2,5	0,01	0			97,5	2,5	0,49	2473	-55,1	250,0
147G-3	14176	1,5	0,01	0,01			98,5	1,5	1,3	2954	-39,3	75,0
147G-4	14177	1,6	0,02	0,01			98,3	1,7	2,1	1975		53,3
147G-5	14178	2	0,04	0,02			98	2	3,2	2128		33,3
147G-6	14179	3,5	0,04	0,01			96,4	3,6	1,5	1525		70,0
149G-1	14180	0,71	0,01	0			99,3	0,72	1	3145	-40,8	71,0
149G-2	14181	0,52	0,01	0			99,5	0,53	1,2	3872	-37,8	52,0
149G-3	14182	0,87	0,01	0,01			99,1	0,89	2,5	2240	-43,2	43,5
149G-4	14183	0,46	0,01	0			99,5	0,46	1,5	2121	-42,3	46,0
149G-5	14184	0,68	0,02	0,01			99,3	0,71	4,2	2761		22,7
149G-6	14185	0,69	0,01	0			99,3	0,7	1,2	2841	-32,4	69,0
63R-1	14186	0,73	0,01	0			99,3	0,74	0,91	420		73,0
143R-1	14187	6,6	0,01	0			93,4	6,6	0,12	5756		660,0

Table 3.3 continued

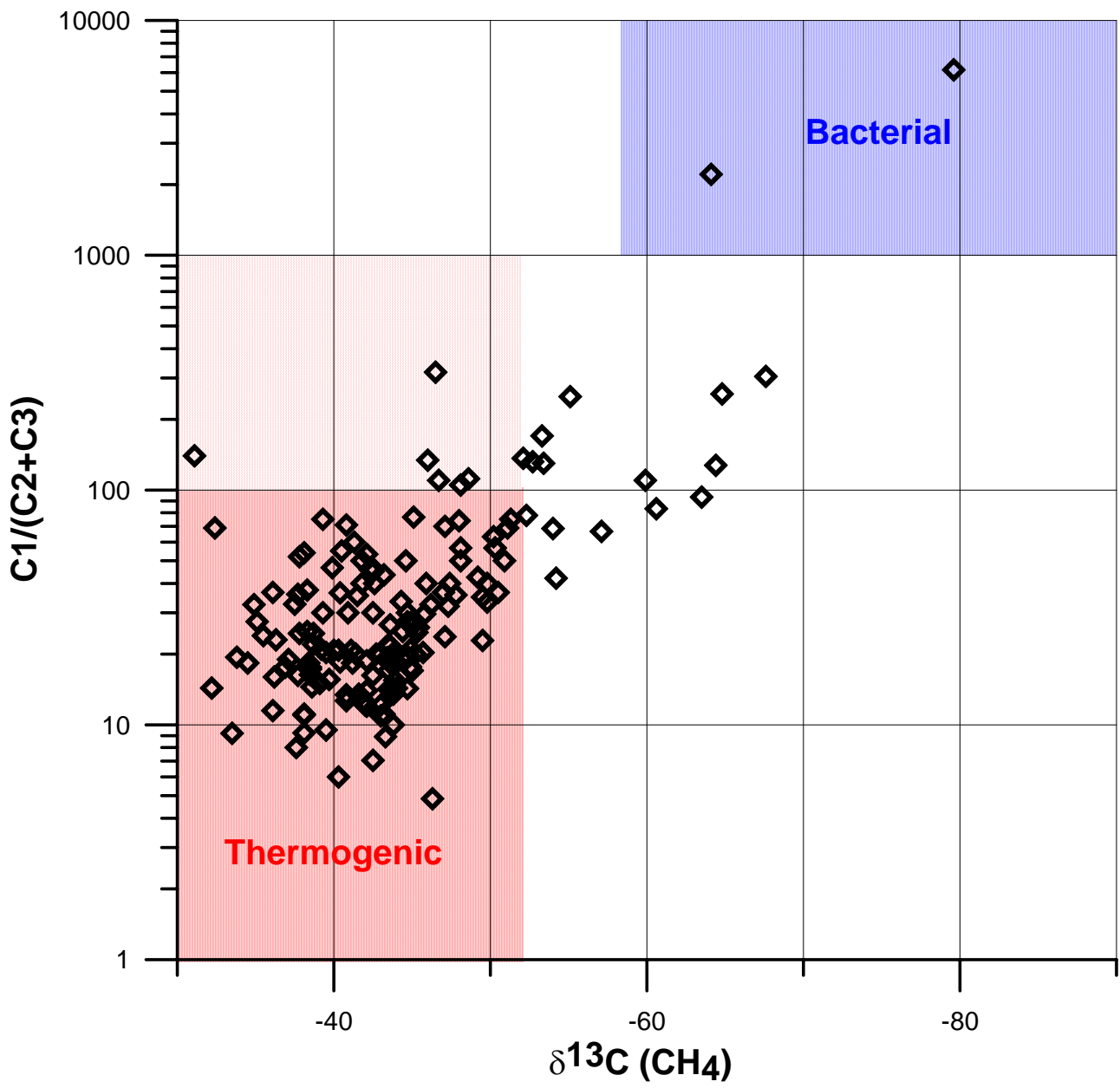


Fig. 3.3.1. Relationship between carbon isotopes of methane and gas composition in a Bernard-type plot, all samples included (Bernard et al. 1978).

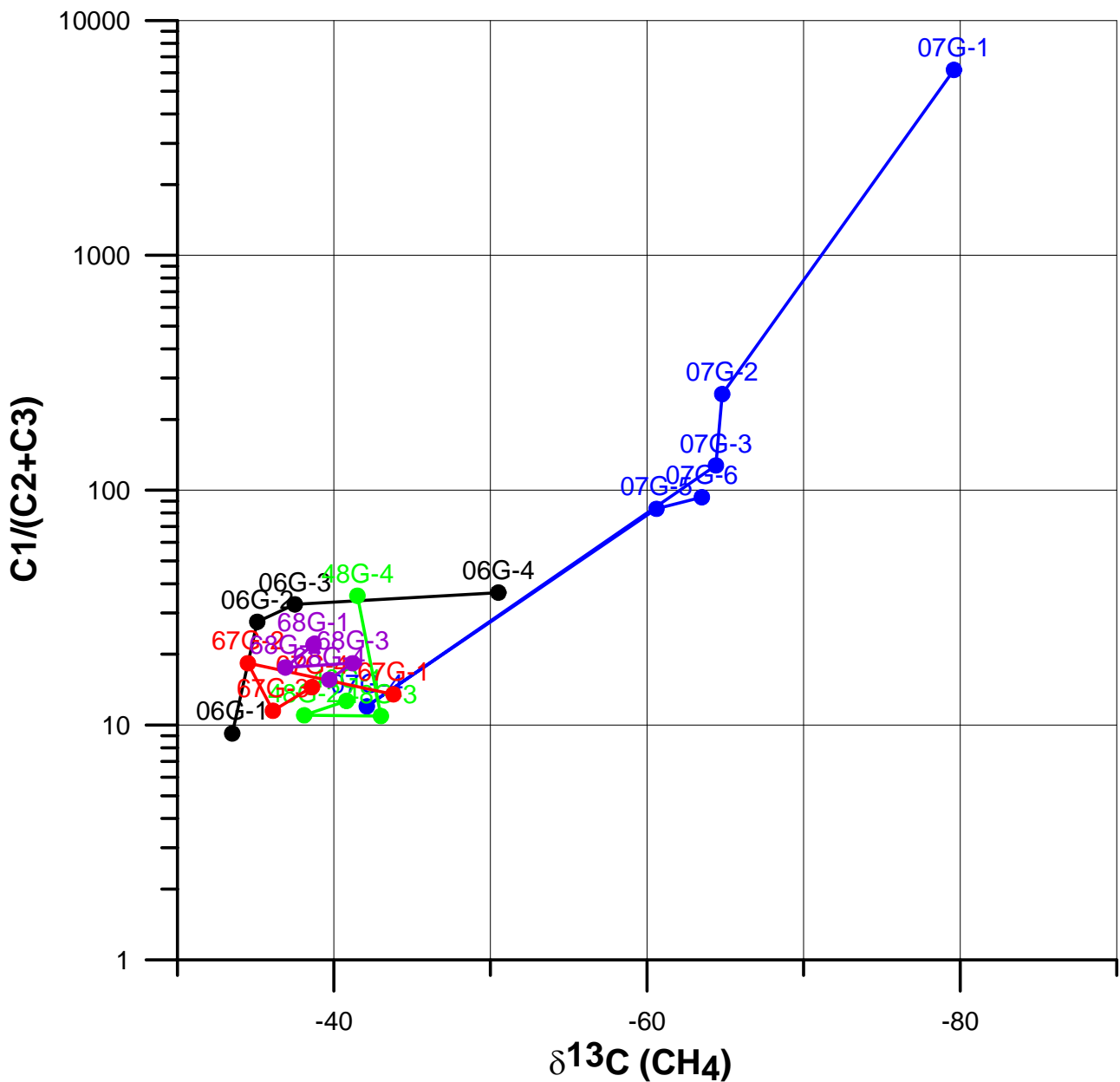


Fig. 3.3.2 Bernard type plot showing subsamples of individual gravity cores. Index 1 indicates the deepest sample (maximum 6 m below the sea bed); higher index numbers represent samples taken progressively closer to the seabed with a spacing of 1 meter.

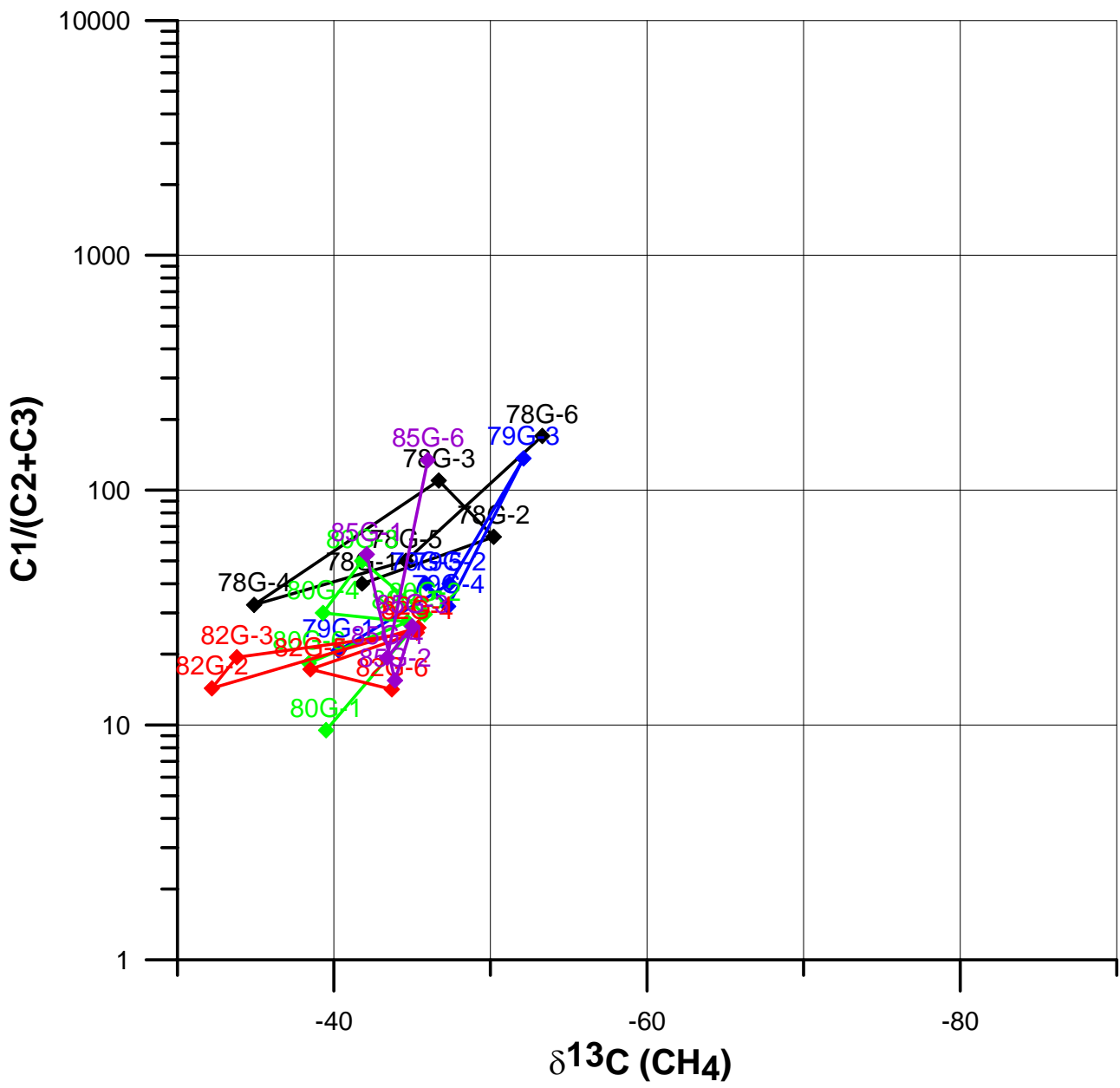


Fig. 3.3.3

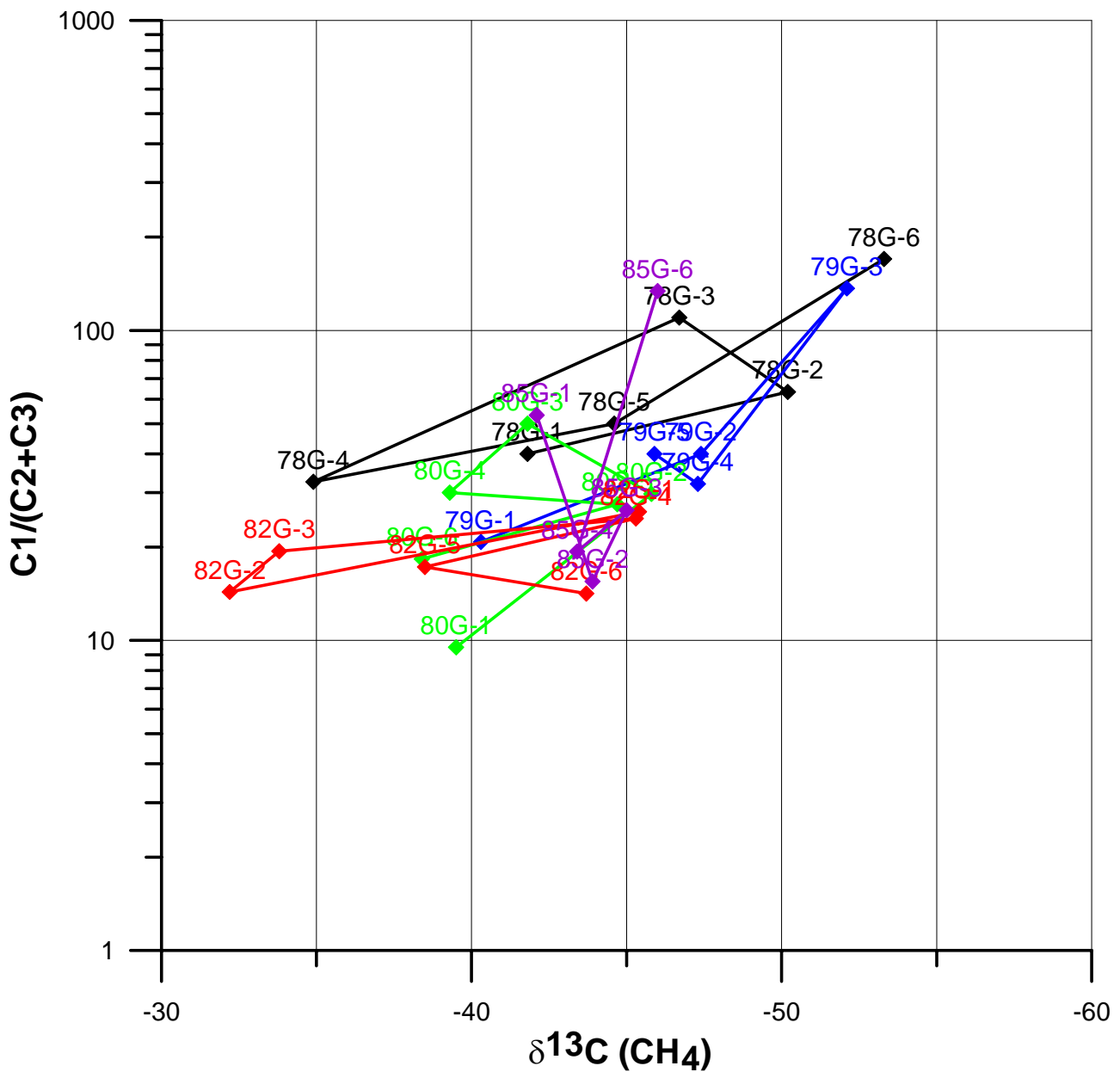


Fig. 3.3.4

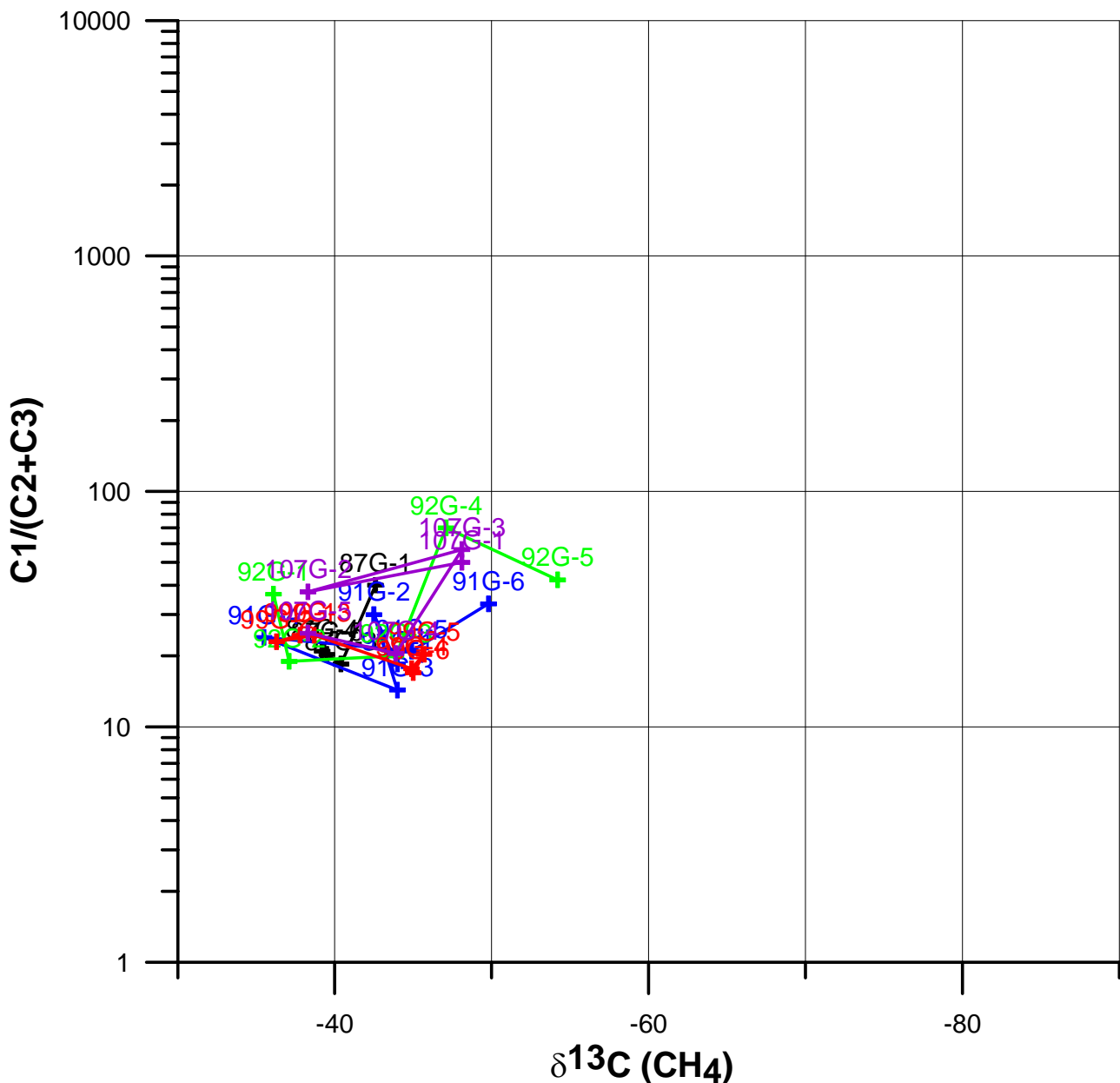


Fig. 3.3.5.

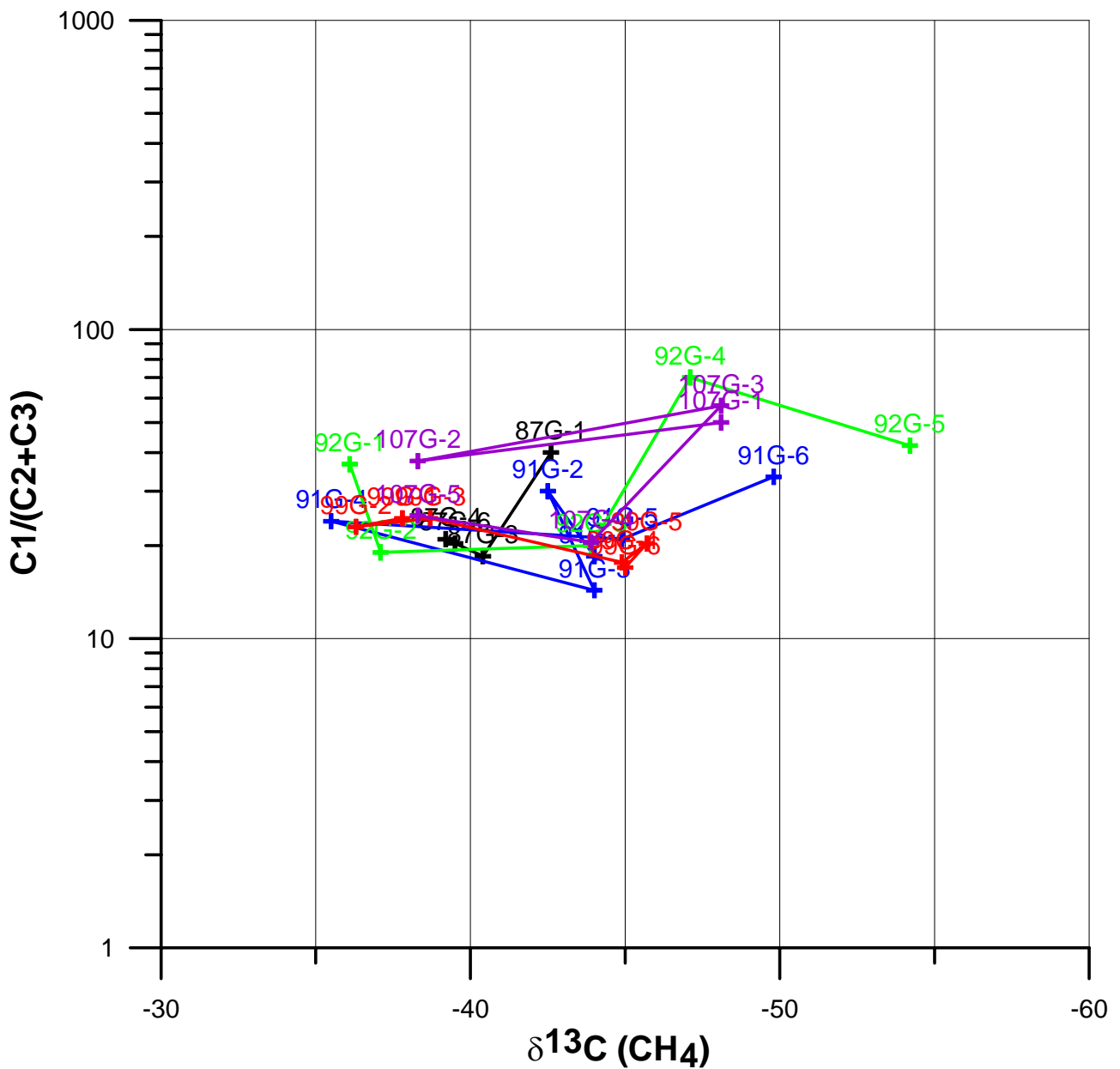


Fig. 3.3.6

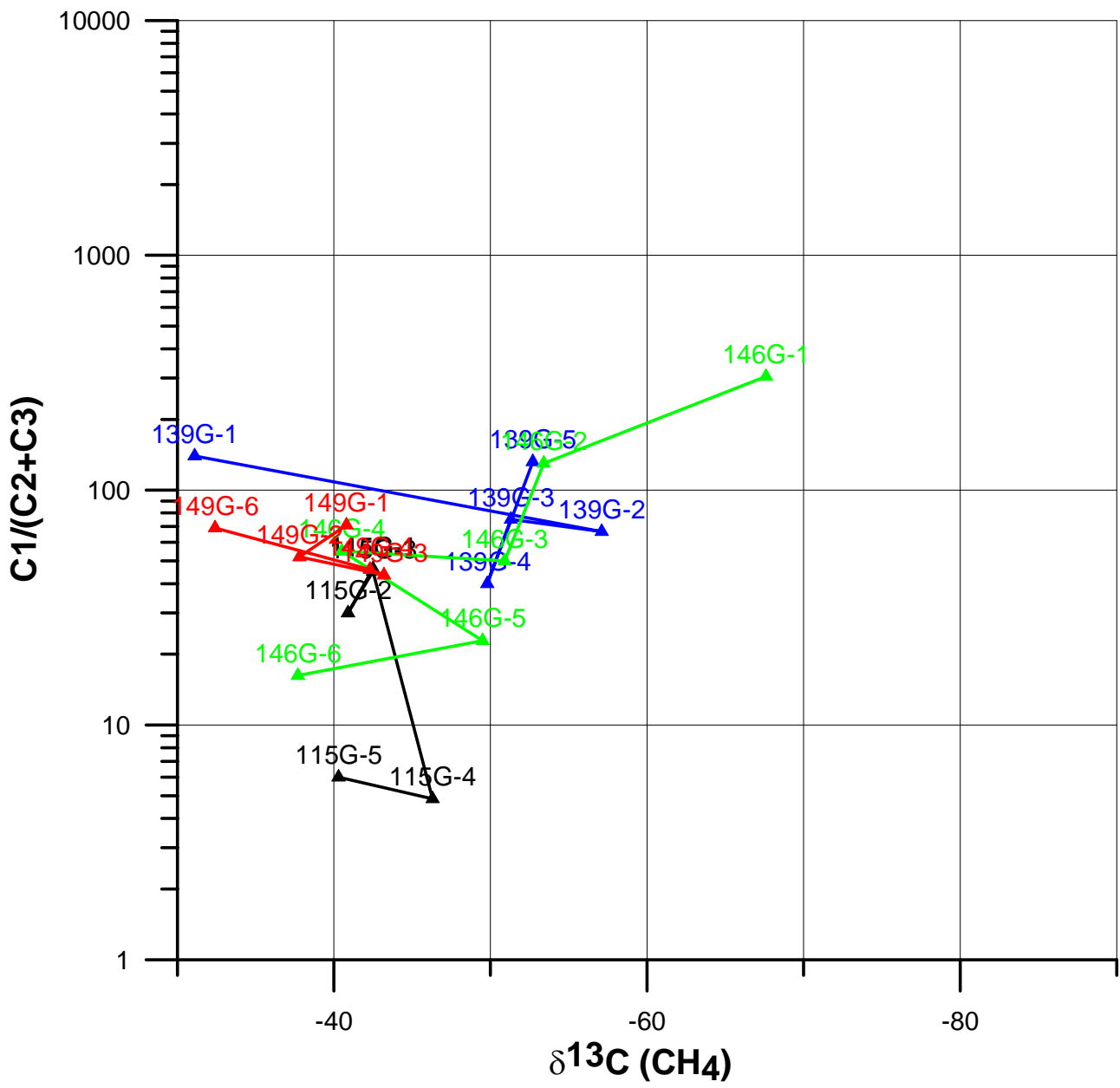


Fig. 3.3.7

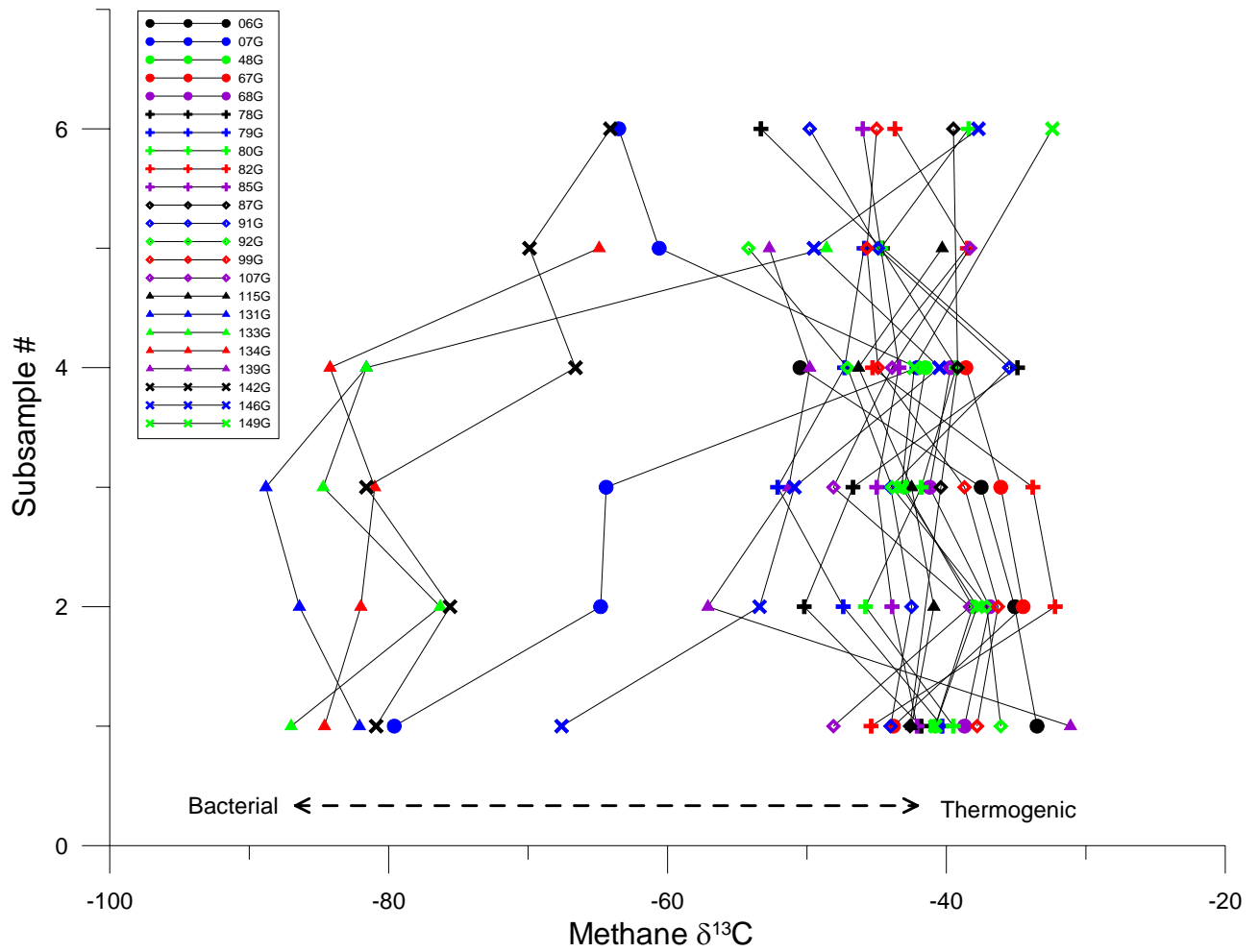


Fig. 3.3.8. Variation in methane carbon isotopic composition. A number of samples show well developed depth-trends.

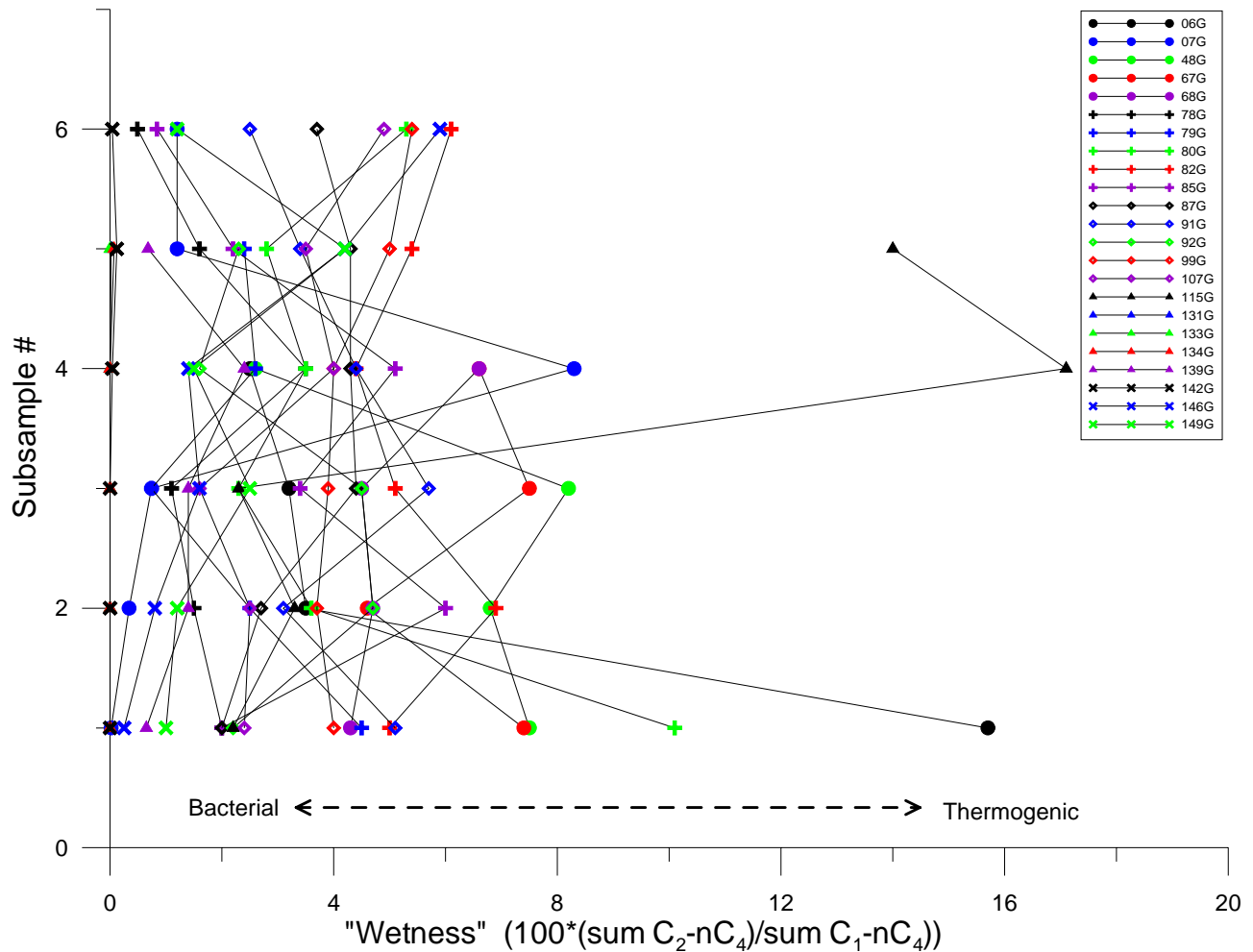


Fig. 3.3.9 Gas “wetness” versus sample depth. Although trends may be difficult to observe, a number of gravity cores yield headspace gas compositions that grow increasingly wetter from the base of the core to its top.

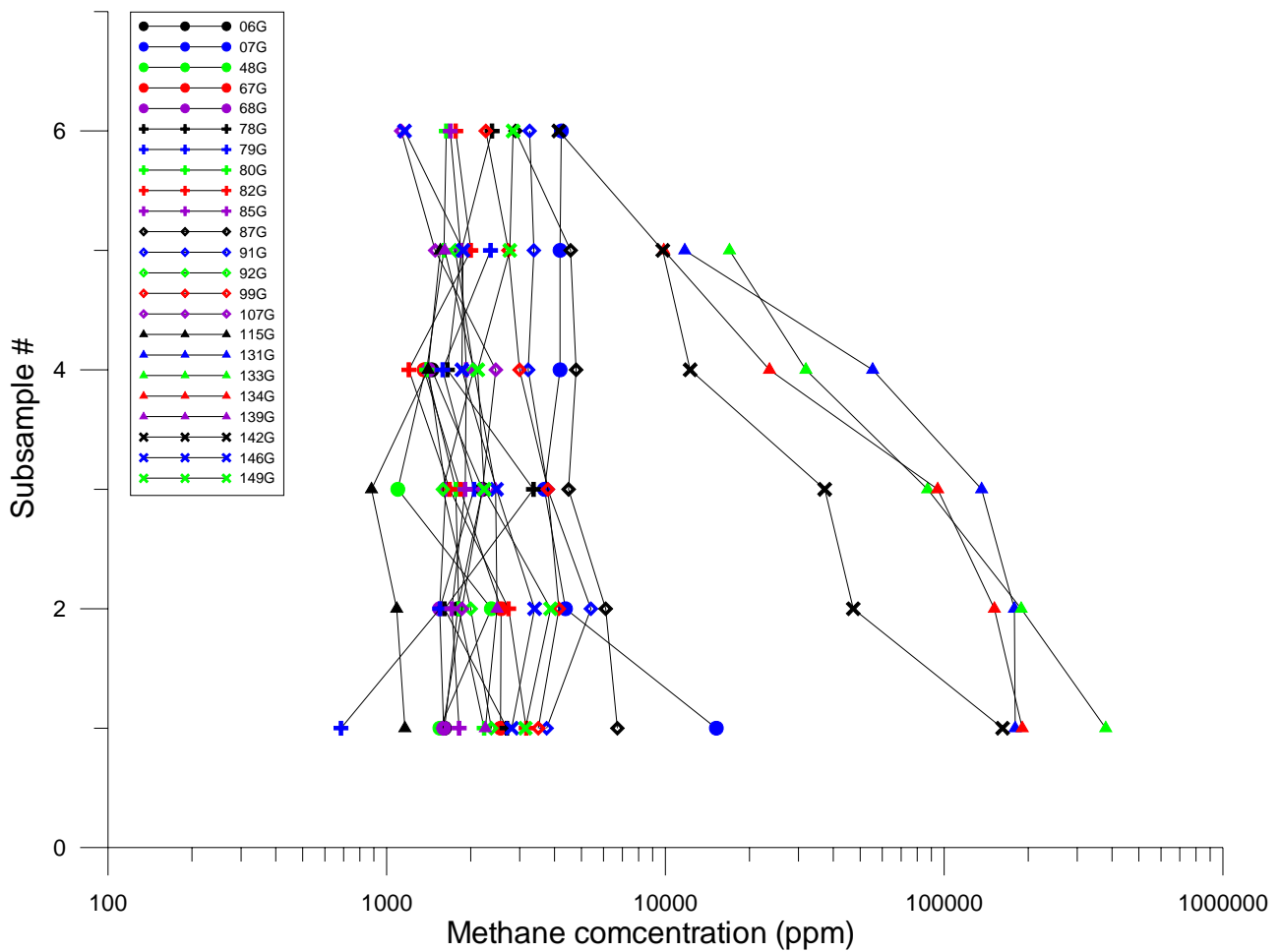


Fig. 3.3.10 Methane concentration versus depth below the sediment water interface. A number of cores show very strong depletion in methane upwards. Cores with overall low methane concentrations show less developed trends.

3.4 Porewater sulphate concentrations

Porewater sulphate concentrations were measured in a number of cores that show gradients in methane concentrations and/or $\delta^{13}\text{C}$ (Dana06-06G, Dana06-07G, Dana06-139G and Dana06-146G). All cores show more or less well developed decreasing trends downwards through the cored interval. The concentrations are significantly lower than in normal oceanic water, but sulphate is present throughout the entire length of all of the gravity cores analysed (Fig. 3.4.1).

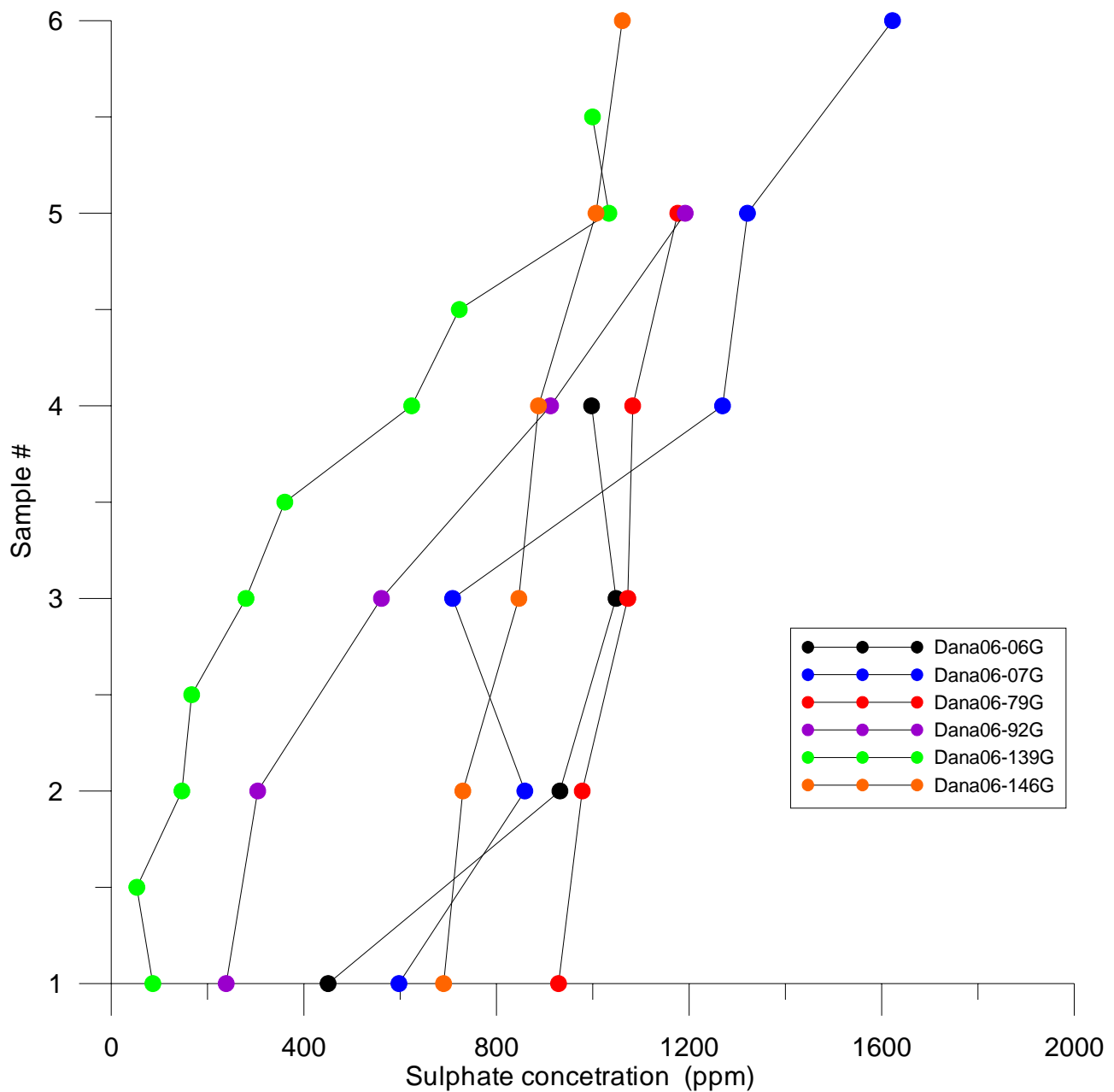


Fig. 3.4.1 Porewater sulphate concentration through cores Dana06-06G, Dana06-07G, Dana06-79G, Dana06-92G, Dana06-139G and Dana06-146G.

4. Discussion

4.1 TC/TOC/TS analysis and Rock-Eval screening pyrolysis

The low levels of TOC and pyrolysis yield generally observed result from low levels of both autochthonous and allochthonous organic input to the sediments, and the decreasing depth trend in TOC frequently observed corresponds to microbial mineralization of the non-refractory part of the sedimentary organic matter. No trace whatsoever of the presence of any ancient sediment with petroleum source rock characteristics has been recorded by the screening analysis.

The Dana06-07G core was collected on a suspected mud diapir, and detailed studies of this feature are currently being undertaken. The results hereof will be reported separately, and the Dana06-07G core will not be discussed further here.

The two populations observed in the TOC vs. TS plot (Fig. 3.1.6) are related to the ability of the sedimentary organic matter to fuel microbial sulphate reduction. The major population is rather similar to the normal marine trend, representing deposits receiving autochthonous organic matter that may sustain microbial sulphate reduction and thus afford the sequestration of sulphur in the form of sulphides in the sediments. The subordinate population is principally defined by subsamples from the Dana06-115G core, that generally shows high TOC and low TS. This core was collected north of Nuussuaq, near the mouth of the large Itilli valley. Runoff from the valley, in which a thick succession of mostly thermally overmature organic-rich Cretaceous mudstones crop out, is likely to carry a significant load of inert organic matter, that can be supplied to seabed sediments in the vicinity of the mouth of the valley. Such organic matter will not serve as substrate for the sulphate reducing community and hence little enrichment in sulphur is observed. The cores Dana06-131G through Dana06-142G are somewhat richer in TOC than most other samples, and show more "normal" TS/TOC ratios. These samples were collected in or in the vicinity of the Vaigat sound, where seabed sediments are likely to receive a notable proportion of ancient organic matter from the brown coals and carbonaceous shales that crop out along the coasts. These are generally of rather low thermal maturity, and may at least to some extent serve as substrate for the sulphate reducing community, hence the more "normal" TS/TOC ratios. This is in agreement with headspace gas data, see below.

4.2 Solvent extract analysis (GC and GC-MS)

GC and biomarker data consistently show a predominance of recent/subrecent organic material in the samples analysed. Although a variable, minor background contribution from ancient sources may be present, neither a trace of thermally mature petroleum components that would point to the presence of seepage, nor any indication of the presence of petroleum source rocks have been found in the data. 28,30-bisnophopane, when occurring unassociated with extended 28-norhopanes is one of the distinguishing characteristics of the Cretaceous shale derived Itilli oil onshore west Greenland. However, the significance of this observation is unclear since 28,30-bisnorhopane is not uncommon in marine sediments.

4.3 Headspace gas analysis and porewater composition

Methane isotopes in natural gases are the principal property that allows a differentiation of low temperature bacterial from high temperature thermogenic origin. For this reason we conducted carbon isotope analyses on the methane that is accumulating in the headspace above the canned core samples. Methane isotope values are reported as δ values relative to the PDB standard i.e.

$$\delta = [(R_{\text{sample}}/R_{\text{standard}}) - 1] * 1000 (\text{\textperthousand})$$

where R represents the $^{13}\text{C}/^{12}\text{C}$ ratio of the sample and the standard, respectively. For natural gases δ values between -20 and -45‰ are indicative of a thermogenic origin whereas δ values more negative than -50‰ are typical for gases of microbial origin. Another characteristic is the presence of higher gaseous hydrocarbons in gases, whereby microbial gases consist only of methane and thermogenic gases contain also C2 (ethane) C3 (propane) and C4 (butane). A crossplot that relates methane isotopes and gas composition (Bernard et al. (1978) allows a differentiation of gas origins. For our samples, the “Bernard plot” (Fig 3.3.1) suggests that the headspace gases are primarily thermogenic, perhaps occasionally with a minor microbial contribution. However, a closer scrutiny of the data shows that this interpretation is not tenable. Core-by-core

Bernard plots (Figs. 3.3.2 through 3.3.7) reveal that a number of gravity cores display systematic depth-related variations through the cored section. For example, headspace gases in core 134G, 68G and 131G have more positive δ values close to the seabed and more negative δ values in deeper samples (Fig.3.3.8). In addition, through several cores, the gas composition shows increase in C2+ gases i.e. have more “thermogenic” characteristics the closer to the seabed the samples are taken. Moreover, hydrocarbon gas concentrations seem to be linked to gas composition, since extremely dry gases are only found where the overall hydrocarbon gas concentration is high. Methane is thus essentially the only hydrocarbon gas that can be detected when hydrocarbon gas concentrations are high. Finally, all gas properties seem to co-vary with the sulphate contents in the porewaters. Together, these observations require a different interpretation than suggested by the Bernard plot.

Since the initial work of Claypool and Kaplan (1974) it is known that methane in unconsolidated sediments is subject to diagenetic alteration. Microbially mediated generation of methane by anaerobic decomposition/fermentation of sedimentary organic matter takes place more or less concurrently with microbially mediated anaerobic oxidation of methane, principally through the action of sulphate reducing bacteria (SRB) (see Whiticar,1999, for a review). Carbon isotope fractionation is taking place as methane is formed by fermentation, resulting in a strong depletion of ^{13}C in the methane and accordingly very negative values of methane $\delta^{13}\text{C}$ from -70 to -110‰. In contrast, anaerobic methane oxidation through the action of SRBs involves an enrichment of ^{13}C in the remaining pool of methane because $^{12}\text{CH}_4$ is preferentially consumed. (and the production of isotopically light CO_2 from oxidation of methane). This enrichment process can result in methane isotope values that are similar and/or equal to thermogenically produced methane with $\delta^{13}\text{C} = -20$ to -50, and thus become indistinguishable from it. These processes are summarised in Fig. 4.3.1 from Whiticar (1999)

In a closed system, the isotope mass balance of the continued preferential elimination of ^{12}C from the carbon substrate and the concurrent progressive enrichment of the residual substrate in ^{13}C is described by the “Rayleigh distillation function” (Rayleigh, 1896), which according to Whiticar (1999) translates into:

$$R_{r,t} = R_{r,i} f^{\alpha-1}$$

and

$$R_{p,t} = R_{r,i} (1-f^\alpha)/(1-f)$$

Where $R_{r,t}$ and $R_{r,i}$ are the isotope ratios of the carbon substrate, at time t and initially i . $R_{p,t}$ is the isotope ratio of the product at time t , f is the fraction of the initial substrate remaining at time t and α is the kinetic fractionation factor. The kinetic fractionation factor is an expression of the relative reactivity of the two isotopes, in the present case ^{12}C versus ^{13}C .

Based on the Rayleigh distillation function, the gradual oxidation of a pool of biogenic methane by SRB we modelled the isotope changes during oxidation using $\alpha = 0.995$ with West Greenland data superimposed (Fig. 4.3.2). A near-perfect match between the model and the measured data is observed, providing strong evidence for the operation of the mechanisms described above. Corroborative evidence is provided by sediment porewater sulphate data shown in Fig. 3.4.1, demonstrating that all samples were indeed collected in the sulphate reduction zone.

It should be noted that it is only in the case of low overall hydrocarbon gas concentrations that ambiguity with respect to gas origin is seen. In the Dana06-07G, Dana06-131G, Dana06-133G, Dana06-134G and Dana06-142G gravity cores that all show high hydrocarbon gas concentrations, there is little doubt as to the biogenic origin of the gases based on isotopic (very light) as well as compositional evidence (extremely dry), although SRB-mediated oxidation of methane is prominent in these cores too, shown by the generally marked trends in CO_2 and CH_4 concentrations, $\delta^{13}\text{CH}_4$ and wetness. Unfortunately isotopic data on CO_2 from these samples are not available, since such data could provide corroborative evidence for methane oxidation. The Dana06-131G, Dana06-133G, Dana06-134G and Dana06-142G gravity cores were all collected in the Vaigat sound, where seismic data often show prominent “Direct Hydrocarbon Indicators” (DHI’s) such as flat spots, brightening of reflectors and gas clouds, and along the coasts, petroleum seepage is common (Bojesen-Koefoed et al. 1999; Bojesen-Koefoed et al. 2007). The DHI’s are, however, deeper seated features, and any possible relation between them and the gases sampled in the gravity cores remains elusive. Compared the other coring sites, both the sedimentation rate and the supply of organic matter are probably higher in the Vaigat, leading to higher overall organic carbon contents in the sediments as

shown by TOC data and a higher level of microbial activity as shown by the prominent gas compositional gradients seen in these cores.

To conclude:

- The presence of thermogenic methane cannot be unambiguously demonstrated in any of the samples collected.
- The apparent thermogenic isotopic signature of a large number of gas samples that typically show low overall hydrocarbon gas concentrations, is an artefact, produced by isotopic fractionation as sulphate reducing bacteria utilise microbial methane as carbon source
- Concurrently with the shift in isotopic composition of the residual methane the overall gas wetness increases as methane concentration decreases.
- All samples that show high hydrocarbon gas concentrations can be unambiguously be identified as microbial, but SRB mediated methane oxidation has a prominent effect on the methane isotope composition in such samples as well.
- The observations made here call for caution using commercial surface geochemical surveys that are sometimes based on analysis of a few samples at essentially the same sediment depth per site, rather than a series of samples representing a section of the sediment at each site.

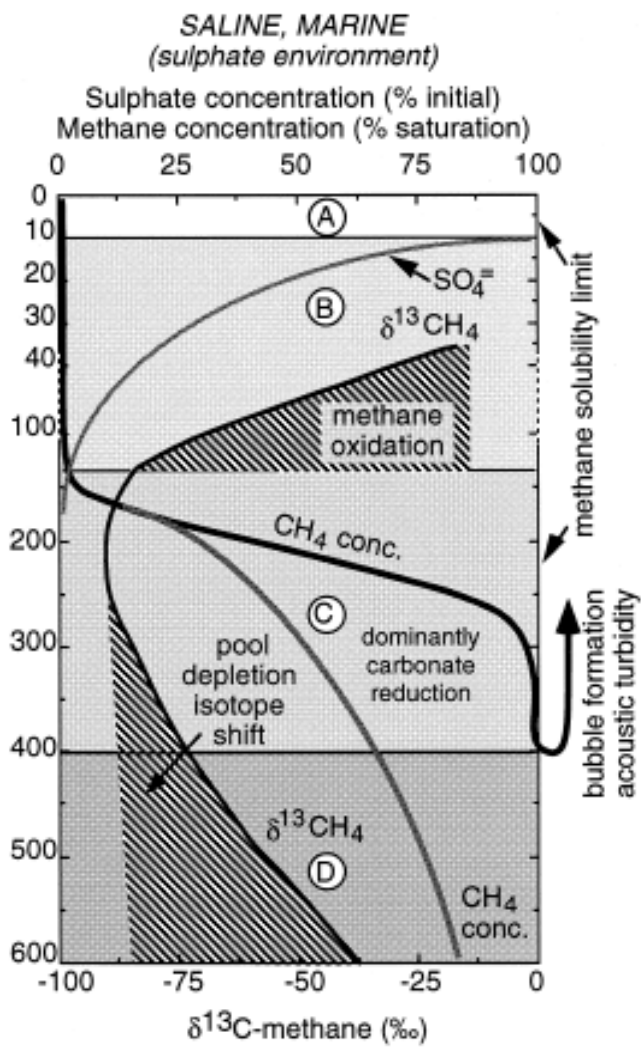


Fig. 4.3.1. Idealised depth profile of methane concentration and isotopic composition in a marine environment. A: oxic zone; B: sulphate reduction zone; C: main zone of methanogenesis; D: zone of substrate depletion or change of processes. (from Whiticar, 1999)

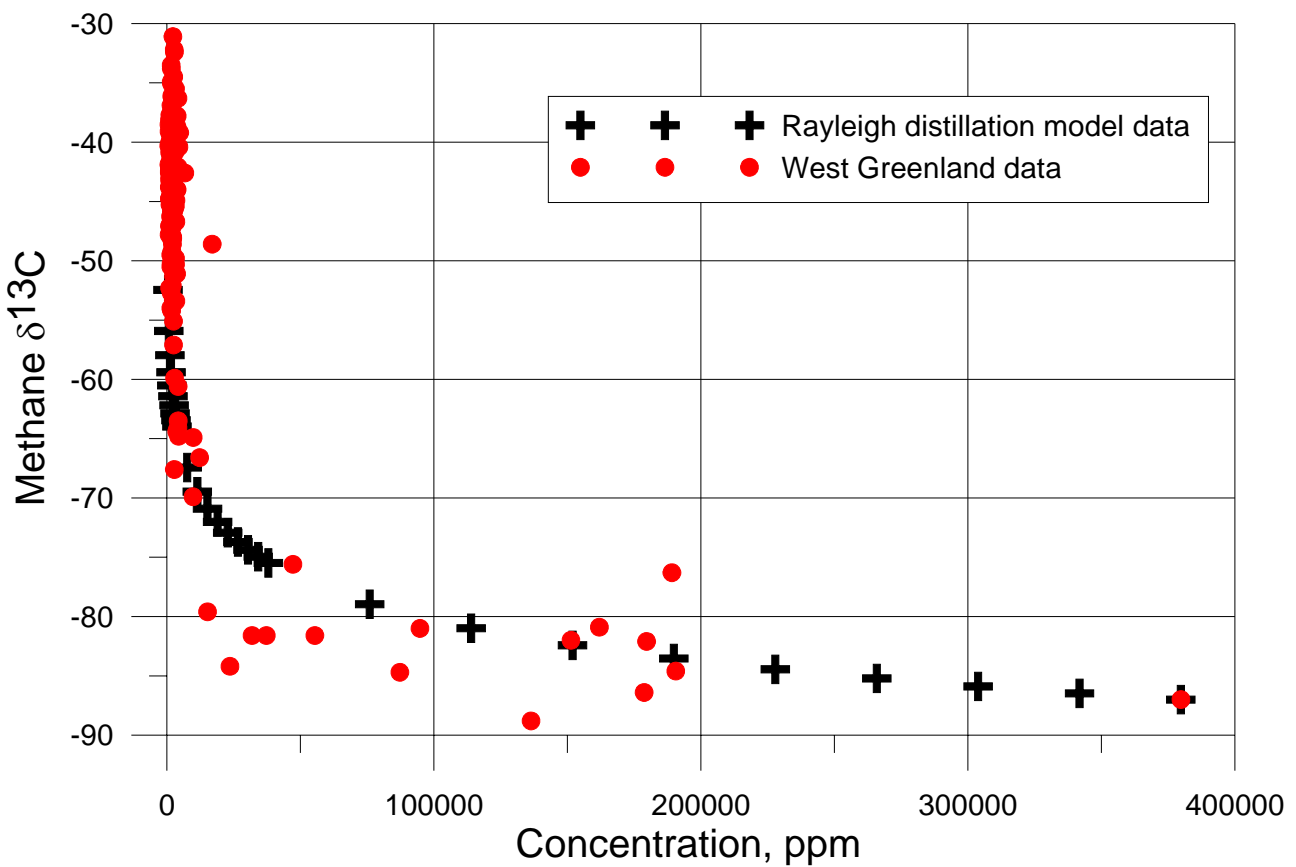


Fig. 4.3.2 Comparison of Rayleigh-type modelling of methane isotopic composition and concentration, using kinetic fractionation factor $\alpha = 0.995$, and measured data from West Greenland. Note near-perfect match between model and real data. See text for discussion.

5. Conclusions

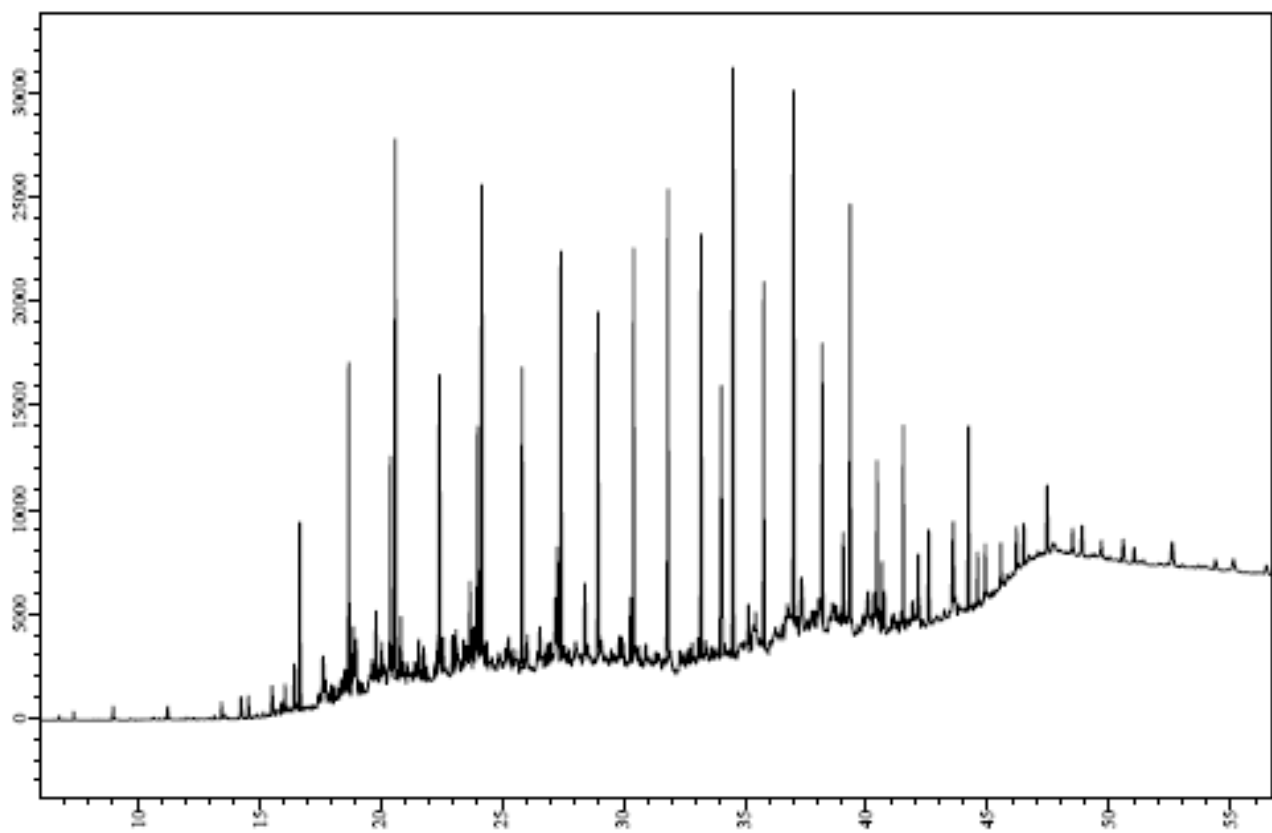
- A total of 196 subsamples, representing 60 different gravity cores (sampling sites) have been analysed.
- Most samples show low or very low levels of TOC and pyrolysis yield.
- Somewhat higher levels of TOC, and S2 pyrolysis yields are shown by three subsamples collected from the Dana06-07G gravity core. This core was collected on a possible diapir, where more detailed investigations are currently being conducted. The result hereof will be reported elsewhere.
- Increased levels of TOC, and to a lesser extent S2 pyrolysis yields are also observed in the Dana06-115G and Dana06-131G through Dana06-142G gravity cores. This is explained by the position of these cores relative to sources of terrestrial runoff carrying organic matter.
- Solvent extract analyses by GC and GC-MS suggest a predominant content of recent/subrecent organic matter in all samples.
- No traces of petroleum seepage or petroleum source rocks have been found in any of the samples.
- In samples with low overall hydrocarbon gas concentrations, a false impression of a thermogenic origin of the methane is produced by in-sediment degradation of biogenic methane by sulphate reducing bacteria (SRB), leading to an isotope shift towards “thermogenic” values and increased gas wetness.
- In samples with higher contents of hydrocarbon gases, methane can readily be demonstrated to be microbial but methane oxidation by SRB affects the gas composition in such samples too.
- The presence of thermogenic hydrocarbon gases has not been demonstrated in any of the samples analysed.
- The results of gas analysis call for caution against surface geochemical surveys providing gas data on single depth samples.
- Hence, standard surface geochemical surveys, providing gas data on single samples, not investigating profiles through the sediment column can be severely misleading, in not affording assessment of the presence of false “thermogenic gases” formed by degradation of microbial methane through the action of SRB.

6. References

- Bojesen-Koefoed, J. A., Christiansen, F. G., Nytoft, H. P. and Pedersen, A. K., 1999: Oil seepage onshore West Greenland: evidence of multiple source rocks and oil mixing. In: Fleet, A. J. and Boldy, S. A. R. (eds.), Petroleum geology of northwest Europe: proceedings of the 5th conference. Geological Society, London, 305–314.
- Bojesen-Koefoed, J. A., Bidstrup, T., Christiansen, F. G., Dalhoff, F., Gregersen, U., Nytoft, H. P., Nøhr-Hansen, H., Pedersen, A. K. and Sønderholm, M. 2007: Petroleum seepage at Asuk, Disko, West Greenland – Implications for regional petroleum exploration. Journal of Petroleum Geology 30, 219-236
- Claypool, G. E. and I. R. Kaplan (1974). The origin and distribution of methane in marine sediments. New York, Plenum Press.
- Coleman, D.D., J.B. Risatti, and M. Schoell (1981) Fractionation of carbon and hydrogen isotopes by methane-oxidizing bacteria. Geochimica et Cosmochimica Acta 45, 1033-1037.
- Bernard, B. B., Brooks, J. M. & Sackett, W. M. 1978: Light hydrocarbons in recent Texas continental slope sediments. Journal of Geophysical Research 83, 4053-4061
- Dalhoff, F. & Kuijpers, A. 2007: Tograpport. Havbundsprøveindsamling ud for Vestgrønland 2006. GEUS rapport 2007/4, 51pp. (*in Danish*)
- Rayleigh, J. W. S., 1896: Theoretical considerations respecting the separation of gases by diffusion and similar processes. Philosophical Magazine 42, 493-499
- Whiticar, M. J. 1999: Carbon and hydrogen isotope systematics of bacterial formation and oxidation of methane. Chemical Geology 161, 291-314

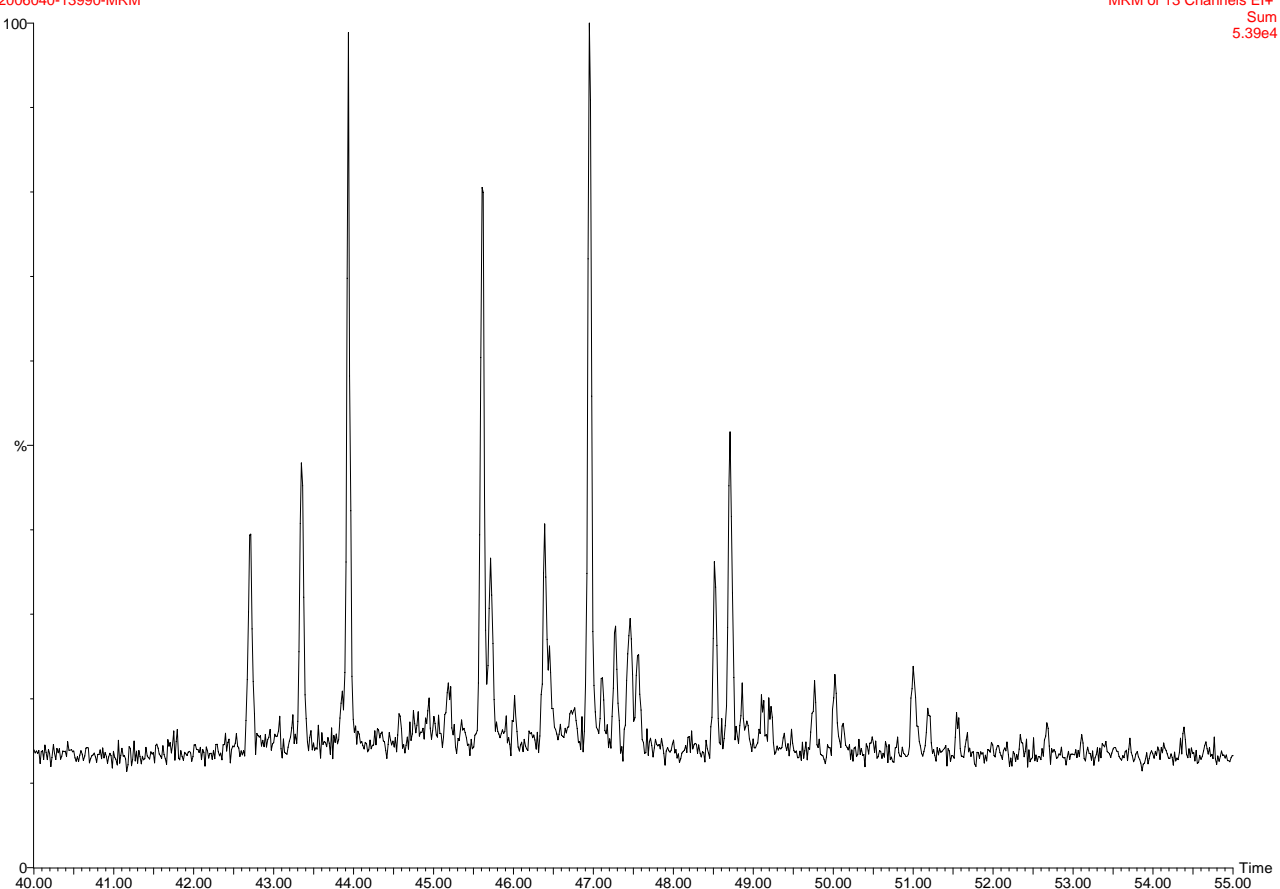
Appendix 1: GC and GC-MS data

DANA06-06G-1



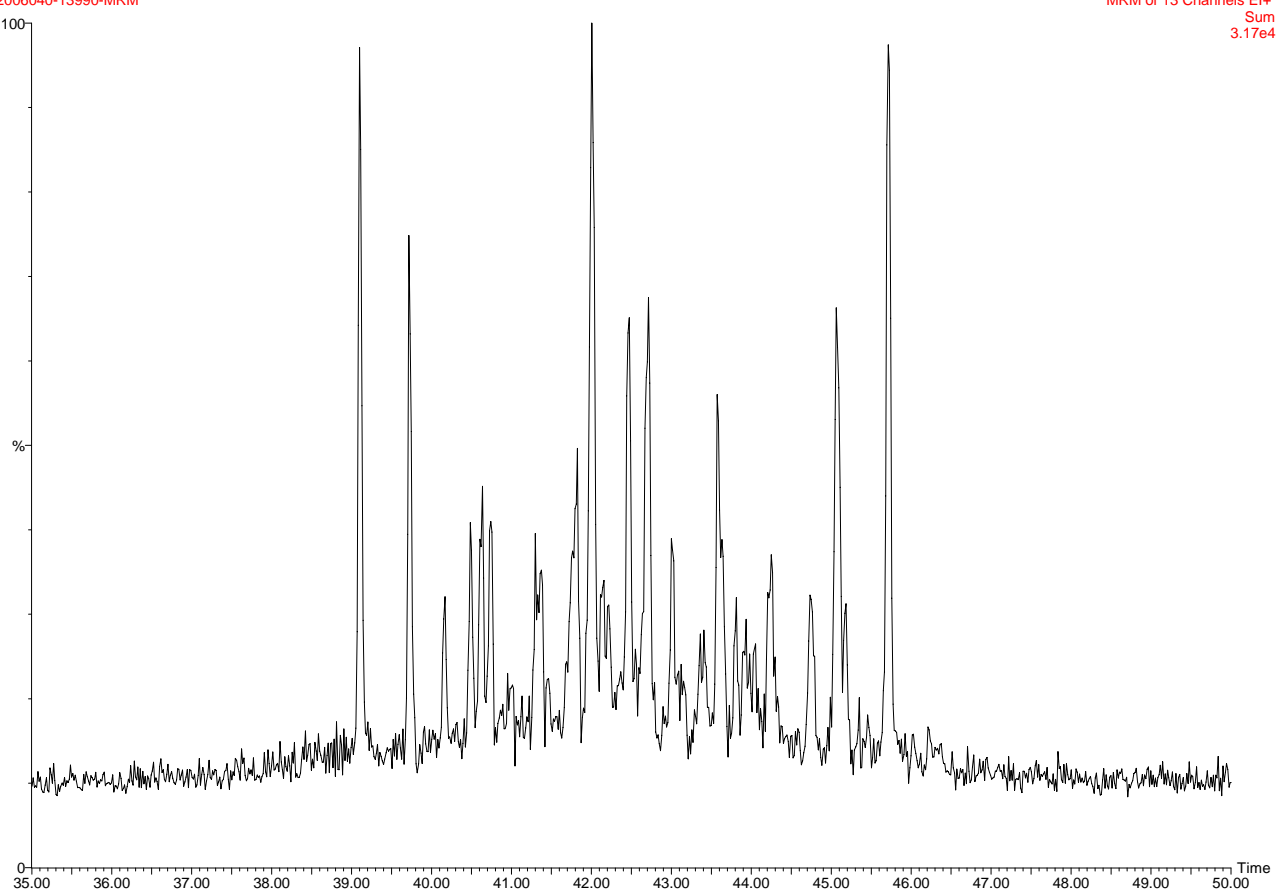
00,2006040-13990-06G-1 ali-aro 0.3 mg
2006040-13990-MRM

MRM of 13 Channels El+
Sum
5.39e4

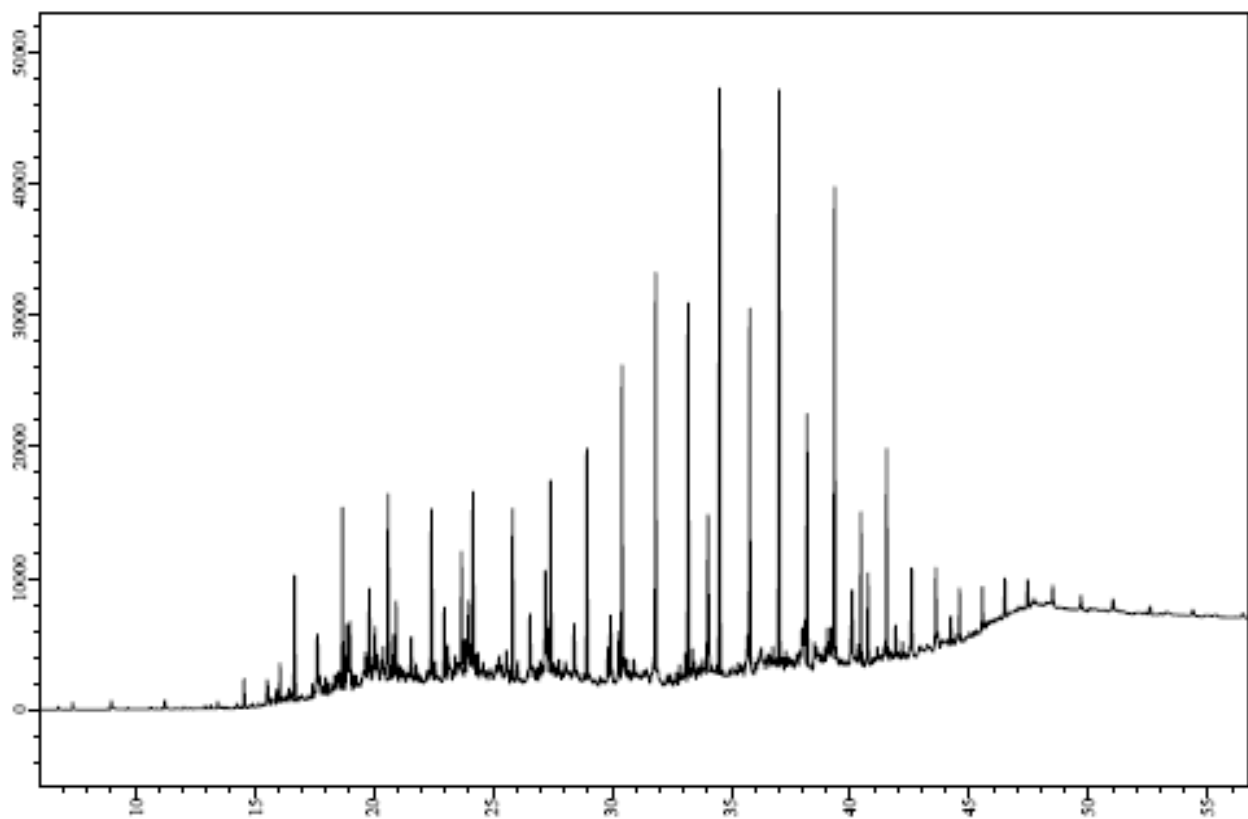


00,2006040-13990-06G-1 ali-aro 0.3 mg
2006040-13990-MRM

MRM of 13 Channels El+
Sum
 $3.17e4$

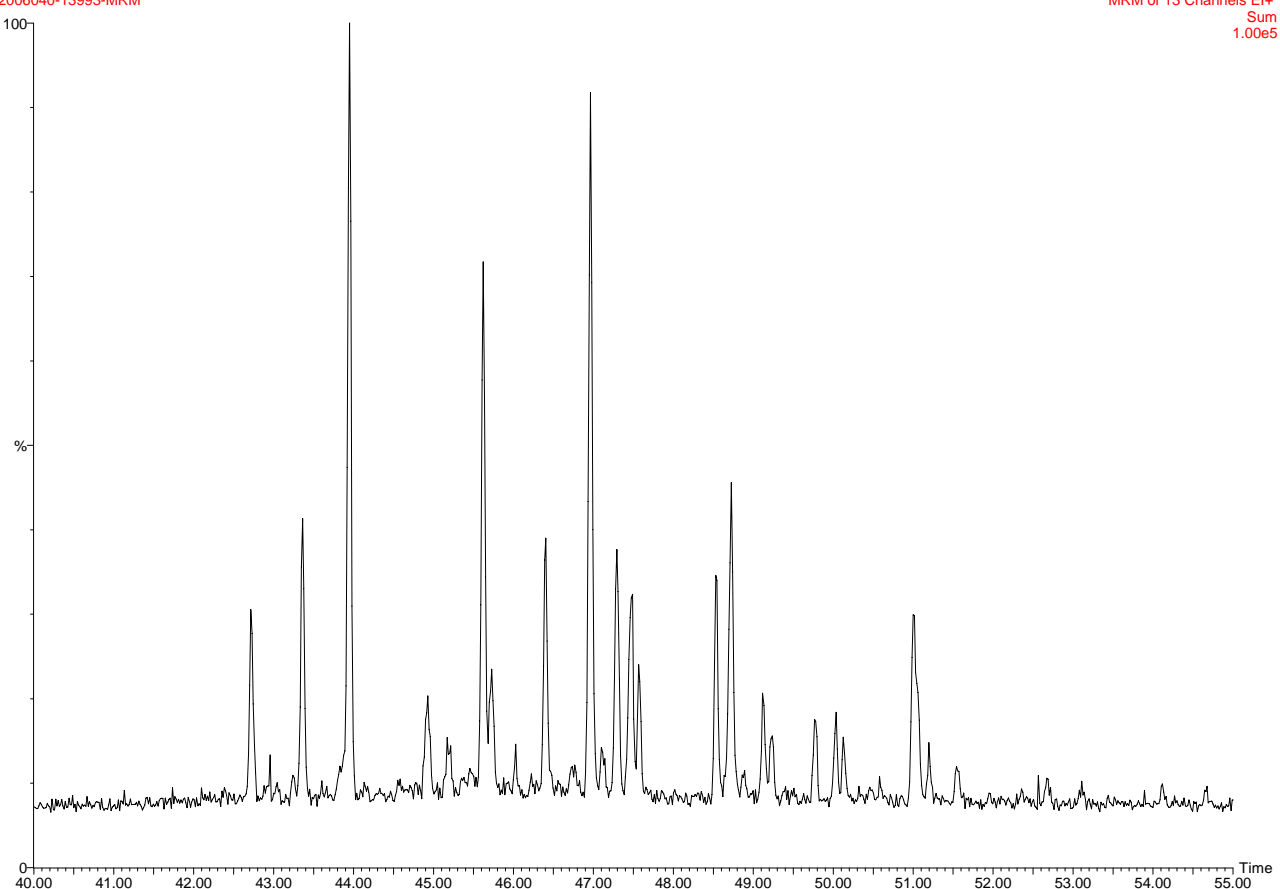


DANA06-06G-4



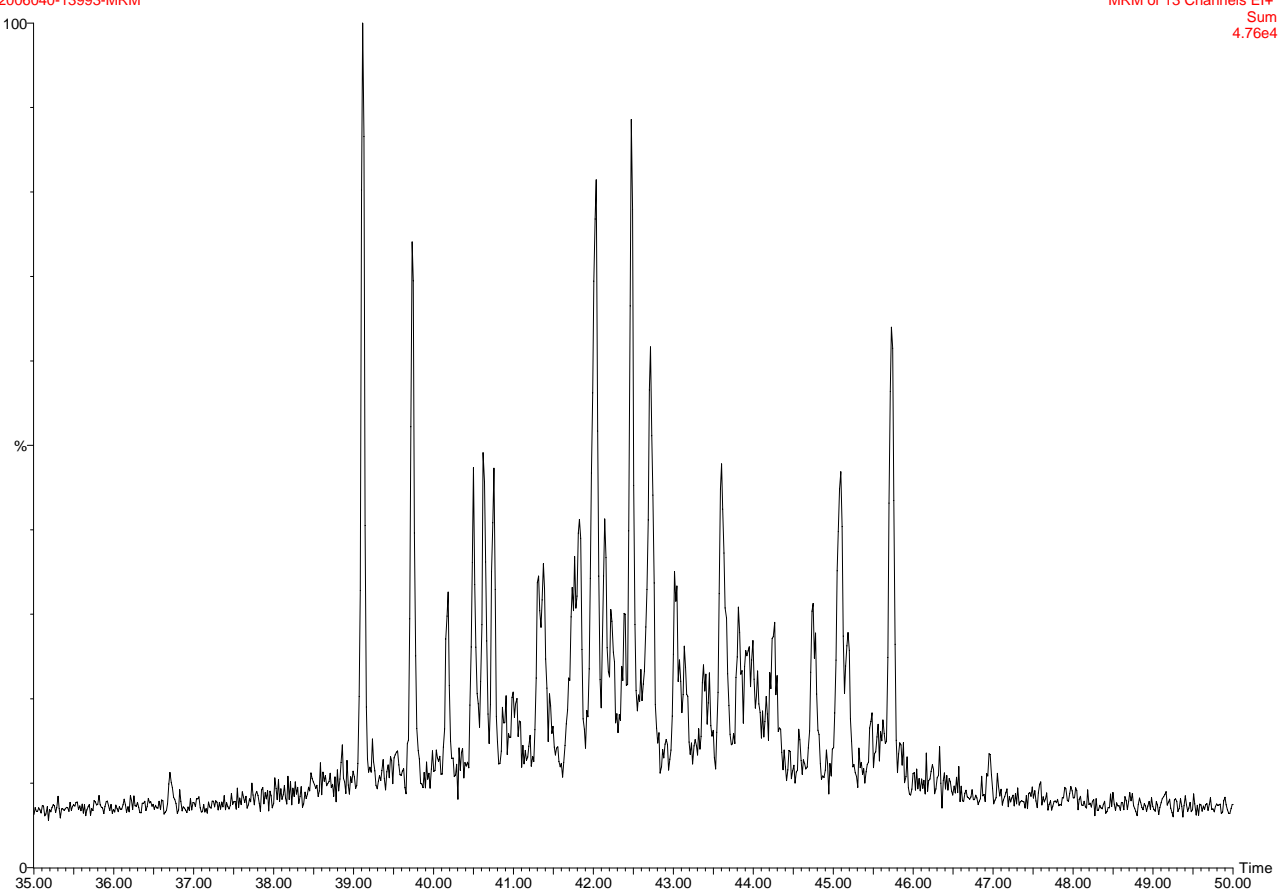
00,2006040-13993-06G-4 ali-aro 0.1 mg
2006040-13993-MRM

MRM of 13 Channels El+
Sum
1.00e5

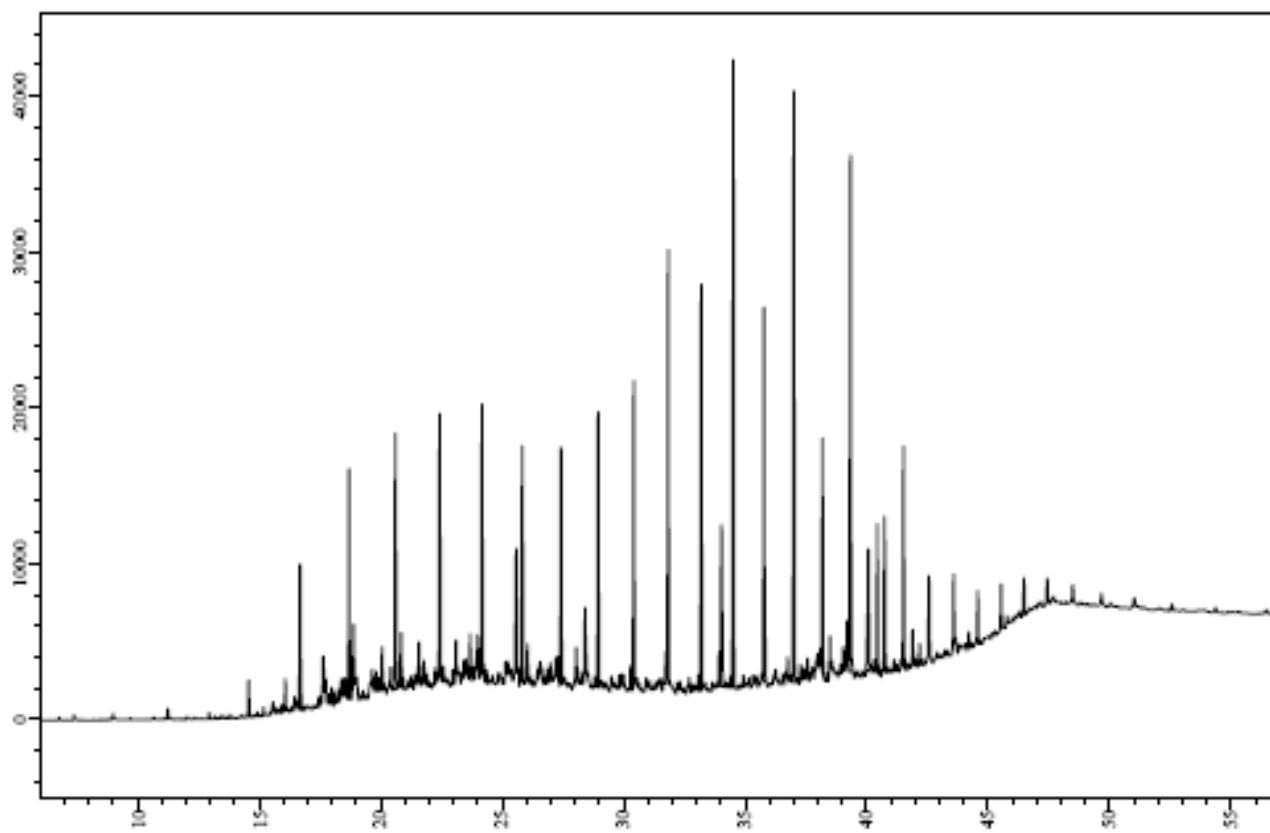


00,2006040-13993-06G-4 ali-aro 0.1 mg
2006040-13993-MRM

MRM of 13 Channels El+
Sum
4.76e4

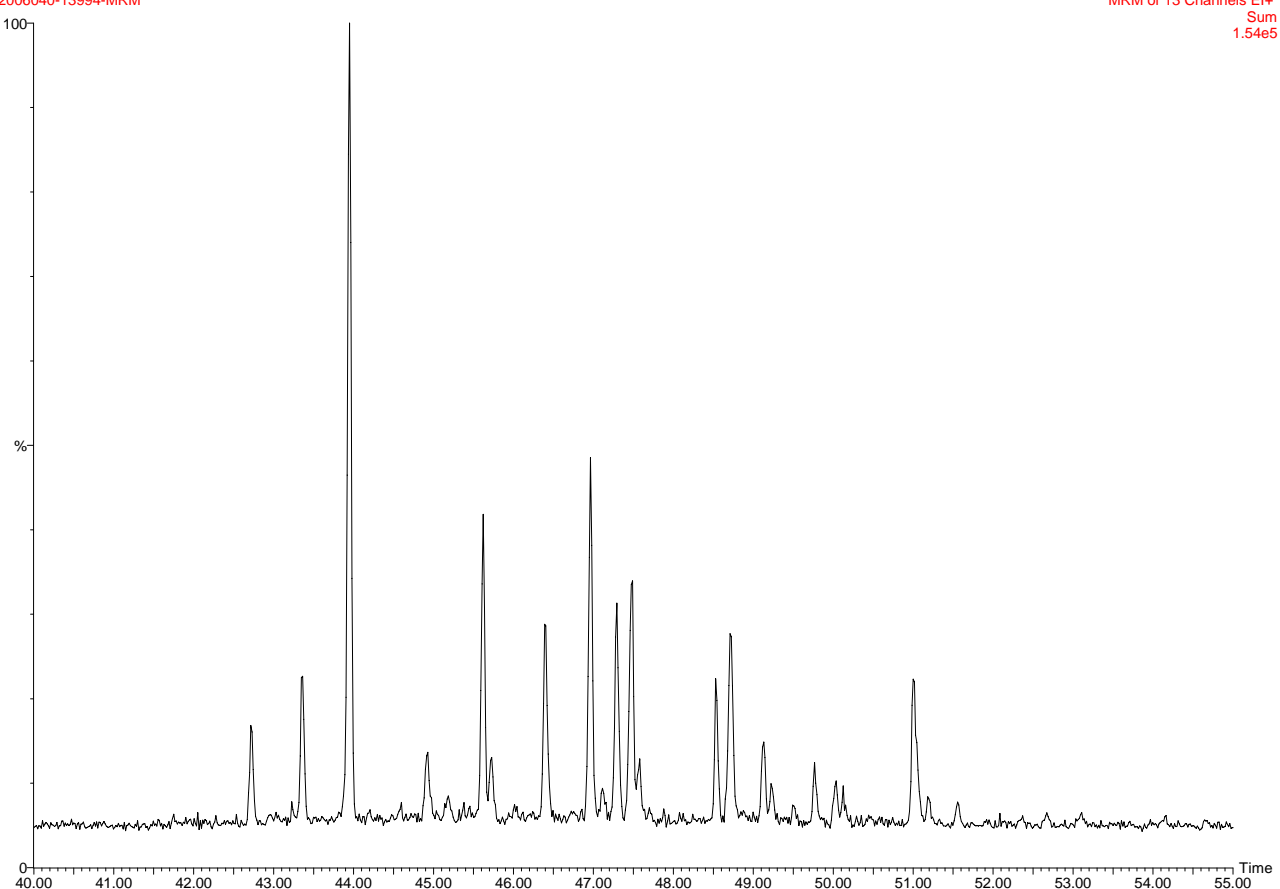


DANA06-07G-1



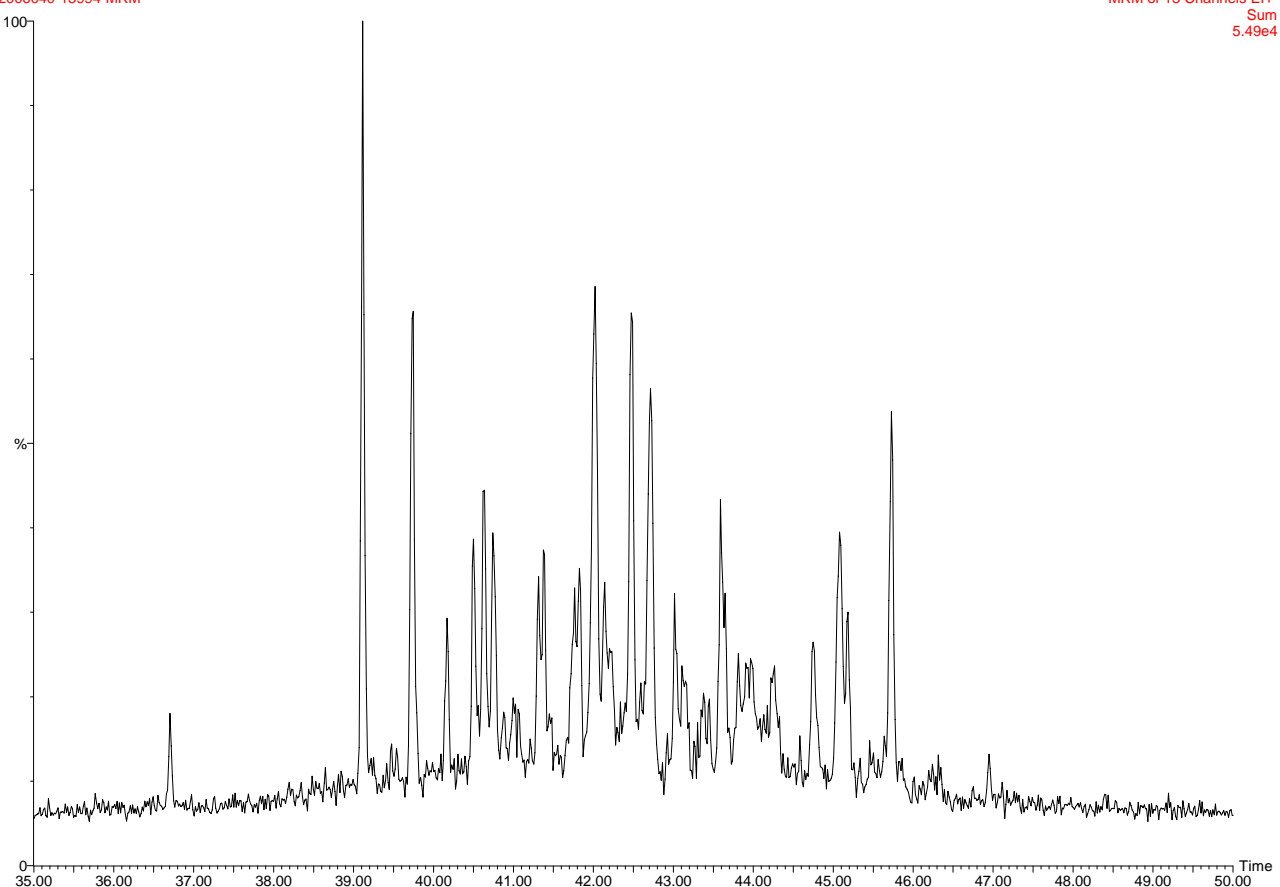
00,2006040-13994-07G-1 ali-aro 0.2 mg
2006040-13994-MRM

MRM of 13 Channels El+
Sum
1.54e5

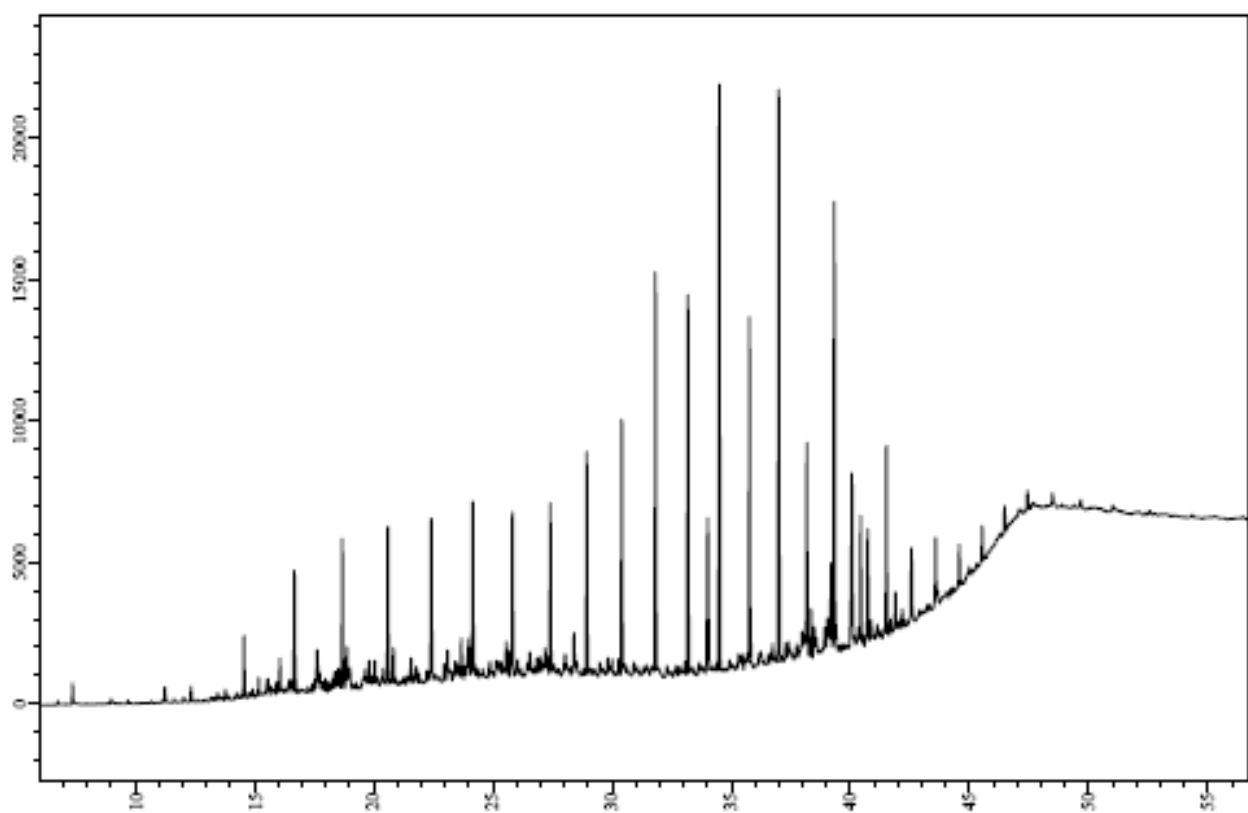


00,2006040-13994-07G-1 ali-aro 0.2 mg
2006040-13994-MRM

MRM of 13 Channels El+
Sum
5.49e4

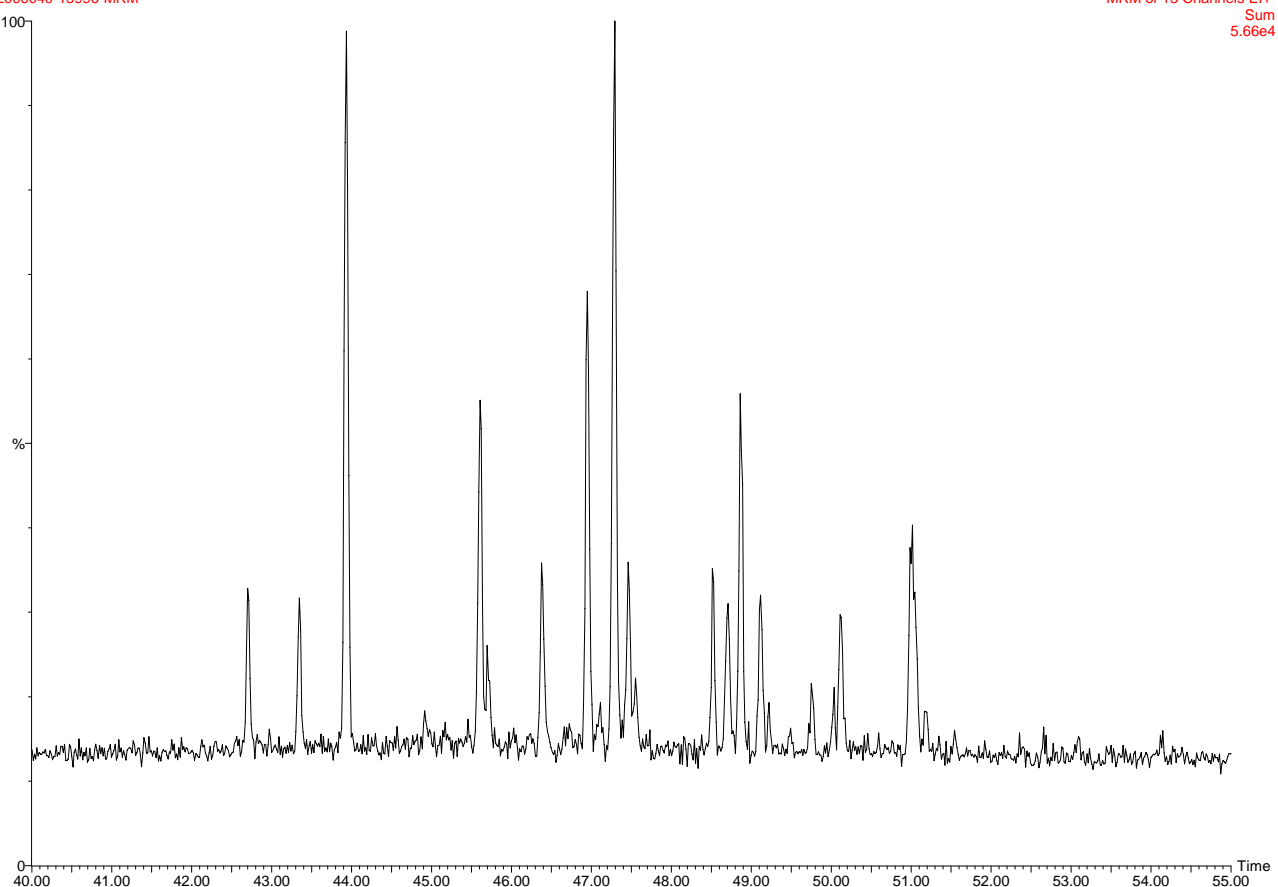


DANA06-07G-3



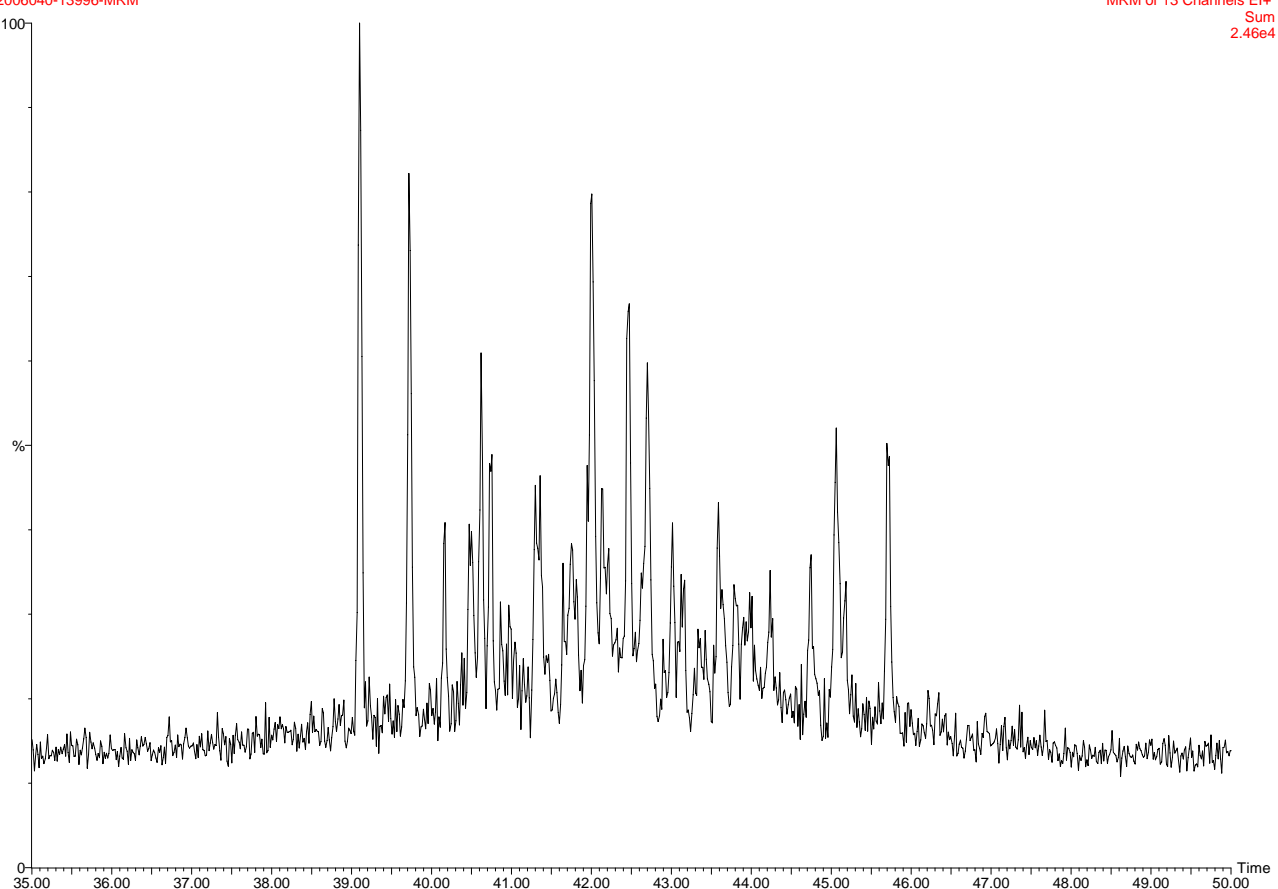
00,2006040-13996-07G-3 ali-aro 0.9 mg
2006040-13996-MRM

MRM of 13 Channels El+
Sum
5.66e4

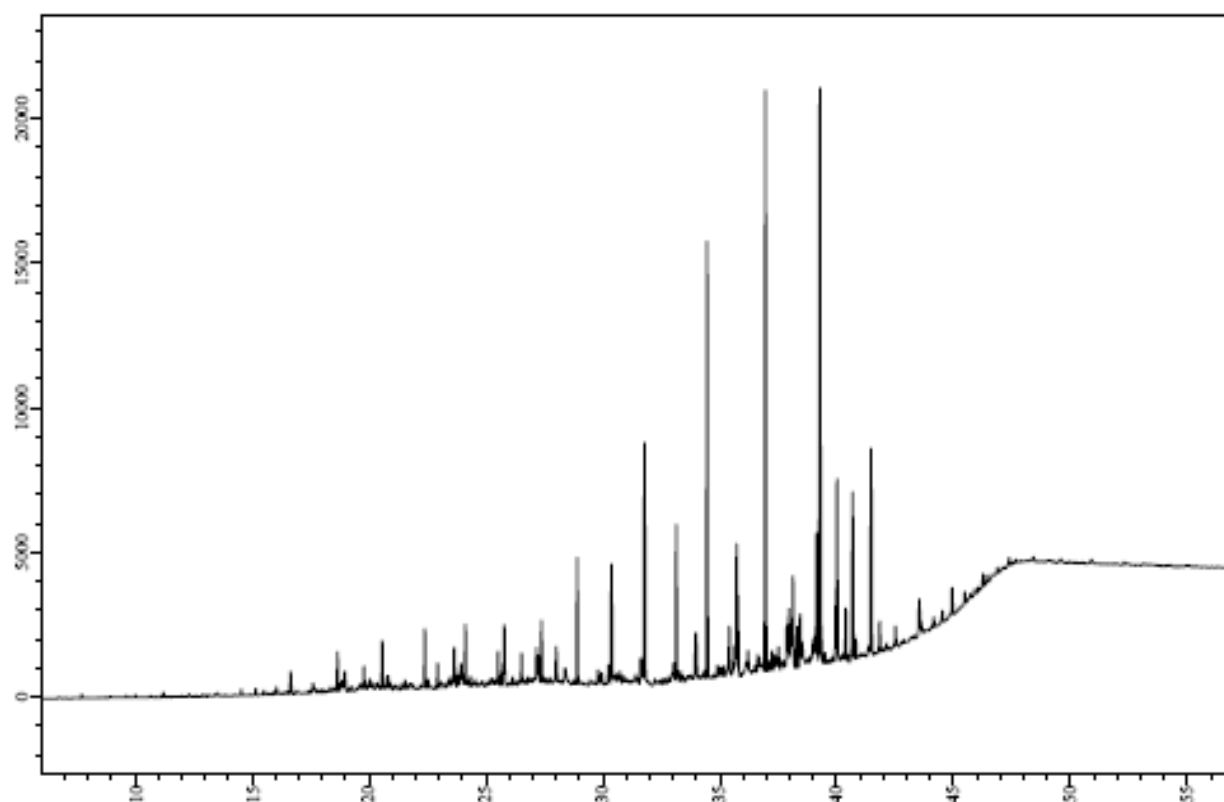


00,2006040-13996-07G-3 ali-aro 0.9 mg
2006040-13996-MRM

MRM of 13 Channels El+
Sum
2.46e4

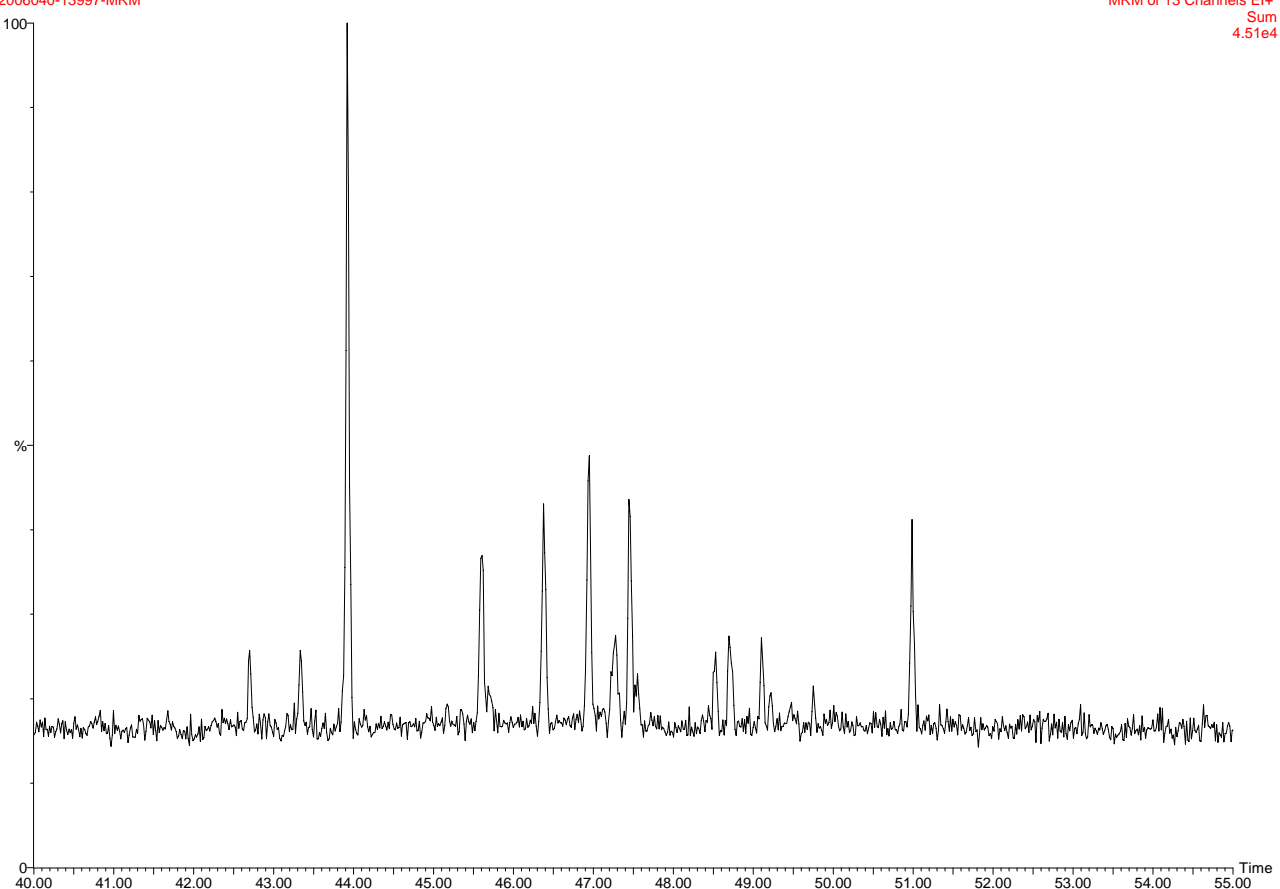


DANA06-07G-4



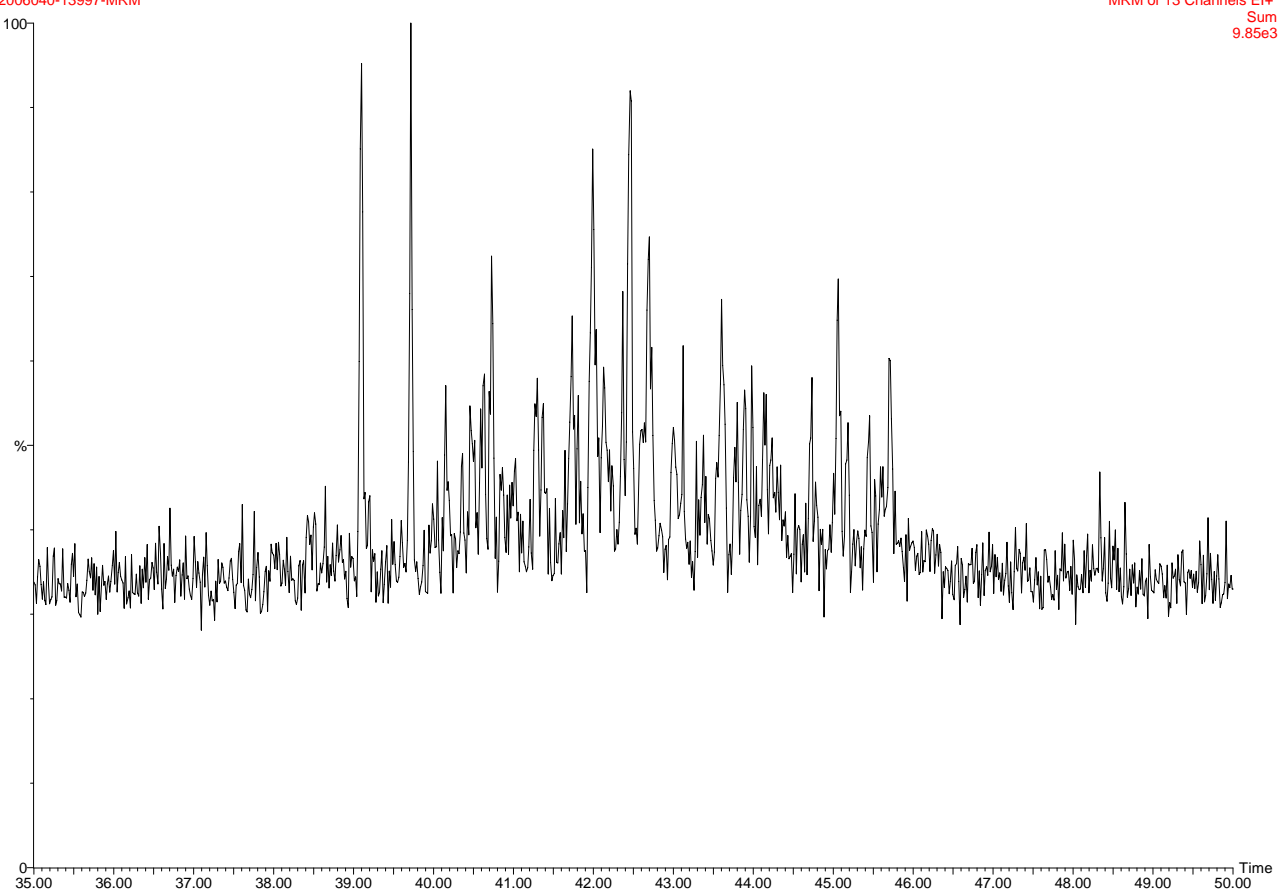
00,2006040-13997-07G-4 ali-aro 3.1 mg
2006040-13997-MRM

MRM of 13 Channels El+
Sum
4.51e4

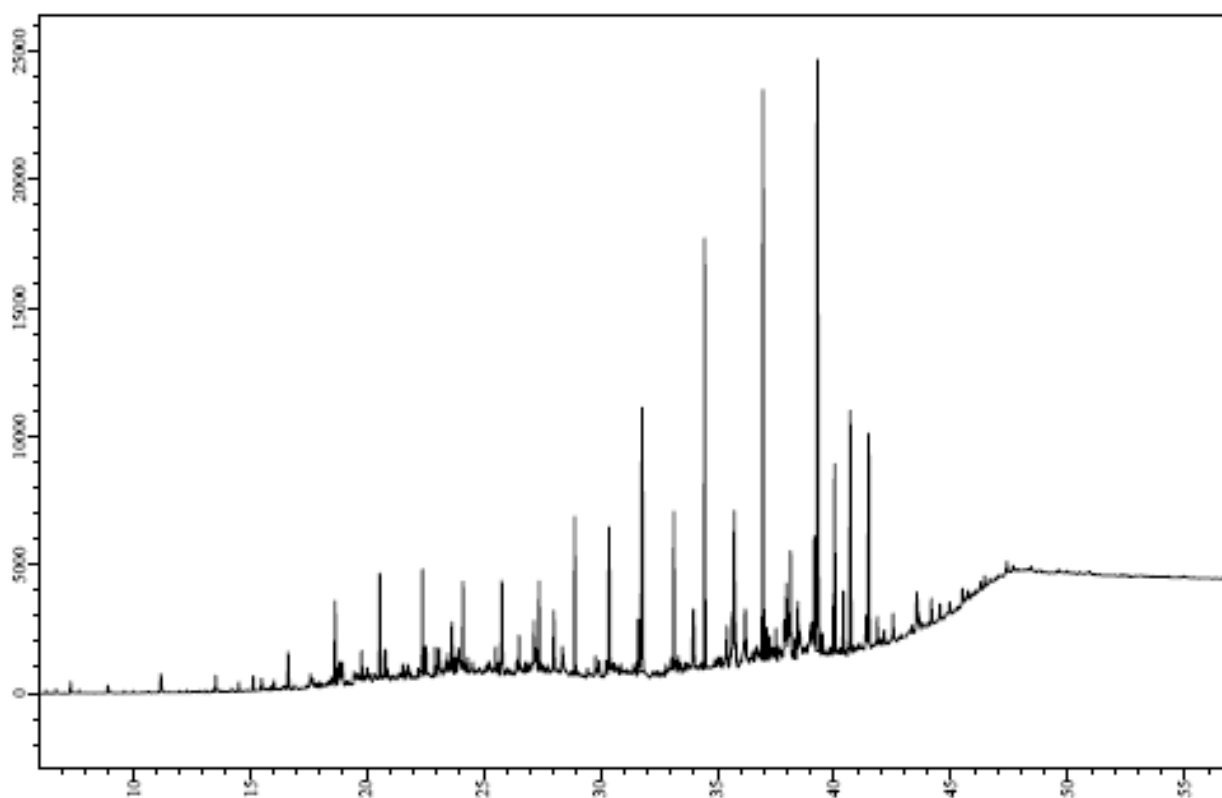


00,2006040-13997-07G-4 ali-aro 3.1 mg
2006040-13997-MRM

MRM of 13 Channels El+
Sum
9.85e3

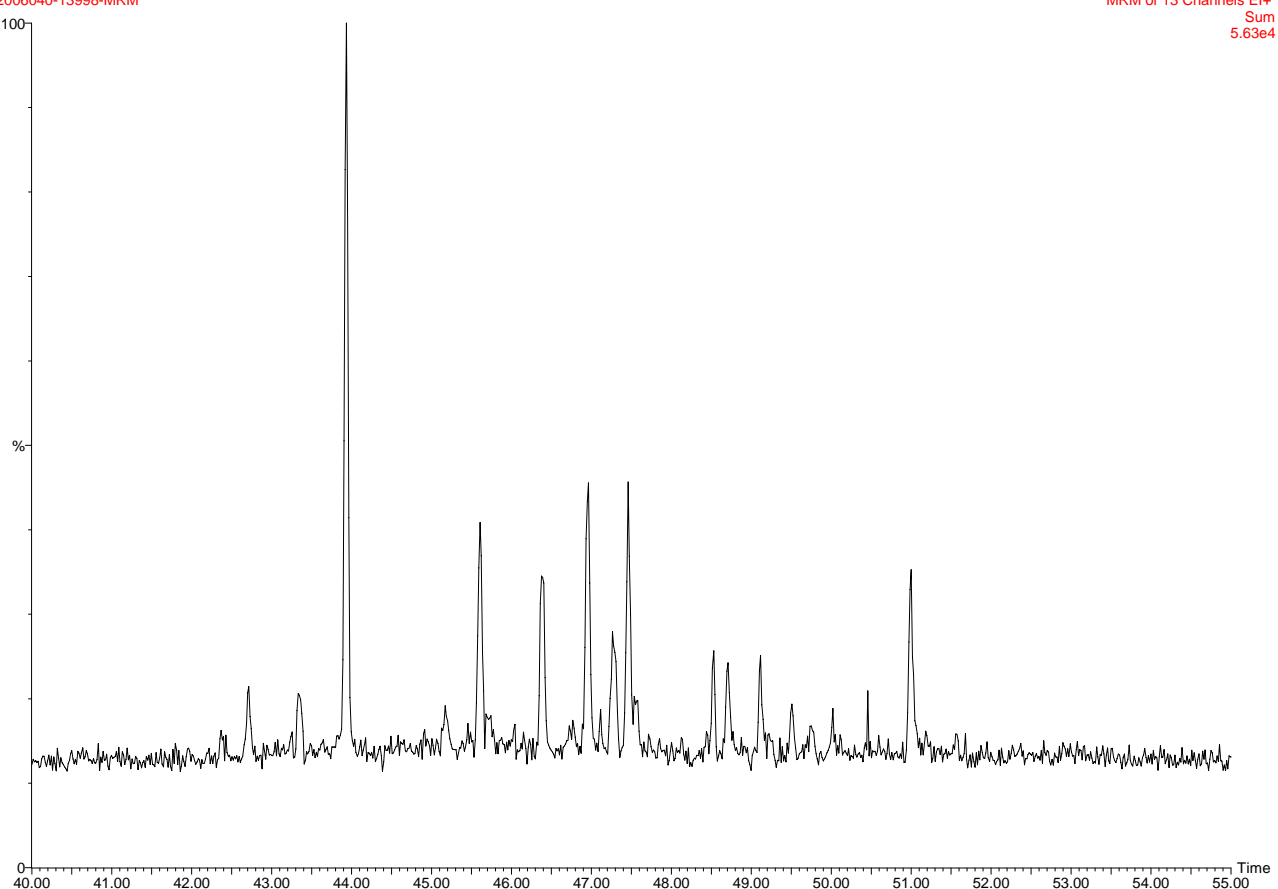


DANA06-07G-5



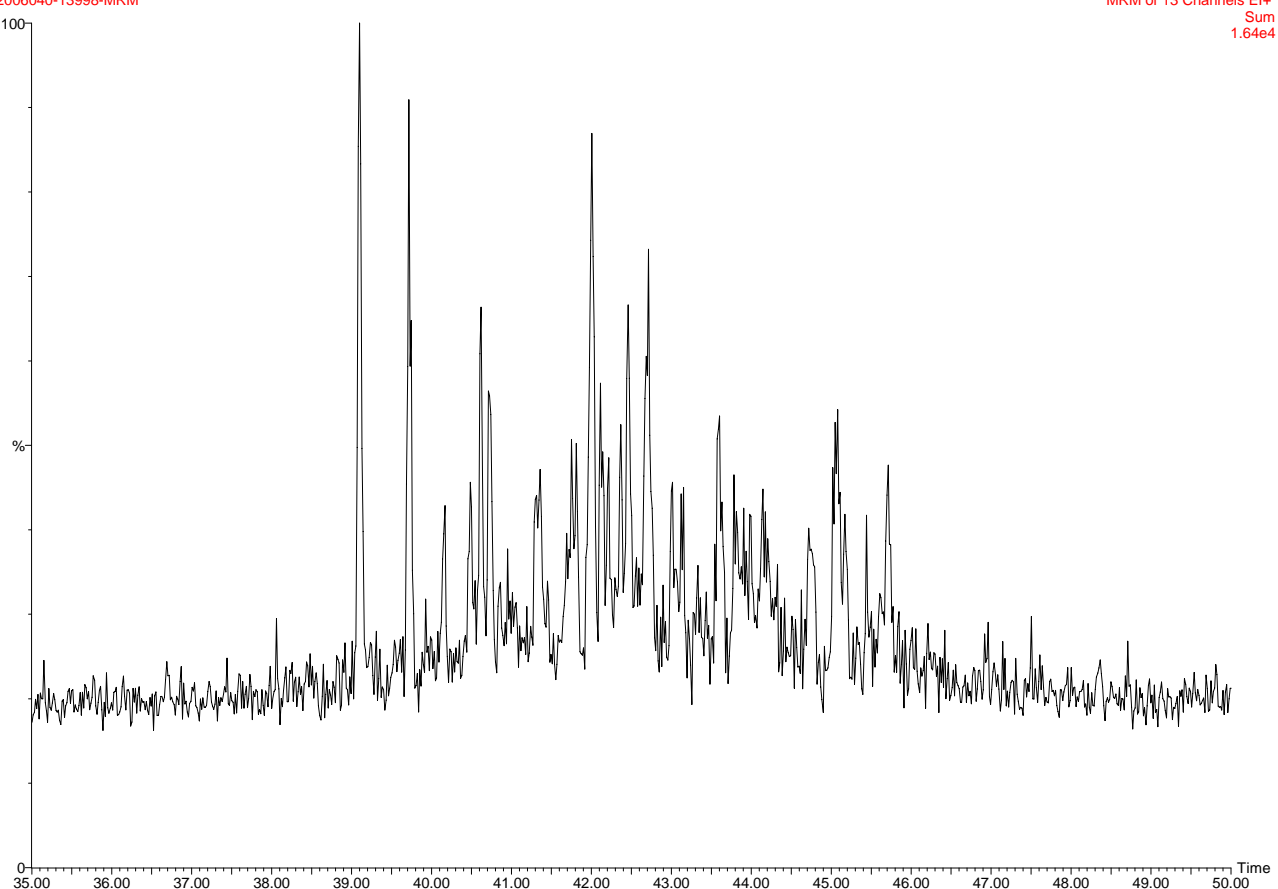
00,2006040-13998-07G-5 ali-aro 2.3 mg
2006040-13998-MRM

MRM of 13 Channels El+
Sum
5.63e4

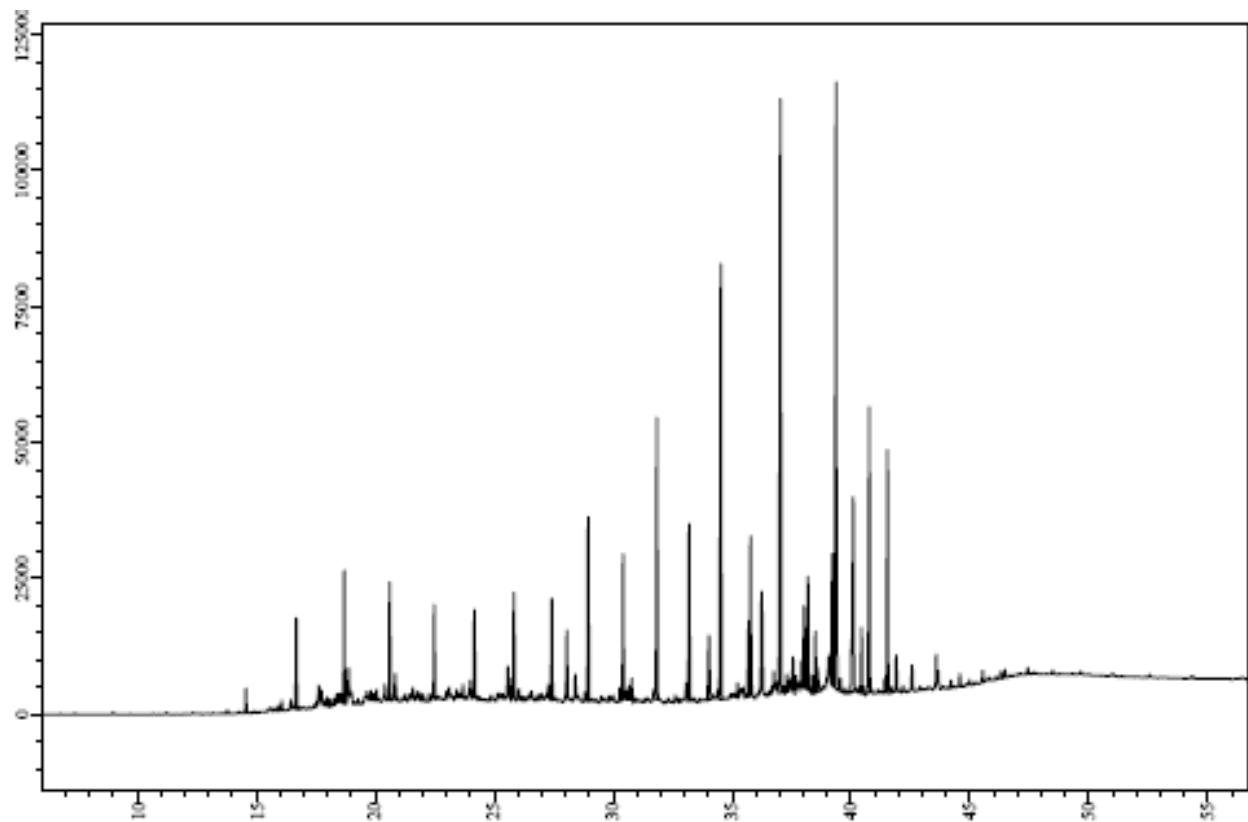


00,2006040-13998-07G-5 ali-aro 2.3 mg
2006040-13998-MRM

MRM of 13 Channels El+
Sum
1.64e4

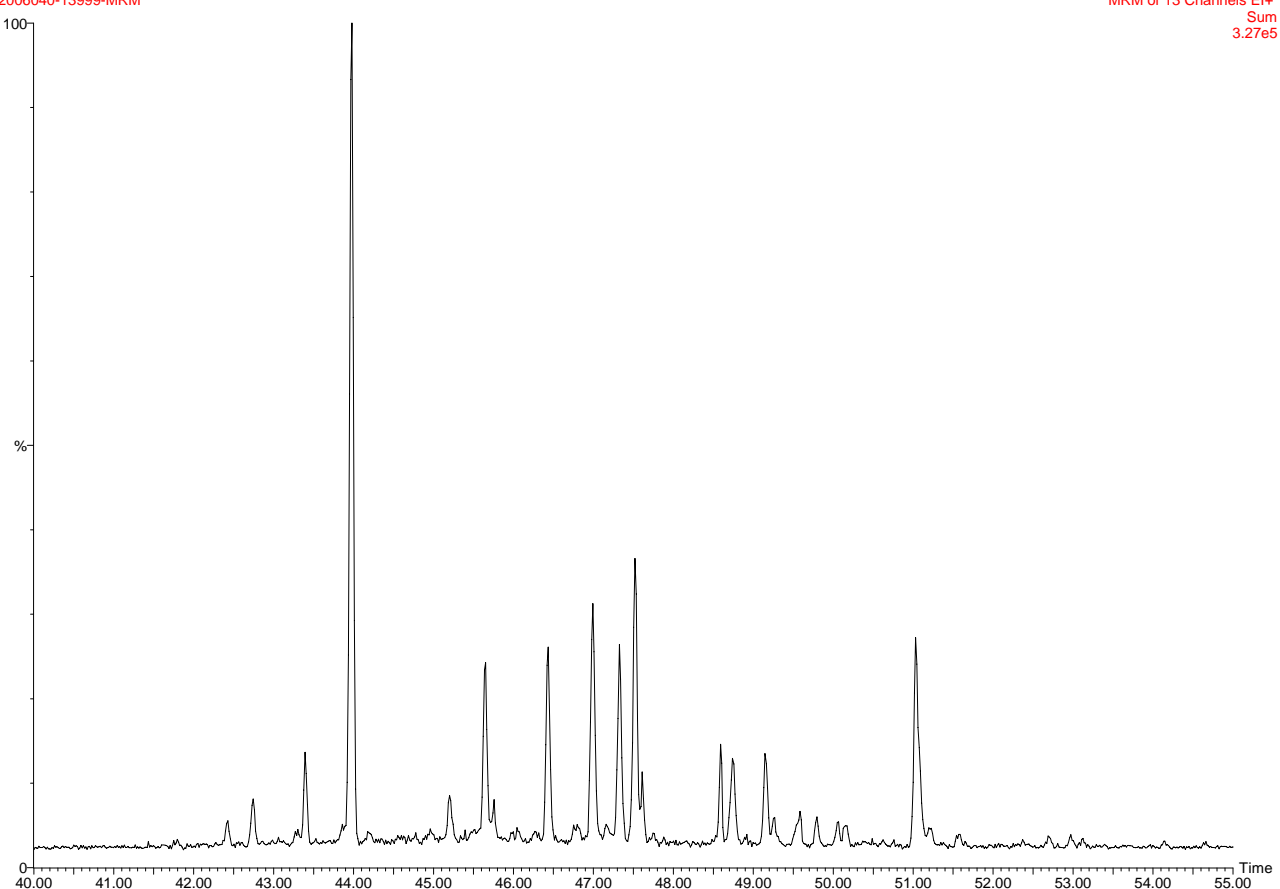


DANA06-07G-6



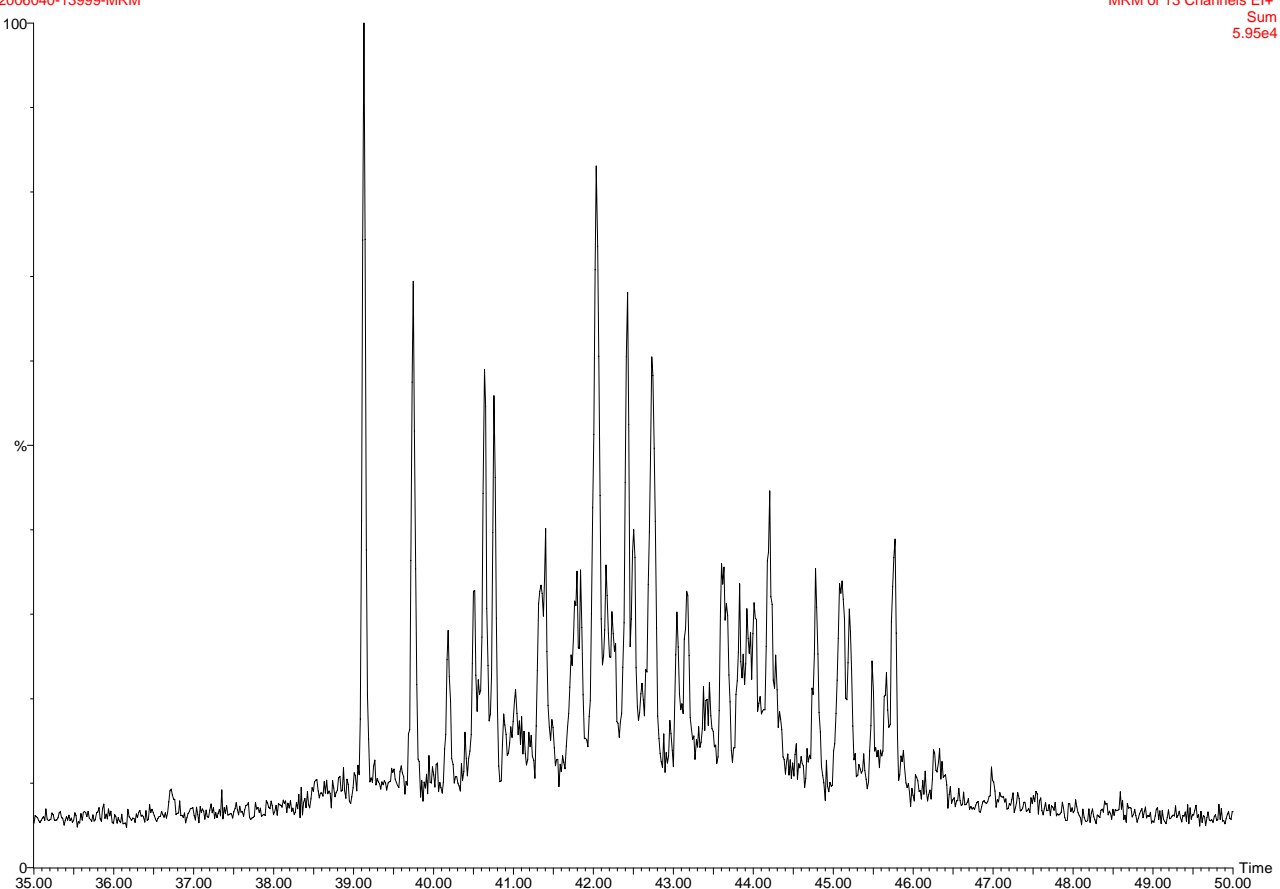
00,2006040-13999-07G-6 ali-aro 0.3 mg
2006040-13999-MRM

MRM of 13 Channels El+
Sum
3.27e5

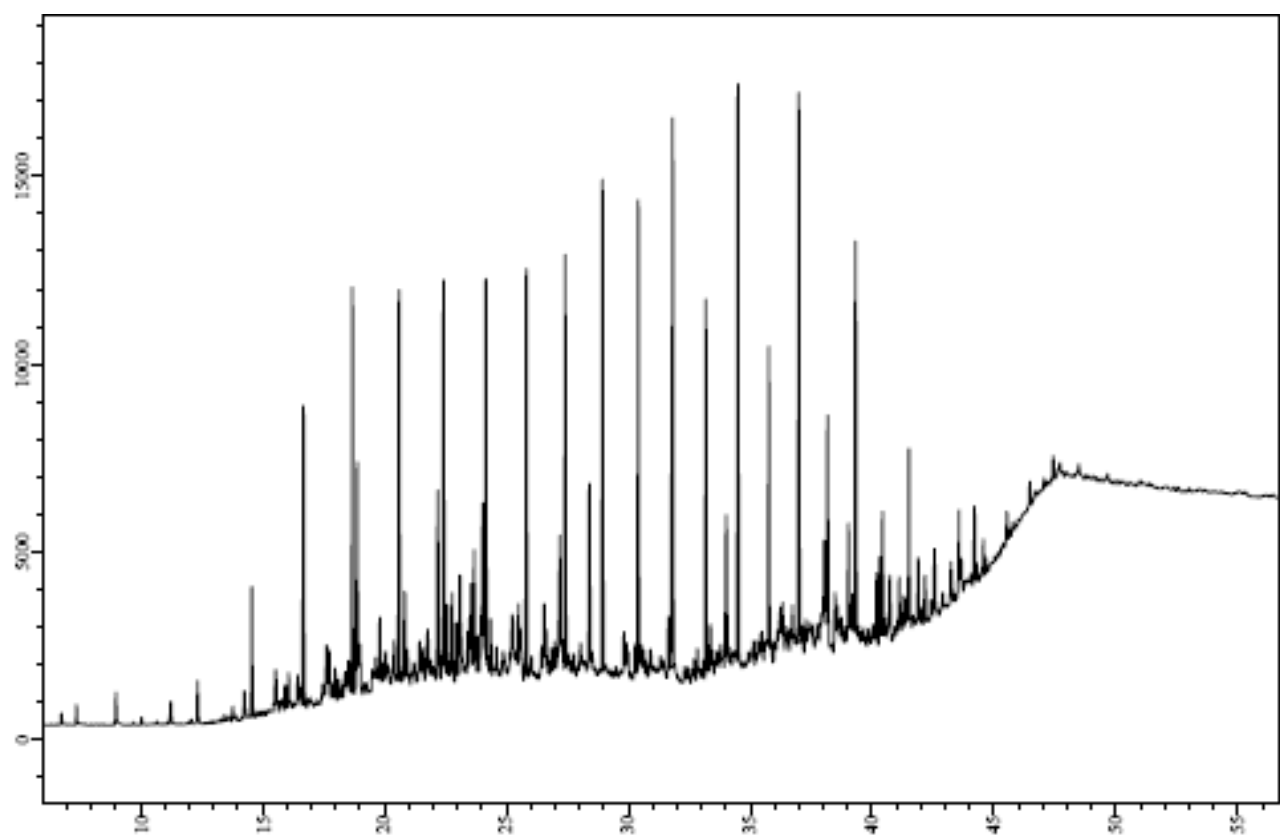


00,2006040-13999-07G-6 ali-aro 0.3 mg
2006040-13999-MRM

MRM of 13 Channels El+
Sum
5.95e4

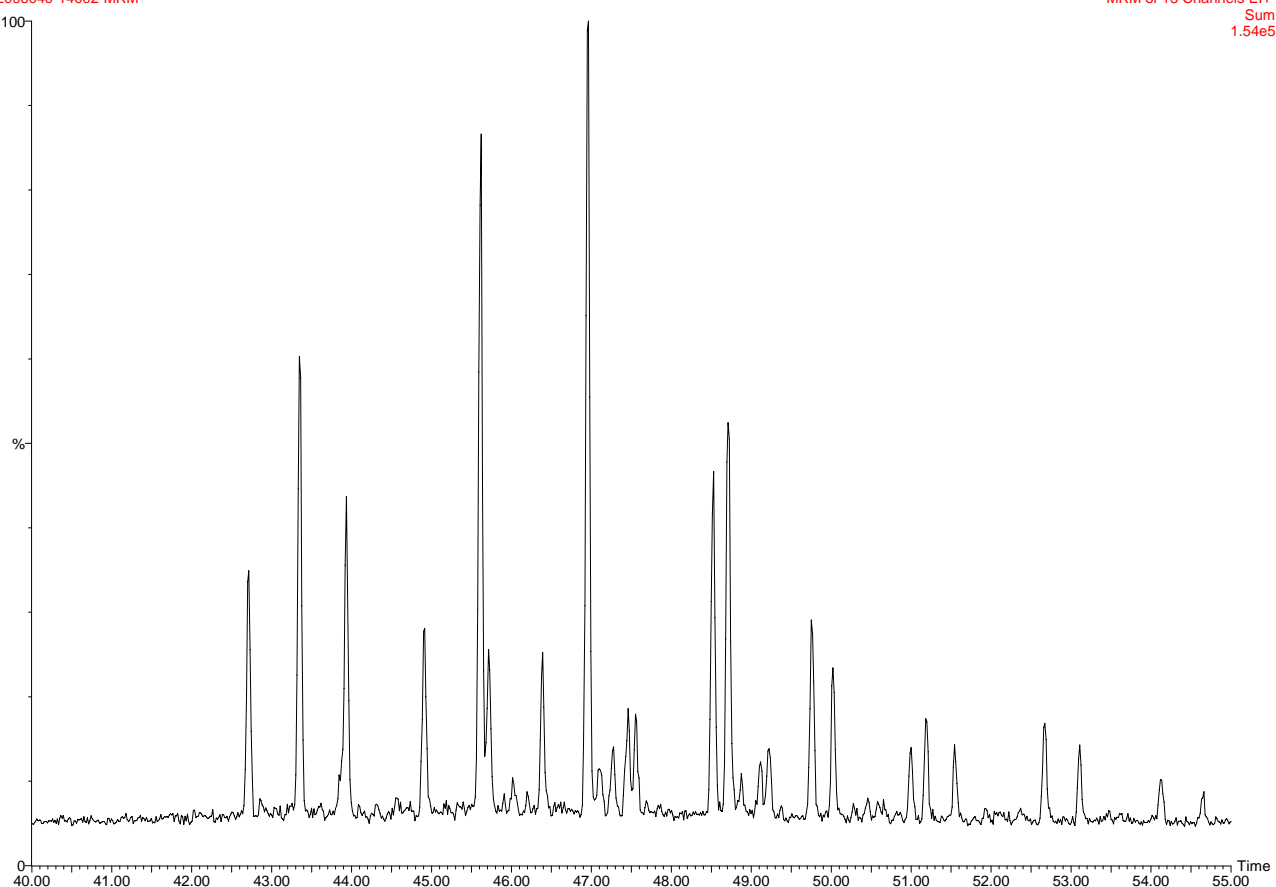


DANA06-21G-1



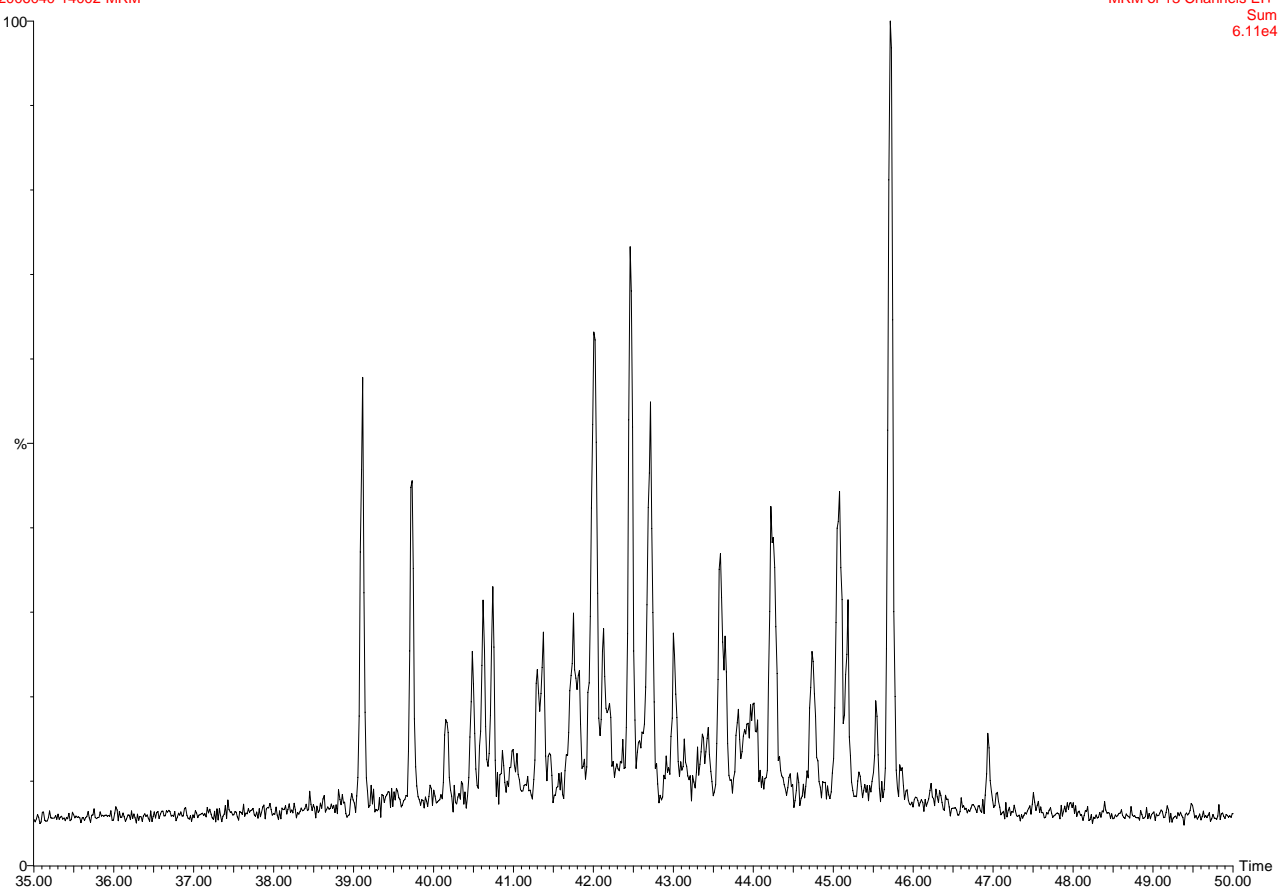
00,2006040-14002-21G-1 ali-aro 0.9 mg
2006040-14002-MRM

MRM of 13 Channels El+
Sum
1.54e5

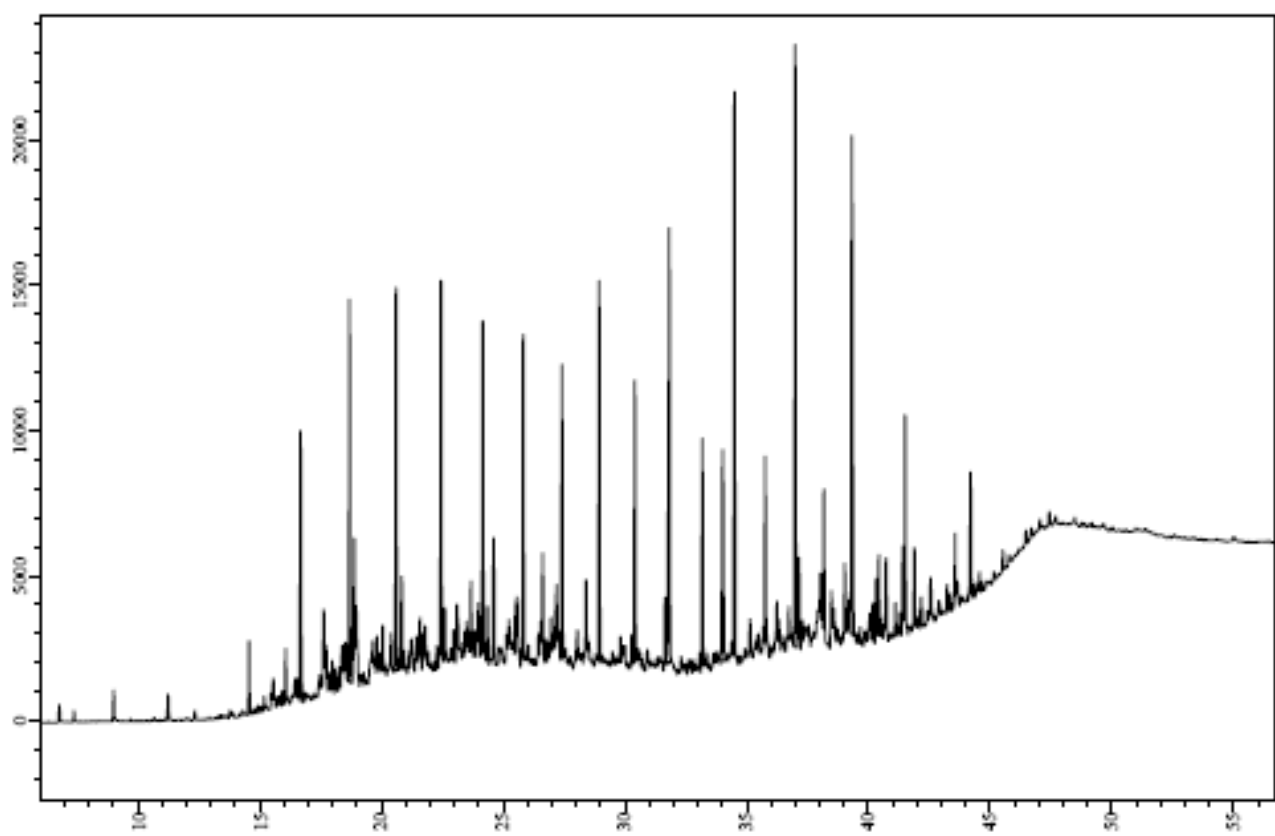


00,2006040-14002-21G-1 ali-aro 0.9 mg
2006040-14002-MRM

MRM of 13 Channels El+
Sum
 $6.11e4$

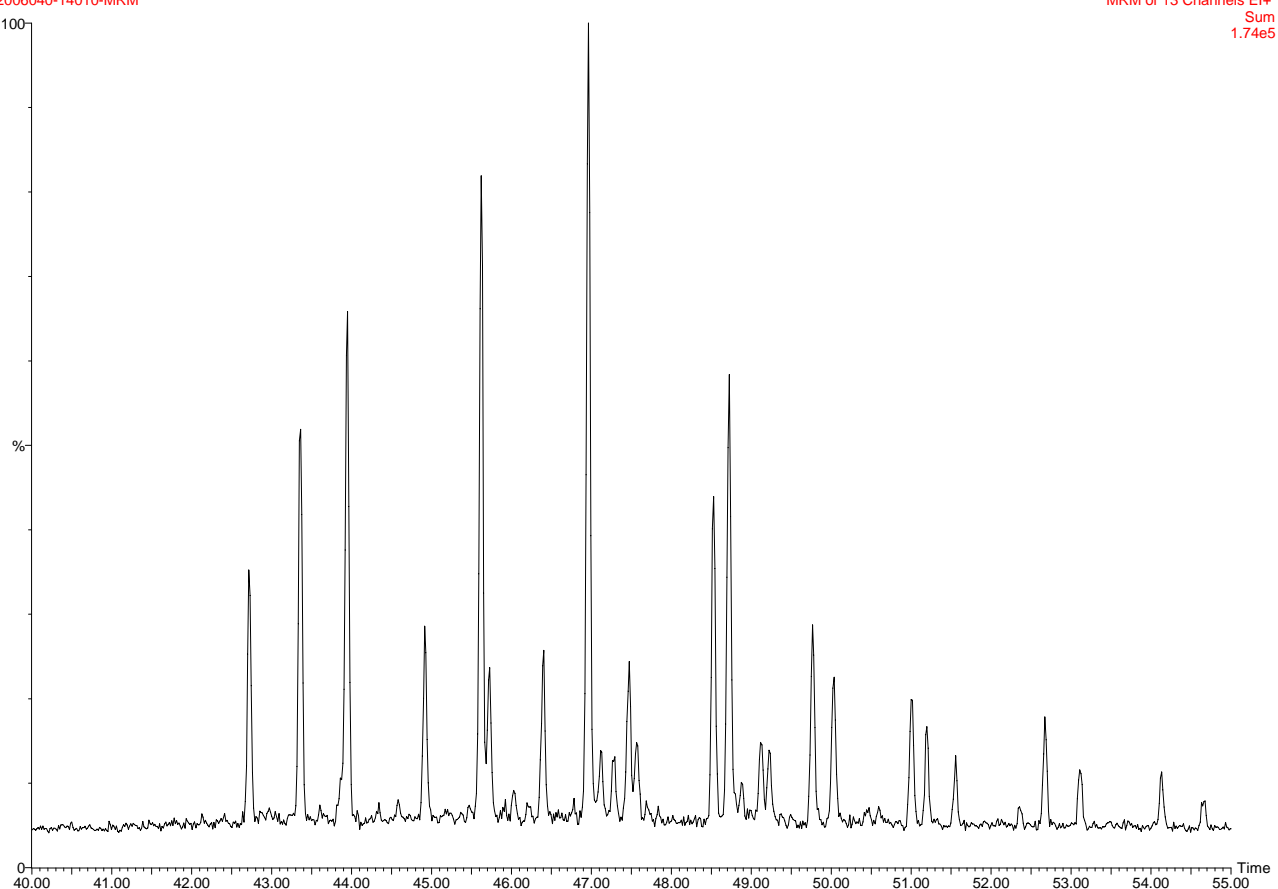


DANA06-48G-1



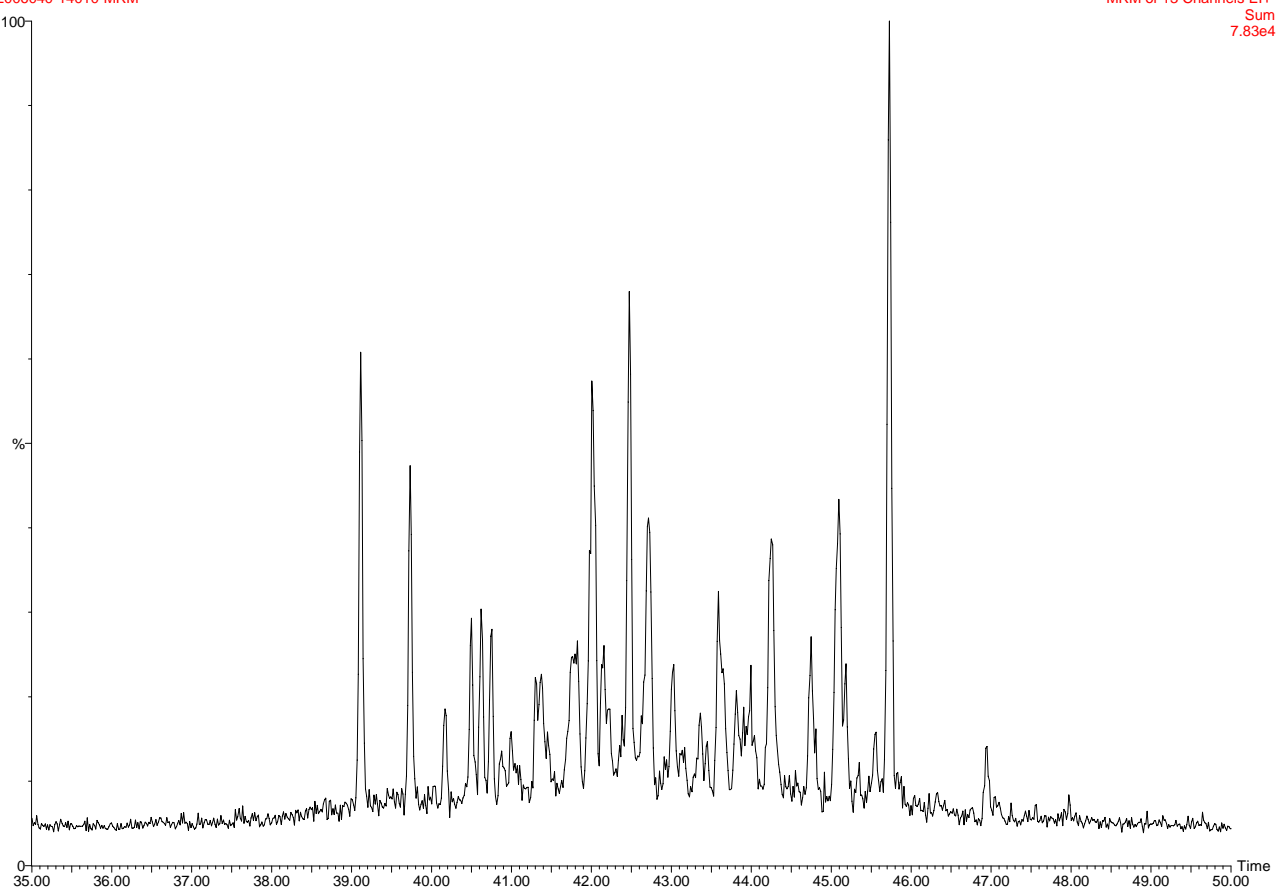
00,2006040-14010-48G-1 ali-aro 0.5 mg
2006040-14010-MRM

MRM of 13 Channels El+
Sum
1.74e5

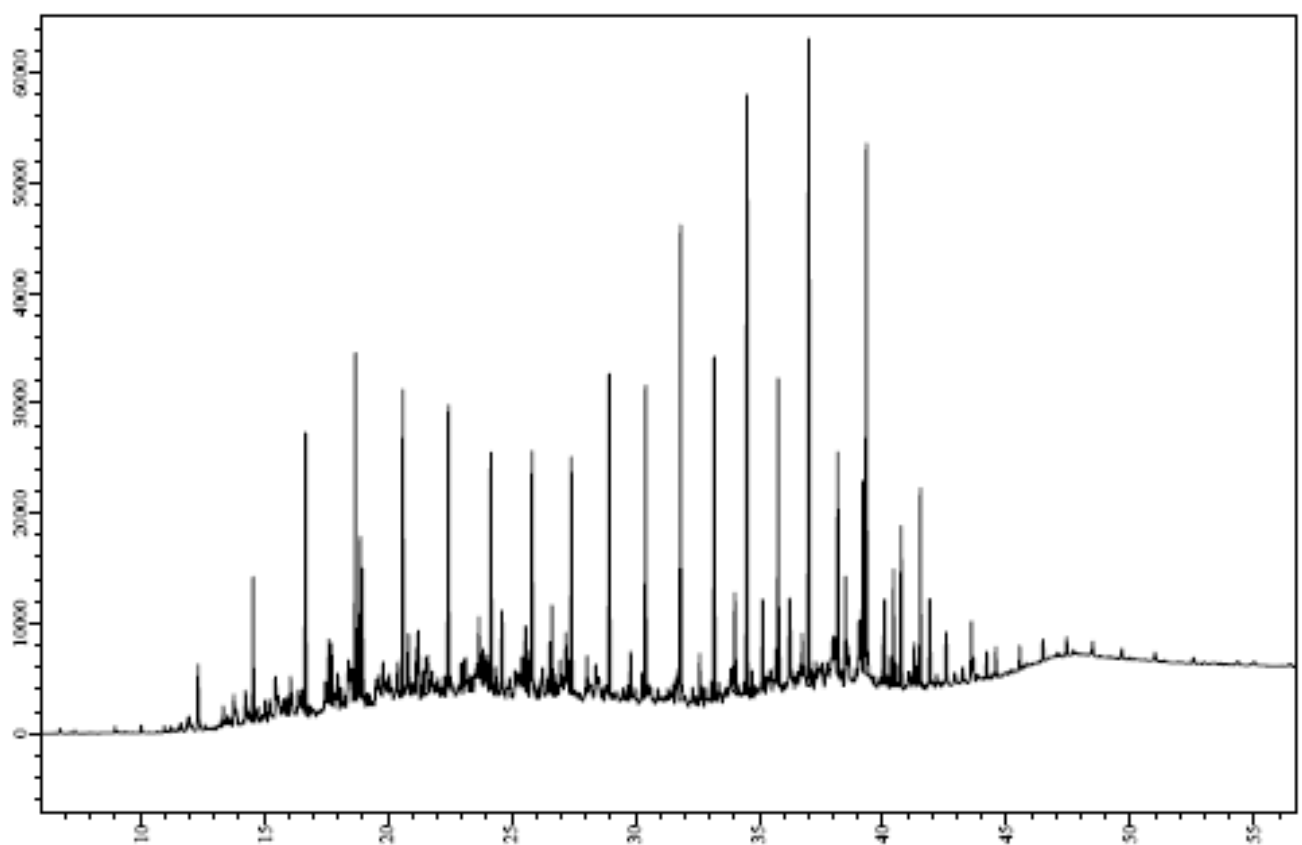


00,2006040-14010-48G-1 ali-aro 0.5 mg
2006040-14010-MRM

MRM of 13 Channels El+
Sum
7.83e4

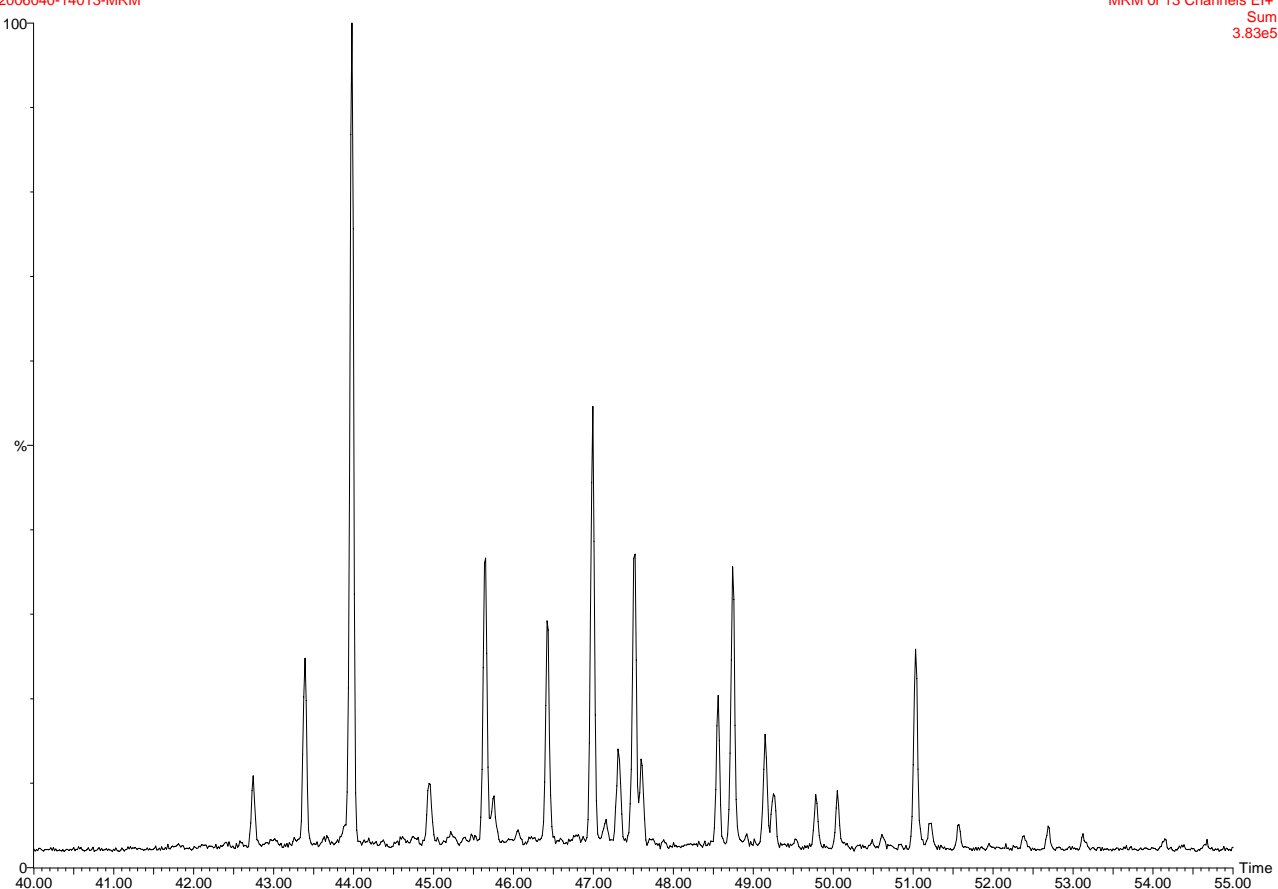


DANA06-48G-4



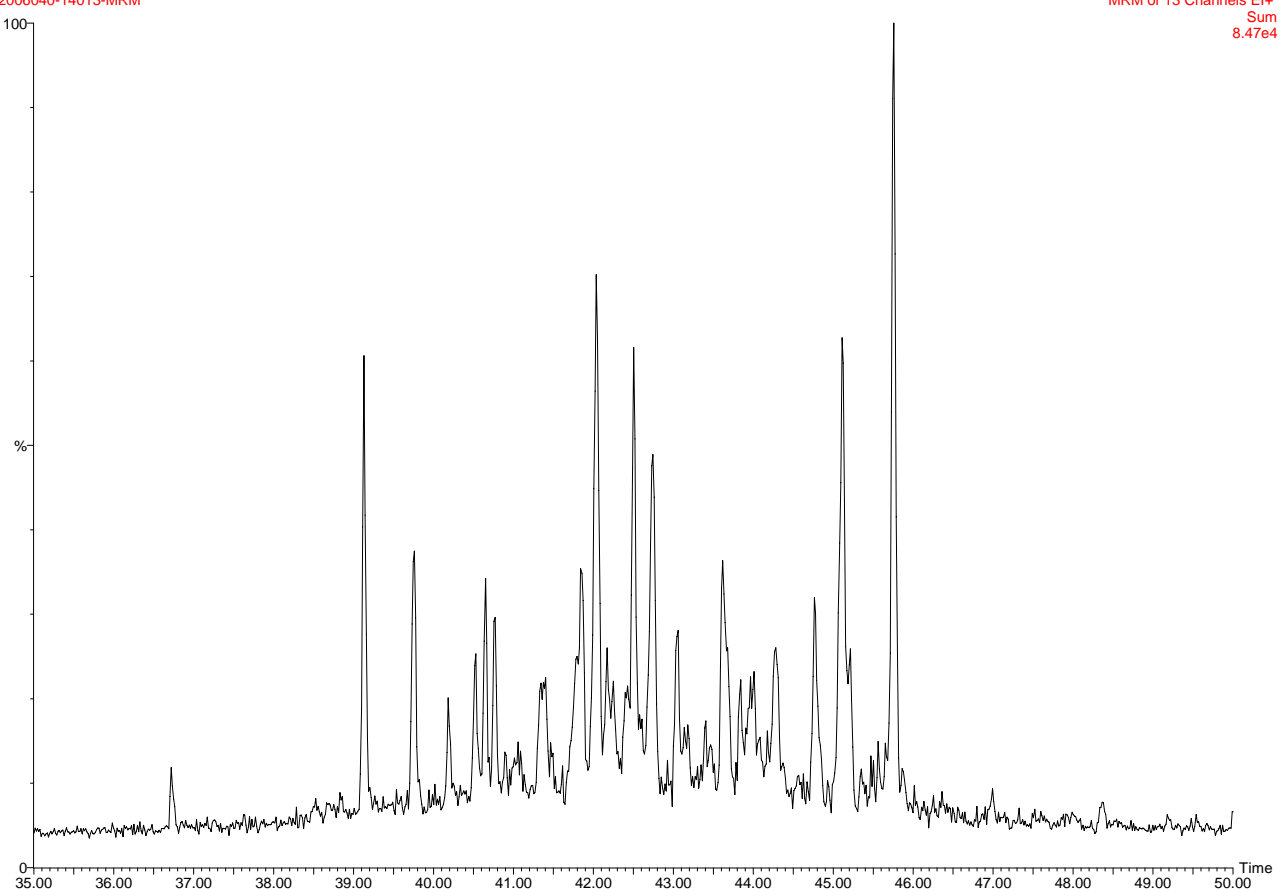
00,2006040-14013-48G-4 ali-aro 0.4 mg
2006040-14013-MRM

MRM of 13 Channels El+
Sum
3.83e5

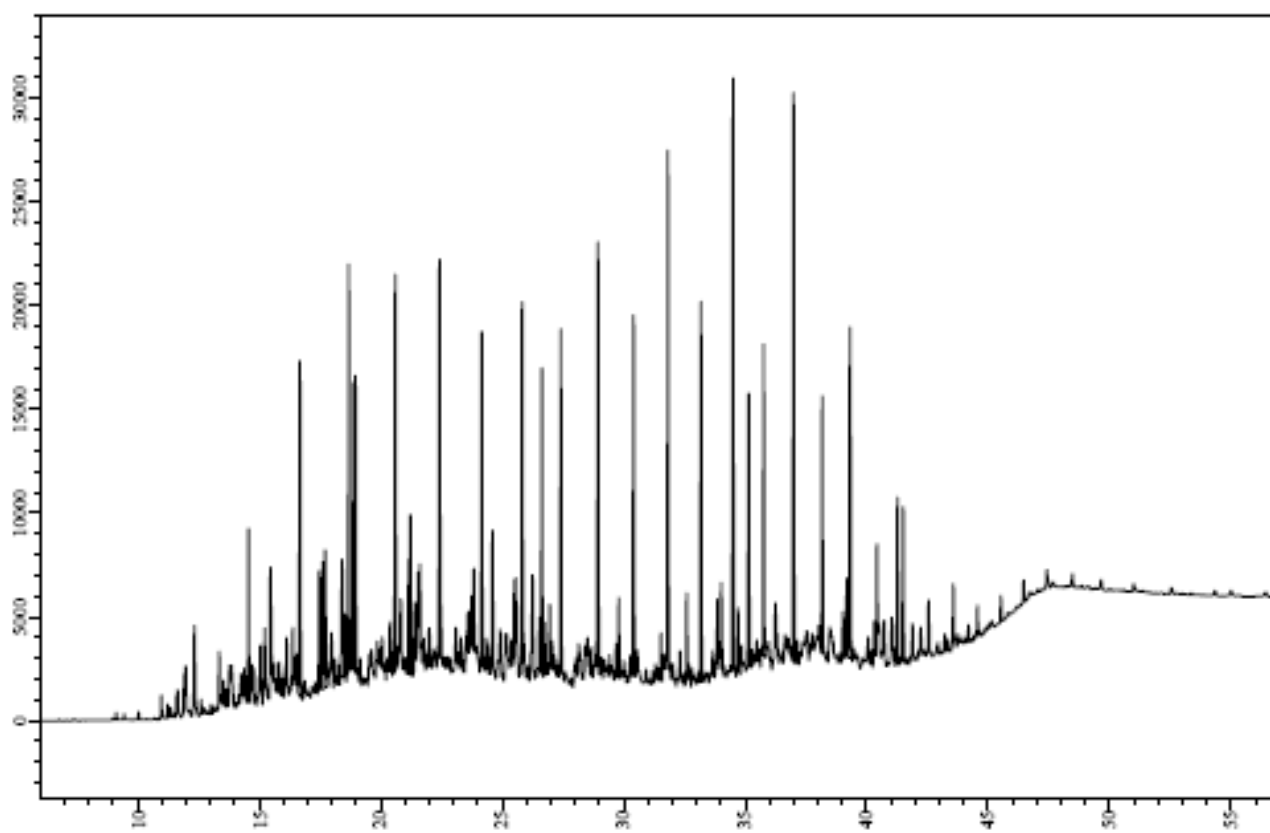


00,2006040-14013-48G-4 ali-aro 0.4 mg
2006040-14013-MRM

MRM of 13 Channels El+
Sum
8.47e4

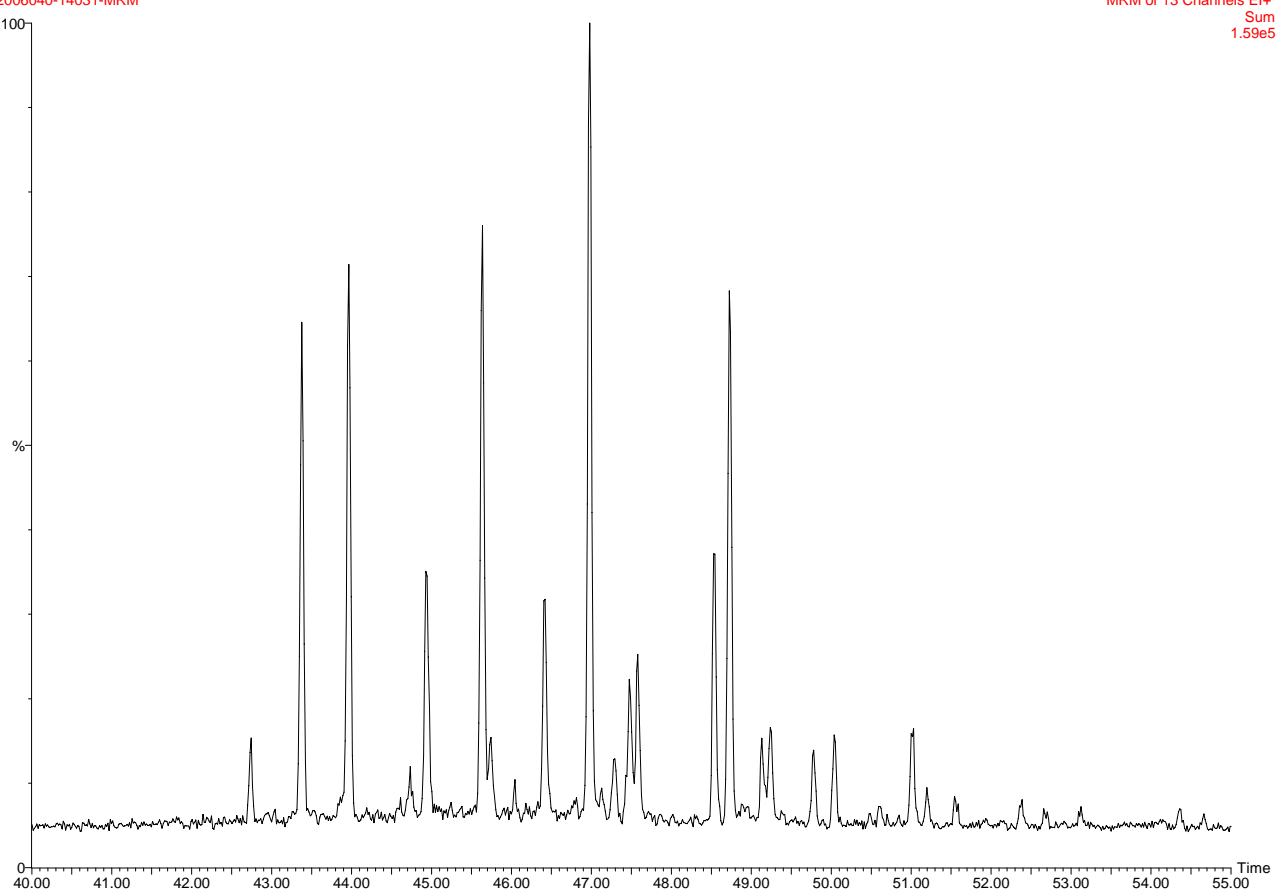


DANA06-61G-2



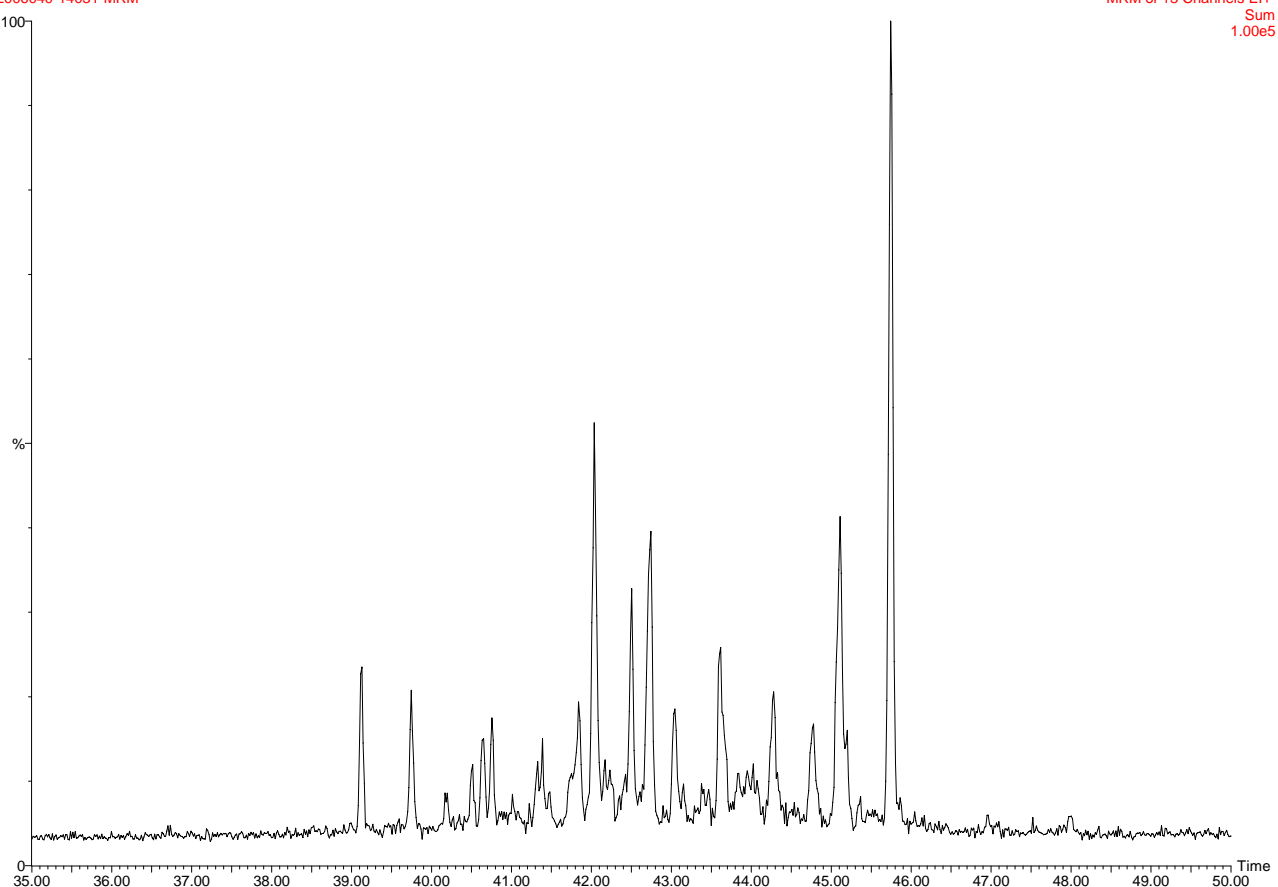
00,2006040-14031-61G-2 ali-aro 1.4 mg
2006040-14031-MRM

MRM of 13 Channels El+
Sum
1.59e5

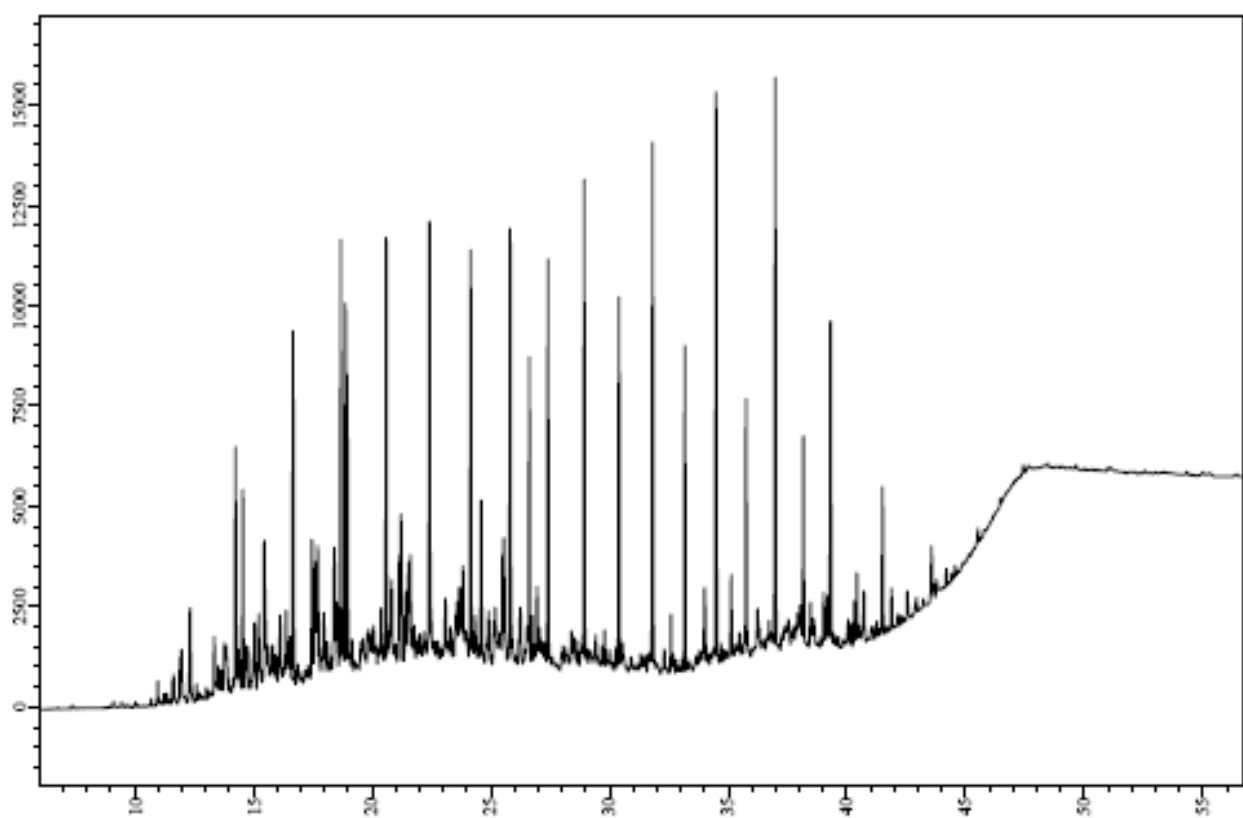


00,2006040-14031-61G-2 ali-aro 1.4 mg
2006040-14031-MRM

MRM of 13 Channels El+
Sum
1.00e5

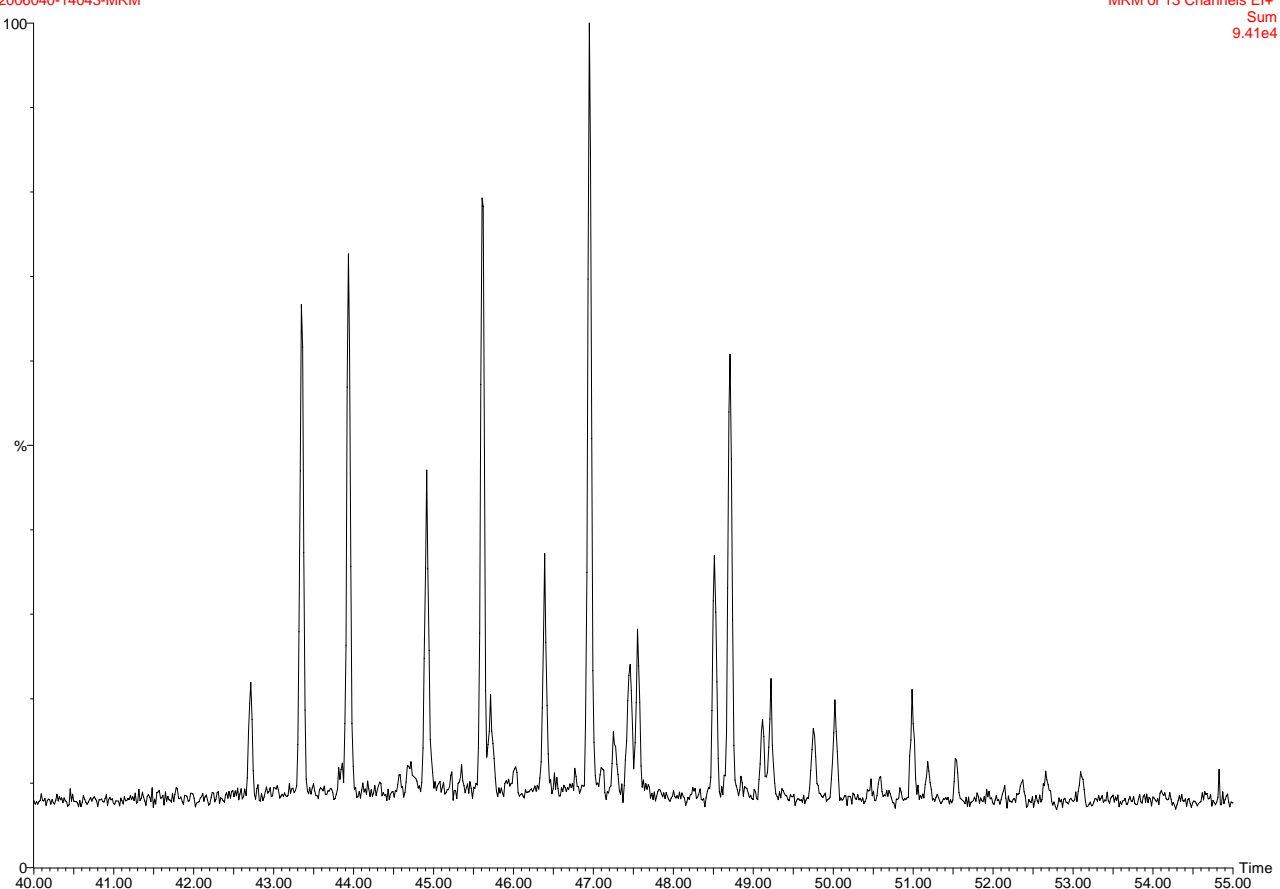


DANA06-69G-1



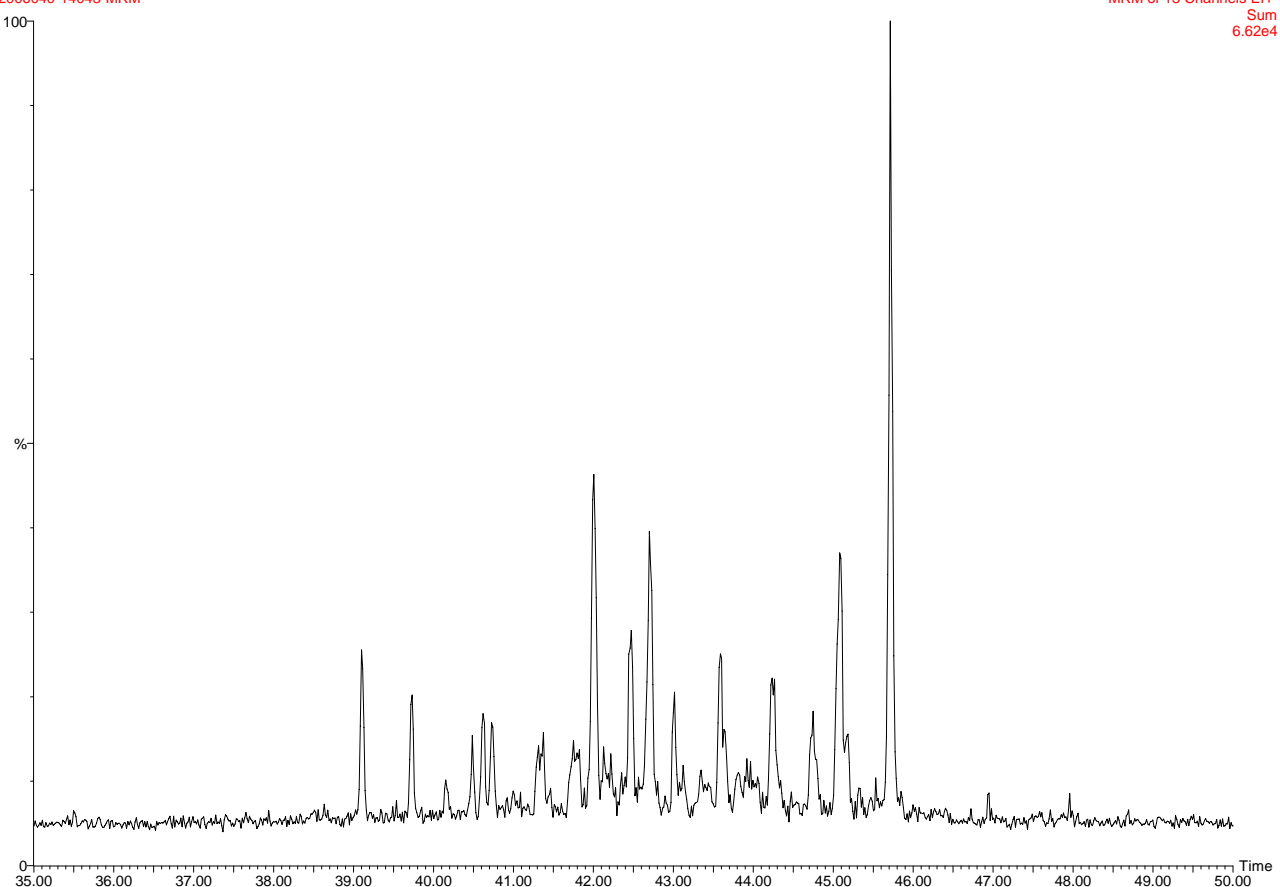
00,2006040-14043-69G-1 ali-aro 2.6 mg
2006040-14043-MRM

MRM of 13 Channels El+
Sum
9.41e4

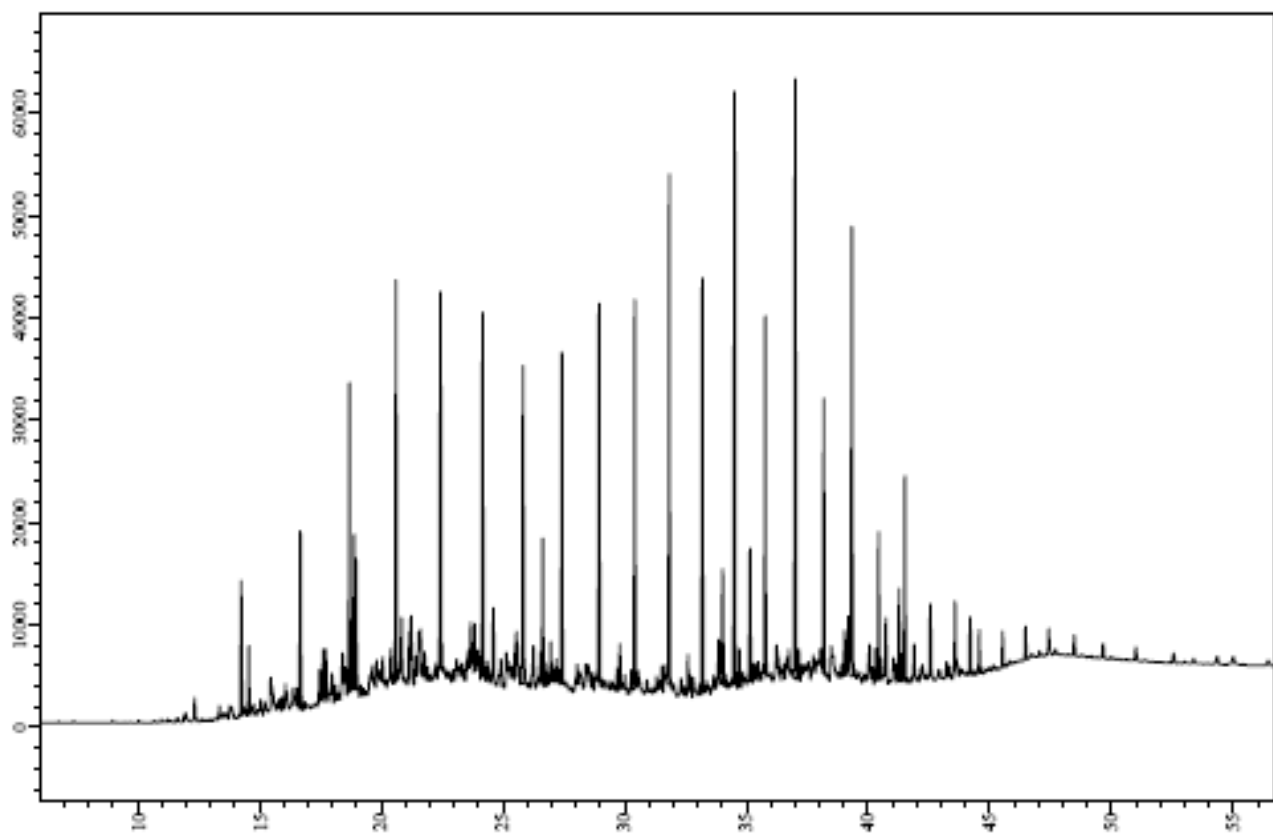


00,2006040-14043-69G-1 ali-aro 2.6 mg
2006040-14043-MRM

MRM of 13 Channels El+
Sum
6.62e4

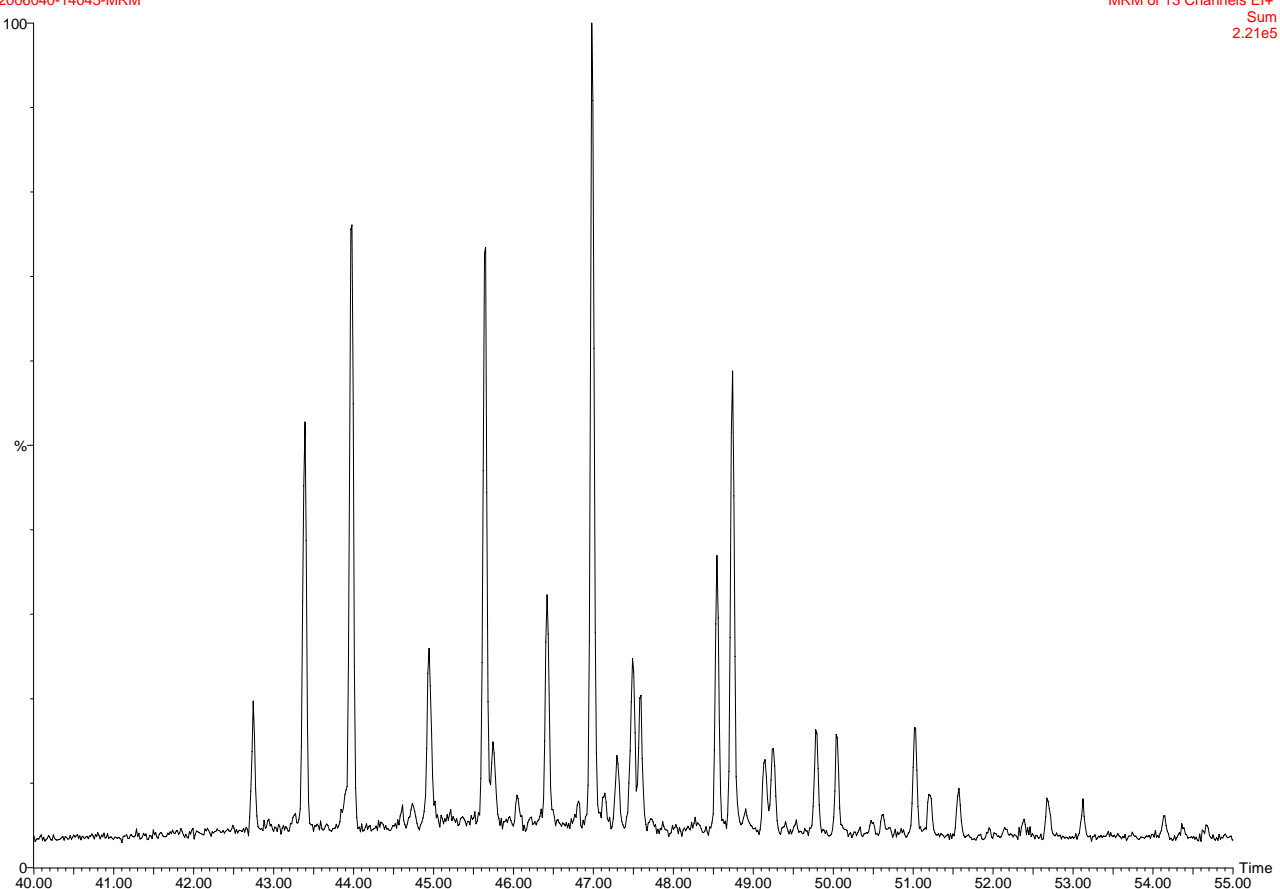


DANA06-69G-3



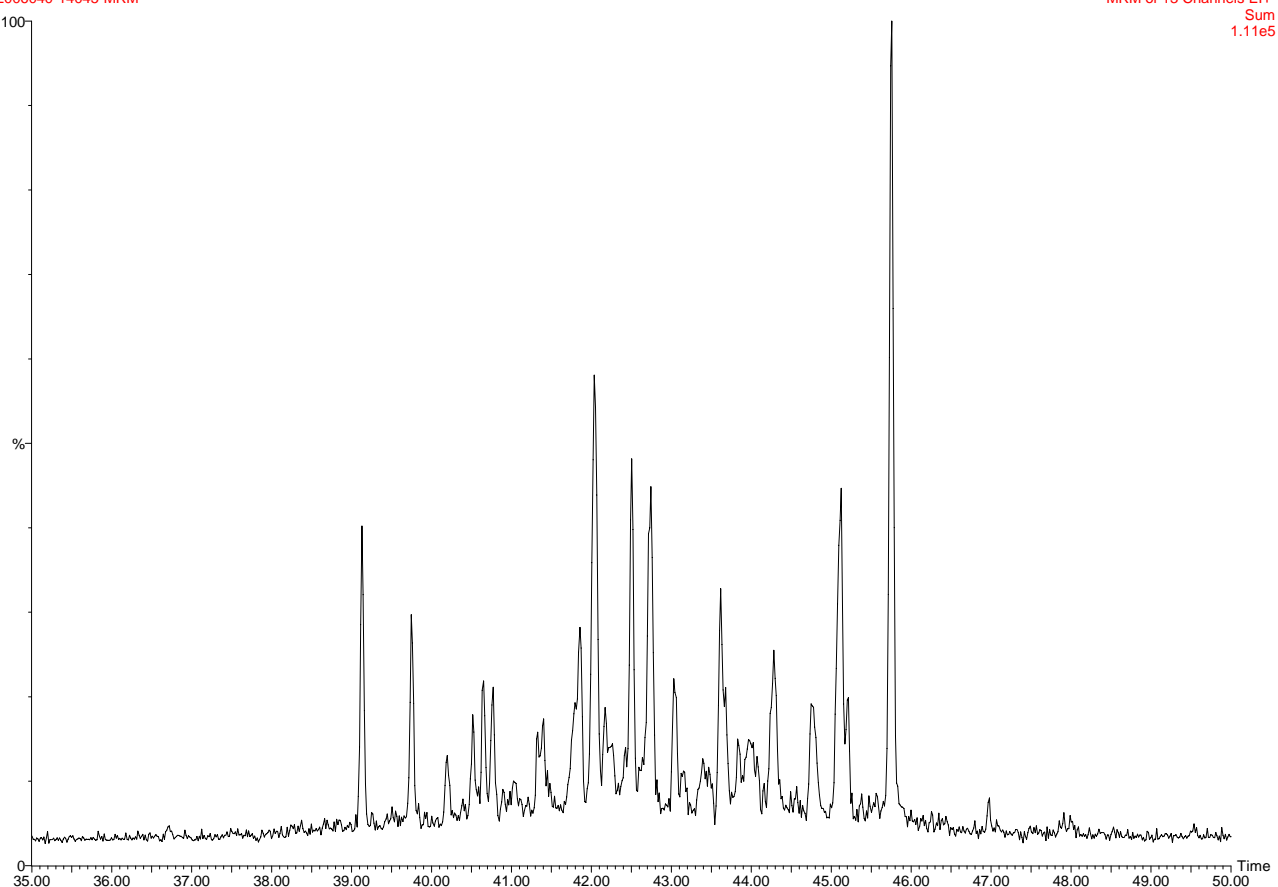
00,2006040-14045-69G-3 ali-aro 0.3 mg
2006040-14045-MRM

MRM of 13 Channels El+
Sum
2.21e5

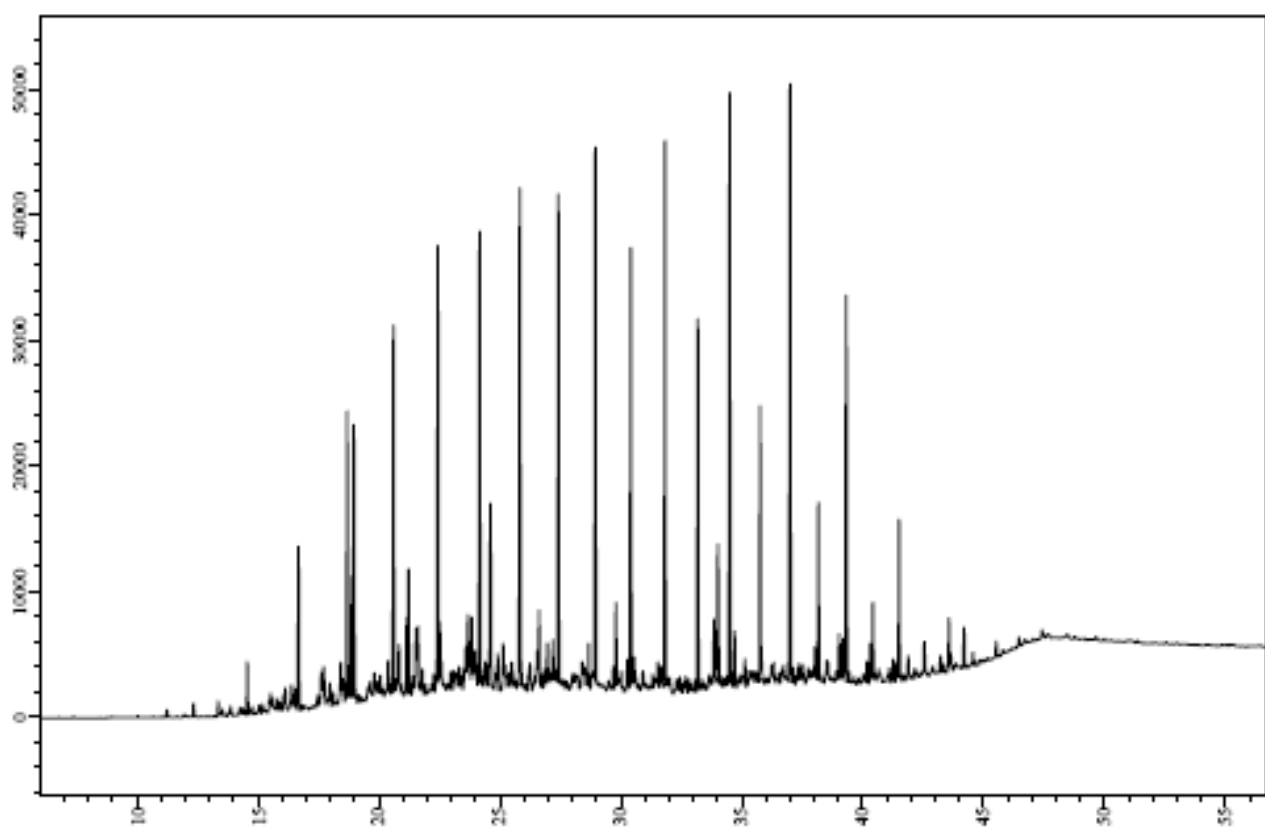


00,2006040-14045-69G-3 ali-aro 0.3 mg
2006040-14045-MRM

MRM of 13 Channels El+
Sum
1.11e5

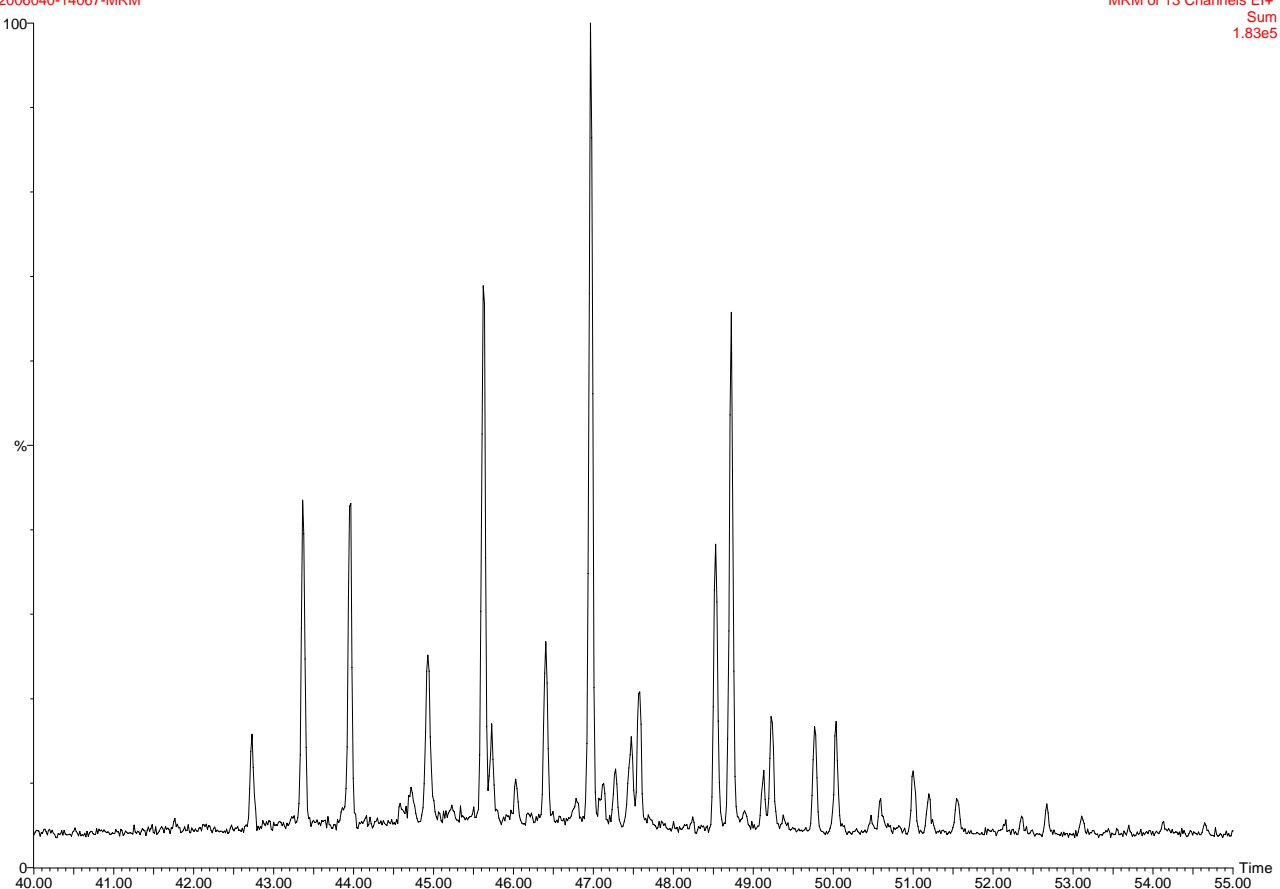


DANA06-79G-1



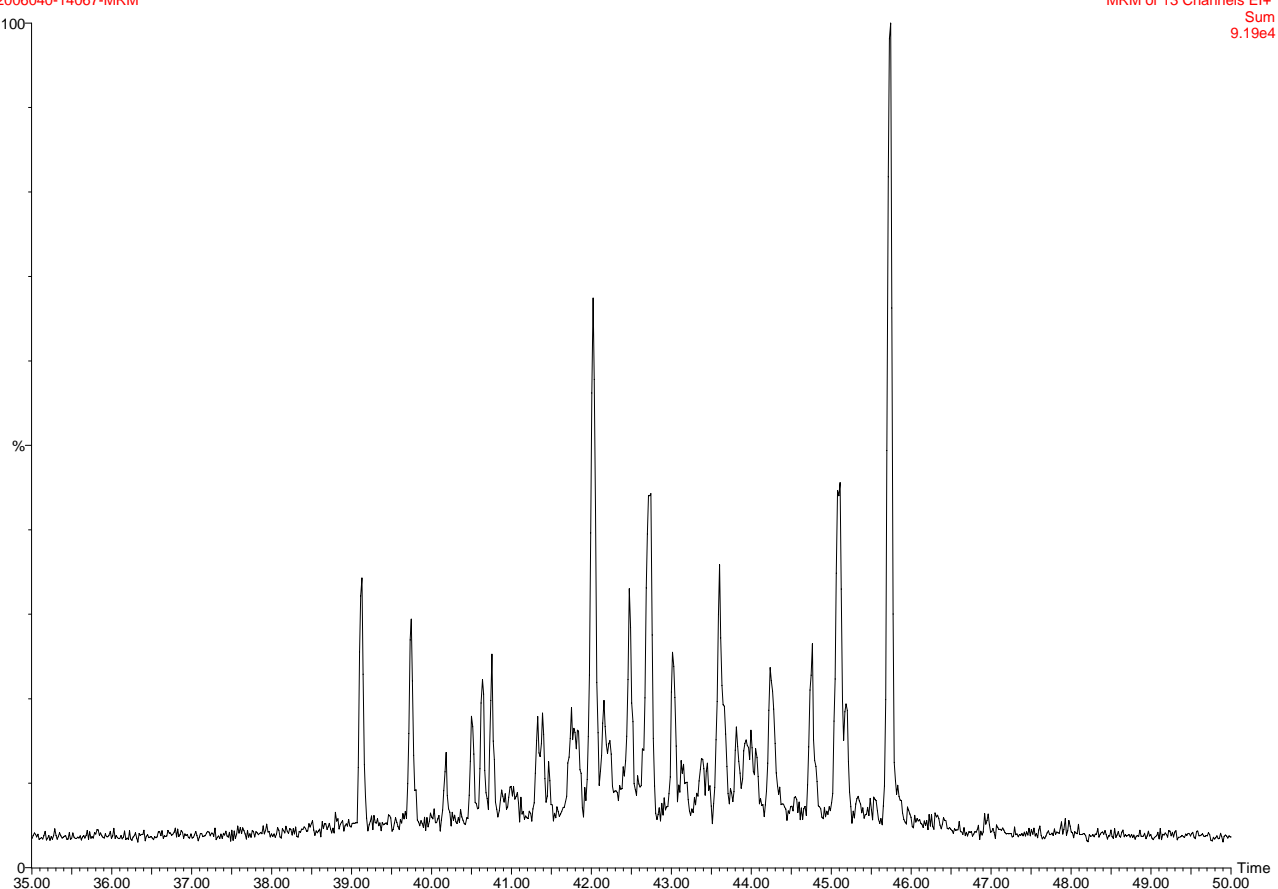
00,2006040-14067-79G-1 ali-aro 0.2 mg
2006040-14067-MRM

MRM of 13 Channels El+
Sum
1.83e5

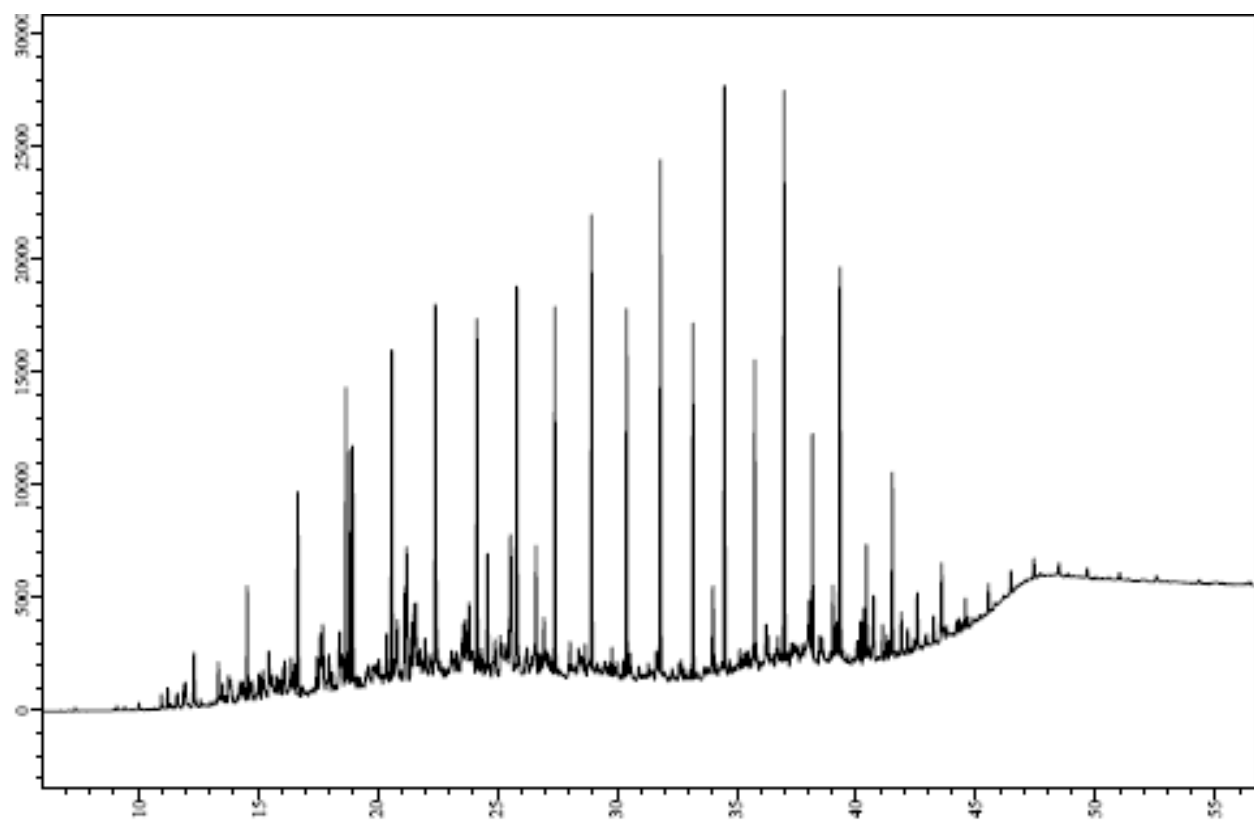


00,2006040-14067-79G-1 ali-aro 0.2 mg
2006040-14067-MRM

MRM of 13 Channels El+
Sum
9.19e4

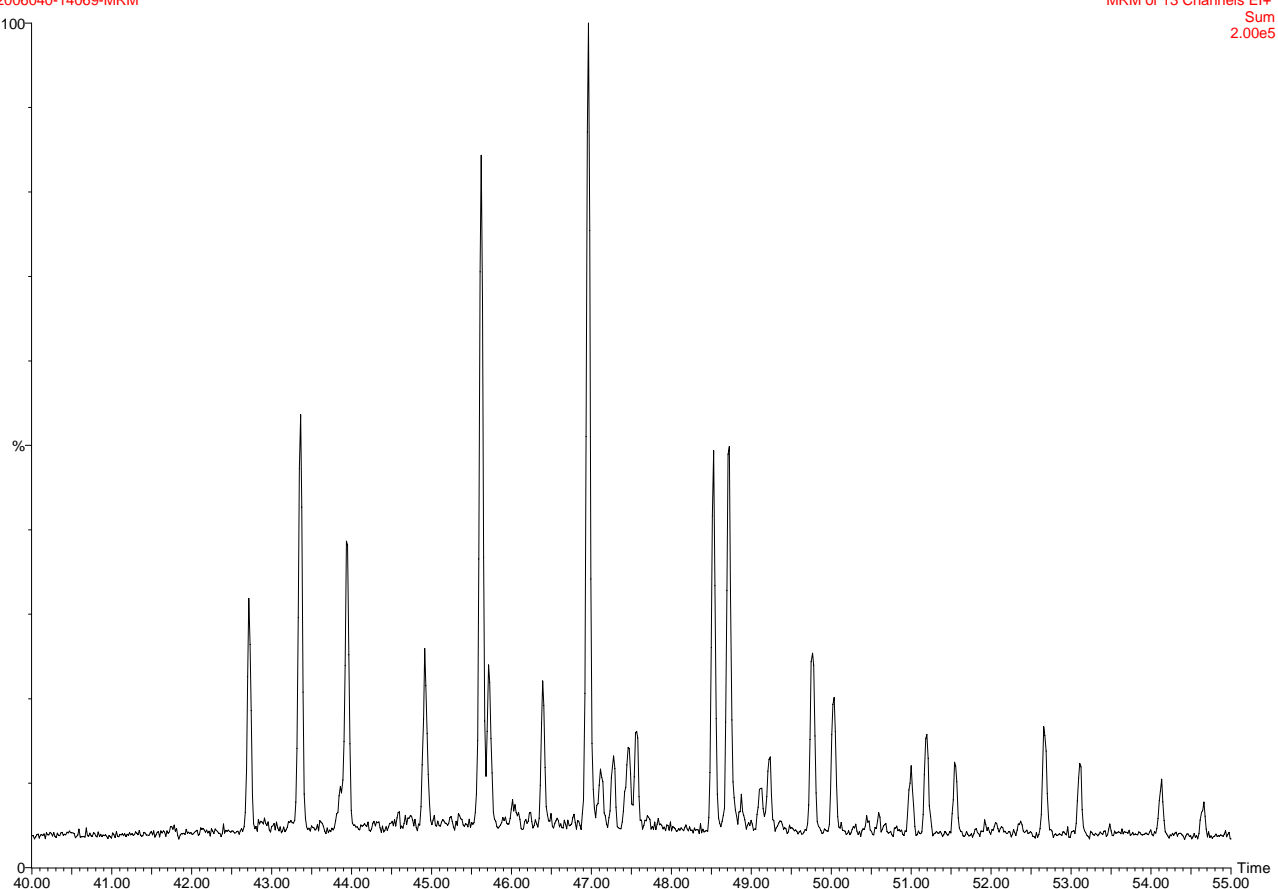


DANA06-79G-3



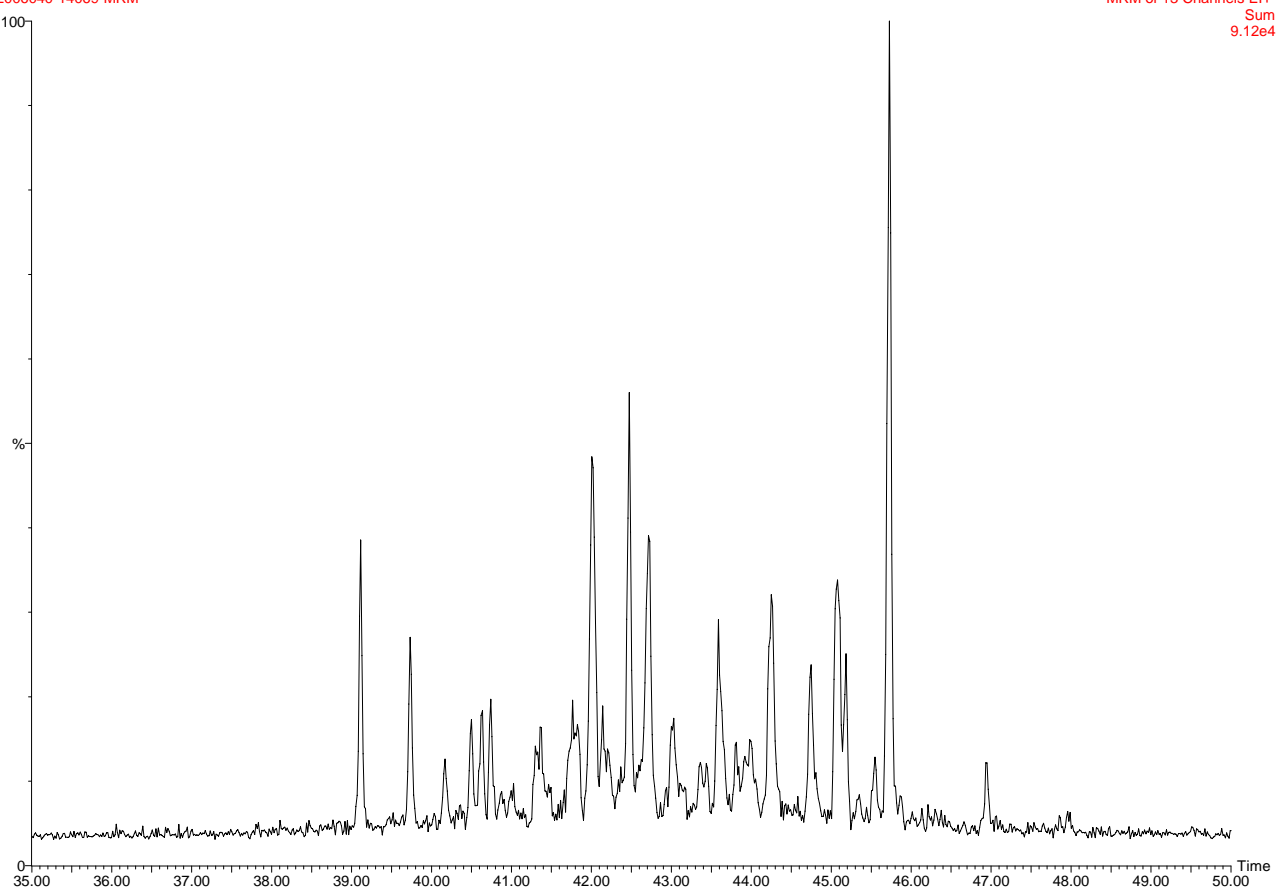
00,2006040-14069-79G-3 ali-aro 1.6 mg
2006040-14069-MRM

MRM of 13 Channels El+
Sum
2.00e5

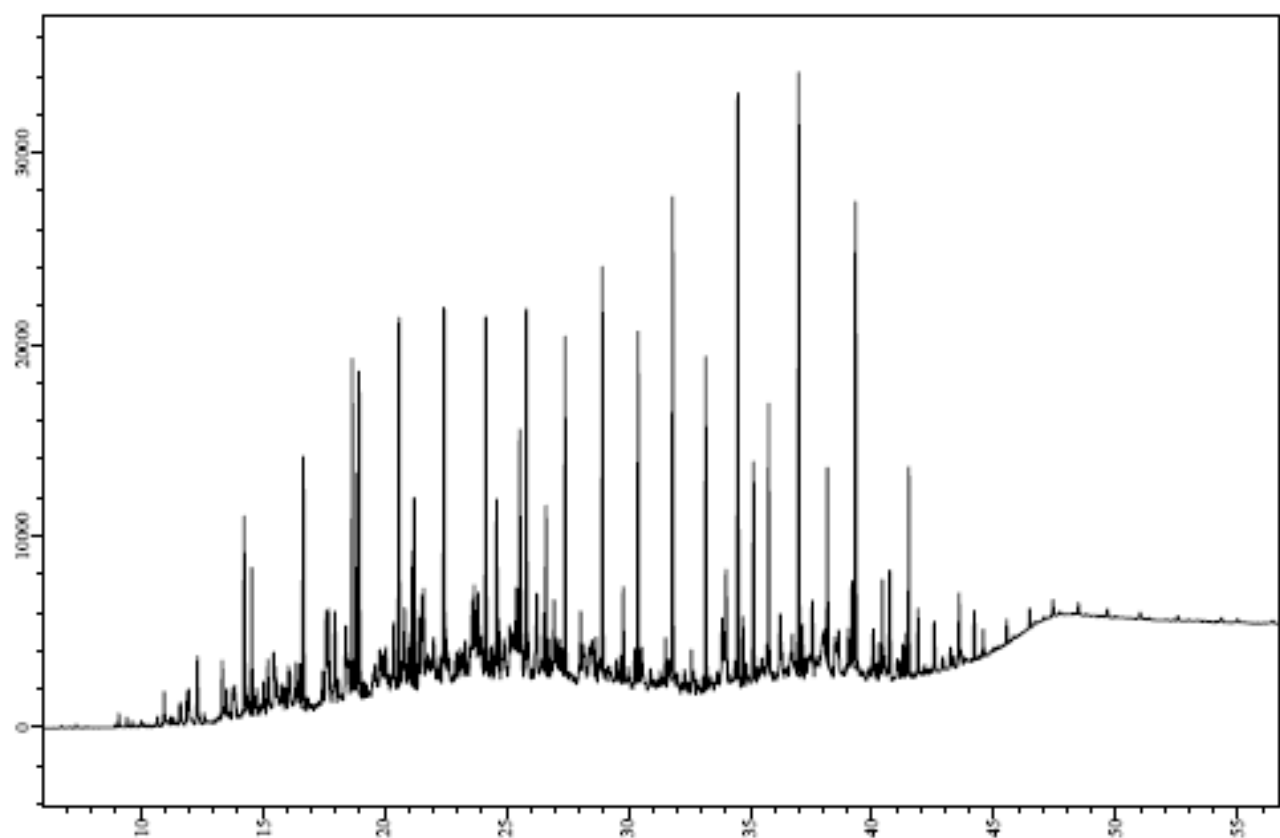


00,2006040-14069-79G-3 ali-aro 1.6 mg
2006040-14069-MRM

MRM of 13 Channels El+
Sum
9.12e4

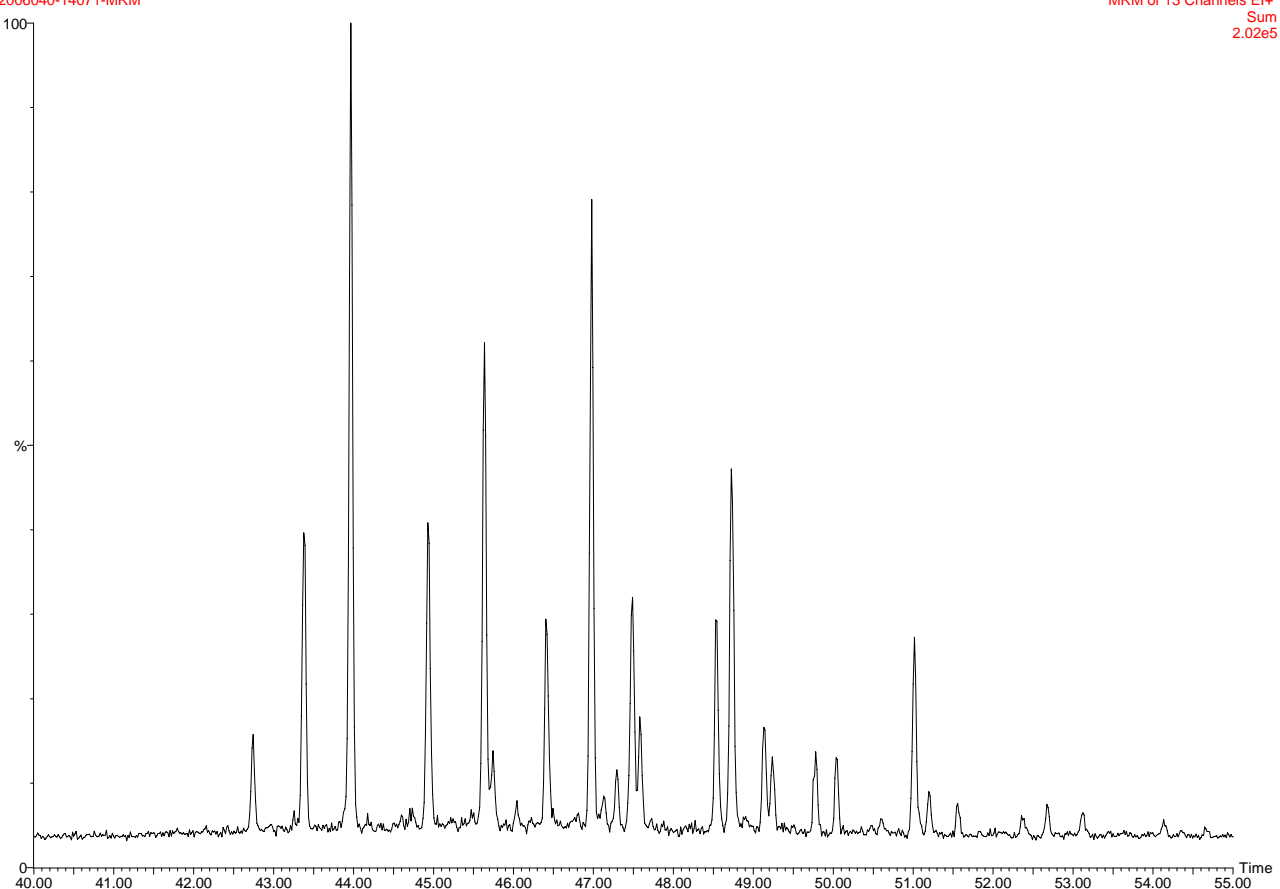


DANA06-79G-5



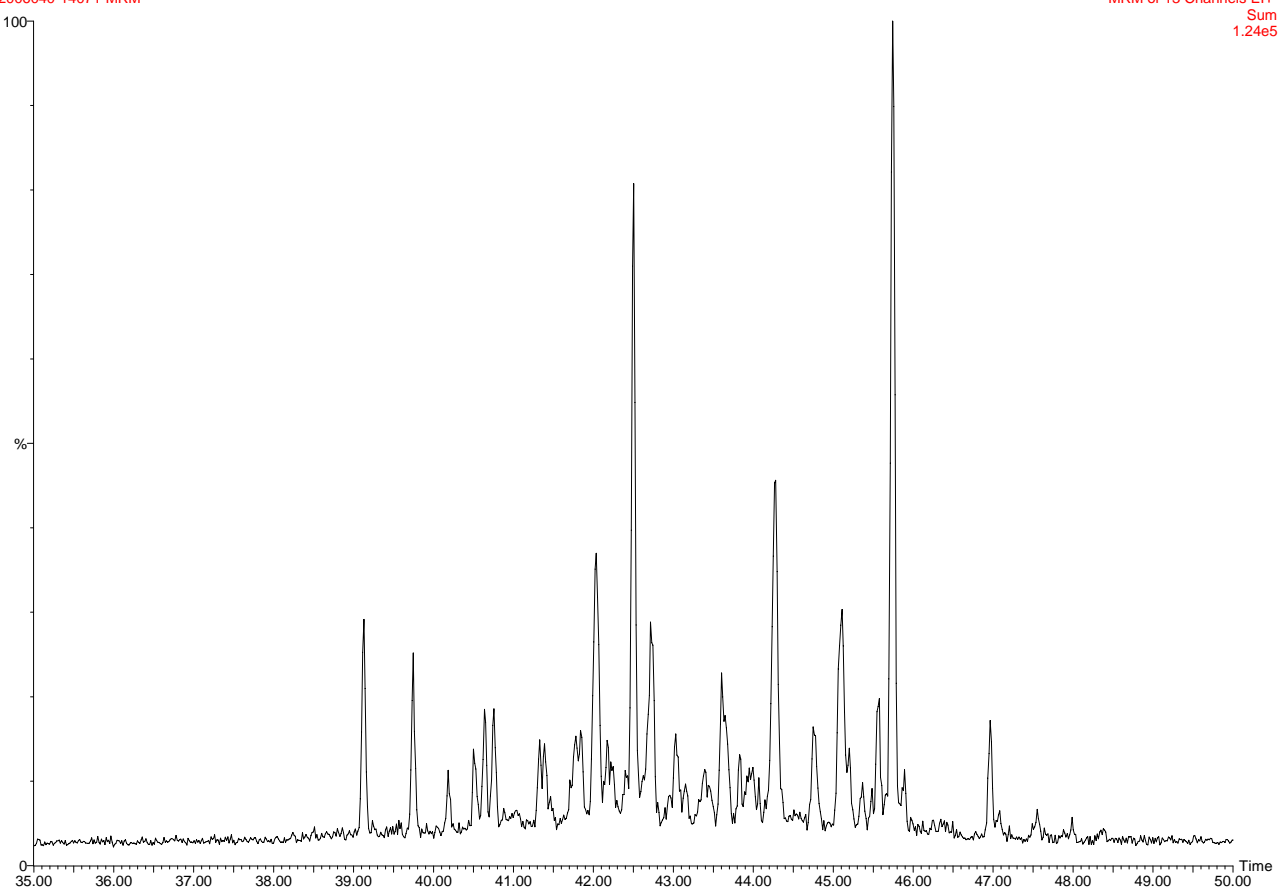
00,2006040-14071-79G-5 ali-aro 0.8 mg
2006040-14071-MRM

MRM of 13 Channels El+
Sum
2.02e5

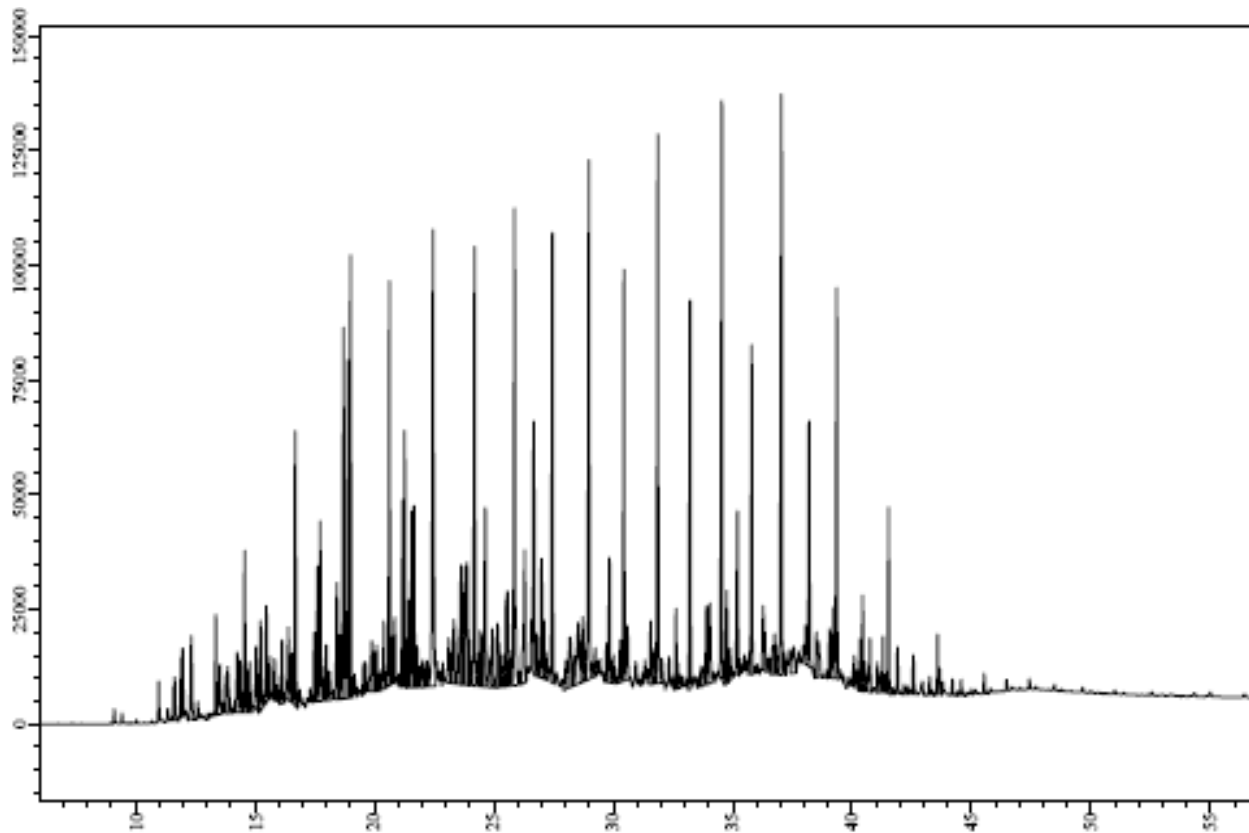


00,2006040-14071-79G-5 ali-aro 0.8 mg
2006040-14071-MRM

MRM of 13 Channels El+
Sum
1.24e5

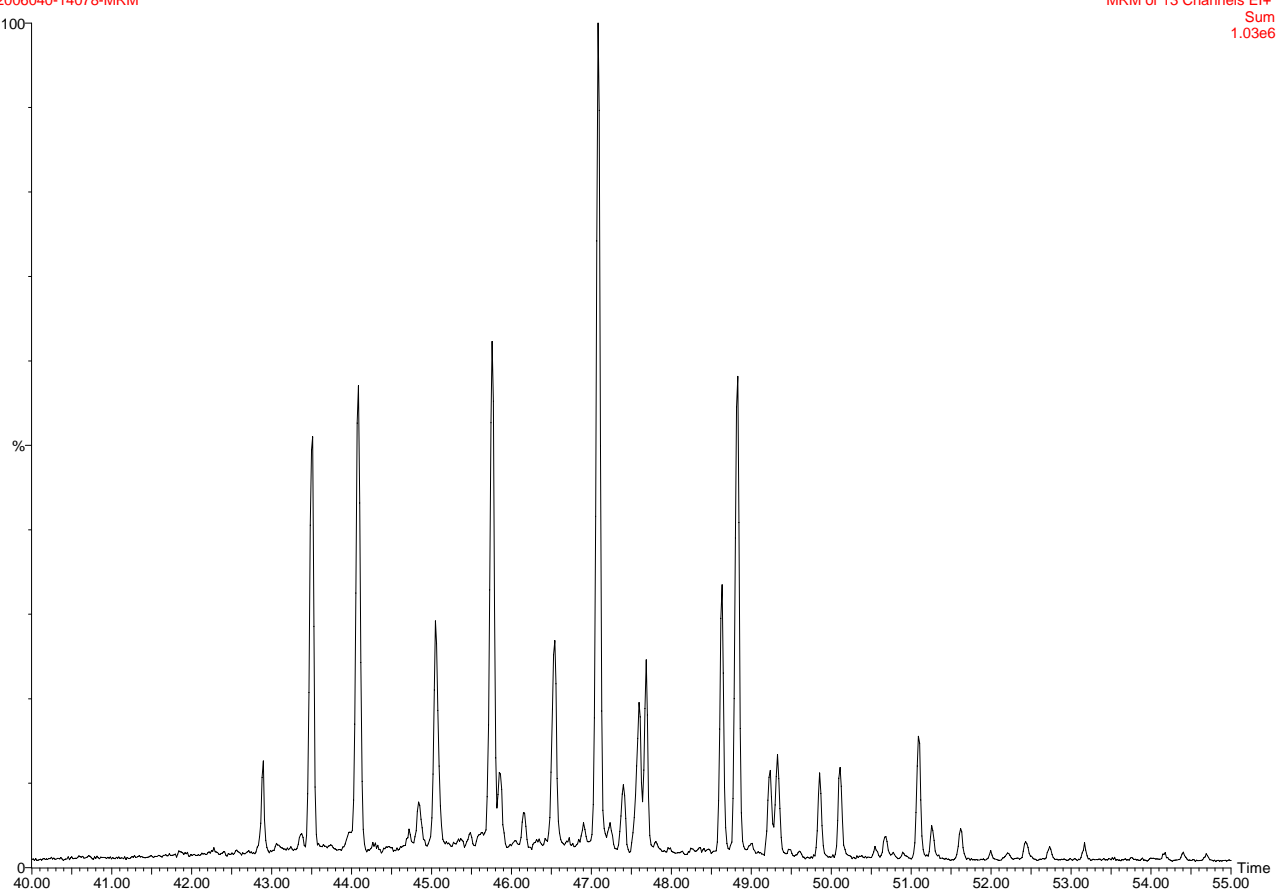


DANA06-82G-1



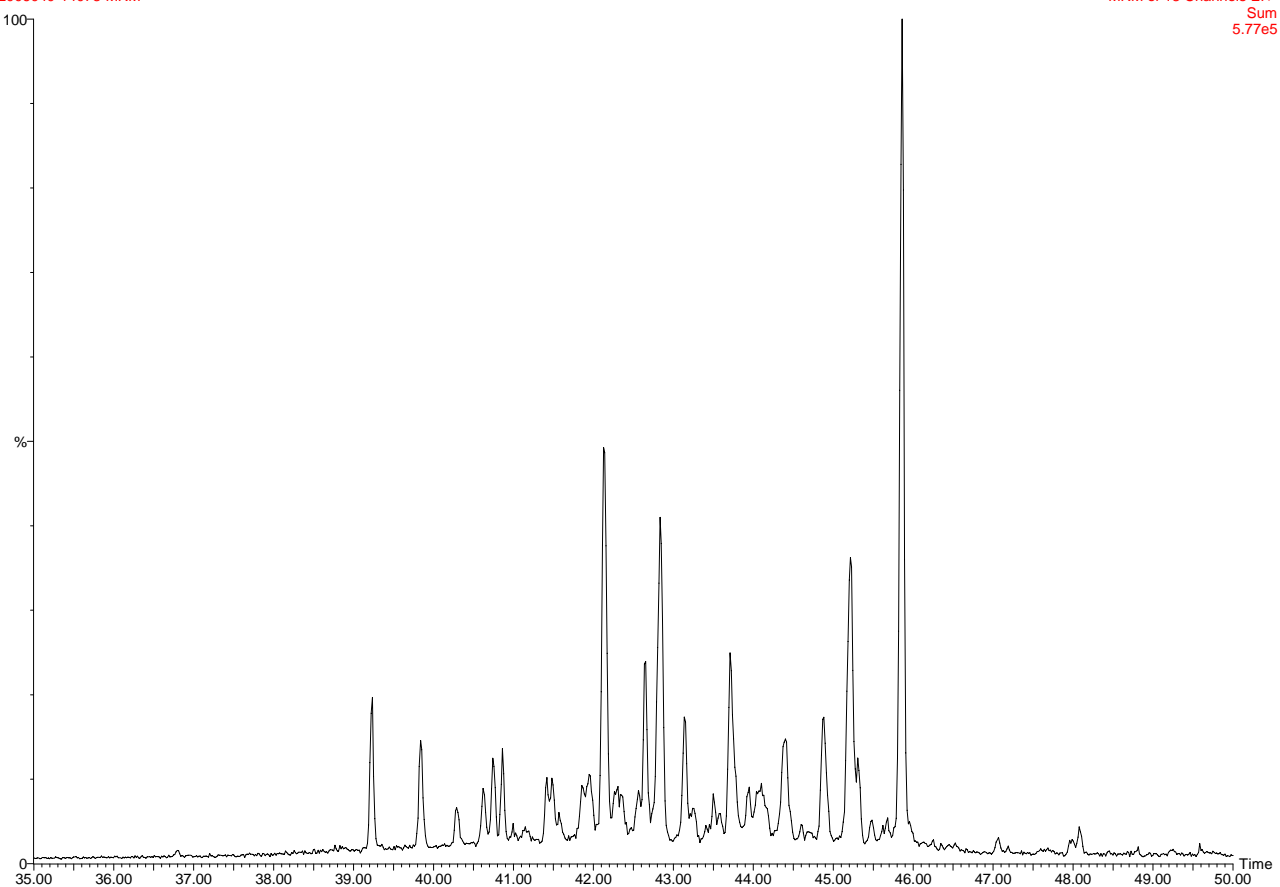
00,2006040-14078-82G-1 ali-aro 0.3 mg
2006040-14078-MRM

MRM of 13 Channels El+
Sum
1.03e6

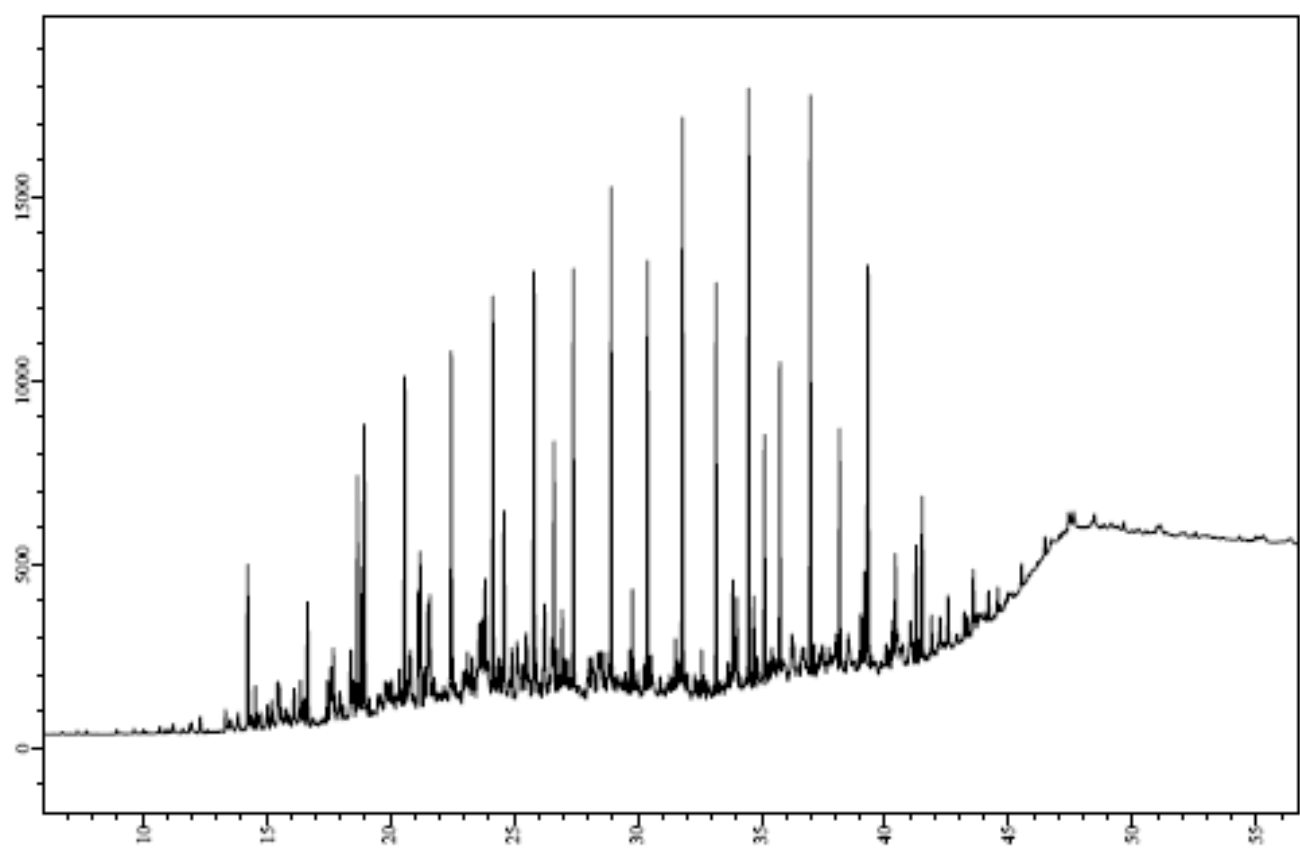


00,2006040-14078-82G-1 ali-aro 0.3 mg
2006040-14078-MRM

MRM of 13 Channels El+
Sum
5.77e5

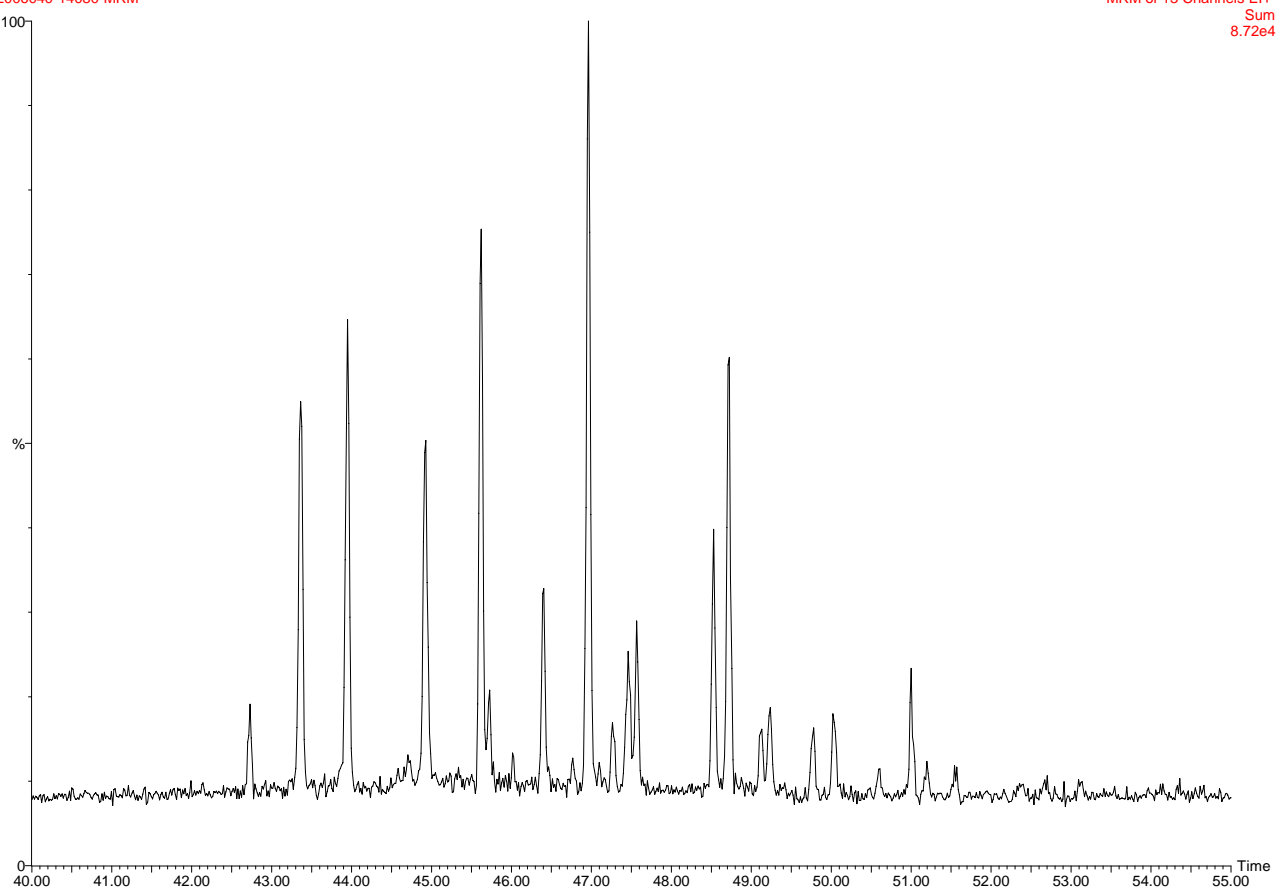


DANA06-82G-3



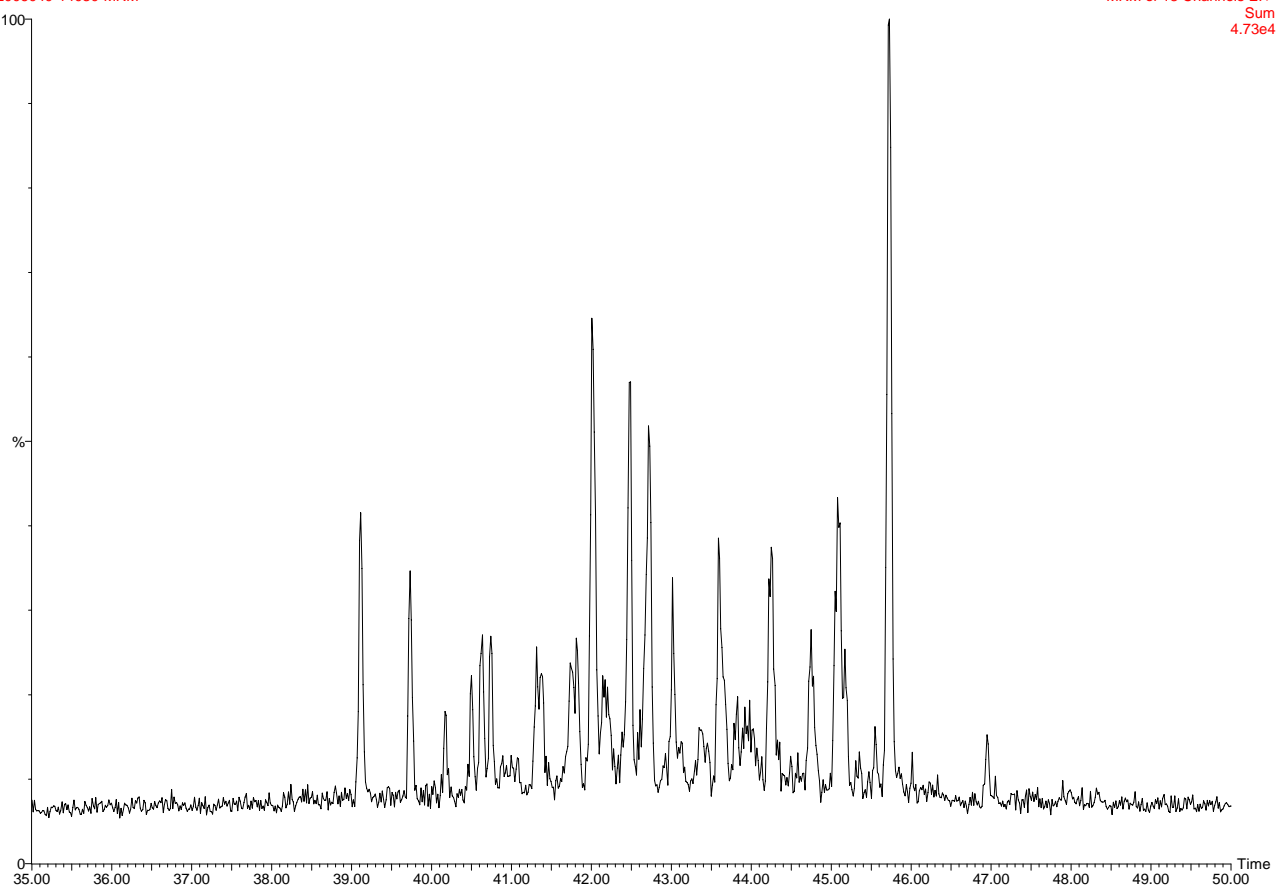
00,2006040-14080-82G-3 ali-aro 2.3 mg
2006040-14080-MRM

MRM of 13 Channels El+
Sum
8.72e4

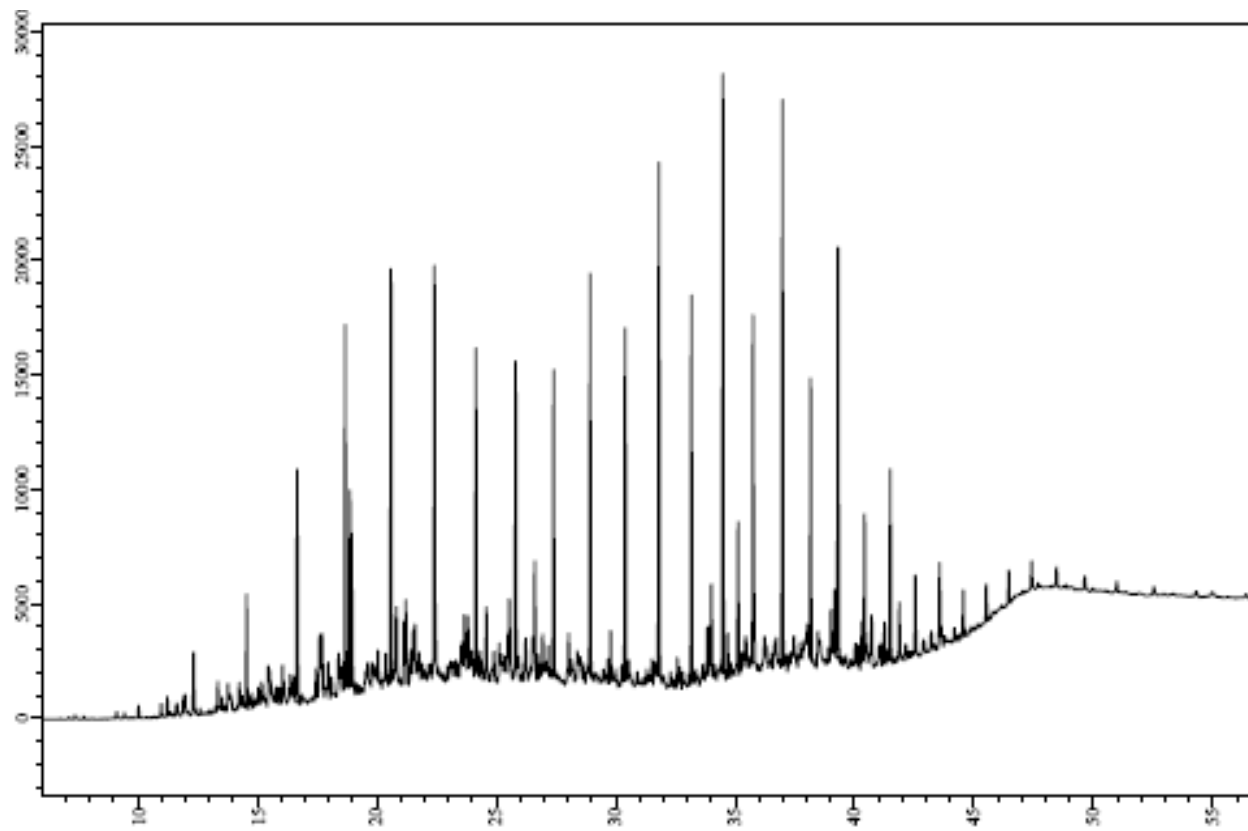


00,2006040-14080-82G-3 ali-aro 2.3 mg
2006040-14080-MRM

MRM of 13 Channels El+
Sum
4.73e4

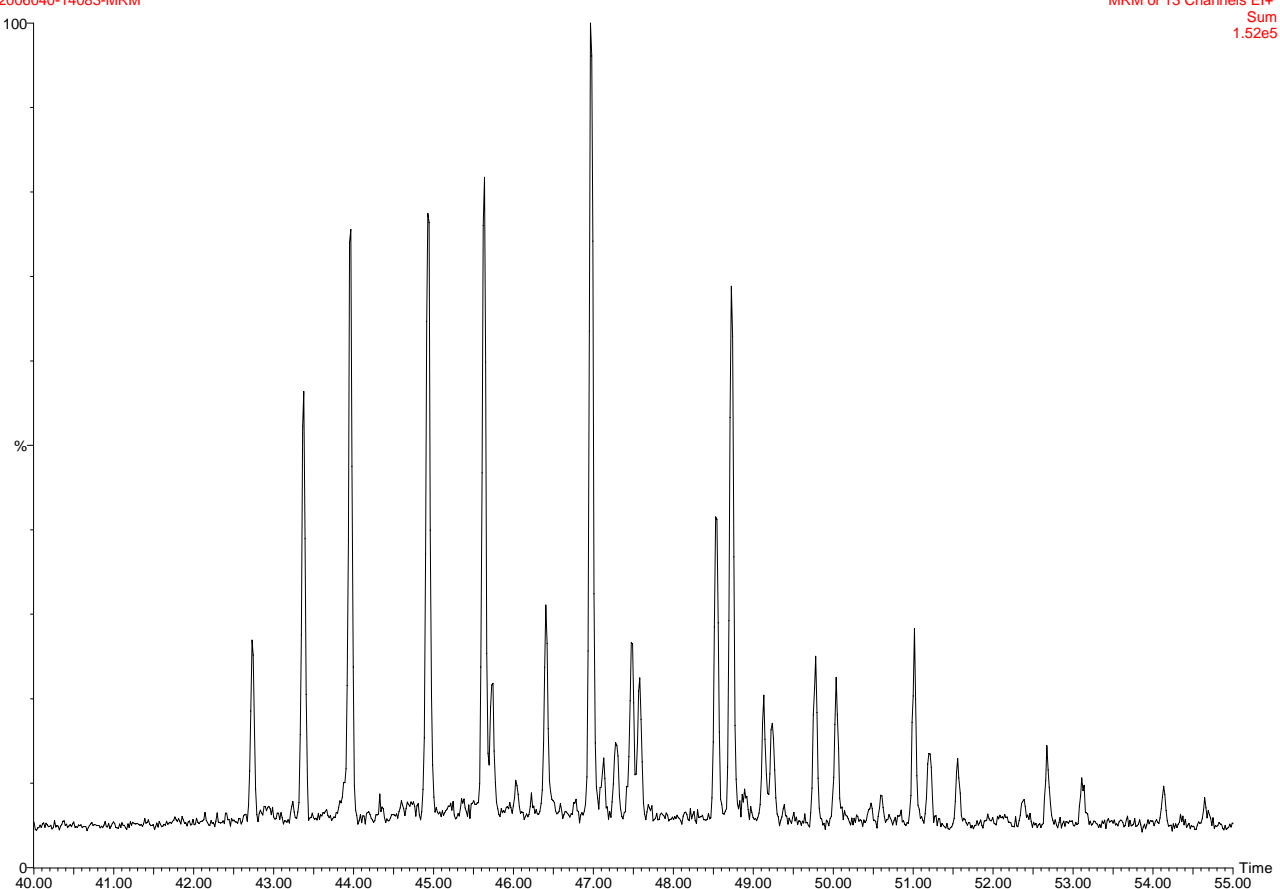


DANA06-82G-6



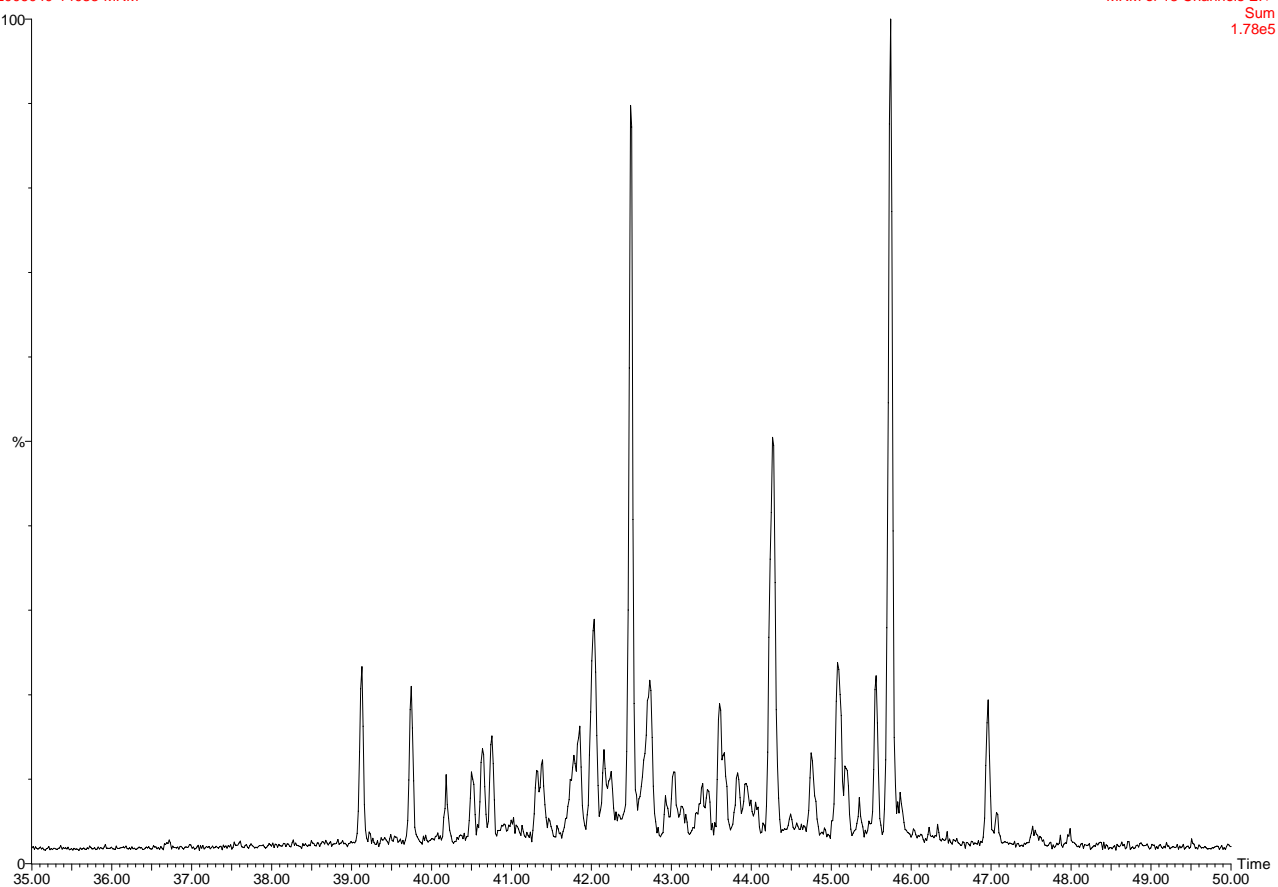
00,2006040-14083-82G-6 ali-aro 1.3 mg
2006040-14083-MRM

MRM of 13 Channels El+
Sum
1.52e5

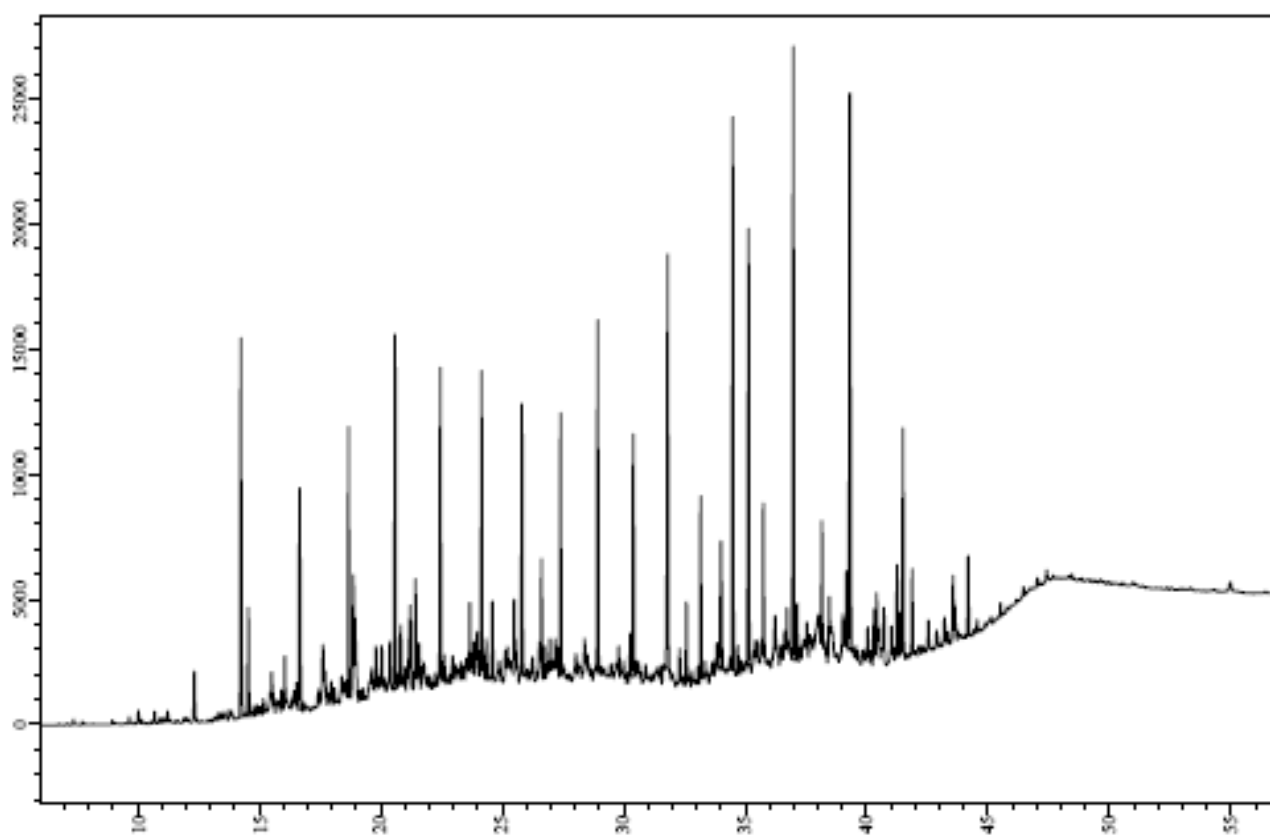


00,2006040-14083-82G-6 ali-aro 1.3 mg
2006040-14083-MRM

MRM of 13 Channels El+
Sum
1.78e5

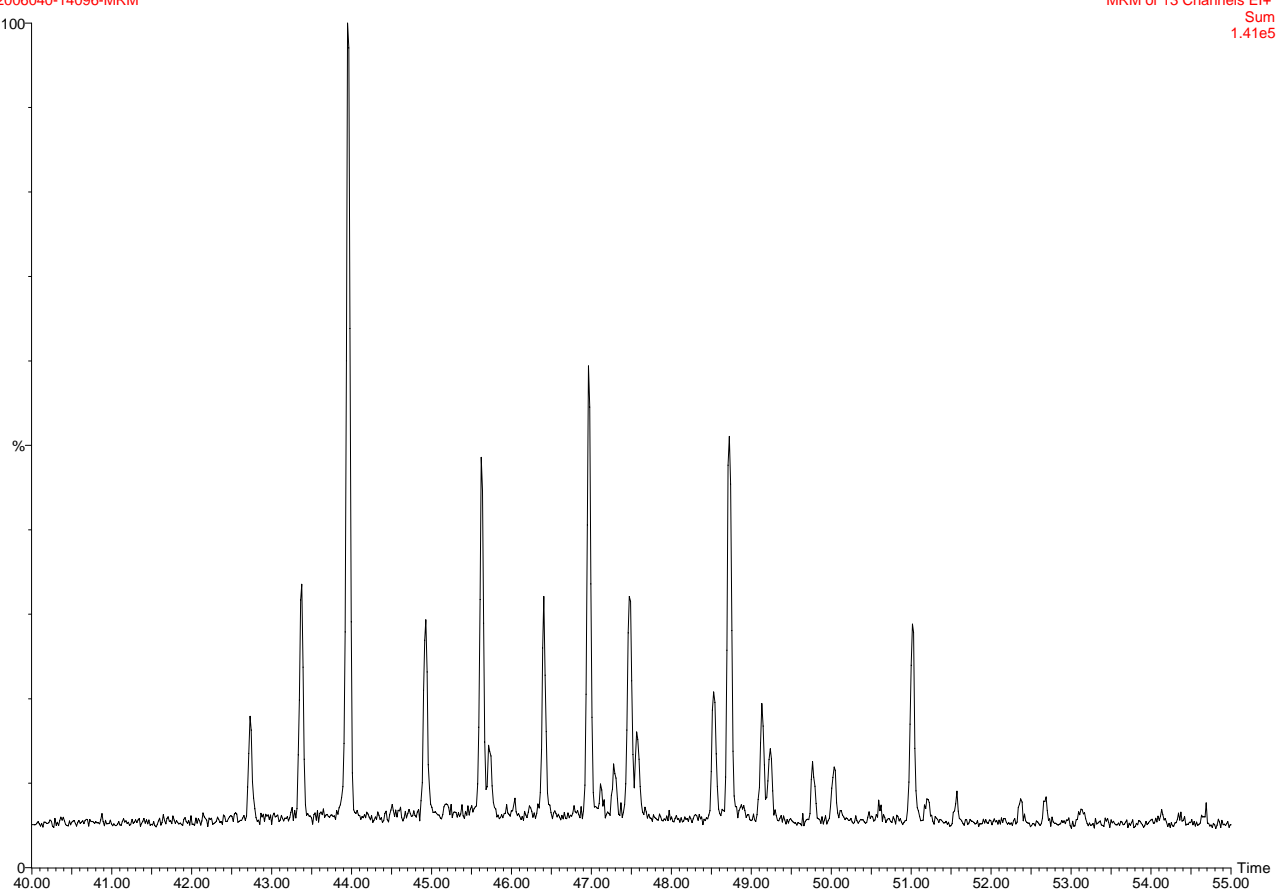


DANA06-91G-1



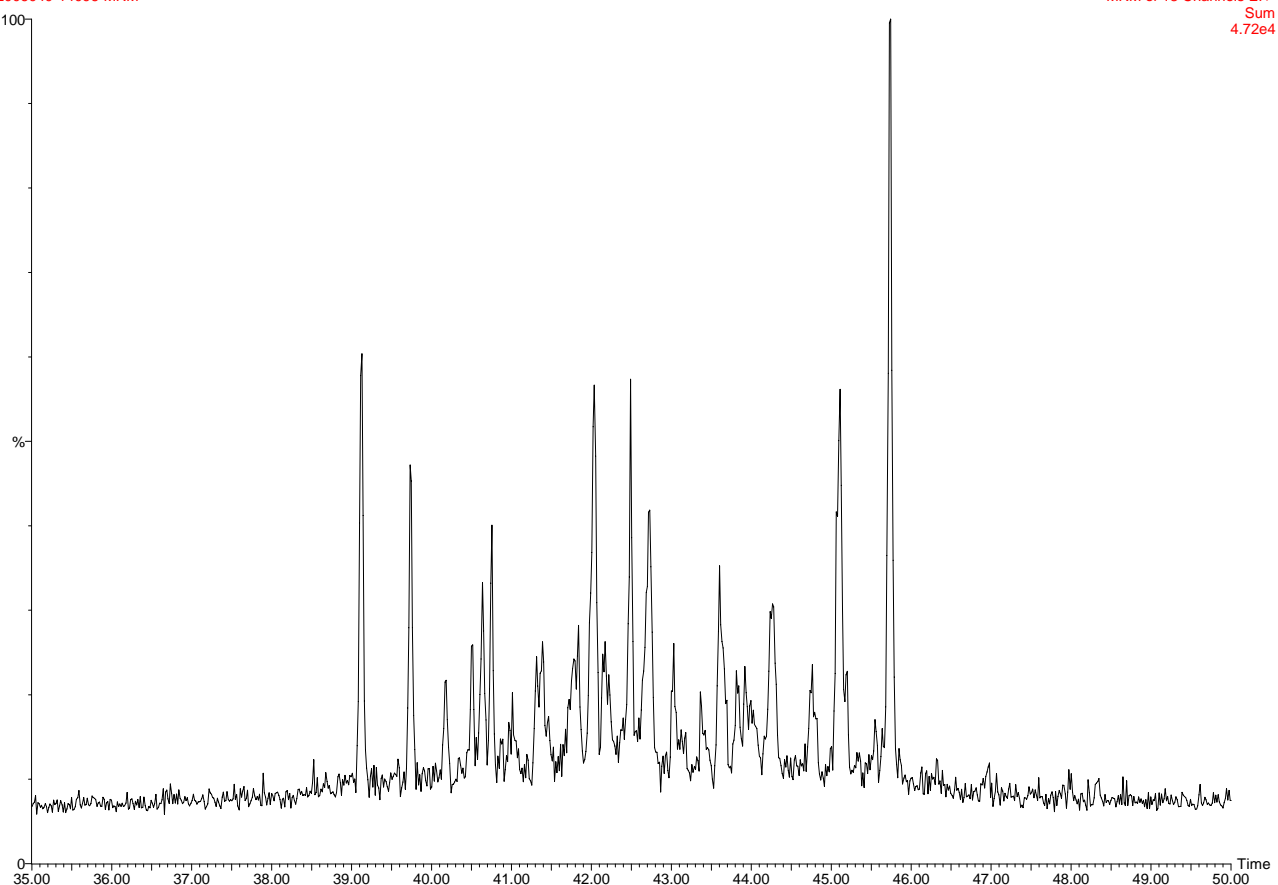
00,2006040-14096-91G-1 ali-aro 0.7 mg
2006040-14096-MRM

MRM of 13 Channels El+
Sum
1.41e5

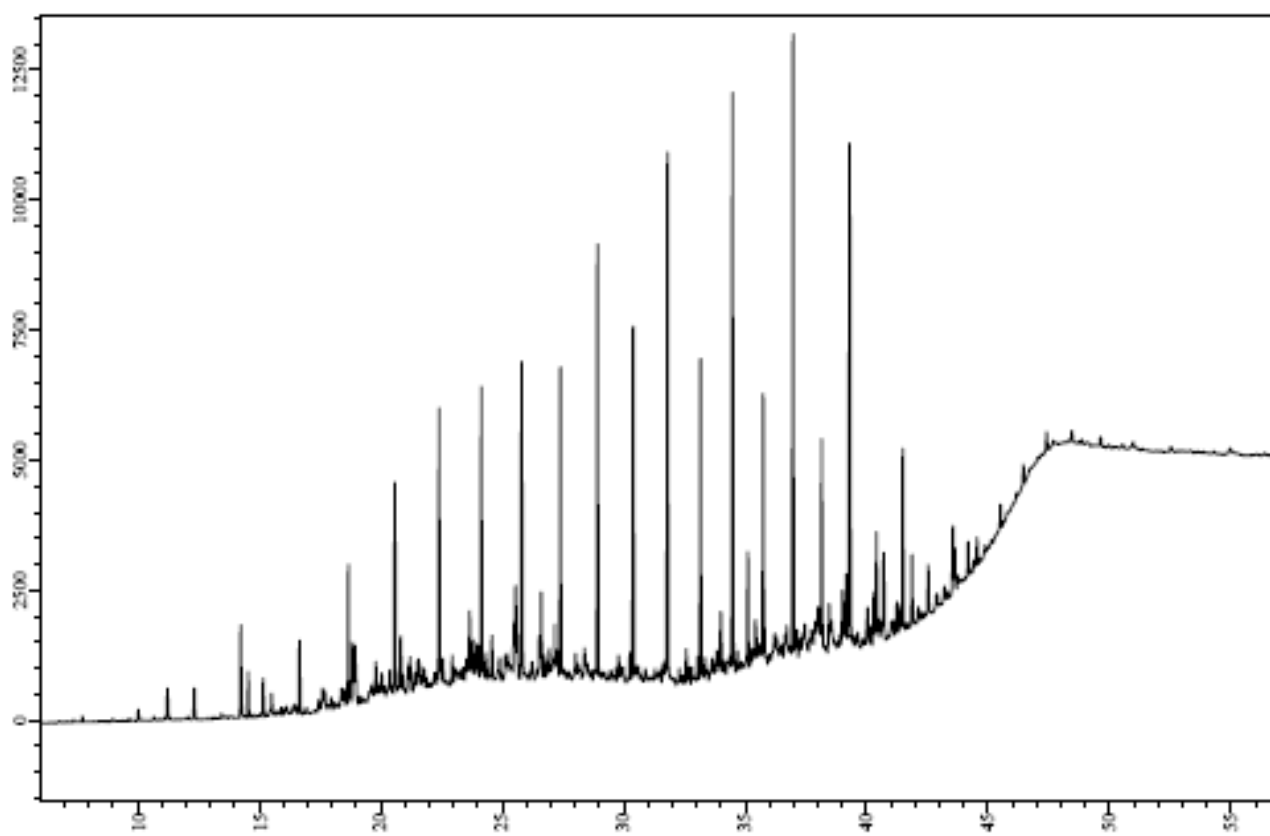


00,2006040-14096-91G-1 ali-aro 0.7 mg
2006040-14096-MRM

MRM of 13 Channels El+
Sum
4.72e4

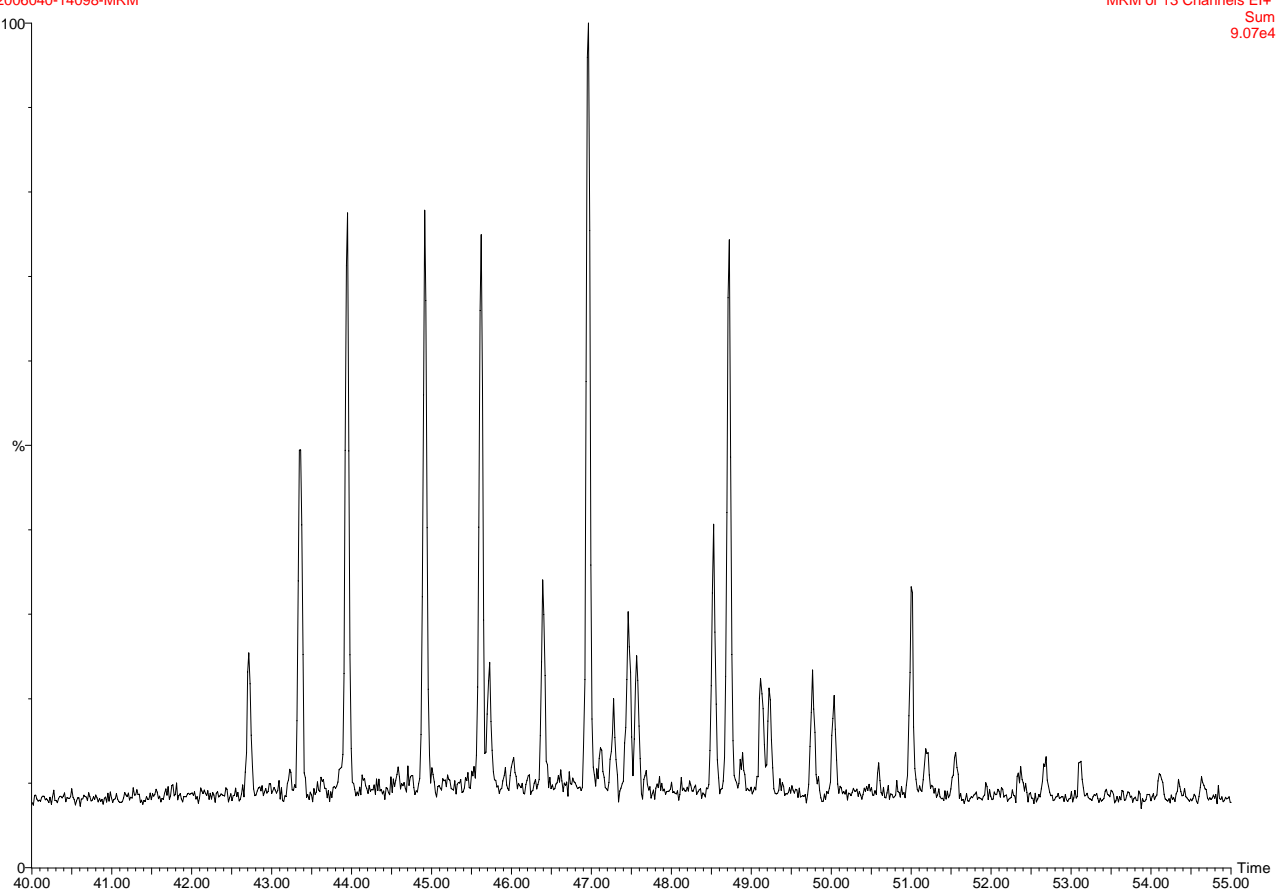


DANA06-91G-3



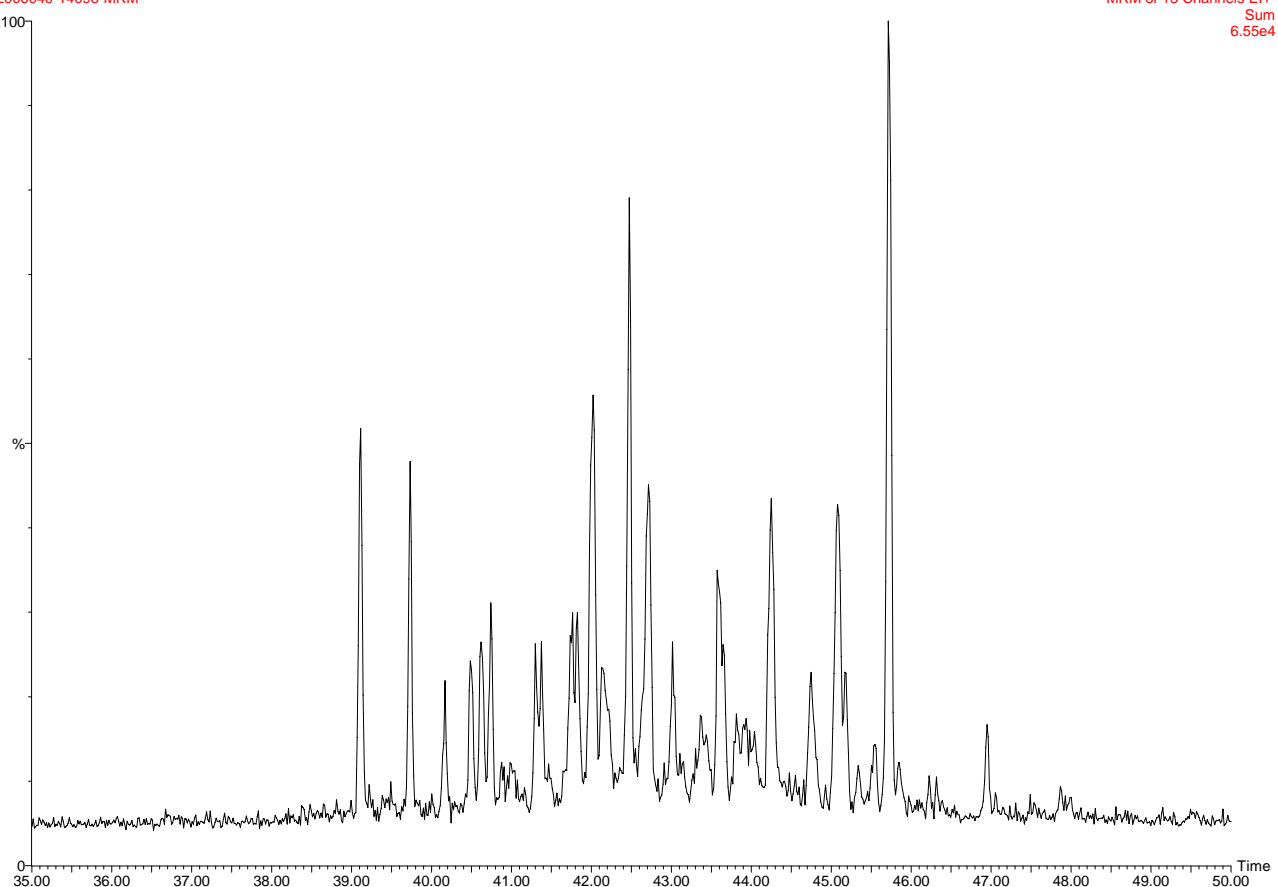
00,2006040-14098-91G-3 ali-aro 2.5 mg
2006040-14098-MRM

MRM of 13 Channels El+
Sum
9.07e4

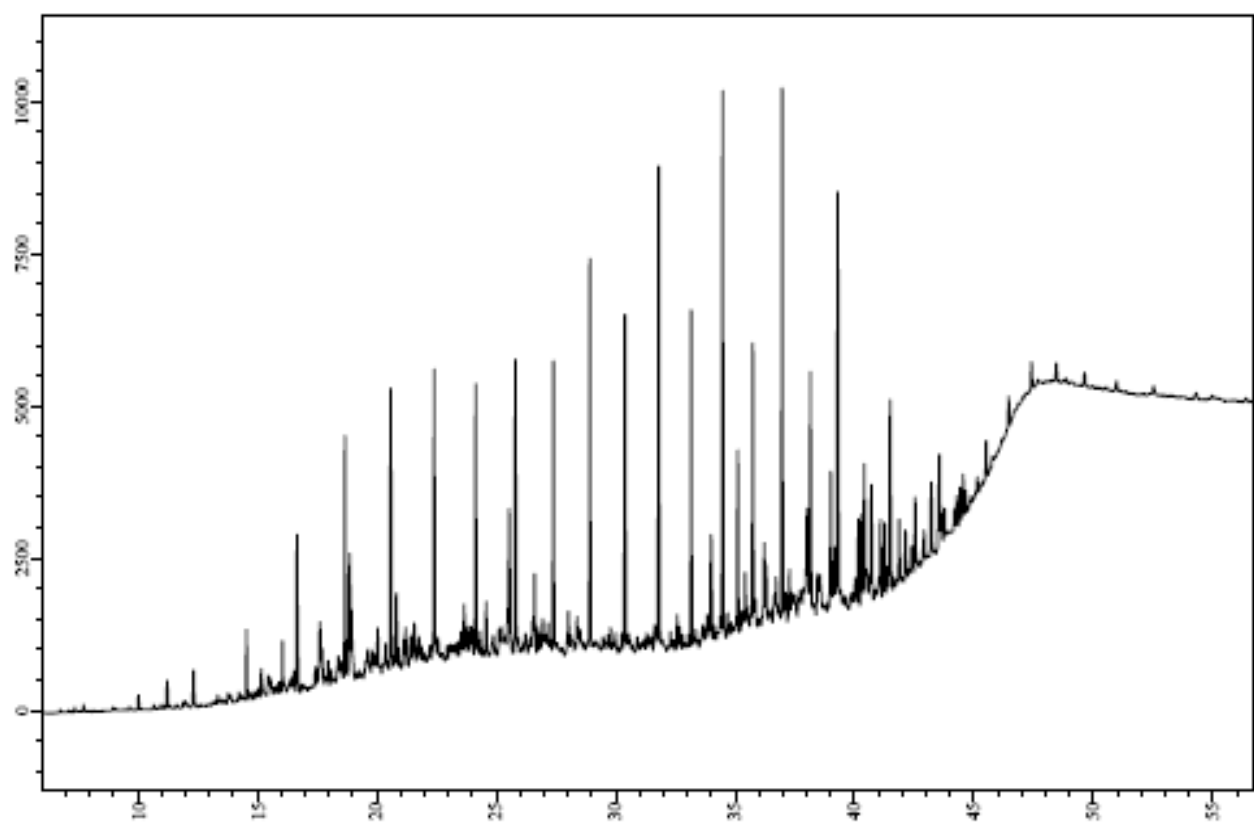


00,2006040-14098-91G-3 ali-aro 2.5 mg
2006040-14098-MRM

MRM of 13 Channels El+
Sum
6.55e4

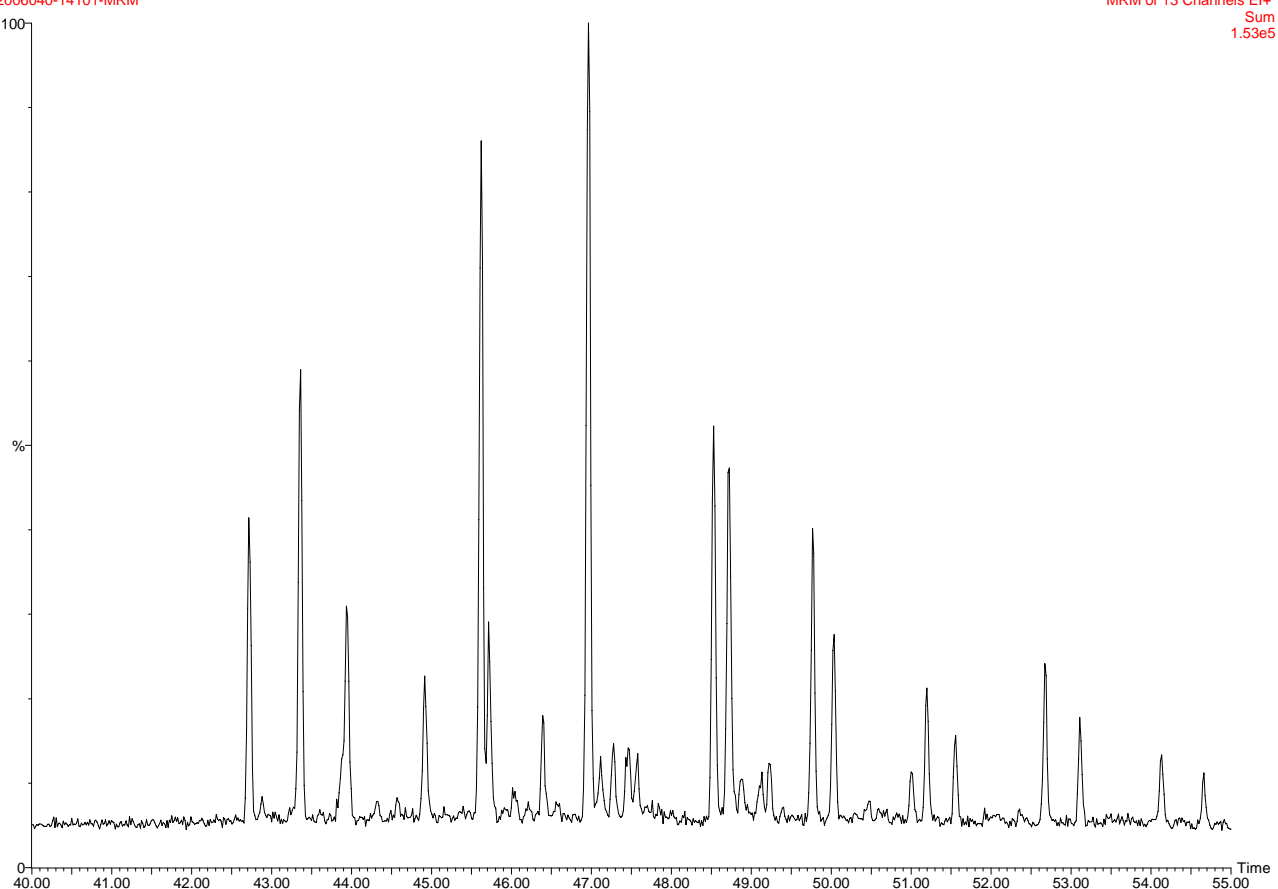


DANA06-91G-6



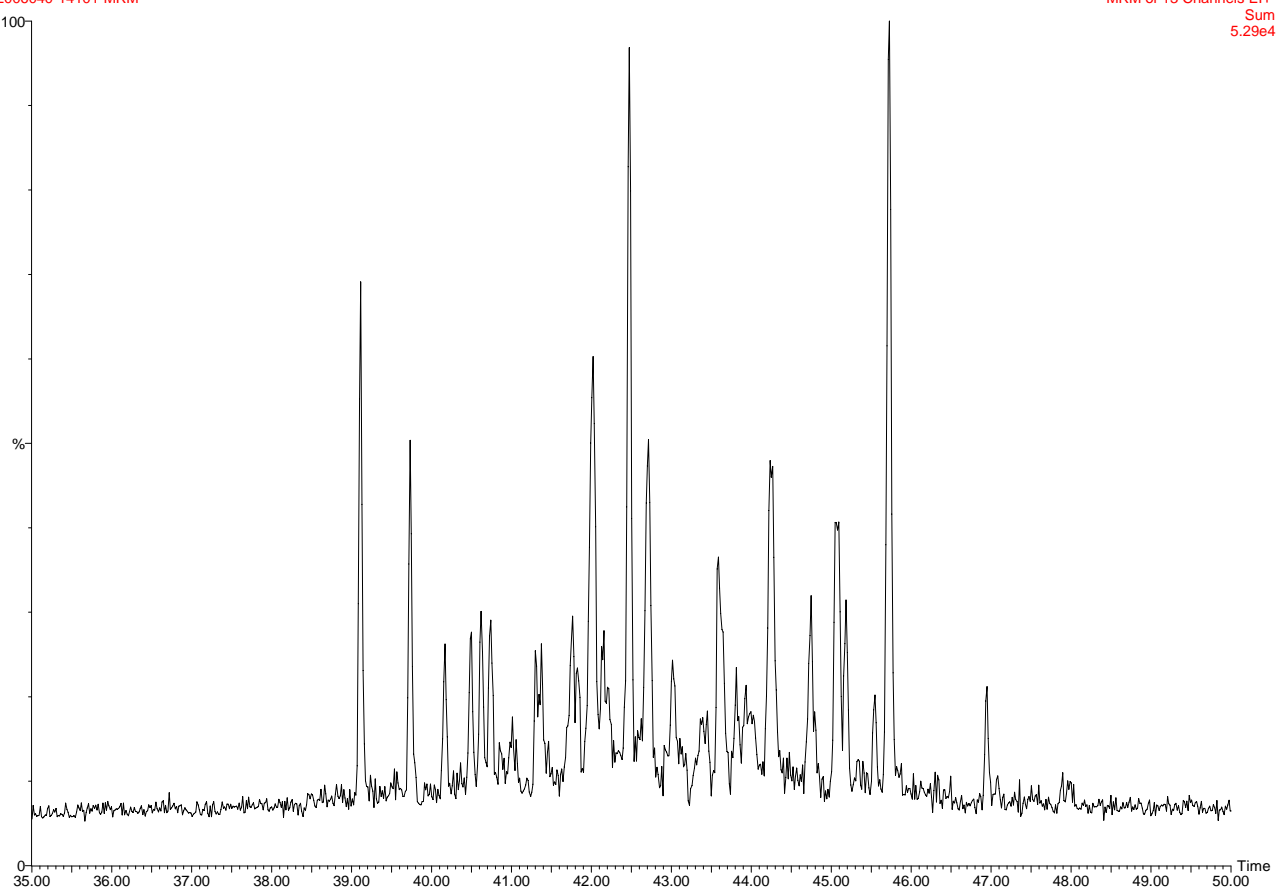
00,2006040-14101-91G-6 ali-aro 2.2 mg
2006040-14101-MRM

MRM of 13 Channels El+
Sum
1.53e5

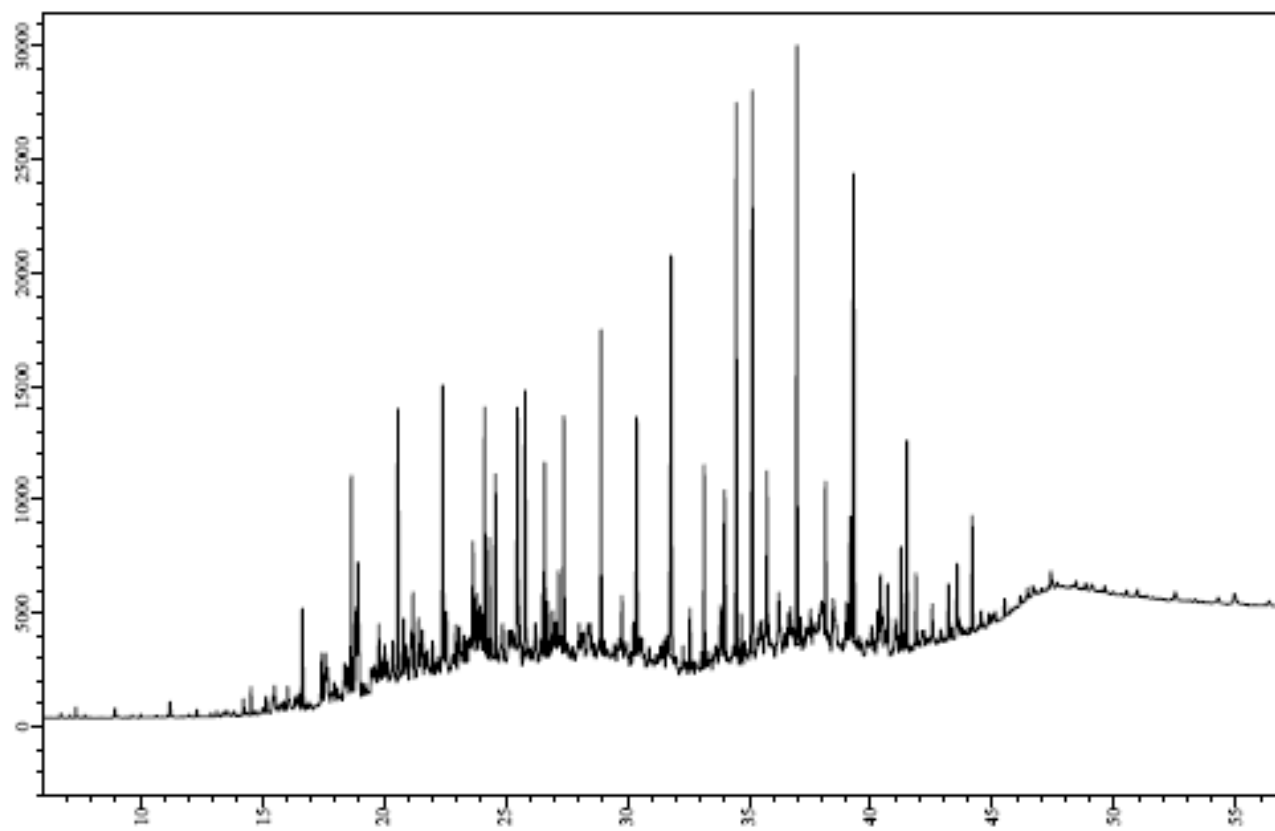


00,2006040-14101-91G-6 ali-aro 2.2 mg
2006040-14101-MRM

MRM of 13 Channels El+
Sum
5.29e4

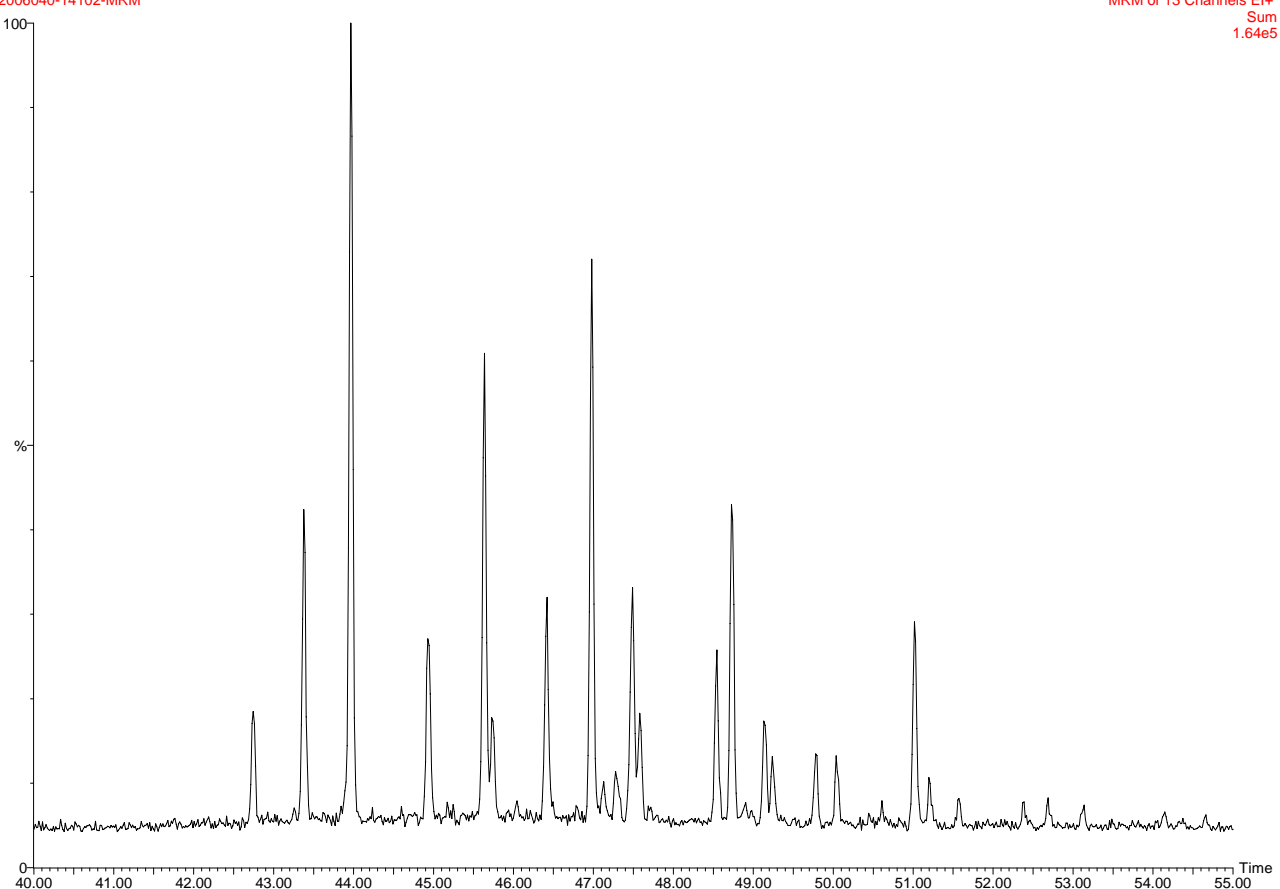


DANA06-92G-1



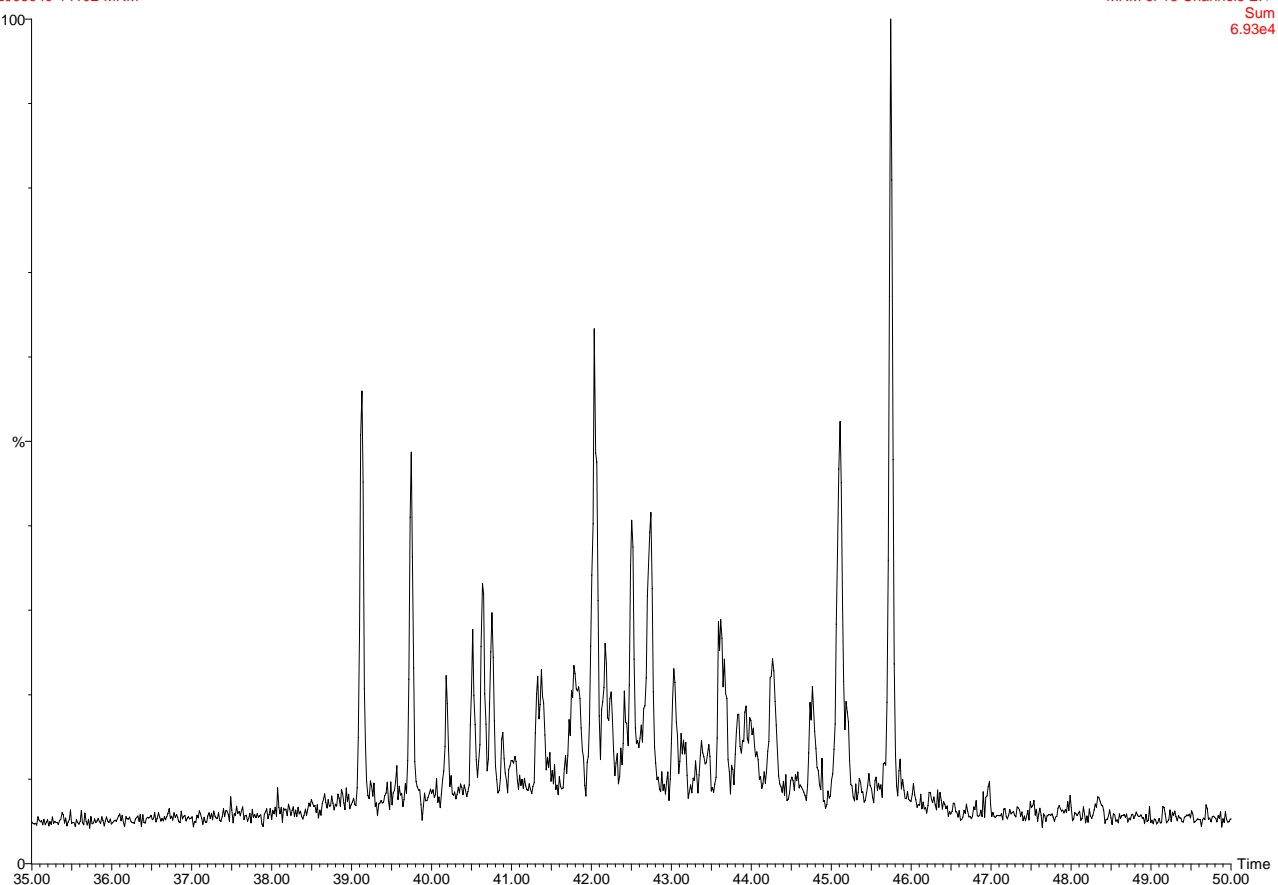
00,2006040-14102-92G-1 ali-aro 0.4 mg
2006040-14102-MRM

MRM of 13 Channels El+
Sum
1.64e5

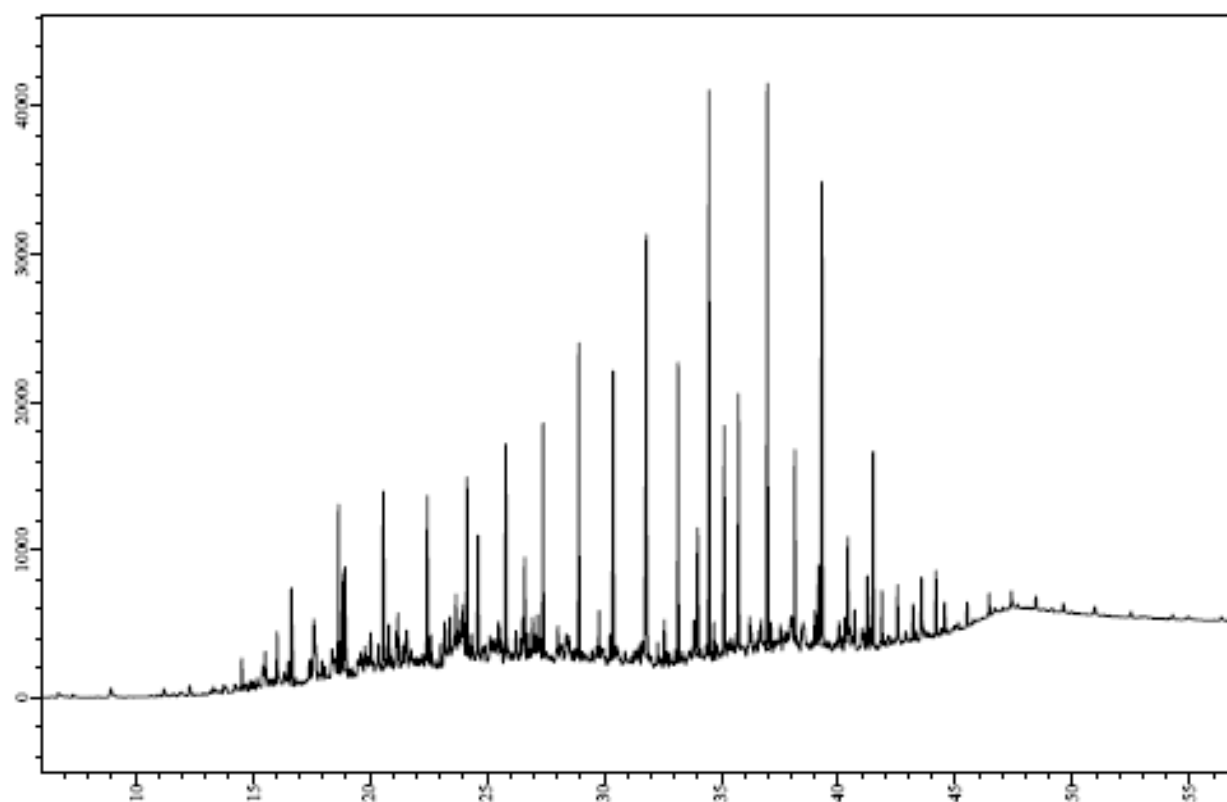


00,2006040-14102-92G-1 ali-aro 0.4 mg
2006040-14102-MRM

MRM of 13 Channels El+
Sum
6.93e4

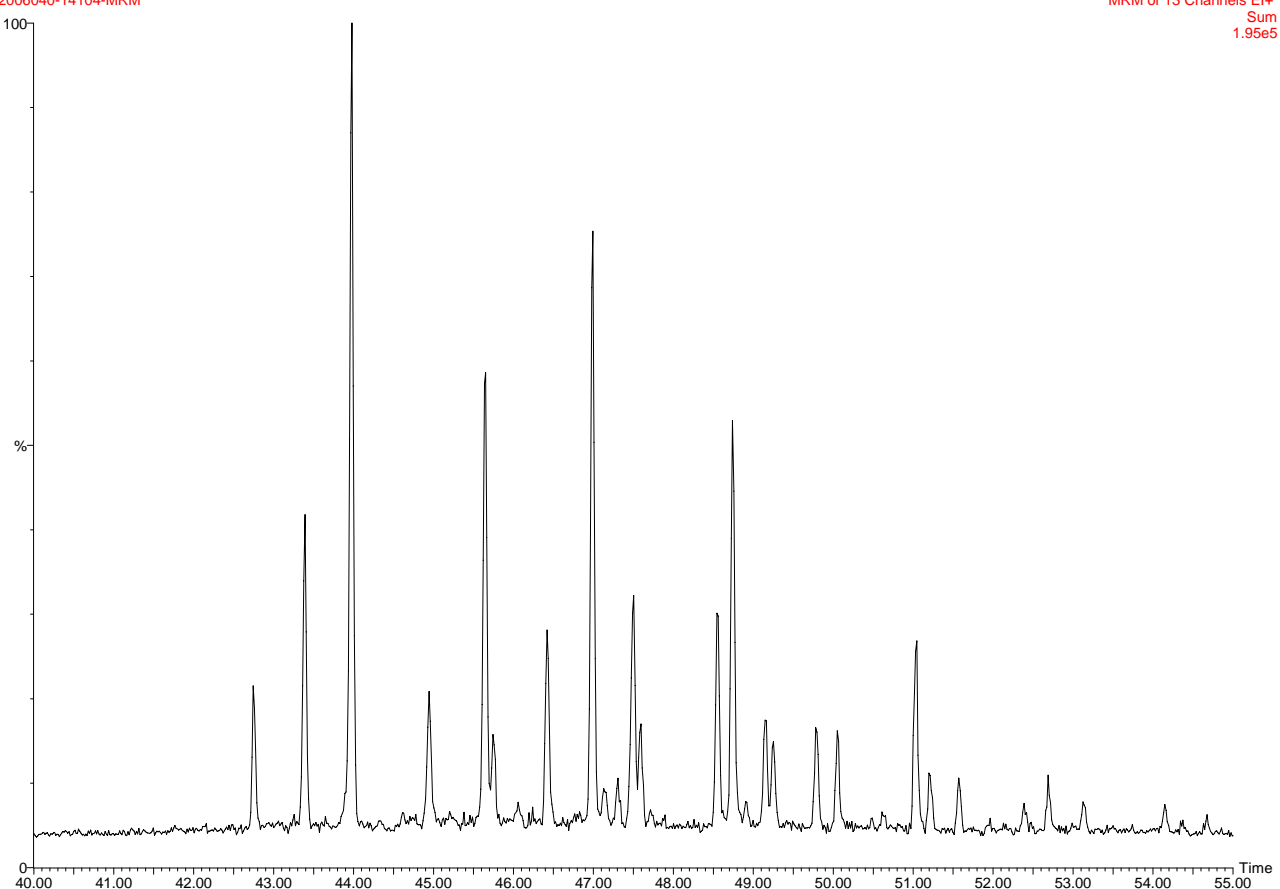


DANA06-92G-3



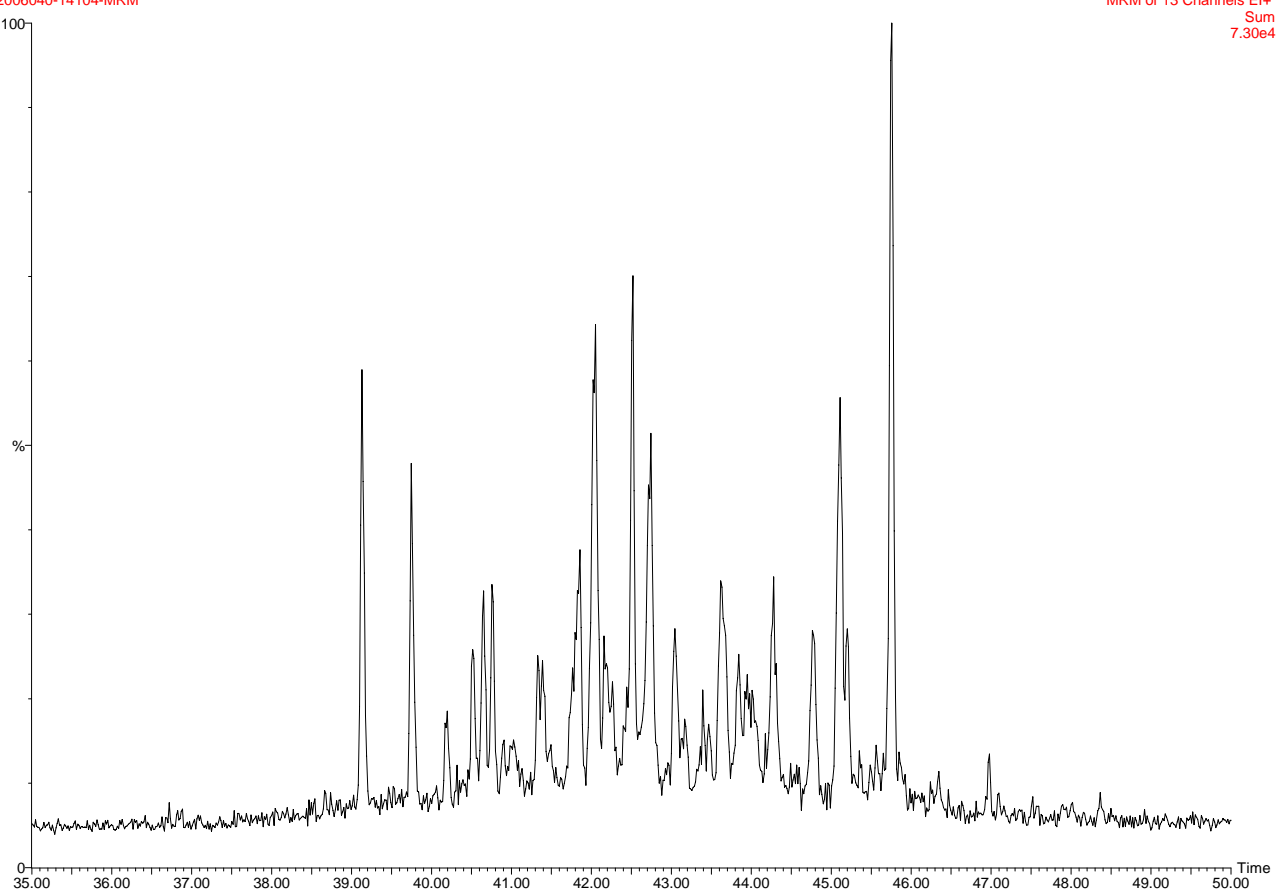
00,2006040-14104-92G-3 ali-aro 0.6 mg
2006040-14104-MRM

MRM of 13 Channels El+
Sum
1.95e5

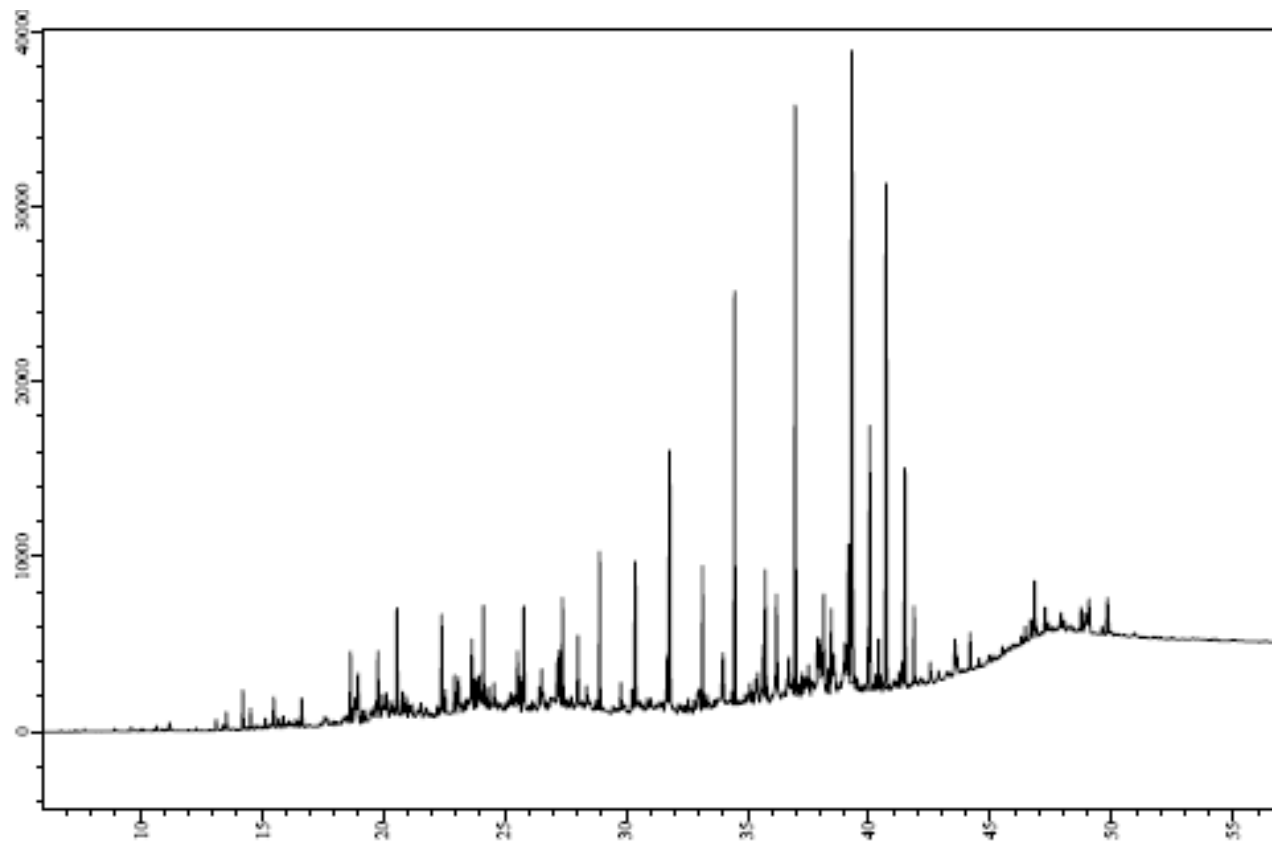


00,2006040-14104-92G-3 ali-aro 0.6 mg
2006040-14104-MRM

MRM of 13 Channels El+
Sum
7.30e4

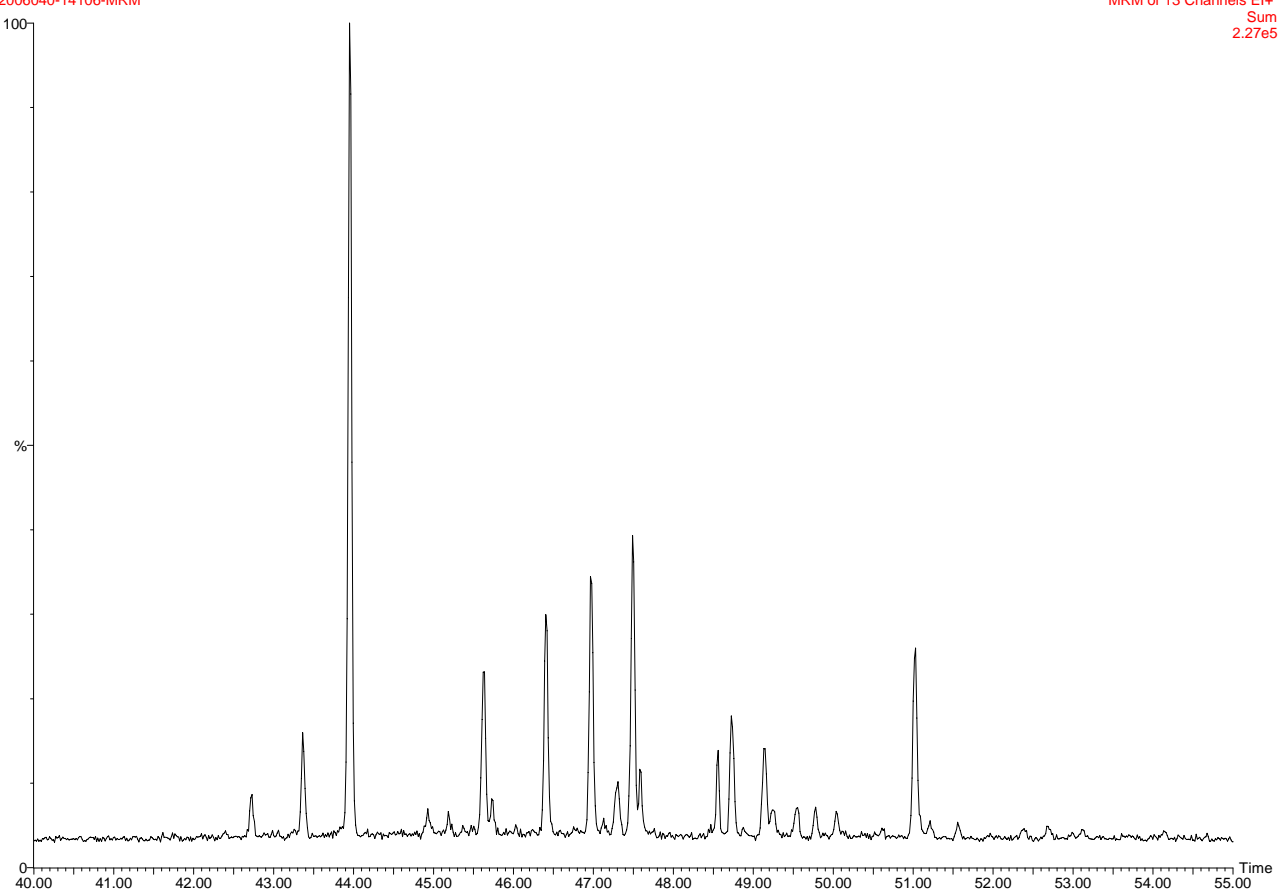


DANA06-92G-5



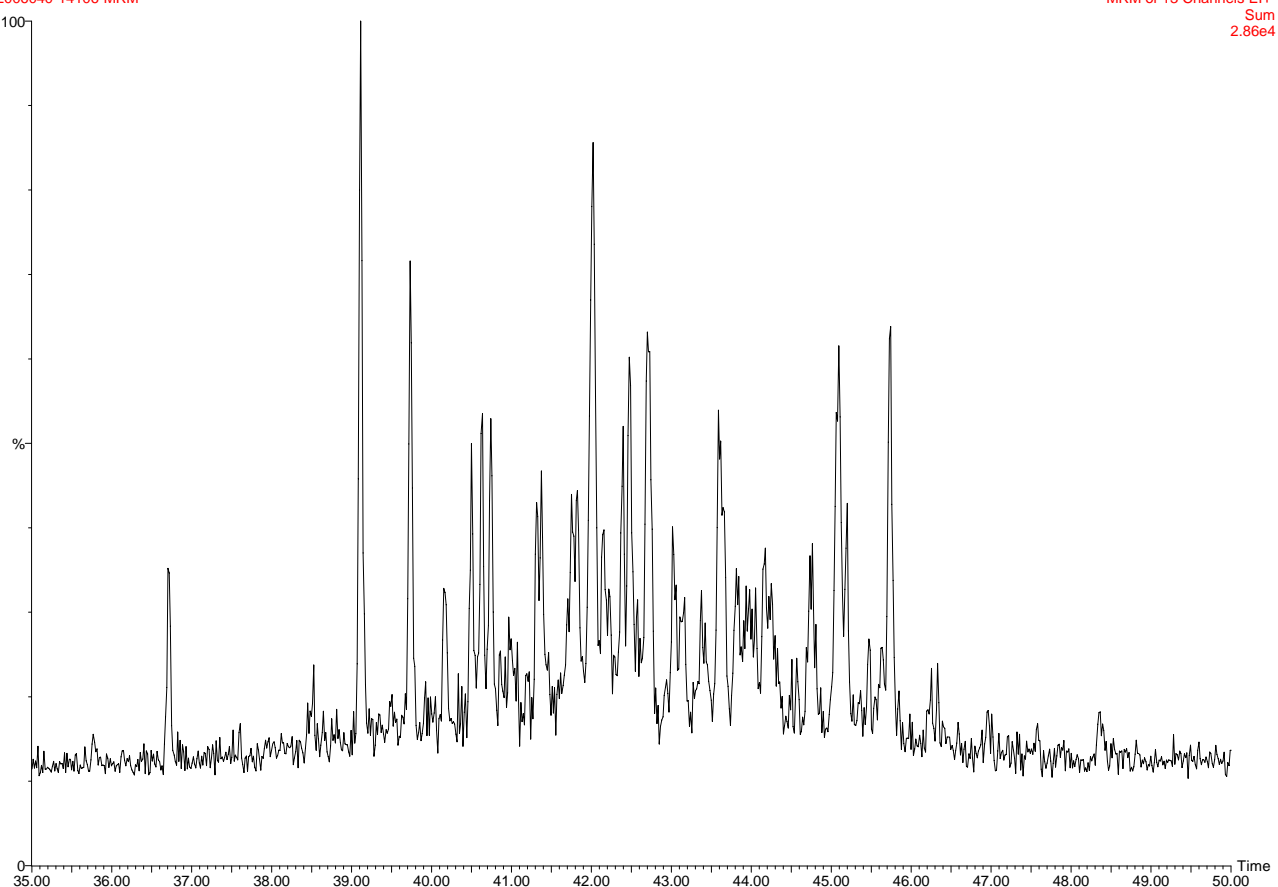
00,2006040-14106-92G-5 ali-aro 1.0 mg
2006040-14106-MRM

MRM of 13 Channels El+
Sum
2.27e5

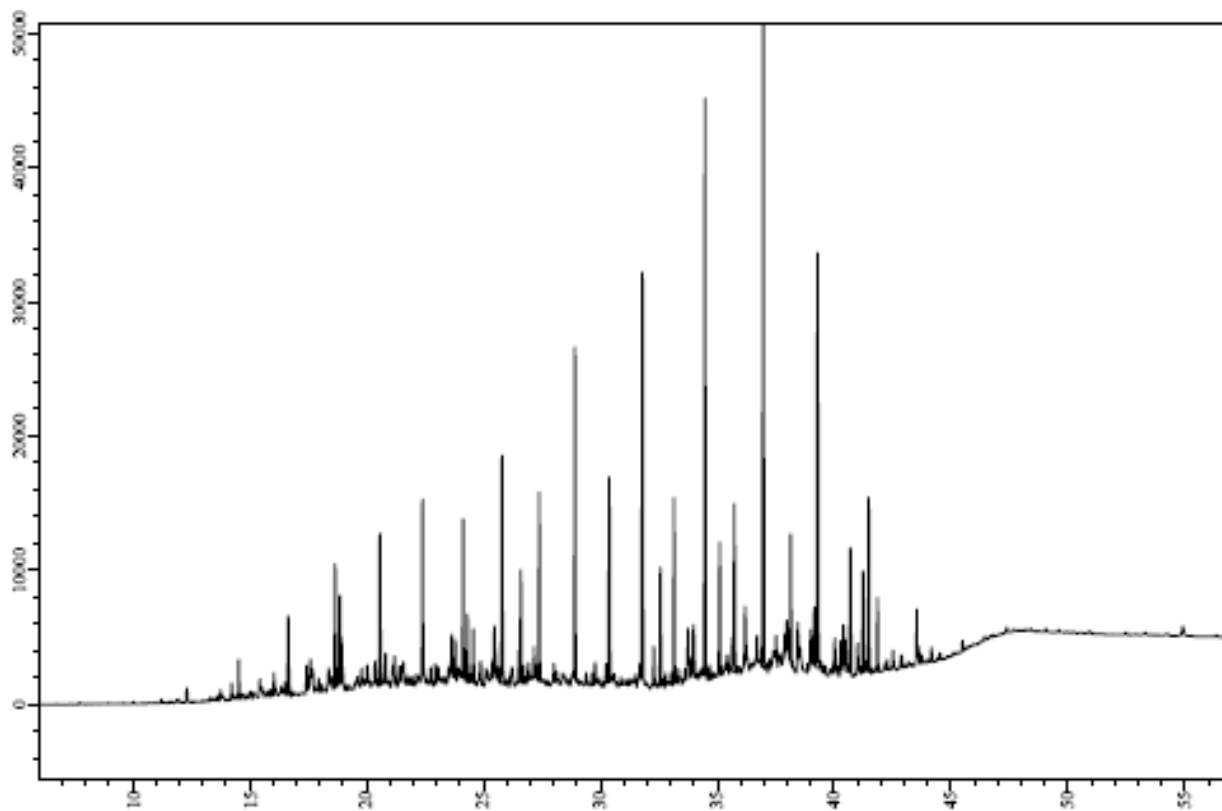


00,2006040-14106-92G-5 ali-aro 1.0 mg
2006040-14106-MRM

MRM of 13 Channels El+
Sum
2.86e4

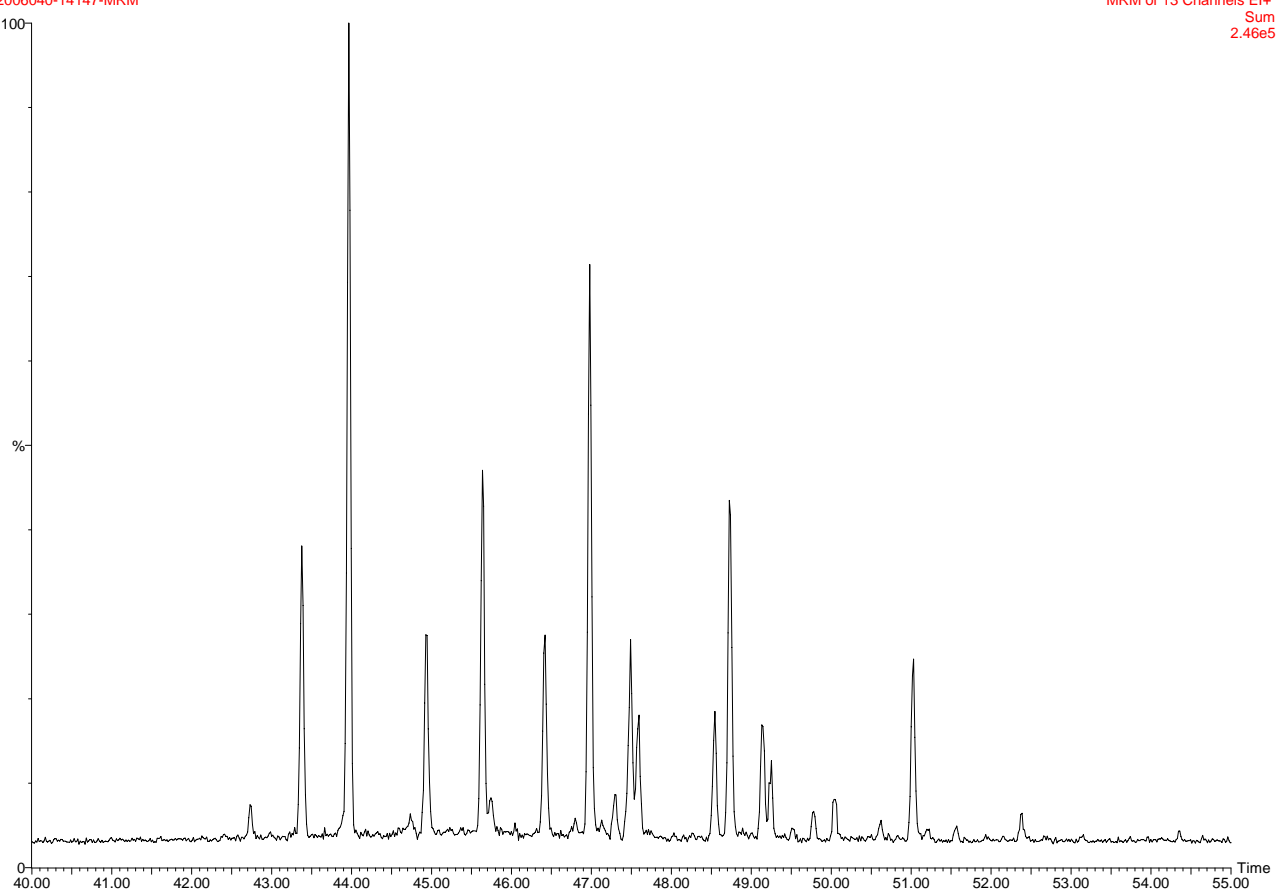


DANA06-133G-1



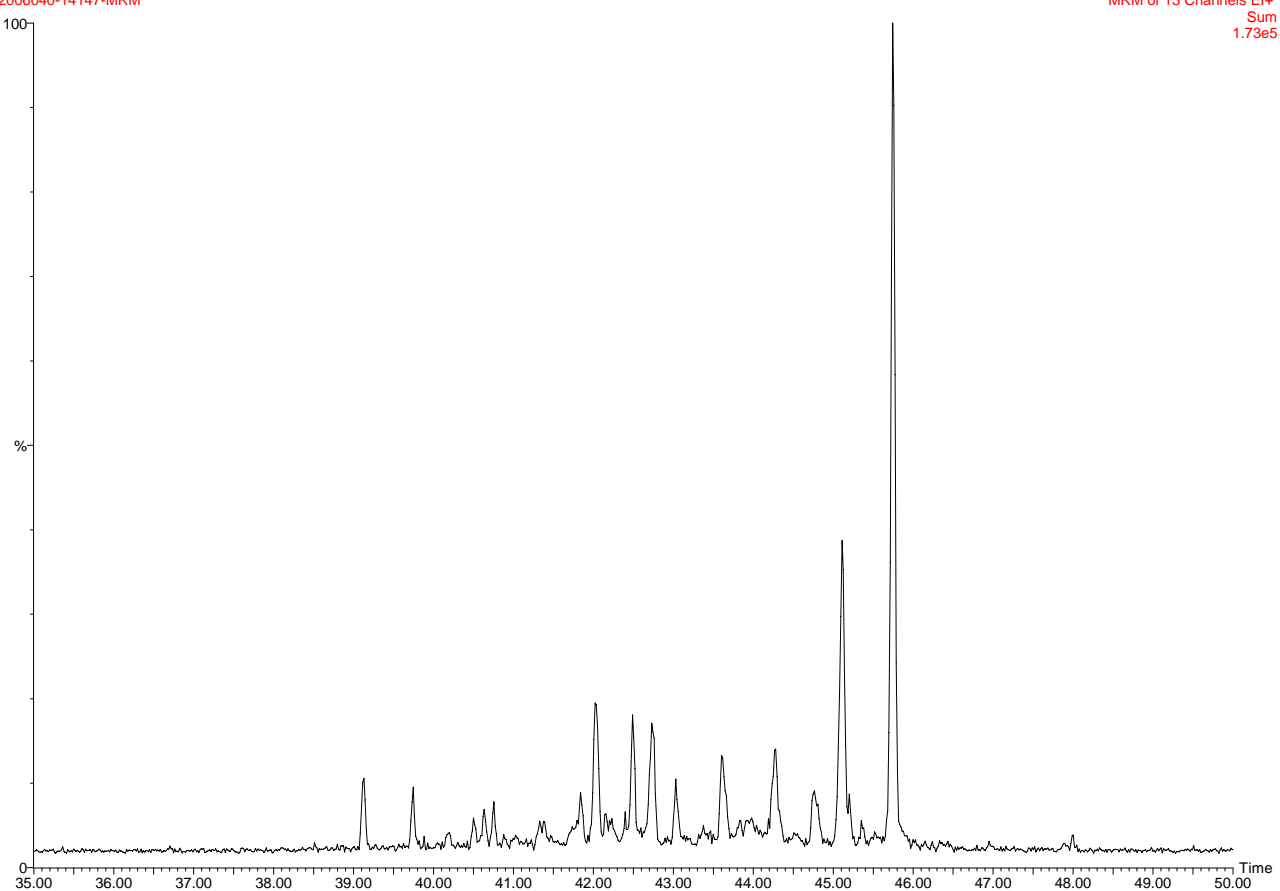
00,2006040-14147-133G-1 ali-aro 1.7 mg
2006040-14147-MRM

MRM of 13 Channels El+
Sum
2.46e5

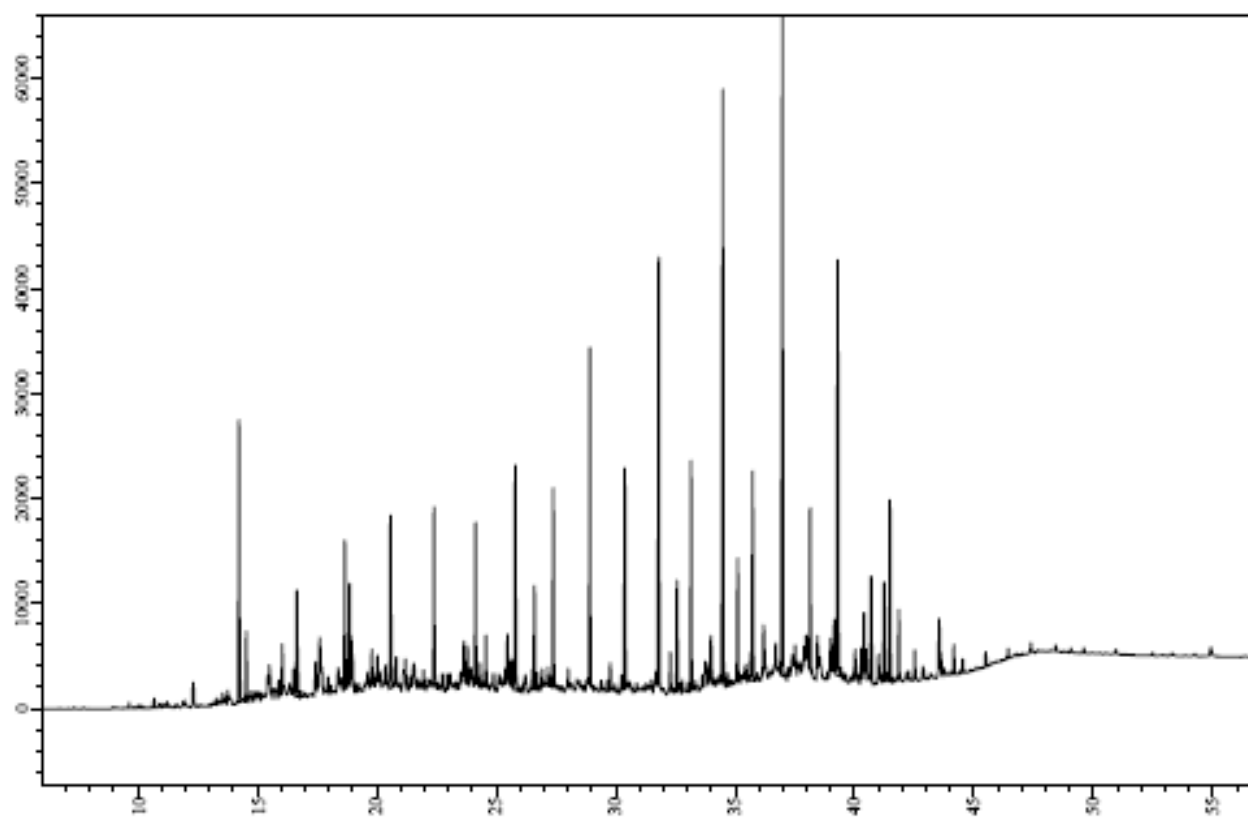


00,2006040-14147-133G-1 ali-aro 1.7 mg
2006040-14147-MRM

MRM of 13 Channels El+
Sum
1.73e5

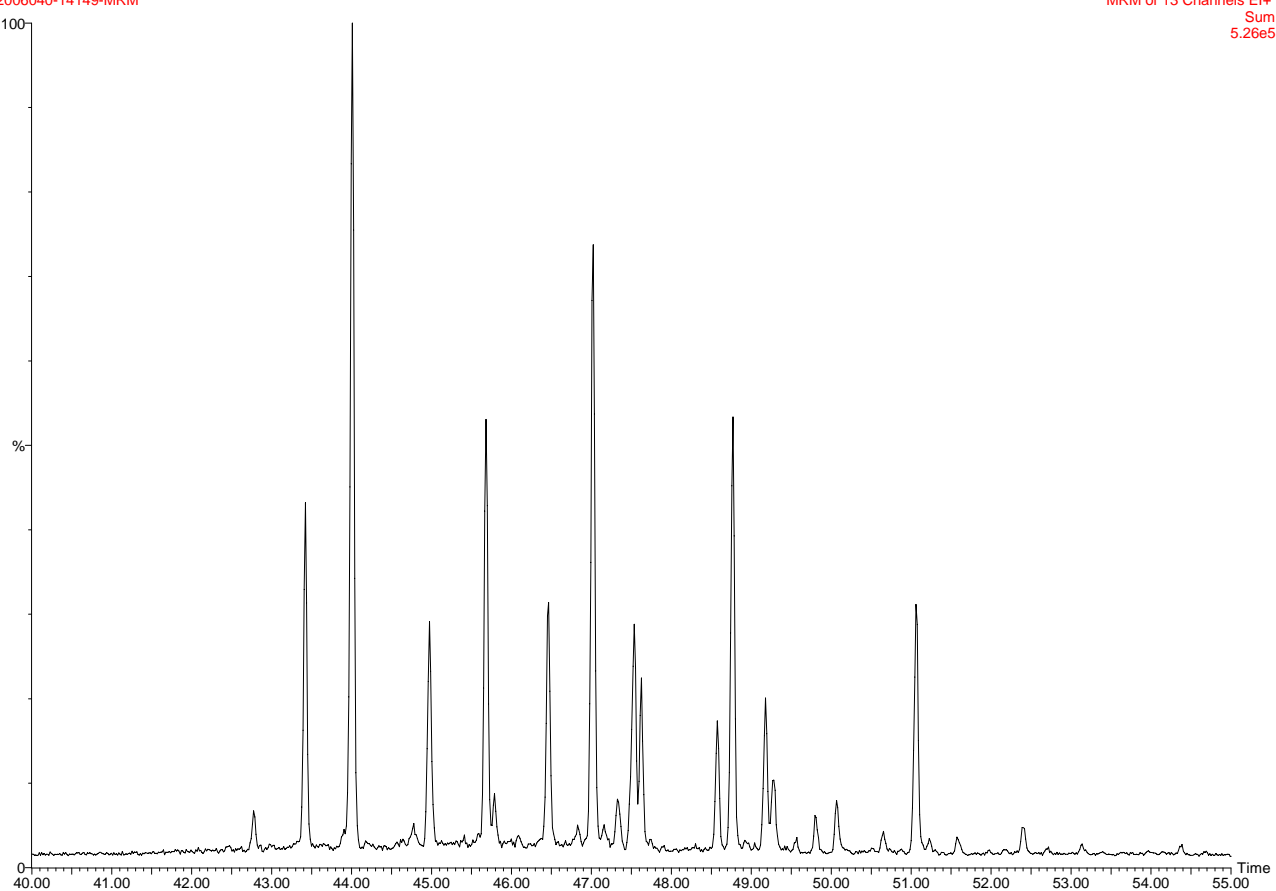


DANA06-133G-3



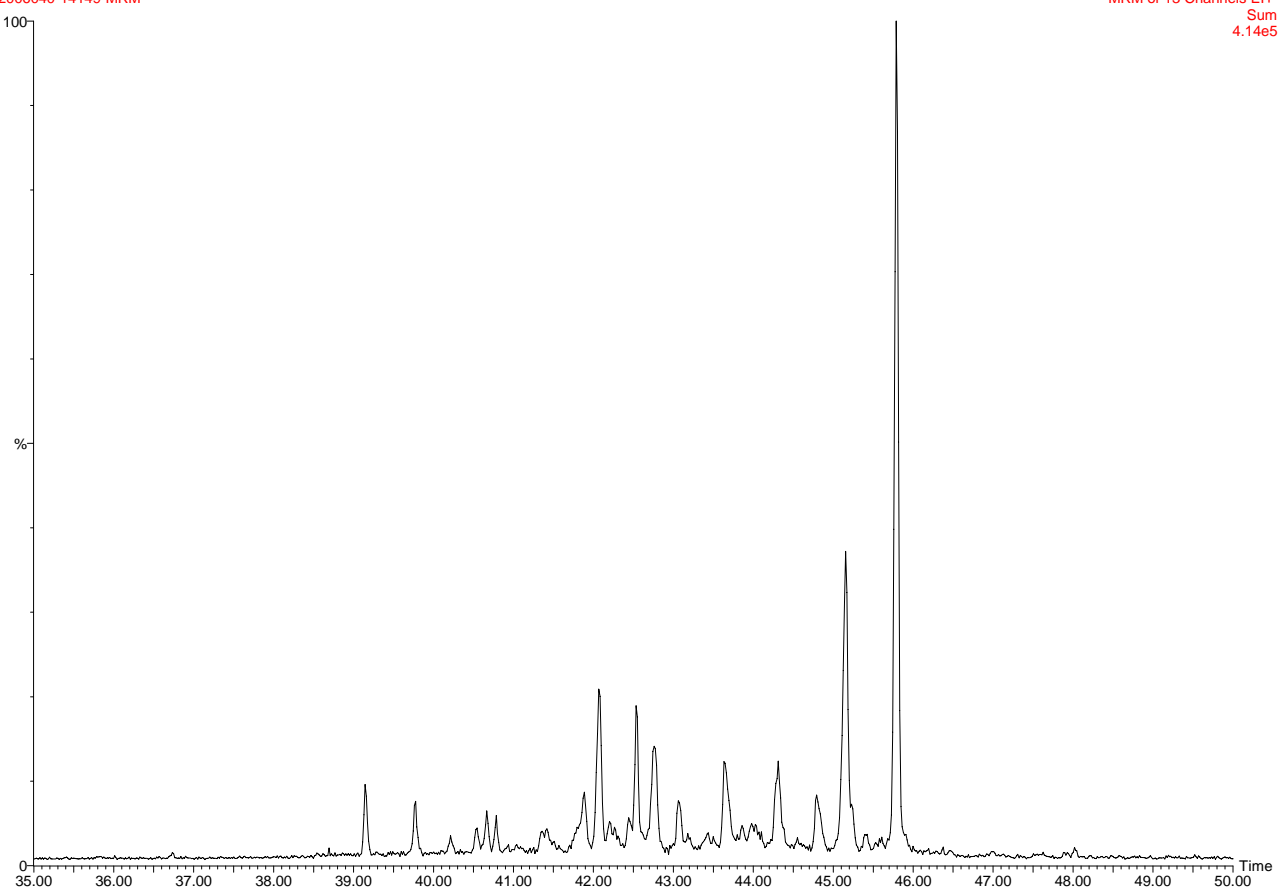
00,2006040-14149-133G-3 ali-aro 1.0 mg
2006040-14149-MRM

MRM of 13 Channels El+
Sum
5.26e5

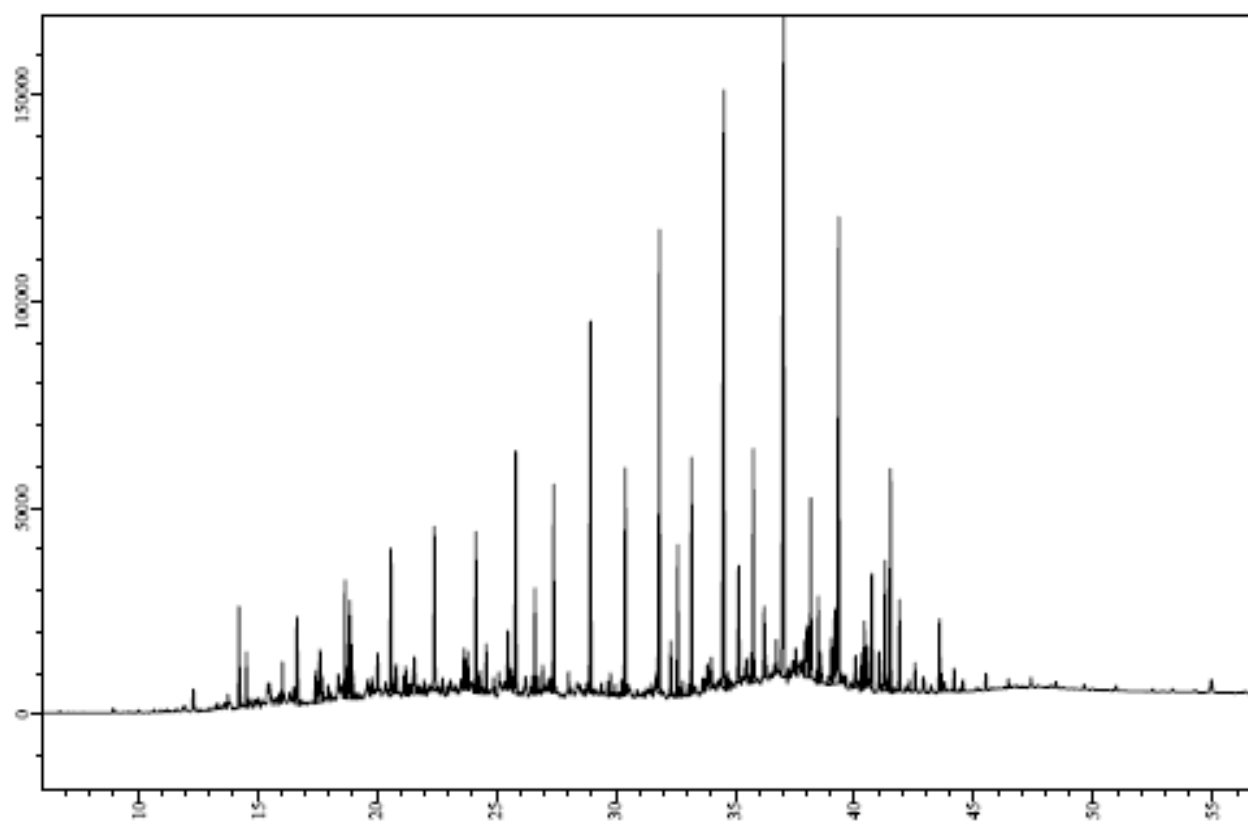


00,2006040-14149-133G-3 ali-aro 1.0 mg
2006040-14149-MRM

MRM of 13 Channels El+
Sum
4.14e5

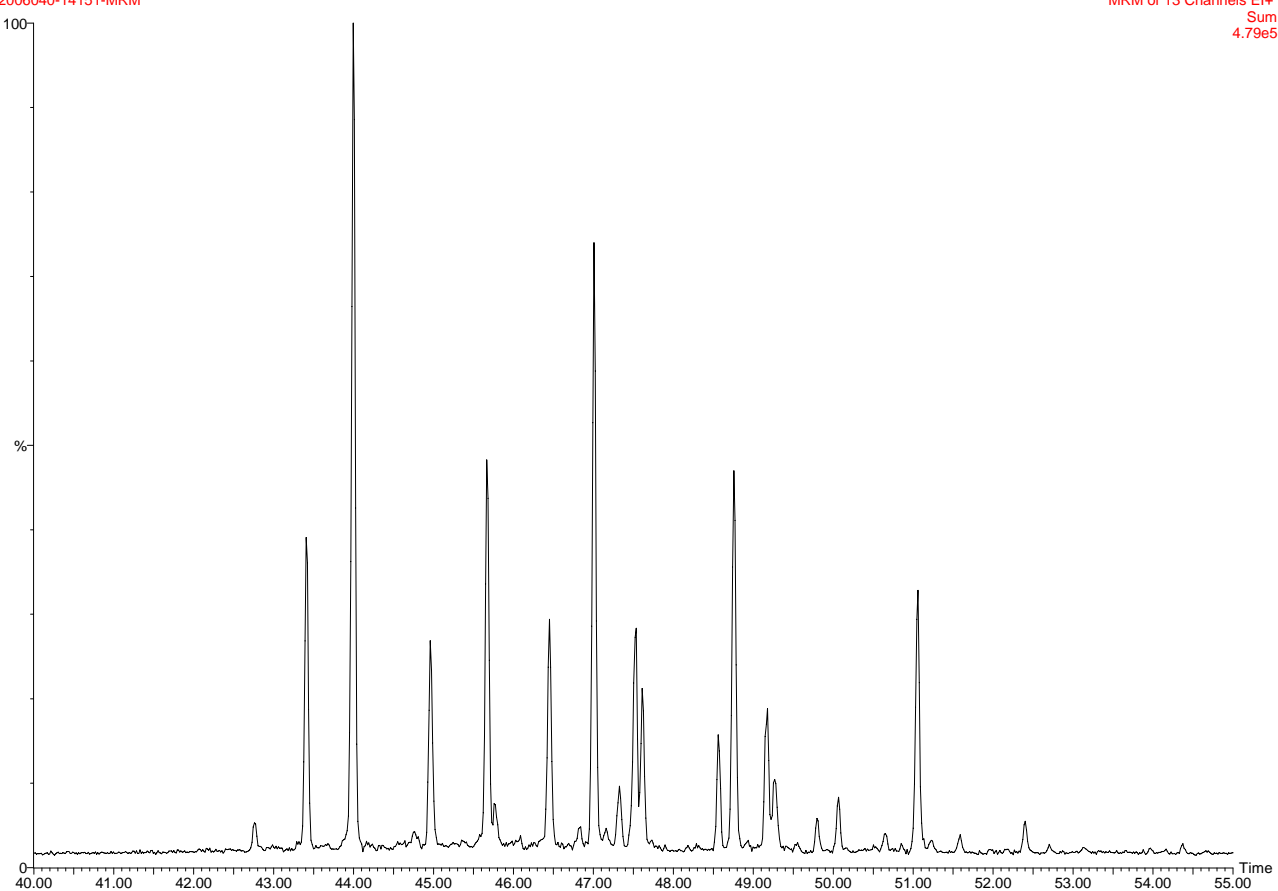


DANA06-133G-5



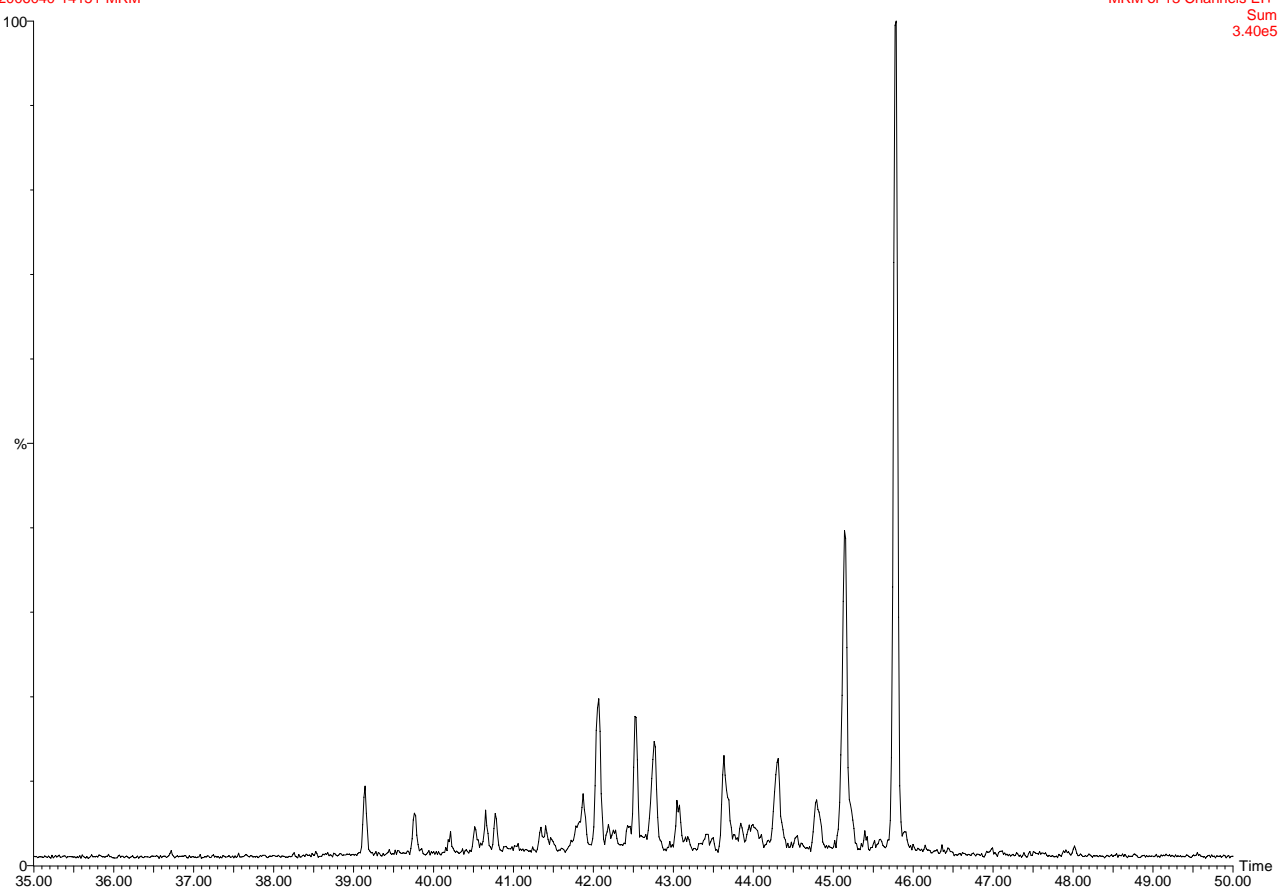
00,2006040-14151-133G-5 ali-aro 0.5 mg
2006040-14151-MRM

MRM of 13 Channels El+
Sum
4.79e5

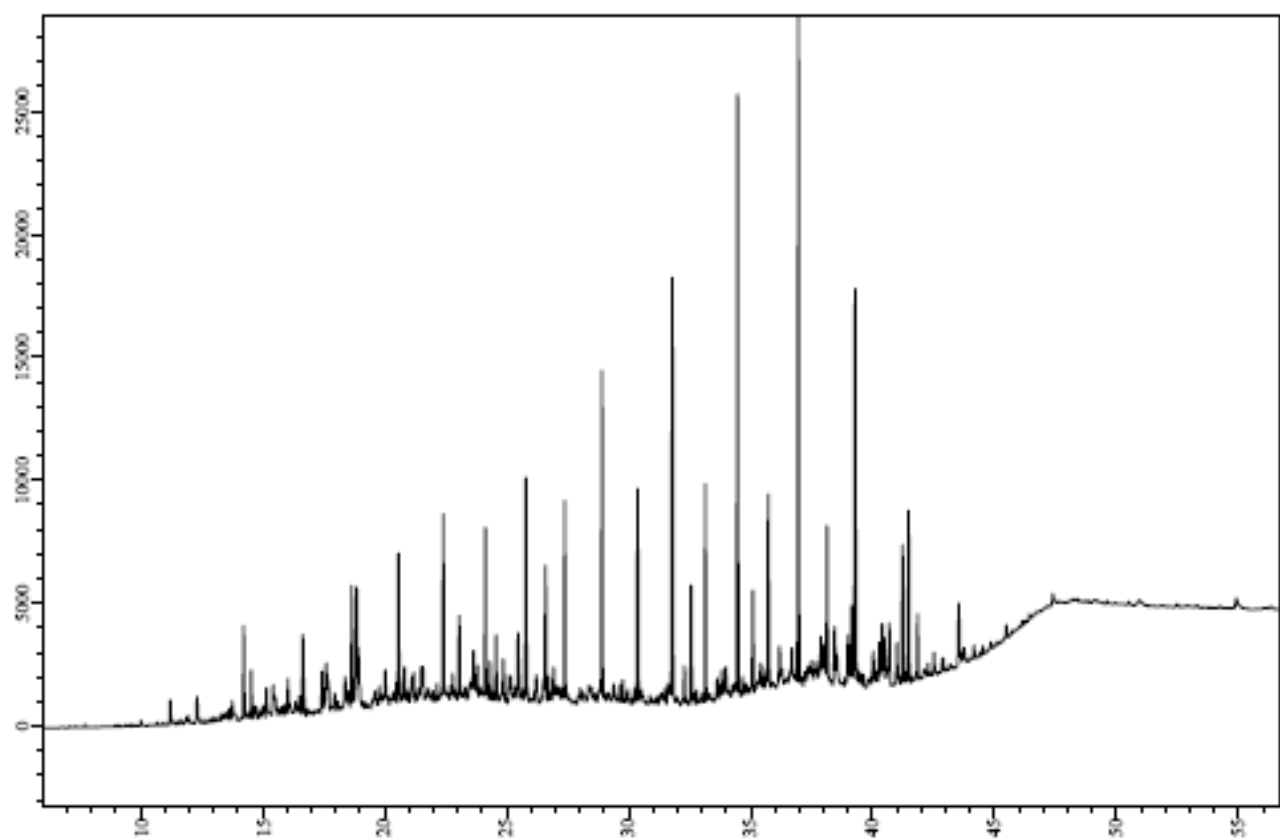


00,2006040-14151-133G-5 ali-aro 0.5 mg
2006040-14151-MRM

MRM of 13 Channels El+
Sum
3.40e5

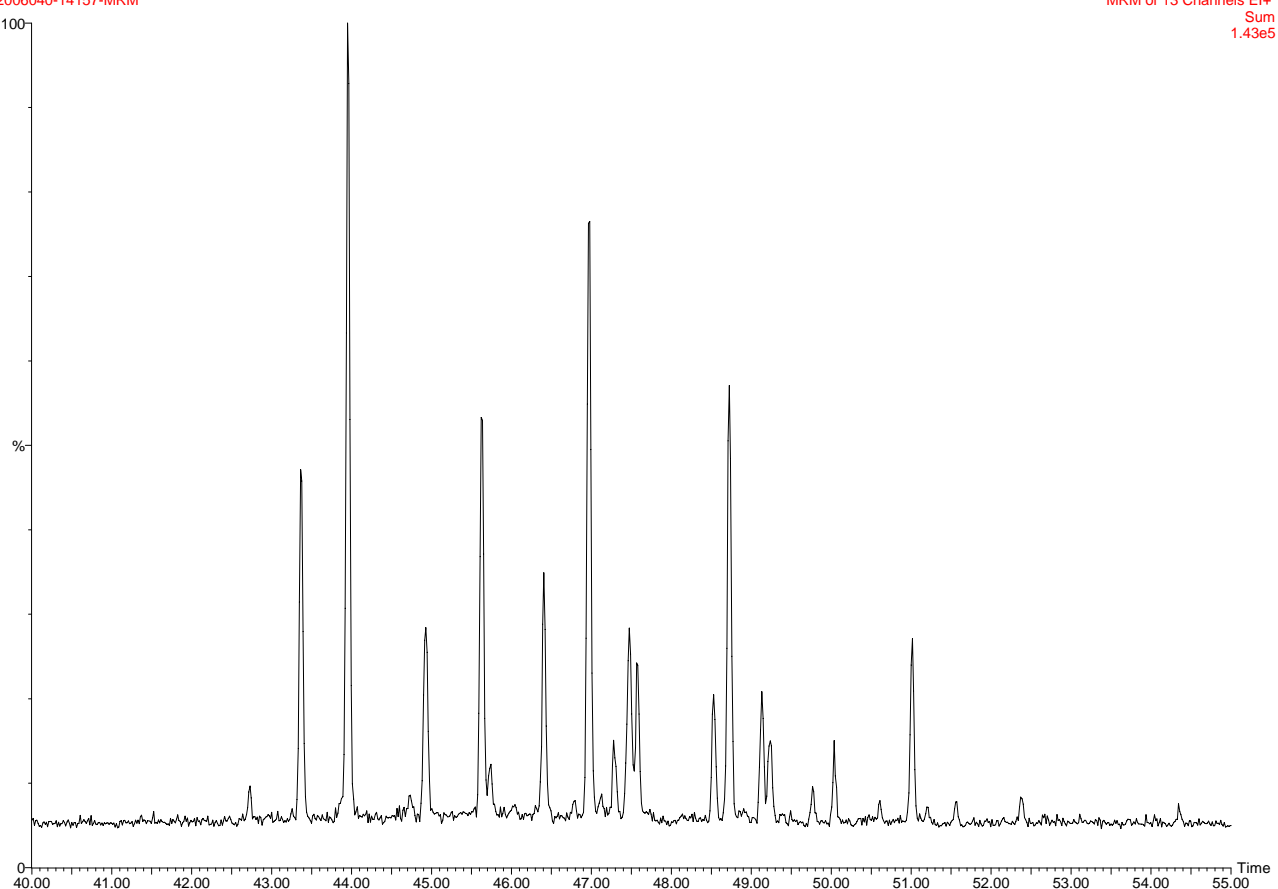


DANA06-139G-1



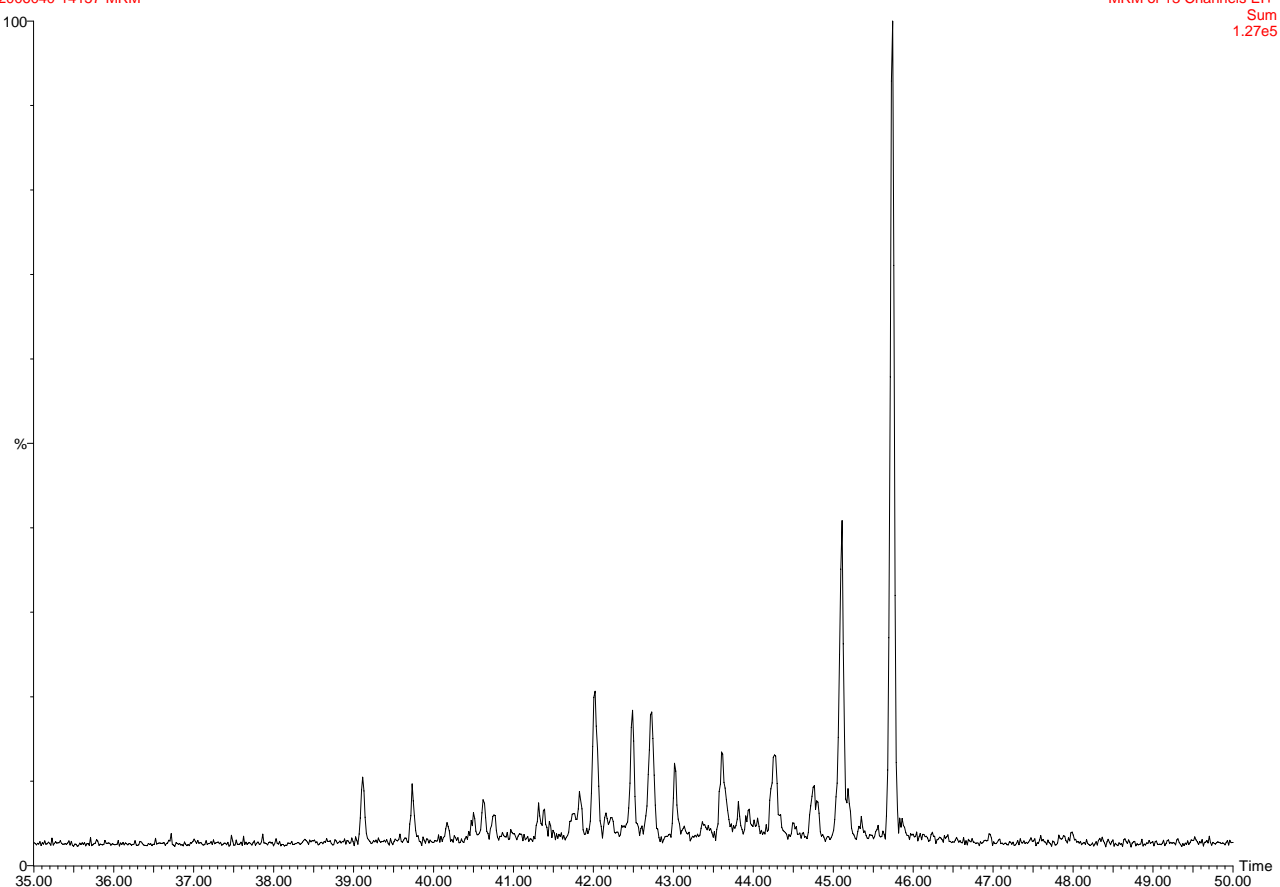
00,2006040-14157-139G-1 ali-aro 0.3 mg
2006040-14157-MRM

MRM of 13 Channels El+
Sum
1.43e5

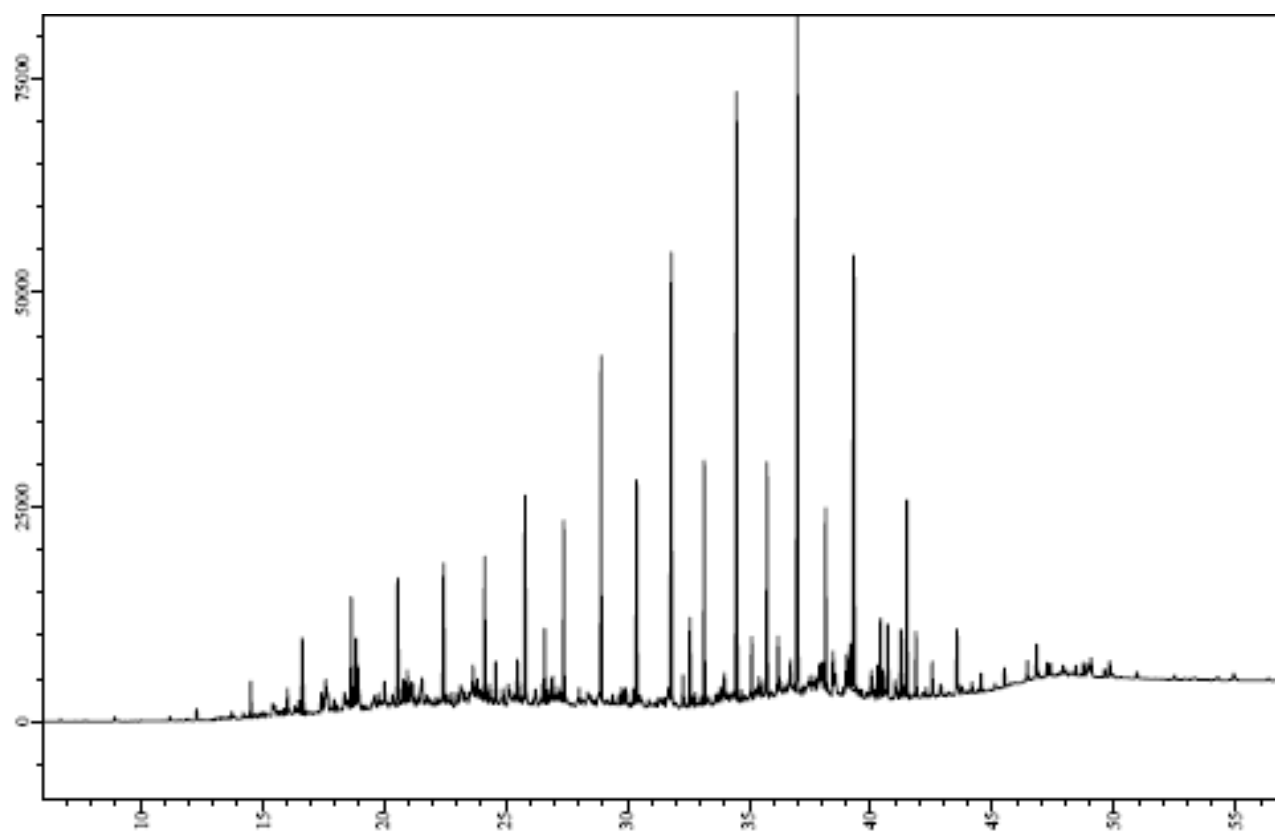


00,2006040-14157-139G-1 ali-aro 0.3 mg
2006040-14157-MRM

MRM of 13 Channels El+
Sum
1.27e5

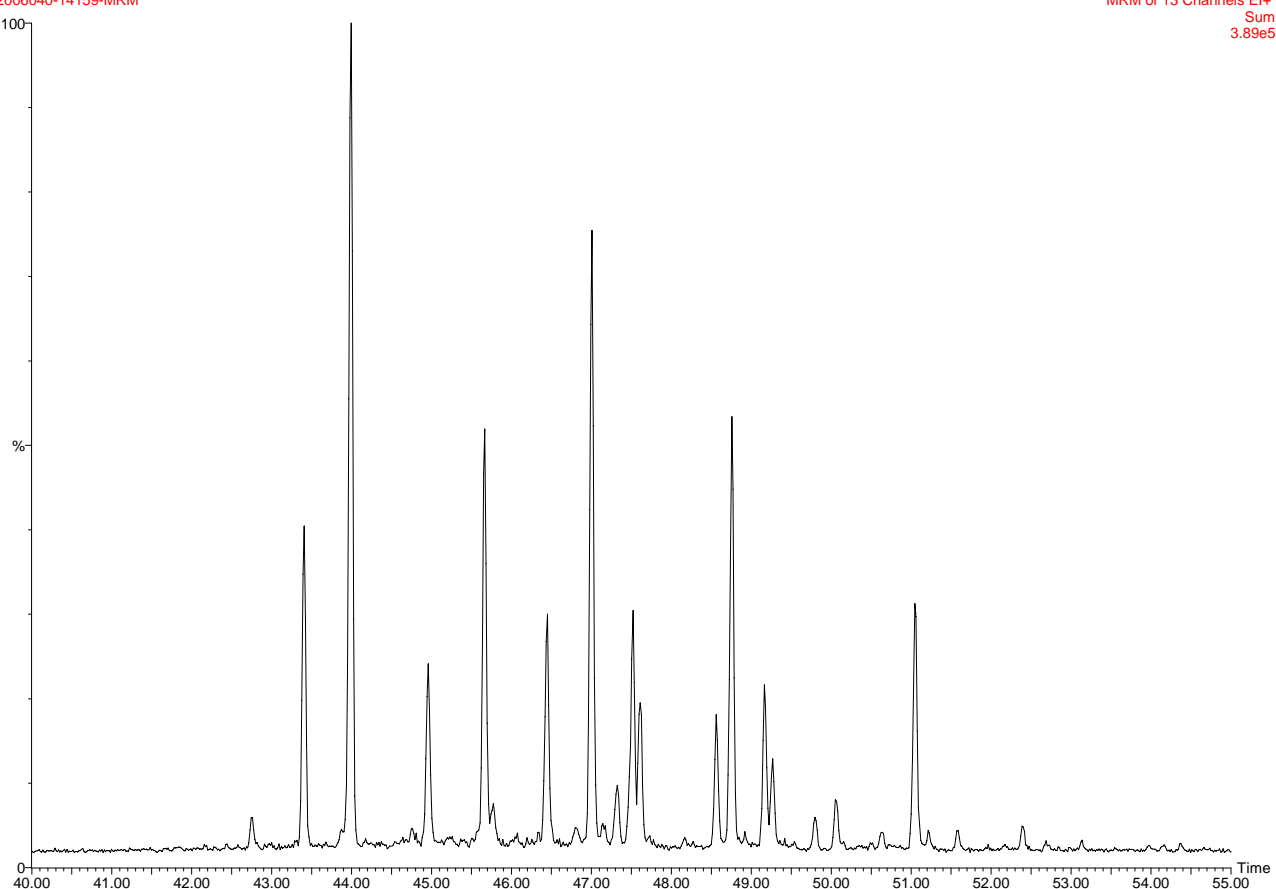


DANA06-139G-3



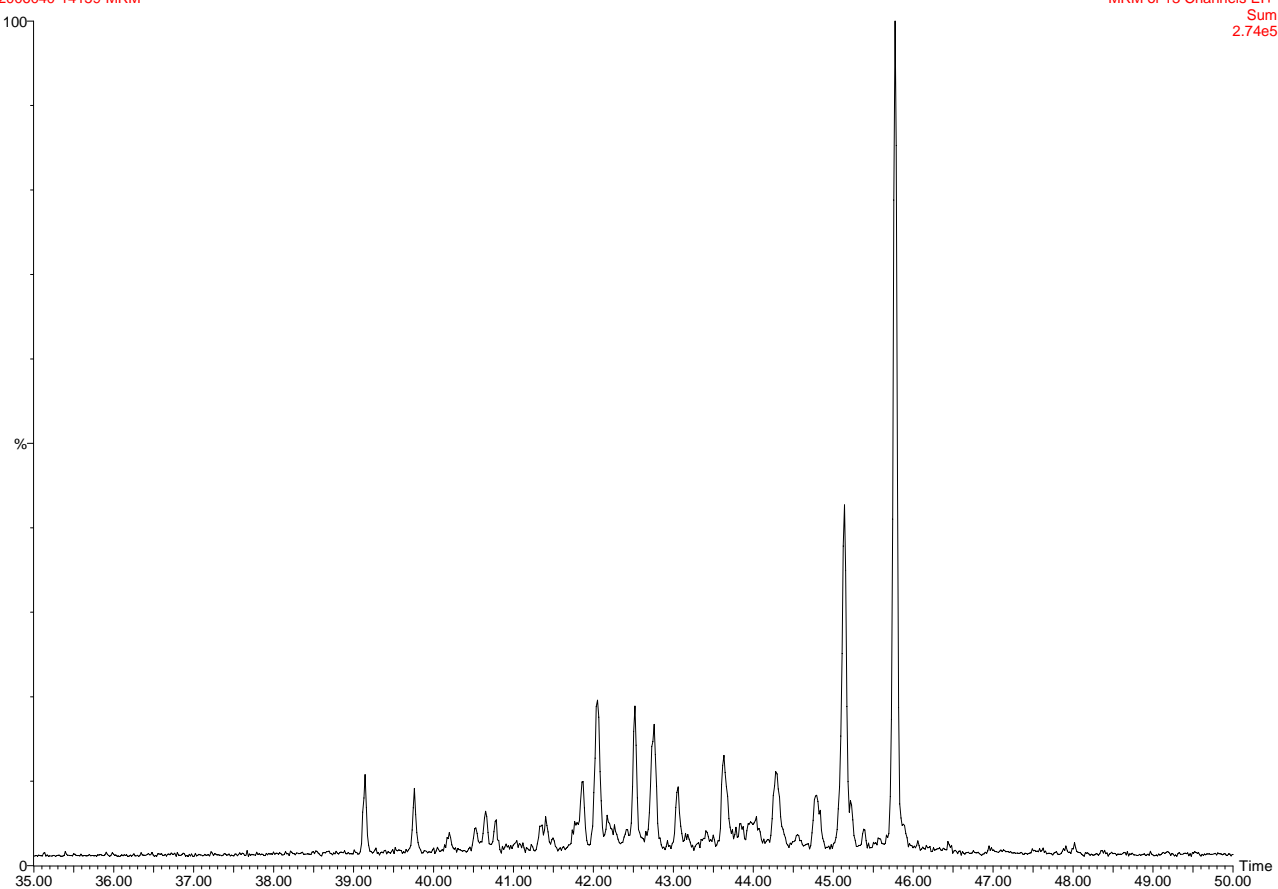
00,2006040-14159-139G-3 ali-aro 0.9 mg
2006040-14159-MRM

MRM of 13 Channels El+
Sum
3.89e5

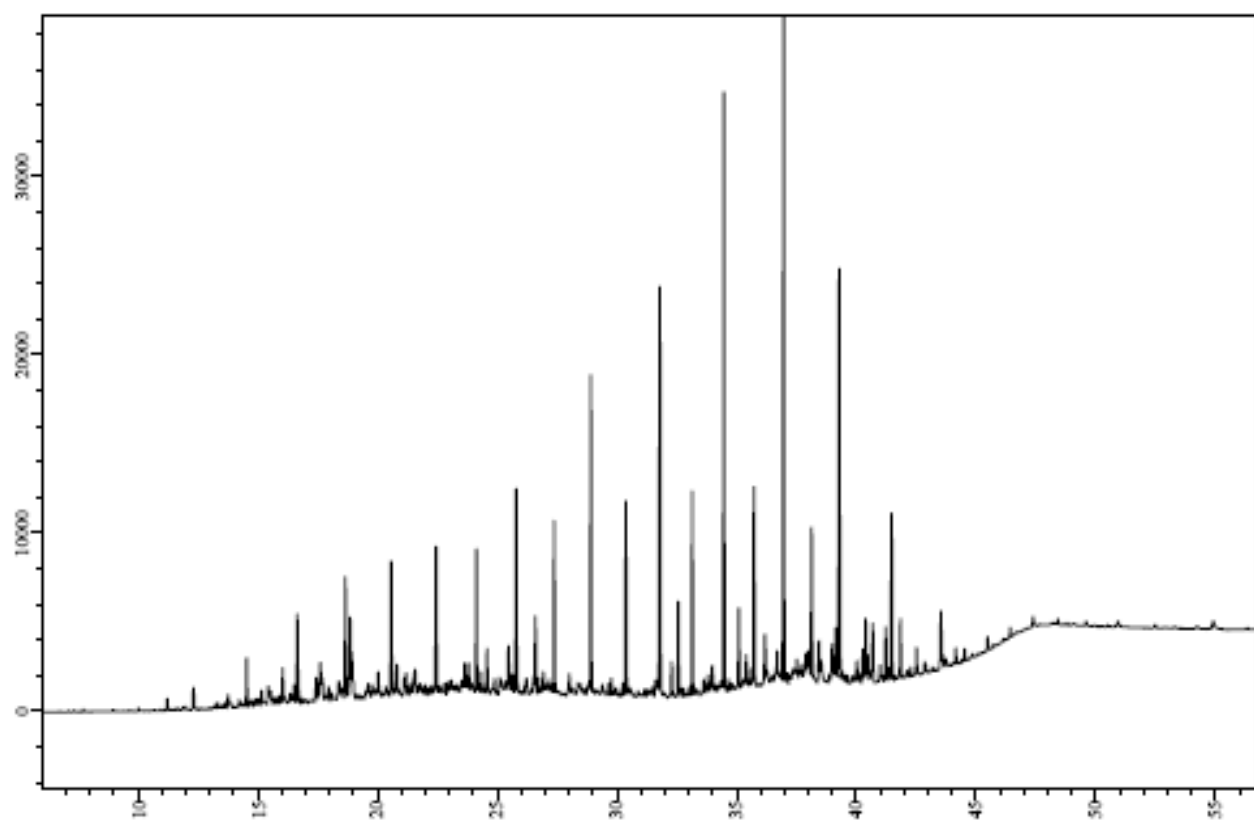


00,2006040-14159-139G-3 ali-aro 0.9 mg
2006040-14159-MRM

MRM of 13 Channels El+
Sum
2.74e5

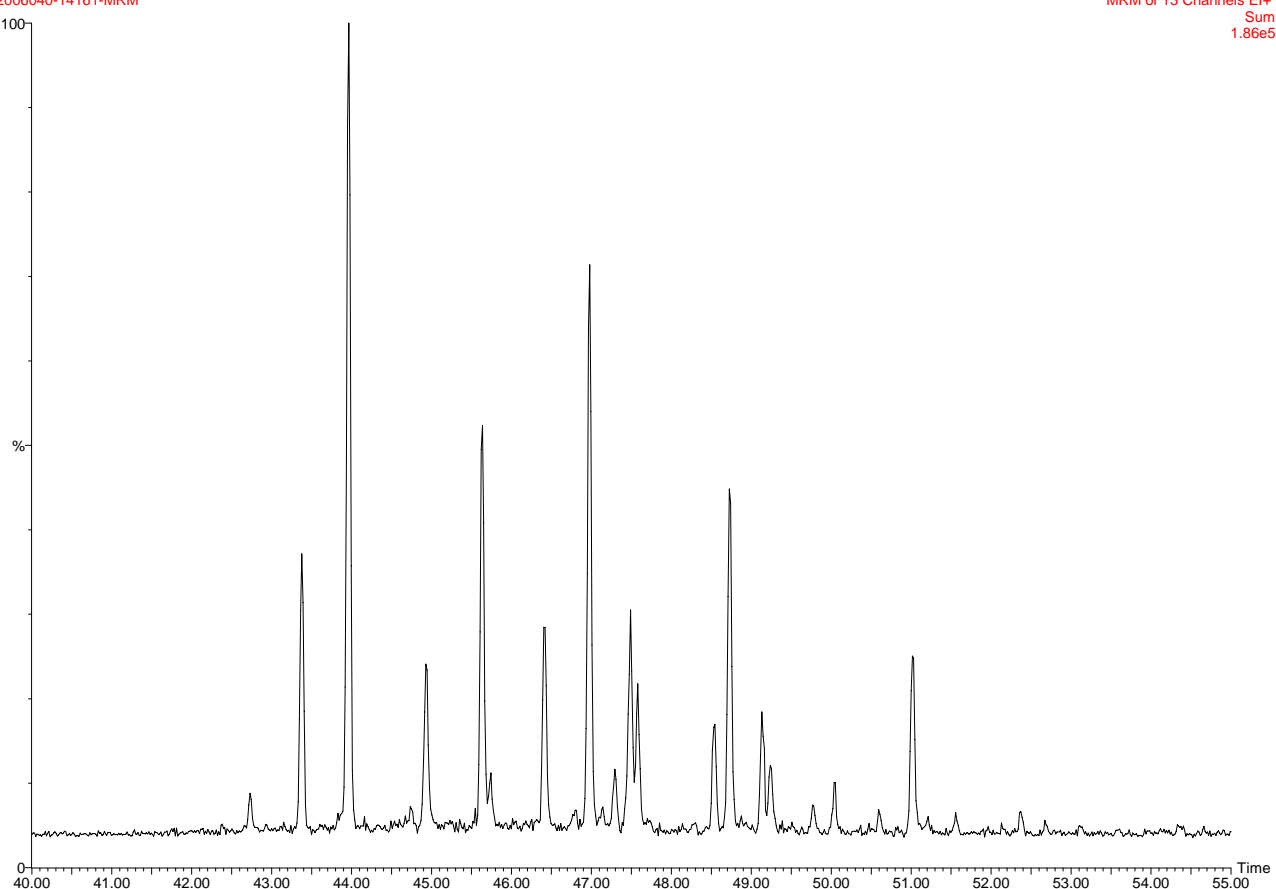


DANA06-139G-5



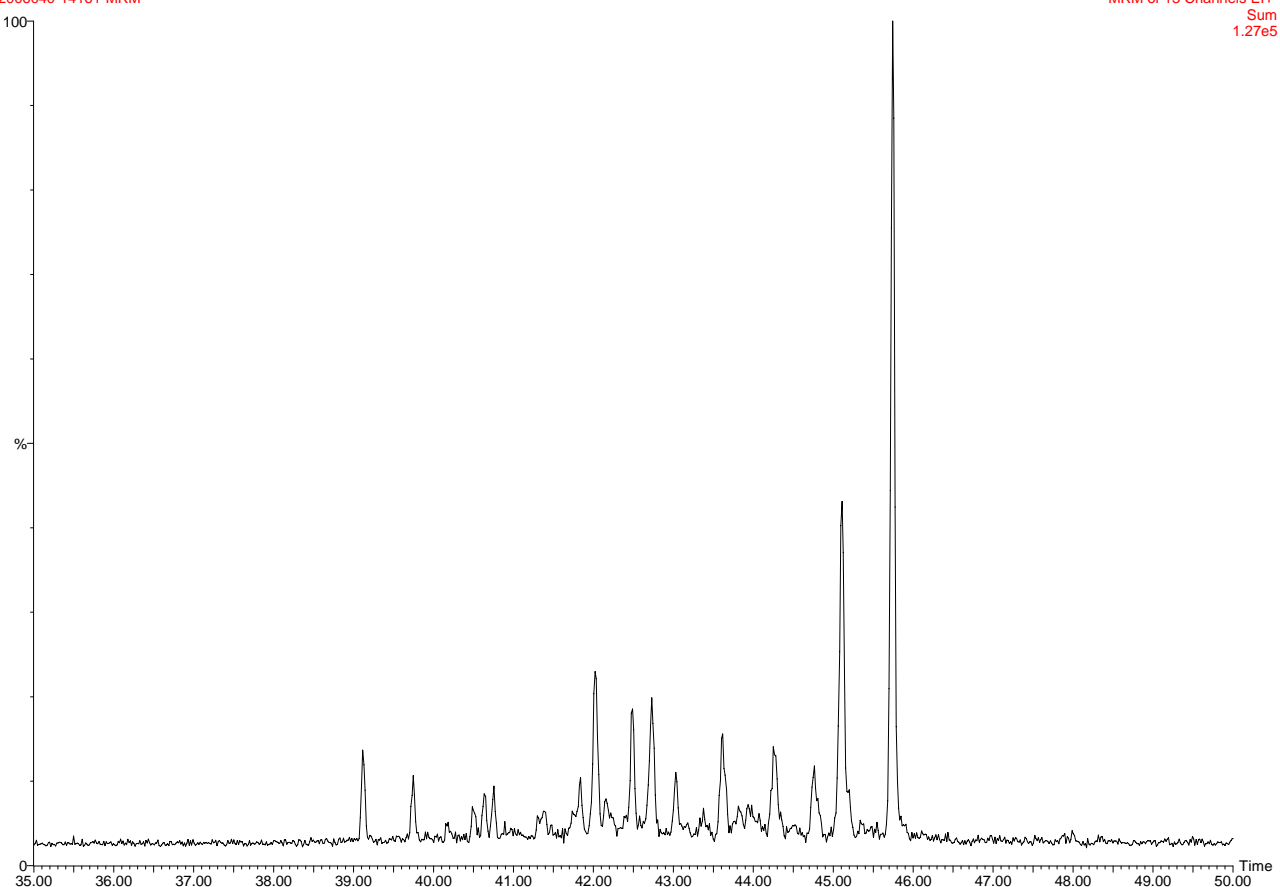
00,2006040-14161-139G-5 ali-aro 2.0 mg
2006040-14161-MRM

MRM of 13 Channels El+
Sum
1.86e5

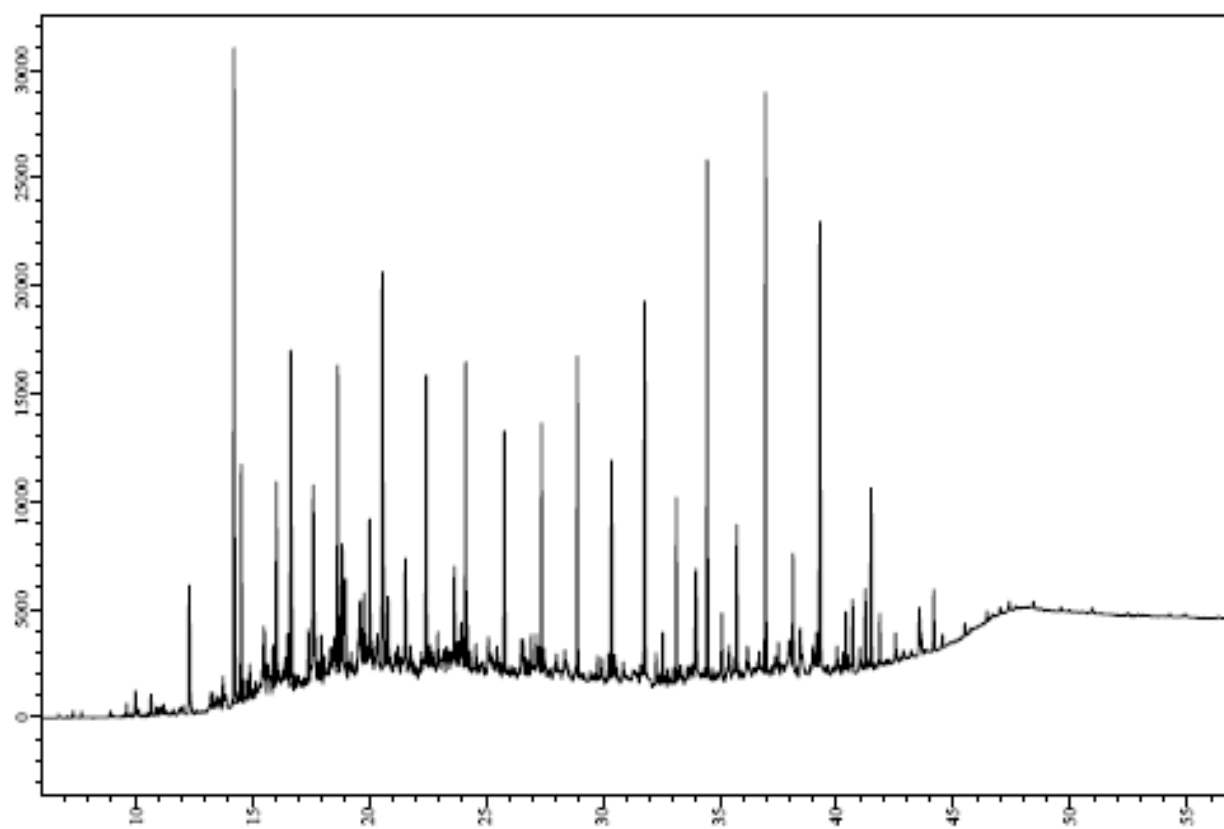


00,2006040-14161-139G-5 ali-aro 2.0 mg
2006040-14161-MRM

MRM of 13 Channels El+
Sum
1.27e5

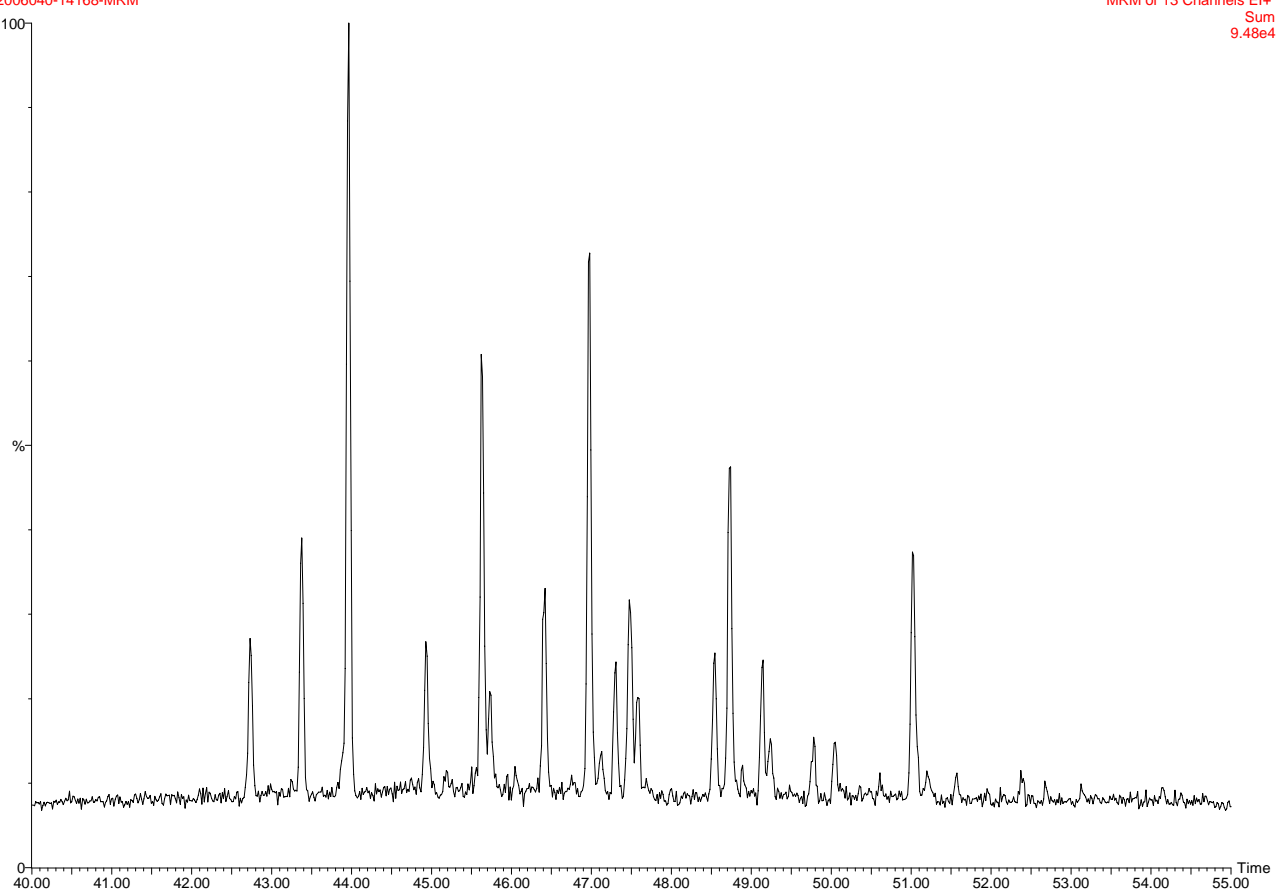


DANA06-146G-1



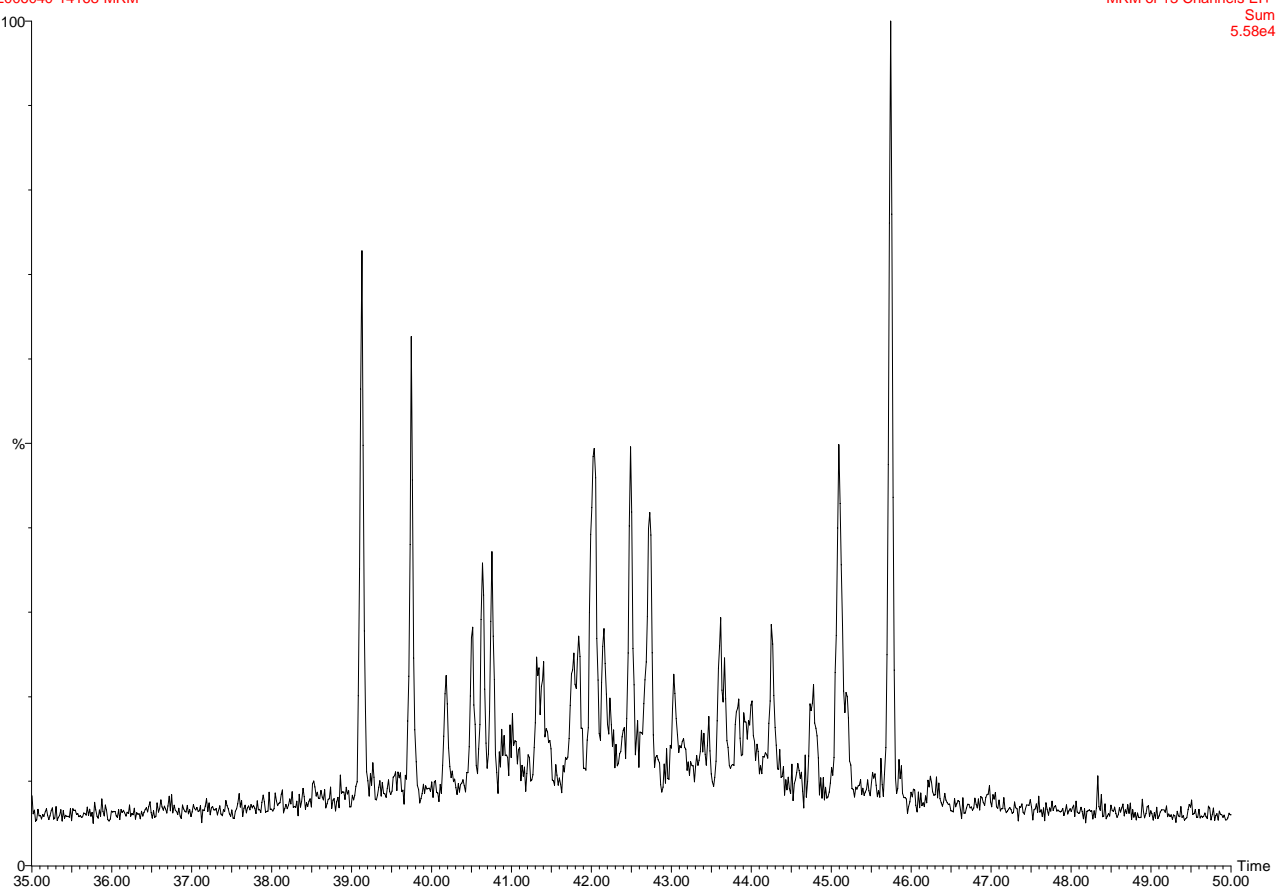
00,2006040-14168-146G-1 ali-aro 0.5 mg
2006040-14168-MRM

MRM of 13 Channels El+
Sum
9.48e4

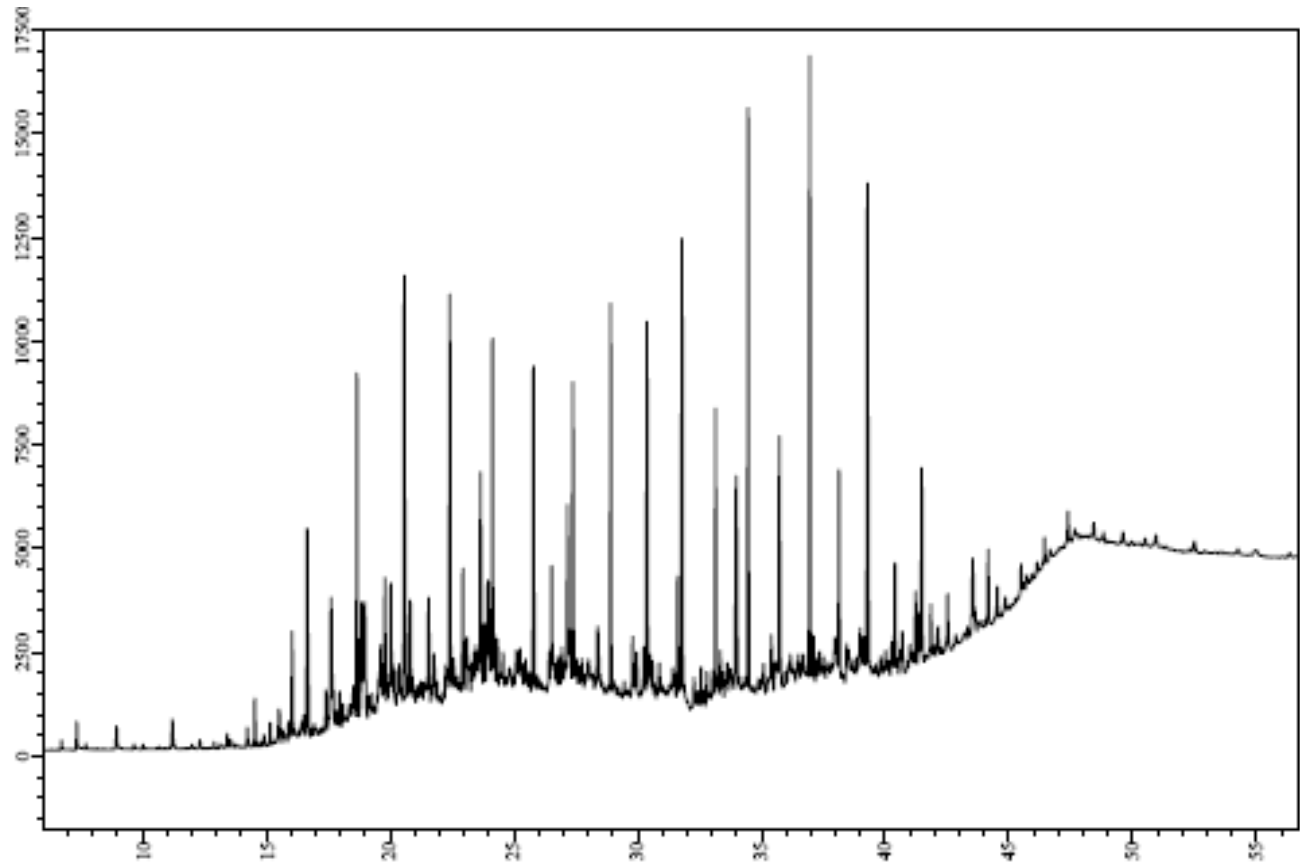


00,2006040-14168-146G-1 ali-aro 0.5 mg
2006040-14168-MRM

MRM of 13 Channels El+
Sum
5.58e4

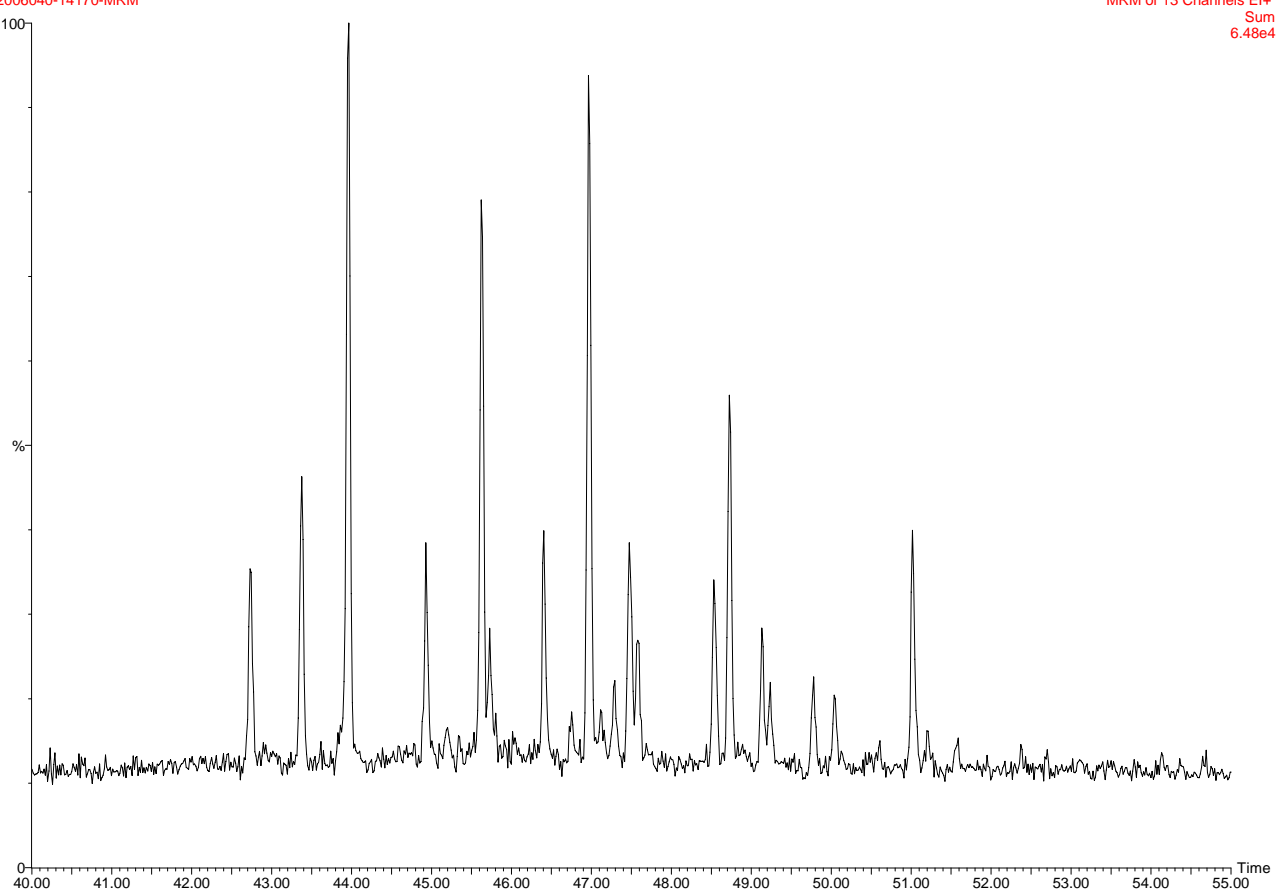


DANA06-146G-3



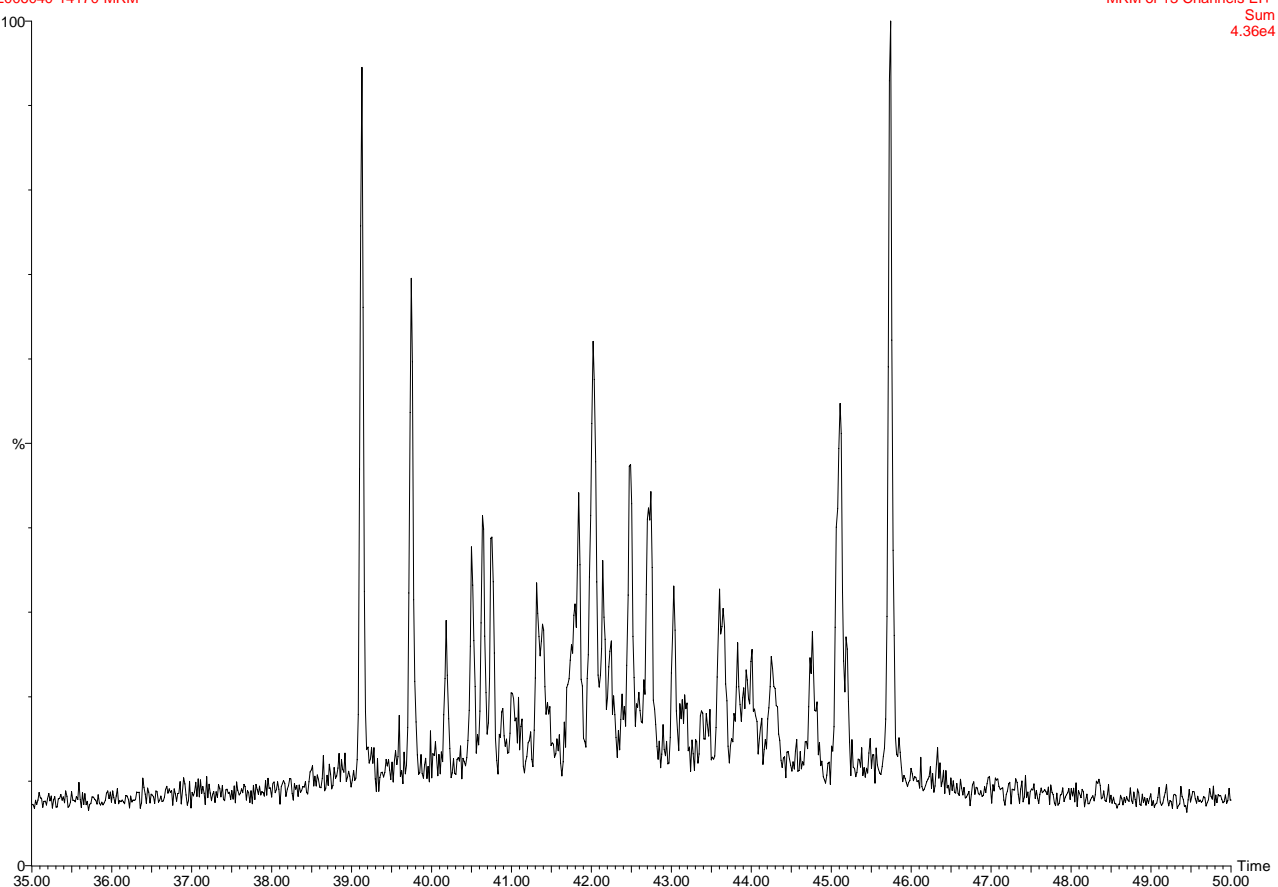
00,2006040-14170-146G-3 ali-aro 1.0 mg
2006040-14170-MRM

MRM of 13 Channels El+
Sum
6.48e4

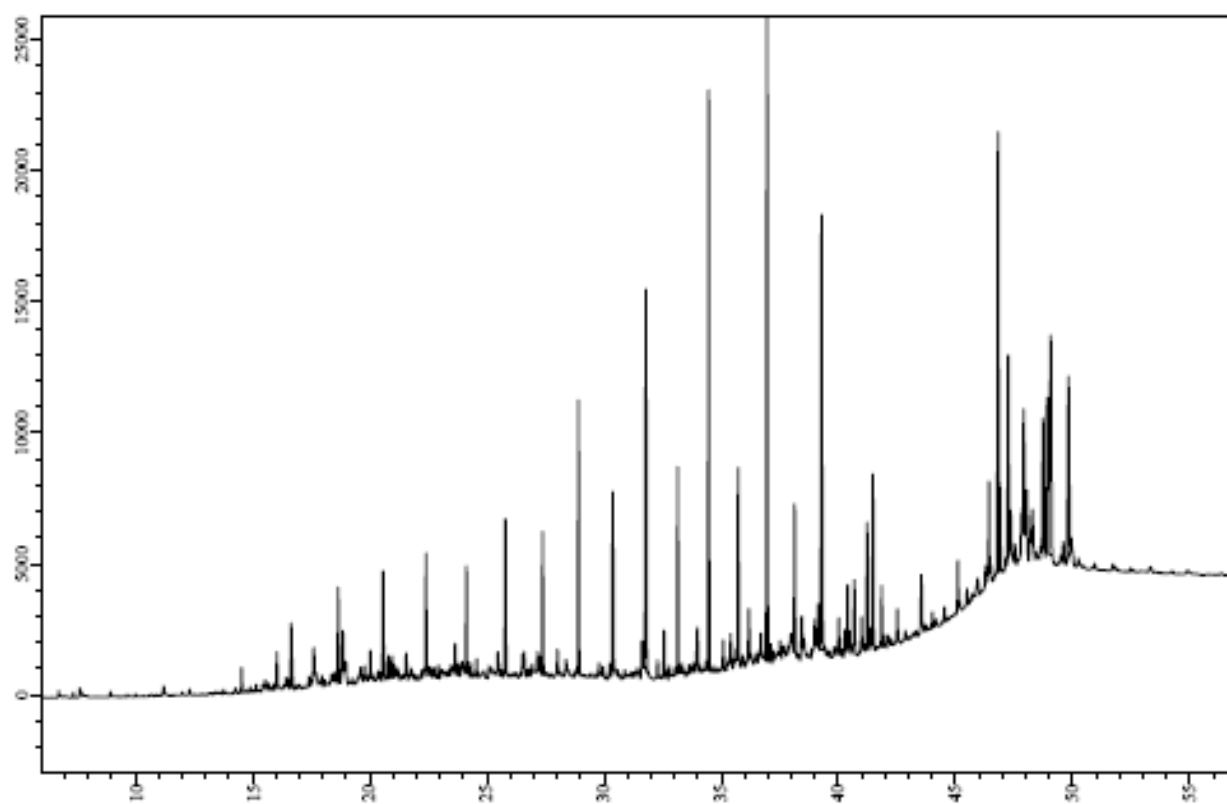


00,2006040-14170-146G-3 ali-aro 1.0 mg
2006040-14170-MRM

MRM of 13 Channels El+
Sum
4.36e4

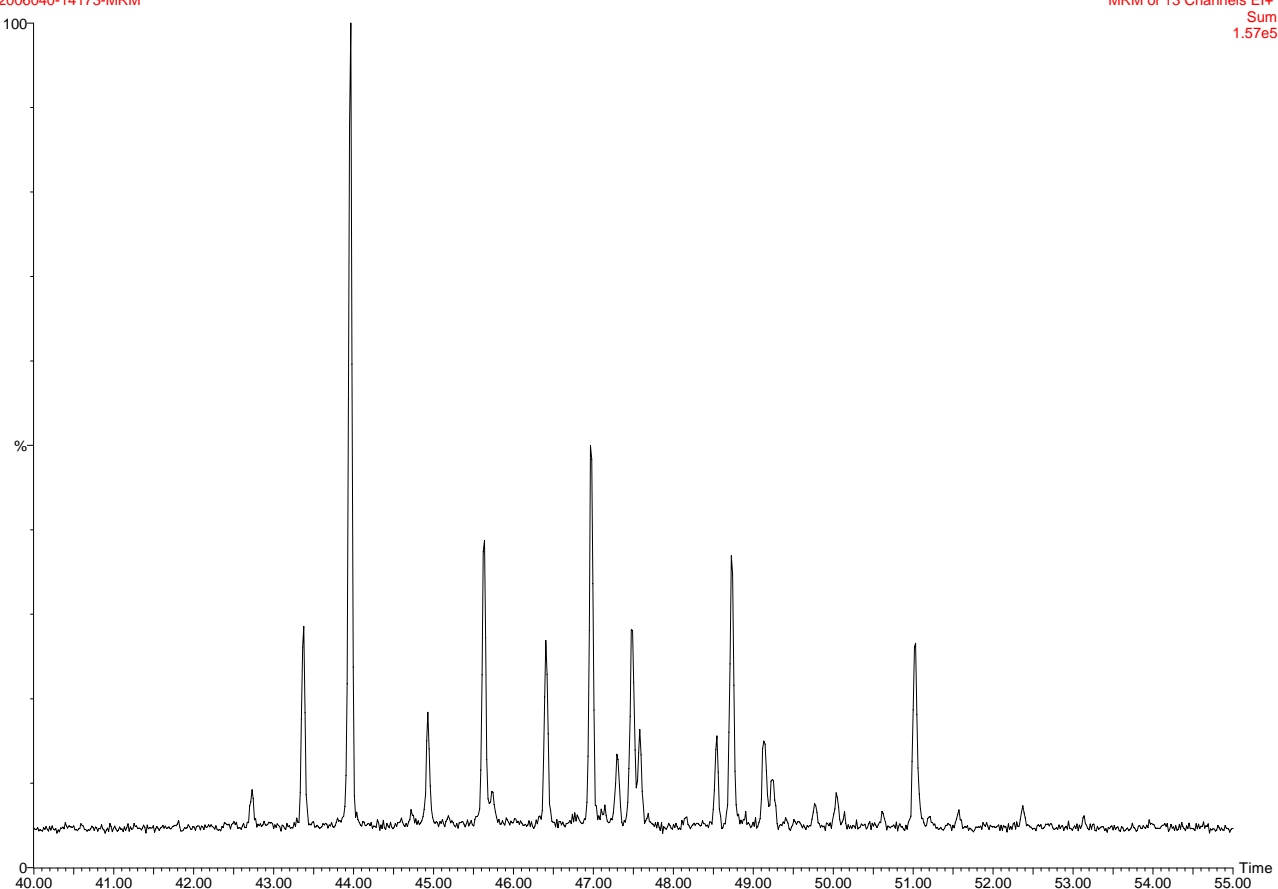


DANA06-146G-6



00,2006040-14173-146G-6 ali-aro 2.9 mg
2006040-14173-MRM

MRM of 13 Channels El+
Sum
1.57e5



00,2006040-14173-146G-6 ali-aro 2.9 mg
2006040-14173-MRM

MRM of 13 Channels El+
Sum
5.85e4

